

The Androgen Receptor Independent Mechanism of Toxicity of the
Novel Anti-tumor Agent 11 β -Dichloro

by

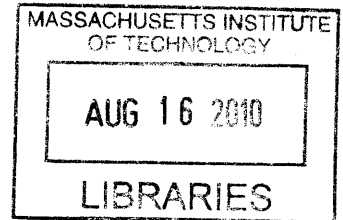
Bogdan I. Fedeleş

B.S. Chemistry, B.S Biology (2002)
Massachusetts Institute of Technology, Cambridge, MA

SUBMITTED TO THE DEPARTMENT OF BIOLOGICAL ENGINEERING
IN PARTIAL FULFILLMENT OF THE REQUIREMENTS
FOR THE DEGREE OF

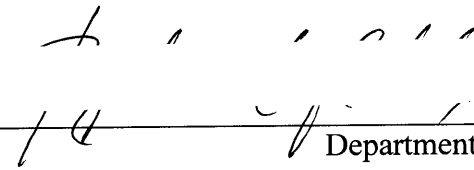
DOCTOR OF PHILOSOPHY IN BIOLOGICAL ENGINEERING
AT THE
MASSACHUSETTS INSTITUTE OF TECHNOLOGY
JUNE 2009


ARCHIVES

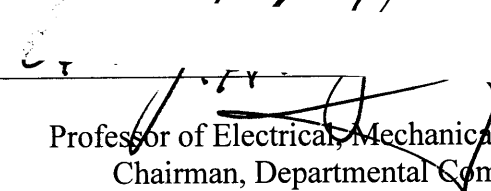


©2009 Massachusetts Institute of Technology.
All rights reserved.

The author hereby grants to MIT permission to reproduce and to
distribute publicly paper and electronic copies of this thesis document in
whole or in part in any medium now known or hereafter created.

Signature of Author:  Department of Biological Engineering
May 22, 2009

Certified by:  John M. Essigmann
William and Betsy Leitch Professor of Chemistry, Toxicology and Biological Engineering
Thesis Supervisor

Accepted by:  Alan J. Grodzinsky
Professor of Electrical, Mechanical, and Biological Engineering
Chairman, Departmental Committee for Graduate Students

Committee

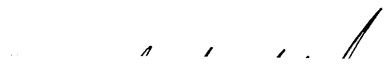
THIS DOCTORAL THESIS HAS BEEN EXAMINED BY A COMMITTEE OF THE DEPARTMENT OF BIOLOGICAL ENGINEERING AS FOLLOWS:



Leona D. Samson
American Cancer Society Professor
Professor of Toxicology and Biological Engineering
Director, Center for Environmental Health Sciences
Chairman

- - -

John Martin Essigman
William and Betsy Leitch Professor of Chemistry, Toxicology and Biological Engineering
Thesis Supervisor



Forrest White
Mitsui Associate Professor of Biological Engineering



Robert G. Croy
Research Scientist in Biological Engineering



The Androgen Receptor Independent Mechanism of Toxicity of the Novel Anti-tumor Agent 11 β -Dichloro

by

Bogdan I. Fedeles

Submitted to the Department of Biological Engineering in Partial Fulfillment of the Requirements for the Degree of Doctor of Philosophy in Biological Engineering

Abstract

Inspired by the toxicity mechanism of cisplatin in testicular cancer, a series of bi-functional genotoxicants has been designed that supplement their DNA damaging properties with the ability to interact with tumor specific proteins. One such compound, 11 β -dichloro links an aniline mustard moiety to a steroid ligand for the androgen receptor (AR). *In vitro* and *in vivo* (cell cultures, mouse xenografts) studies highlighted the potent antitumor properties of the molecule, which can prevent growth of AR positive tumor xenografts in mice. However, 11 β -dichloro also proved highly effective against many cancer lines that do not express the AR, more so than other nitrogen mustards commonly used in chemotherapy.

To understand better the AR independent mechanism, the toxicity of 11 β -dichloro was investigated in *Saccharomyces cerevisiae*, by interrogating the complete yeast single-gene deletion mutant library. Surprisingly, the screen revealed that the mutants most sensitive to 11 β -dichloro are not the ones lacking genes involved in DNA repair, but rather mutants lacking genes involved in mitochondrial and ribosomal function. While some of the sensitive mutants are also sensitive to other DNA damaging agents, almost half of them are uniquely sensitive to 11 β -dichloro, suggesting a DNA-damage independent mechanism of action.

Based on the yeast findings, we tested mechanistic hypotheses in HeLa cells (an AR negative human cancer cell line), and discovered that 11 β -dichloro induces a large amount of reactive oxygen species (ROS), accompanied by a significant depletion of the antioxidant pool and a perturbation of the mitochondrial inner membrane potential. We also discovered that co-treatment with antioxidants such as N-acetyl cysteine or vitamin E alleviates the toxicity of 11 β -dichloro, suggesting that ROS play an important role in the mechanism of toxicity. In terms of transcriptional responses, previous observations were confirmed that 11 β -dichloro upregulates expression of genes involved in the unfolded protein response (UPR) and sterol biosynthesis. Additional cellular responses consistent with these pathways were the striking increase in cytosolic calcium and significant changes in the size of the cells. Taken together, our results highlight the multifaceted toxicological profile of 11 β -dichloro, indicating that besides DNA damage, the generation of ROS and induction of UPR may be the additional pathways responsible for the potent anticancer effects of this agent.

Abstract

Thesis Supervisor: John M. Essigmann

Title: William and Betsy Leitch Professor of Chemistry, Toxicology and Biological Engineering

Acknowledgements

Research on the scale required for doctoral work always involves significant human interaction and collaborative efforts. I am greatly indebted to all the people that have influenced and shaped my doctoral career; their wisdom, advice and friendship have made all the difference, transforming these seven long years of PhD into an unforgettable life experience.

My deepest gratitude goes to my advisor, John Essigmann, who has been a tremendous source of inspiration, motivation and guidance. Ever since our first encounter at a student dinner, back in my college senior year, I have been fascinated by John's brilliant scientific ideas, his unstoppable enthusiasm and captivating story-telling ability. John has always been extremely supportive of all my overly-creative ideas and he encouraged me to explore paradigm-shifting approaches to research. I am very grateful for his laid-back mentoring style, which has been instrumental for allowing me to occasionally pursue interests outside the lab. Yet, I have always found John extremely available to consult on any matter, ranging from science to life and career advice. John, through his kind and selfless example, not only taught me how to become a better scientist, but he inspired me to become a better person. I have always been amazed by John's ability to gracefully handle a tightly packed research schedule with his family duties and an entire dorm full of MIT undergraduates. For that, I consider John a true role model for me, and I hope to follow in his footsteps towards an exciting and fulfilling academic career.

I would like to thank my thesis committee members. Leona Samson has been another source of inspiration for me. Her fascinating research and innovative approaches have been instrumental for shaping my project. I am also very grateful to her for allowing me to work in her lab and learn all about yeast genomic phenotyping, and for her sharing of the yeast mutant library. Additionally, I would like to thank Leona for being the chair on my thesis committee; in this quality, she has played a pivotal role in focusing and guiding my research towards a fruitful completion. Her feedback, at every step of my graduate career has always been poignant and invaluable. I would like to thank Forest White for being a very supportive committee member. His insightful and goal-oriented comments have always been very helpful in structuring my work and focusing on the positive results of my research. I would also like to thank Bob Croy, the co-founder of the programmable chemotherapeutics project. Bob has helped me a great deal, both by personal example and by sharing his wealth of scientific knowledge with me. Bob has also been an excellent and avid critic of my work, helping me pose and search the answers for all the hard research questions, and thus helping me strive for scientific excellence. I am also grateful to all my thesis committee members for being accommodating and flexible with their schedules, which has allowed me to successfully overcome crunch times that seemed virtually insurmountable.

Throughout my graduate career, all my scientific colleagues have been very helpful, friendly and supportive. Especially, the people in the Essigmann lab have often had a positive impact on my work and life. I would like to thank Nicole for being my very first Essigmann lab mentor, while I was still transitioning to grad school. Her neatness and attention to detail, doubled by a friendly, laid-back attitude have been attributes I have tried to emulate during

Acknowledgements

my own work. I am greatly indebted to John Marquis, who has been an amazing on-site consultant for most of my experiments, until he decided to move on. I have always admired John's patience with my random questions and his subtle wit that made all our conversations immensely enjoyable. I would also like to thank Kaushik for introducing me to the then-called "fatal engineering" project and for making all the experiments look easy. To all the hard-working synthetic chemists, Alfio, Aida, Denise, Uday, Pei-Sze and Eunsuk, I thank you for creating excellent compounds that kept the rest of the lab busy for years. I would like to thank Peter for always providing quick answers to my quick questions. I am very grateful to Shawn for having written a very well-documented thesis, which served as a model for my own. To Jim, I am thankful for always knowing the way to the nearest free food opportunity. To Charles, for being a cool wordsmith. To Lauren and Sarah, the most serious people in the lab, I am thankful for setting a high standard of dedication and work ethics, but also for organizing some excellent trips to Maine. I would like to thank Jeannette for proofreading some of my thesis and for being very supportive especially during my final grad days. I would also like to thank Jenn, Yuri, Francis, Will, Mayuree and Tang for always being very friendly. To Leslie, I am grateful for her help with proofreading and for her kind and friendly career insights and advice. I would like to thank Deyu for his excellent suggestions for my thesis defense talk. To Sreeja, I am grateful for all the help with the comet assays and other complicated protocols. Finally, I would like to thank Kyle for being a great year mate and friend. Our countless discussions about "figuring it out" yielded some of the most helpful ideas for my research. Kyle has also been extremely supportive and helped me through some trying emotional times with a positive outlook and sound advice.

I would like to thank the people from other laboratories that I have collaborated with. Especially, Tom Begley, Rebecca Fry and Rachel Ehrlich from the Samson lab, who have patiently taught me so many things about working with yeast, deserve an important acknowledgment. I would also like to thank Andrea from the Manalis lab, who helped me with the cell size measurements. I am also grateful to Michael Jie and Glenn Paradis for teaching me how to design and run flow cytometry experiments.

In my graduate career, I have been fortunate to have the opportunity to mentor several undergraduate students as they discover the joys and frustrations of experimental science. It has been a pleasure to teach them and it also helped me understand my work better. I would like to thank Angela, Kellie, Jessica, Alvin, Ryan and Daniel for being wonderful UROPs, very eager to learn new things, very dedicated and very receptive to my sometime eccentric ideas. The sheer amount of experimental data gathered throughout my project would not have been possible without your hard work. I have also learned a lot from you and had a great time working together.

I would like to extend a warm thank you to all my friends who have been helpful and supportive all throughout my long grad school journey. The moments we shared at the occasional festive gatherings, on the town or around some intriguing board game have been immensely enjoyable and helped me keep my sanity after endless days of experiments. Many thanks go, in no particular order to: Daniel (Pylot), Stefan, Florin A., Florin C., Mihai B., Mihai & Simona, Theo & Smaranda, Simona T., Daniel N., Iuliu, Ioanid, Viorel and Florin M.

Acknowledgements

I would like to thank the Ashdown housemasters Terry and Ann Orlando, who have done a wonderful job in making me feel at home in the old Ashdown. Their dedication and genuine care has been reflected in the vibrant Ashdown community, which often constituted a welcome oasis of diversion during the trying moments of grad school.

A special thank you goes to all my music teachers and coaches I have had at MIT. Music has always been an integral part of my life and you helped me to continue to nurture it throughout grad school. I would like to thank John Harbison, Randall Hodgkinson, Judith Gordon, Tim McFarland, Marcus Thompson and David Deveau. I would also like to thank all my music colleagues from all the chamber music groups I have been a part of, in particular to : Way, Tracy, Joyce, Katherine, Katie, Sunny, Jodie, Sophie, Lanthe, Boris and Benjamin. Making music together has been a tremendous experience and a necessary respite from the lab grind.

Most importantly, I would like to extend the warmest thank you possible to my wonderful family. Many thanks go to my grandparents, who have always been supportive of me pursuing a scientific career. Sadly, none of them lived long enough to see me get my doctorate. My siblings, Flavia and Sorin and my sister-in-law Antonia, have also been extremely helpful and supportive. They have encouraged me every step of the way and I am very thankful for that. My parents deserve my most heartfelt gratitude; their unyielding love and dedication, their constant faith in my abilities and their unconditional support have made a world of difference to me. None of my accomplishments, including the present thesis would have been possible without their amazing optimism, care and emotional support.

Finally, my most special thank-yous go to the most important person in my life, the adorable Abby Men. Meeting Abby has been a momentous event in my graduate career, because it happened at a time of great emotional distress and seemingly insuperable difficulties in my work. She has been the miraculous catalyst that empowered me to find the ways to overcome the technical difficulties and persevere in my work towards a successful conclusion. I am forever indebted to her for her patience and understanding, for her amazing support and dedication, and for her love. Her efforts for easing my frustrating research toil have been unforgettable; after a long and laborious day of work, she would often surprise me with an exquisitely delicious, home-cooked dinner. I often feel that without her, my graduate school career would have been so much longer. I would never be able to thank her enough for the joy and inspiration she brought into my life, for making me a better, more efficient person and for helping me graduate. Thank you, Abby, with all my heart!

Acknowledgements

Table of Contents

Abstract	5
Acknowledgements	7
Table of Contents	11
List of Abbreviations	14

CHAPTER 1

Introduction.....	17
1.1 Cancer	18
1.2 Chemotherapy	23
1.3 DNA-damaging agents as chemotherapeutics	26
1.4 Developing better chemotherapeutic agents	29
1.4.1 The inspiration – the mechanism of cisplatin in testicular cancer	29
1.4.2 The vision – engineering programmable cytotoxins.....	31
1.4.3 The proof of principle – the phenyl-indole compounds.....	32
1.4.4 E2-7 α – optimizing a compound targeted towards ER.....	33
1.5 11 β -Dichloro – an androgen receptor targeted compound	36
1.5.1 Physico-chemical properties	36
1.5.2 Toxicological properties	37
1.5.3 Investigating the mechanism of toxicity of 11 β -dichloro	40
1.6 Figures.....	42
1.7 References.....	55

CHAPTER 2

Investigating the Mechanism of Toxicity of the Anticancer Agent 11 β -Dichloro in <i>Saccharomyces cerevisiae</i> by Genomic Phenotyping.....	61
2.1 Introduction.....	62
2.2 Materials and Methods.....	67
2.2.1 Reagents	67
2.2.2 Yeast cell lines and culture	67
2.2.3 Survival analysis	67
2.2.4 Library screening approach.....	68
2.2.5 Statistical analysis	69
2.3 Experimental Results	70
2.3.1 Validation of the spectrophotometric quantitation of cell growth	70
2.3.2 Choosing and characterizing the control strains	71
2.3.3 Screening the complete single gene knockout mutant yeast library	72
2.3.4 The GO localization, processes and functions of mutants sensitive to 11 β -dichloro	74
2.3.5 Common mutants between most sensitive mutants to 11 β -dichloro and most sensitive mutants to other DNA alkylating agents.....	76
2.3.6 The GO localization, processes and functions of mutants uniquely sensitive to 11 β -dichloro	77
2.4 Discussion	78
2.5 Tables and Figures	82

2.6	References.....	100
CHAPTER 3		
The Anticancer Agent 11 β -Dichloro Generates Reactive Oxygen Species in HeLa Cells ..		103
3.1	Introduction.....	104
3.2	Materials and Methods.....	109
3.2.1	Reagents.....	109
3.2.2	Cell lines and culture	109
3.2.3	Assays for cell growth, cell viability and cytotoxicity	109
3.2.4	Determination of intracellular ROS using flow cytometry.....	110
3.2.5	Determination of the mitochondrial potential and reduced GSH	111
3.2.6	Determination of H ₂ O ₂ , lipid peroxidation and cellular NADPH.....	111
3.2.7	Statistical analysis.....	112
3.3	Experimental Results	113
3.3.1	11 β -Dichloro exhibits remarkable acute toxicity against HeLa cells <i>in vitro</i> , higher than simpler nitrogen mustards.....	113
3.3.2	11 β -Dichloro exposure is accompanied by generation of ROS.....	114
3.3.3	Antioxidants attenuate 11 β -dichloro toxicity	115
3.3.4	11 β -Dichloro depletes cellular NADPH and the free thiol pool.....	115
3.3.5	Glutathione depletion sensitizes cells to 11 β -dichloro	116
3.3.6	11 β -Dichloro treatment affects inner mitochondrial membrane polarization	116
3.3.7	11 β -Dimethoxy displays cellular responses similar to 11 β -dichloro, but of lower magnitude.....	117
3.4	Discussion.....	119
3.5	Figures.....	128
3.6	References.....	146
CHAPTER 4		
The Anticancer Agent 11 β -Dichloro Induces the Unfolded Protein Response in HeLa Cells		151
4.1	Introduction.....	152
4.2	Materials and Methods.....	157
4.2.1	Reagents.....	157
4.2.2	Cell lines and culture	157
4.2.3	Quantifying changes in cell size	157
4.2.4	Determination of intracellular Ca ⁺⁺ using flow cytometry	158
4.2.5	Determination of transcript levels using RT-PCR.....	158
4.2.6	Determination of relative protein levels using Western blotting	159
4.2.7	Determination of cell viability in the presence of cell death inhibitors.....	160
4.2.8	Determination of acidic cellular compartments using acridine orange staining 161	
4.3	Experimental Results	162
4.3.1	11 β -Dichloro upregulates the expression of genes involved in the UPR response and sterol biosynthesis	162
4.3.2	11 β -Dichloro increases the levels of the SREBP protein	163
4.3.3	11 β -Dichloro causes an increase in cytosolic Ca ⁺⁺	163

Table of Contents

4.3.4	11 β -Dichloro causes an increase in cell size.....	164
4.3.5	11 β -Dichloro induces the proliferation of acidic compartments in the cell..	164
4.4	Discussion.....	166
4.5	Conclusions and Future Directions.....	171
4.6	Tables & Figures.....	180
4.7	References.....	190
APPENDIX A		
	The Complete List of Yeast Mutants Sensitive to 11 β -Dichloro.....	197
A.1	Description.....	198
A.2	References.....	198
A.3	Table.....	199
APPENDIX B		
	Effects of the Medium Components on 11 β -Dichloro Toxicity in <i>Saccharomyces cerevisiae</i>	269
B.1	Introduction.....	270
B.2	Materials & Methods.....	270
B.3	Results and Discussion.....	271
B.3.1	The phenotypes of the control strains	271
B.3.2	The influence of the low ionic strength of the buffer.....	271
B.3.3	The influence of glucose	272
B.3.4	The influence of divalent cations	273
B.4	Figures.....	274
B.5	References	280
	CURRICULUM VITAE	281

List of Abbreviations

4NQO	4-nitro-quinoline oxide
AIF	apoptosis inducing factor
AMS	accelerator mass spectrometry
ANT	adenine nucleotide translocase
AO	acridine orange
AR	androgen receptor
ATP	adenosine triphosphate
BSO	buthionine sulfoximine
CFA	colony forming assay
CMFDA	chloromethylfluorescein diacetate
CM-H ₂ DCFDA	5- (and 6-)-chloromethyl-2',7'-dichlorodihydrofluorescein diacetate
CML	chronic myelogenous leukemia
CTB	cell-titer blue
DHE	dihydroethidine
DHT	dihydrotestosterone
DMSO	dimehtylsulfoxide
DNA	deoxyribonucleic acid
ER	estrogen receptor (chapter 1)
ER	endoplasmic reticulum (chapter 4)
ERK	extracellular-signal regulated kinase
ETC	electron transport chain
GO	gene ontology
GPX	glutathione peroxidase
GR	glutathione reductase
GRID	general repository for interaction datasets
GSH	glutathione
GSSG	glutathione dimer
HMG	high mobility group
HMGCR	3-hydroxy-3-methyl-glutaryl-CoA reductase

List of Abbreviations

HMGCS	3-hydroxy-3-methyl-glutaryl-CoA synthase
HN2	mechlorethamine
HPF	hydroxyphenyl fluorescein
HPV	human pappiloma virus
HRP	horseradish peroxidase
hUBF	human upstream binding factor
IP	intra-peritoneal
JNK	c-jun N-terminal kinase
LBD	ligand binding domain
LDLR	low density lipoprotein receptor
LFC	log2 fold change
MAPK	mitogen activated protein kinase
MDA	malondiadehyde
MEK	MAPK/ERK kinase
MMS	methylmethane sulfonate
MnSOD	manganese superoxide dismutase
MPT	mitochondrial permeability transition
NAC	N-acetyl L-cysteine
NADH	nicotinamide adenine dinucleotide hydride
NADPH	nicotinamide adenine dinucleotide phosphate hydride
NCI	national cancer institute
PARP	polyadenineribonucleotide polymerase
PBS	phosphate buffered saline
PCR	polymerase chain reaction
PDI	protein disulfide isomerase
RNA	ribonucleic acid
ROS	reactive oxygen species
rRNA	ribosomal RNA
SCAP	SREBP cleavage activating protein
SERCA	sarco-endoplasmic reticulum calcium ATPases
SGD	saccharomyces genome database

List of Abbreviations

siRNA	short interfering RNA
SOD	superoxide dismutase
SQLE	squalene epoxidase
SREBP	sterol responsive element-binding protein
TBP	tert-butyl peroxide
TCA	tricarboxylic acid
TH	transhydrogenase
thioTEPA	n,n',n''-triethylenethiophosphoramidate
UPR	unfolded protein response
UV	ultra-violet
WT	wild-type
YPD	yeast-extract/peptone/dextrose
zVADfmk	carbobenzoxy-valyl-alanyl-aspartyl-[o-methyl]- fluoromethylketone

CHAPTER 1

Introduction

1.1 Cancer

In many ways, cancer has become the plague of our times. Predicted to become by 2010 the most common death cause in the world (Boyle and Levin, 2008), cancer undoubtedly represents a formidable scientific challenge. Although significant advancements have been made in detection technologies and available therapies, we are still far from effective treatments and cures for most malignancies, especially for advanced stage cancers. However, as our knowledge about the causes and biochemical mechanisms of cancer expands, we are approaching the critical mass of data necessary to map a path towards novel, paradigm-shifting treatments for cancers that are currently incurable.

Cancer constitutes a significant public health problem, accounting currently for about 25% of the total number of deaths in the US (Jemal et al., 2008), and for about 13% of the total number of deaths worldwide (Boyle et al., 2008). The incidence of cancer in the Western world is staggering; it is estimated that one in two men and one in three women will develop a form of invasive cancer throughout their lifetime (Ries et al., 2009). Moreover, the incidence of cancer is growing annually by about 1% worldwide. This growth is predicted by some estimates to establish cancer as the leading cause of death worldwide as soon as 2010 (Boyle et al., 2008). In fact, in the US population aged 85 years or less, the death rate from cancer has already surpassed the death rate from cardiovascular diseases (Jemal et al., 2008).

Cancer can affect people irrespective of their gender, race, locale's climate, micro-environment, or income, but it shows a strong dependence on age. On average, the lowest incidence of cancer occurs between the ages 20 to 40 years; the incidence increases about 10-fold for the ages 40 to 60 years and then another 2- to 3-fold for the ages 60 to 80 years. The cancer incidence then drops for people aged 80 years or more. Interestingly, children and teenagers (aged less than 20 years) have also an elevated risk of developing certain kinds of cancer (Jemal et al., 2008).

Cancer is not a singular disease. The term “cancer” usually refers to a set of over 100 distinct malignancies caused by an aberrant and excessive cell growth (Stratton et al., 2009). Cancers can occur in virtually every organ of the human body and in every type of tissue, and are usually classified by the location in which the primary tumor – the initial malignant outgrowth, occurs. However, additional complexity is imparted by the extensive diversity at the cellular and molecular level; cancers occurring in the same kind of tissue may have very different genetic compositions and phenotypic manifestations, and thus exhibit variable and often unpredictable responses to treatments.

In 2008, in the US, the estimated top five most prevalent cancers have been cancers of prostate, lung, colon/rectum, urinary bladder and non-Hodgkin lymphoma for men, and cancers of breast, lung, colon/rectum, uterus and non-Hodgkin lymphoma for women (Figure 1.1). The most deadly cancers have been predicted to be the lung, prostate, colon/rectum, pancreas and liver cancers for men, and lung, breast, colon/rectum cancer, pancreas and ovarian cancers for women (Figure 1.1).

A great body of work, which started in the 1980s, has firmly established that the molecular basis for cancer is an accumulation of mutations in the cellular DNA (Hanahan and Weinberg, 2000). These genetic changes range from point mutations to large scale chromosomal rearrangements, duplications and deletions. Often, changes also occur in the number and organization of the chromosomes, generating aneuploidy (Hede, 2005). Such genomic transformations alter the function of a number of genes involved in cell proliferation — either activating genes that promote growth (oncogenes), or inactivating genes that suppress growth (tumor suppressor genes). Several such specific mutations are usually required for the cell to become cancerous, acquiring the six fundamental traits common to most malignancies (Hanahan et al., 2000) : unlimited replicative potential (immortality), self-sufficiency in growth stimuli, resistance to growth-inhibitory stimuli, avoidance of apoptosis, ability to trigger angiogenesis (blood vessel growth) and finally, invasiveness - the ability to metastasize (spread) to other parts of the body and generate secondary tumors. These traits are not acquired all at once, but rather one at a time through selective pressures in the micro-

environment of each cell. Once a cell in a tissue gains an ability to proliferate slightly faster than its neighbors, it will generate several generations of cells with similarly enhanced growth abilities. Most of these cells will not lead to disease, being controlled by the inhibitory signal of their environment or the immune system. However, if one of these mutated cells acquires a second advantageous mutation, it proliferates even more. This cycle of mutation and selection goes on until cells acquire most of the cancer hallmarks; at that point, the growth of those cells becomes malignant. Unfortunately, cancer cells in the patient's body continue to evolve, becoming more invasive, faster growing and more resistant to therapies. They metastasize and generate secondary tumors throughout the body, affecting the function of various organs. The loss of function in multiple systems due to secondary tumors is the cause of death in 90% of cancers (Sporn, 1997). This is why the earlier the cancer is detected, the higher the chance an effective therapy has for preventing the cancer from advancing to its deadly metastatic stage.

Understanding the molecular mechanisms responsible for the accumulation of the mutations that lead to cancer is essential for evaluating risk factors, designing better diagnostics and better treatments. In all living cells, there is a background mutation rate due to errors made by polymerases when DNA is replicated. Taking into account all the proofreading and repair mechanisms in the cell, mutation rates have been estimated to be between one in 10^9 replicated base pairs for somatic cells (Albertini et al., 1990) and one in 10^{11} replicated base pairs for stem cells (Cervantes et al., 2002). This rate translates into about one mutation for every somatic cell division and about one mutation for every four stem cell divisions. In addition to polymerase errors, environmental exposure to genotoxic agents can contribute to an even greater mutagenic load. Despite this barrage, most mutations that accumulate over a lifetime in our genomes will not lead to cancer. These benign mutations have been termed "passenger mutations." However, an occasional mutation that can contribute to cancer will occur – these are termed "driver mutations" (Greenman et al., 2007; Haber and Settleman, 2007). In general, the background and environmental rates of mutation are relatively low; therefore, it is unlikely that a cell will accumulate the necessary driver mutations leading to cancer within a human lifetime (Loeb et al., 2008). To explain the epidemiological data on cancer incidence, it has been proposed that on their way to becoming cancerous, cells must

acquire a mutator phenotype, a mutation that increases dramatically the background mutation rate and hence will favor the accumulation of the subsequent mutations leading to full malignancy (Loeb et al., 2008). It has been mathematically proven that the mutator phenotype hypothesis can satisfactorily explain the incidence of certain cancers (Beckman and Loeb, 2006). Additionally, a large number of clinical cancers exhibit a mutator phenotype, which can be detected experimentally and used for diagnostic purposes. Unfortunately, a mutator phenotype usually indicates a poor prognosis (Bielas et al., 2006; Loeb et al., 2008).

Genetic predispositions can significantly affect the probability of developing cancer. In light of the considerations above, inherited mutations in oncogenes or tumor suppressor genes shorten the time, sometimes dramatically, required for carcinogenesis, because fewer mutations are needed for cells to become cancerous (Pollard and Ratcliffe, 2009). Additionally, mechanisms by which inherited mutations predispose the cells harboring them for acquiring dramatic mutator phenotypes and aneuploidy have also been documented (Hede, 2005). Recent efforts have focused on completely mapping many different cancers at genomic levels to understand better the genetic differences between cancerous and normal cells. More than 350 driver genes have been identified; interestingly 10% of these genes are already known to be associated with hereditary risk for cancer (Stratton et al., 2009). Among the genes most commonly mutated in cancers are the tumor suppressor gene TP53 (mutated in more than 50% of cancers) and the oncogene K-RAS (mutated in 20-30% of cancers). However, most mutated genes tend to be cancer specific; for example gliomas almost always have a mutation in K-RAS or another gene in the K-RAS pathway (Parsons et al., 2008), whereas many breast cancers show mutations in genes like BRCA1, BRCA2 and ERBB2, but very few show mutations in K-RAS (Bos, 1989).

There are numerous environmental risk factors that have been associated with increased incidence of cancer. These factors include smoking and tobacco use, exposure to sun light without UV protection, exposure to radiation (both cosmic and radioactive materials), obesity and high fat diet, exposure to chemical carcinogens and mutagens and various pathogenic microorganisms (including bacteria and viruses). Sometimes, the exposure to certain

environmental factors increases the incidence of a specific cancer, suggesting an underlying causative relationship. For example, exposure to cigarette smoke has been associated with lung cancer; exposure to naturally occurring aflatoxin has been associated with liver cancer; exposure to high amount of UV light has been associated with skin cancer; and human papilloma virus (HPV) infection has been associated with cervical cancer. Some environmental agents have been shown to be mutagens – they can directly induce mutations in cellular DNA. Other agents, although not mutagenic, can still cause cancer by stimulating proliferation, hyperplasia or by causing chronic inflammation. Most of the time, it is the combination of these actions over a long period of time that leads to an increased risk of cancer.

Modern therapies for cancer are aimed at improving survival of the patient and managing the disease, given that in many cases, there is no cure. If the primary tumor is accessible, surgery is performed to remove the malignant tissue. This is, however, not an option for all hematological cancers, such as leukemias and lymphomas. Given the risk of metastasis, even in the early stages of cancer, oncologists then prescribe courses of systemic treatments aimed at killing metastases and preventing the recurrence of the disease. Such treatments include radiation therapy, hormonal therapy, immunotherapy and chemotherapy, the best results usually being achieved by these approaches given in combination.

Significant progress has been made in last 30 years in improving the relative five year survival expectancy for all cancers, which has increased from 50% between 1975-1977 to about 66% between 1996-2003 (American Cancer Society, 2008). However, these numbers not only reflect the advancements in therapies, but also reflect better, earlier diagnoses and lifestyle changes in the US population (e.g., a reduction in smoking). The sobering reality is that for advanced cancers, the current available therapies prolong life, on average, only a few months more than the prevailing therapies did 30 years ago (American Cancer Society, 2008). Such statistics strongly underline the need for more research and development of better, more effective therapies. The work presented here, aimed at investigating the mechanism of a novel synthetic agent with chemotherapeutic potential, is a small step towards fulfilling this need.

1.2 Chemotherapy

Chemotherapy – the use of chemical toxicants to kill cancer cells – is sometimes used alone, but in most cases it accompanies or follows other cancer treatment methods such as surgery, radiation therapy or hormonal therapy. Oncologists routinely prescribe chemotherapeutic regimens following surgery in an effort to eradicate local and distant micrometastases and to prevent the relapse. Due to its systemic nature, chemotherapy is among the very few treatment choices for advanced, metastatic cancers.

All traditional chemotherapeutic agents act by preventing proliferating cells to divide further, thereby inducing cell arrest, necrosis or apoptosis (Perry, 2001). Often, these compounds are termed *cytotoxic*, reflecting on their ability to kill cells. Most cancer cells are actively proliferating and thus, they would be preferentially targeted. However, other tissues in the human body, such as the bone marrow, the digestive tract epithelial lining and the hair follicles, have a high normal turnover rate; these cells will also be collaterally affected by chemotherapeutics. The toxicity to these normal tissues is responsible for the most common side-effects of chemotherapy: myelosuppression (decrease in white blood cells), mucositis (inflammation of the digestive tract lining leading to nausea and loss of appetite) and alopecia (hair loss).

The most common target of chemotherapeutics is DNA and its associated processes. By interfering with the normal function of DNA, anti-neoplastic agents can slow down cell growth and trigger apoptosis (Hurley, 2002). As a function of their mechanism of toxicity, chemotherapeutic agents can be divided in several classes (Perry, 2001):

- Chromosomal apparatus inhibitors: agents that interfere with the chromosomal microtubules assembly and disassembly during replication (e.g., paclitaxel, vincristine)
- DNA antimetabolites: agents that interfere with the metabolic pathway required for the synthesis of new DNA. The common enzymes inhibited are folate synthase

- (e.g., methotrexate, aminopterin), thymidylate synthase (e.g., 5-fluoro uracil, floxuridine), ribonucleotide reductase (e.g., gemcitabine, fludarabine)
- DNA polymerase inhibitors: agents that block the activity of DNA polymerases inhibiting DNA replication (e.g., cytarabine)
 - DNA topoisomerase inhibitors: agents that interfere with the unwinding activity of the topoisomerases, thus blocking DNA replication and inducing single-strand and double-strand breaks in DNA (e.g., camptothecin, etoposide)
 - DNA intercalating agents: agents that block DNA and RNA polymerases by intercalating between the bases (e.g., doxorubicin, mitoxantrone). Doxorubicin is also a potent topoisomerase II inhibitor.
 - DNA alkylating agents: agents that form covalent modifications (adducts) on the bases in DNA (e.g., mechlorethamine, chlorambucil, cisplatin, carmustine, busulfan, thioTEPA, dacarbazine, mitomycin C)

Other classes of chemotherapeutics have been targeted at features of cancer cells other than DNA. One common strategy is to inhibit the growth signals received by cancer cells and slow down their growth. It has been observed that a large number of breast and prostate cancers depend, at least initially, on growth signals received from steroid hormones. About 50% of breast cancers overexpress the estrogen receptor (ER) and depend on it for growth (Fernö et al., 1990); therefore, anti-estrogens (aromatase inhibitors such as anastrozole, testolactone) and ER antagonists (tamoxifen) are successfully used as anticancer agents. In prostate cancer, the expression of the androgen receptor (AR) makes cells susceptible to anti-androgens (flutamide, bicalutamide). Unfortunately, although very effective initially, the signaling antagonists eventually fail when the cancers progress to a hormone refractory state.

Other strategies include targeting features that cancer cells acquire during their transformation and that are not found in normal cells. A classic example is the major translocation that occurs between the chromosomes 9 and 22 in chronic myelogenous leukemia (CML) and in other leukemias. The newly formed chromosome 22, named “Philadelphia chromosome,” now contains a chimeric oncogene (BCR-Abl), formed by the fusion of the BCR gene from chromosome 22 and the gene for the tyrosine kinase Abl from

chromosome 9. The BCR-Abl kinase is constitutively active and plays an important role in driving carcinogenesis. Therefore, the BCR-Abl kinase constitutes an excellent target for chemotherapy. Antibody-based inhibitors against the BCR-Abl proteins (imatinib, market name Gleevec) have been notably successful in preventing the growth of cancer cells that express the chimeric oncoproteins. In clinical treatments, Gleevec has been shown to be more effective than previous chemotherapeutic regimens (O'Brien et al., 2003).

Another cancer-specific protein successfully identified and targeted with antibodies is ErbB2 (Her2), a pro-mitotic membrane tyrosine kinase amplified in about 15-30% of breast cancers, which was associated with reduced survival of breast cancer patients (Lohrisch and Piccart, 2001). Her2 overexpression was correlated with resistance to chemotherapy and hormonal therapy, and thus poor prognosis (Bange et al., 2001). Trastuzumab (Herceptin), the antibody against Her2, proved to be very effective at reducing the number of Her2 proteins on the cell surface, inhibiting cell growth and attracting an immune system response that killed the cancer cells (Sliwkowski et al., 1999). In combination with other chemotherapeutics, Herceptin regimens have been shown to improve median survival time of breast cancer patients by 25% compared with chemotherapy alone (Baselga, 2001).

The sad reality is that cancer cells also acquire resistance in almost all of the antibody based therapies, a phenomenon due to the large heterogeneity of the cells in a tumor (Jabbour et al., 2009; Bedard et al., 2009). For this reason, even the very specific chemotherapeutics are given in combination with broader spectrum, classical antineoplastic agents, in hopes of overcoming the development of therapy-refractory tumors. Unfortunately, in many cases, resistance to chemotherapy cannot be overcome, highlighting the dire need for development of better, more potent and more specific chemotherapeutics.

1.3 DNA-damaging agents as chemotherapeutics

Among all chemotherapeutic agents, the DNA damaging agents have been in clinical use for the longest time. They also prove to be among the most versatile agents, being included in regimens for almost all types of cancers (Perry, 2001). Their versatility comes from the fact that although all alkylating drugs damage DNA, each agent has a slightly different reactivity and specificity.

Among the DNA-damaging chemotherapeutics, nitrogen mustards constitute an important class. All nitrogen mustards are structurally derived from the parent compound, mechlorethamine (HN2, Figure 1.2), an agent initially designed for chemical warfare. The presence of the electron pair on the nitrogen greatly increases the reactivity of the chloroethyl arms; an elimination-addition mechanism with the formation of an aziridine cation intermediary is believed to be the mechanistic explanation for the remarkable reactivity of HN2 (Colvin et al., 1976). The chemotherapeutic use of HN2 was suggested in 1943 when it was observed that an accidental exposure to HN2 causes significant loss of white blood cells (Rappeneau et al., 2000). Although still in use today for certain aggressive leukemias, HN2 is an extremely toxic agent, causing massive non-specific damage to healthy tissues. Being a potent mutagen, HN2 can also induce secondary cancers (Povirk and Shuker, 1994).

A large number of nitrogen mustard derivatives have been synthesized in the last 30 years. The chemical modifications were aimed at tempering the high reactivity of HN2 and at introducing specificity. The nitrogen mustards commonly used in clinical treatments maintain the two chloroethyl arms, but lower the nitrogen electron density by linking it to either a phenyl ring or to a more electropositive phosphorus (Figure 1.2). Although the reactive portion of each molecule (the warhead) is the same, the substituents on the mustard determine the reactivity, solubility and other biochemical properties, which then influence the toxicity and specificity of the agent.

Most cells are able to repair efficiently simple DNA alkylation damage; this is why nitrogen mustards are designed to be bifunctional, with one molecule of the drug alkylating the DNA

twice. The resulting lesions, called crosslinks (intrastrand or interstrand) are considerably more toxic than simple alkylation damage and are quite hard to repair efficiently and correctly (McHugh et al., 2001). Most mechanisms of repair involve multiple pathways such as nucleotide excision repair, homologous recombination and translesion repair. Given the complex mechanism required, the repair of crosslinks is likely to generate mutations and chromosomal aberrations (Dronkert and Kanaar, 2001). It is believed that the clinical efficacy of a nitrogen mustard is closely related to its ability to form DNA crosslinks.

Nevertheless, most normal cells with intact repair pathways can eventually repair crosslinks and thus tolerate crosslinking agents at reasonably low doses (Nojima et al., 2005). This observation suggests that nitrogen mustards would be most effective against cancer cells that lack (or have lost due to mutations) certain DNA repair abilities. It is believed that particular cancer cells exhibiting mutator phenotypes, have lost their ability to repair DNA faithfully and, hence, they are susceptible to toxicity induced by DNA-damage. Indeed, cells with impaired repair capabilities are orders of magnitude more sensitive to crosslinking agents (McHugh et al., 2001; Nojima et al., 2005; Trimmer and Essigmann, 1999).

Certain cancers develop resistance to DNA alkylating agents, either by upregulating efflux pumps that lower the effective intracellular drug concentration (Sharom, 2008), by upregulating enzymes that can directly inactivate the reactive portion of the molecules (e.g., glutathione S-transferases) (O'Connor, 2007), or by a combination of the two mechanisms (Meijerman et al., 2008). Some malignancies, such as lung and prostate cancers, are inherently resistant to alkylating agents because of their relatively slow growth and resistance to apoptosis. The long doubling times of these cancer cells allows more time for DNA repair, while the resistance to apoptosis prevents cell death in the wake of extended DNA damage. Hence, the effectiveness of DNA damaging agents in slow growing lung and prostate cancers is very limited.

The ability to form crosslinks is only part of the asset pool of an effective DNA alkylating drug. In the case of cisplatin (*cis*-diamminedichloroplatinum(II), (Figure 1.3 A), one of the most successful DNA-alkylating chemotherapeutics, the mechanism of toxicity has been

postulated to include interactions with tumor specific proteins in addition to crosslink formation (Kartalou and Essigmann, 2001). The example of cisplatin underlines the significance of multifunctional compounds, and given the limitations of current DNA-alkylating drugs, it should inspire the development of new generations of multifunctional, more effective chemotherapeutics.

1.4 Developing better chemotherapeutic agents

1.4.1 The inspiration – the mechanism of cisplatin in testicular cancer

Cisplatin and its analog carboplatin (Figure 1.3 A) are chemotherapeutic agents most effective in the treatment of metastatic testicular cancer. These drugs are also used in various combinations to treat ovarian, head, neck, cervical, colon, lung, bladder and other cancers (Zamble and Lippard, 1995). In fact, the efficacy of cisplatin against testicular cancer is unprecedented; regimens including cisplatin achieve a cure rate of over 95% (Masters and Köberle, 2003; Ries et al., 2009), making cisplatin one of the most successful stories in chemotherapy.

It has been established that the cytotoxic properties of cisplatin are due to its ability to modify DNA covalently (Kartalou et al., 2001). Inside the cells, the two chloride ions are replaced with water molecules yielding a cationic aquated complex that is even more reactive towards DNA than the parental dichloro species, preferentially forming adducts at the N7 positions of guanine and N3 position of adenine (Bancroft et al., 1990). *In vitro* studies have shown that most of the adducts formed by cisplatin are in fact crosslinks: 65 % are 1,2-d(GpG) intrastrand crosslinks, 25% are 1,2-d(ApG) intrastrand crosslinks and 5-10% are 1,3-d(GpG) intrastrand crosslinks. Only a minor fraction of adducts are interstrand crosslinks or monoadducts (Kartalou et al., 2001). A similar adduct profile is also observed *in vivo*, in cells isolated from cancer patients treated with cisplatin (Fichtinger-Schepman et al., 1987).

The ability of cisplatin to form a variety of DNA crosslinks is insufficient to explain its potent antitumor activity. The trans isomer (transplatin, *trans*-diamminedichloroplatinum(II)) (Figure 1.3 B) also forms a large number of DNA crosslinks, yet it is therapeutically ineffective. It was shown that due to its geometry, the trans isomer forms a different pattern of crosslinks, mostly 1,3-d(GpC) intrastrand crosslinks and, unlike cisplatin, a great number of G-C interstrand crosslinks (Leng and Brabec, 1994). This result suggested that the cisplatin adducts were more than just crosslinks, but also substrates for some ulterior biochemical interactions that, potentially, interfered with the repair process. Indeed, the major adducts of cisplatin, 1,2-d(GpG) and 1,2-d(ApG), force the DNA into unusual

conformations. According to the crystal structures, the DNA helix is bent towards the major groove by 50° or more and also unwound by about 20° (Takahara et al., 1995; Fouchet et al., 1997; Gelasco and Lippard, 1998). Such structures have been shown to have high affinity for a class of proteins containing the high-mobility group (HMG) domain - a DNA binding motif found in various non-histone components of chromatin. The HMG-domain proteins bind tightly to the DNA structures generated by the 1,2 crosslinks of cisplatin, but do not bind to the DNA structures generated by the 1,3 crosslinks, suggesting that these proteins might play a role in the mechanism of cisplatin toxicity. This observation could also explain why transplatin does not display the same effectiveness (Pil and Lippard, 1992). The presence of HMG-domain proteins is thought to prevent the repair proteins from accessing the DNA crosslink, hence significantly extending the lifetime of the DNA adduct and its cytotoxic effect (Zamble et al., 1995). This mechanism has been labeled “repair shielding” (Figure 1.4 A).

Some of the HMG proteins have been shown to bind extremely tightly to the cisplatin adducts. An important example is the human upstream binding factor (hUBF), a transcription factor involved in regulating transcription of ribosomal RNA (rRNA), which binds the 1,2 adducts of cisplatin with an affinity ($K_d = 60 \text{ pM}$) very close to the affinity for its natural response element in the rRNA promoter ($K_d = 18 \text{ pM}$). This high affinity suggests that increasing levels of cisplatin adducts will have a significant impact on the availability of hUBF, effectively titrating hUBF away from its natural binding site (Treiber et al., 1994). Disrupting the natural function of transcription factors such as hUBF may also be a mechanistic explanation for the toxicity of cisplatin. This mechanism has been labeled “transcription factor hijacking” (Figure 1.4 B).

A significant body of experimental work has demonstrated that both repair shielding and transcription factor hijacking are possible players in the high effectiveness of cisplatin against testicular cancer cells. *In vitro* assays showed that the repair of cisplatin adducts is significantly inhibited in the presence of HMG domain proteins, such as HMG1, tsHMG and SRY (Huang et al., 1994; Zamble et al., 2002; Trimmer et al., 1998). Notably, the tsHMG and SRY proteins are commonly overexpressed in testicular cancers. Additionally, sensitivity

to cisplatin can be modulated *in vivo* by the levels of HMG-domain proteins. It was shown that mammalian cells overexpressing HMG1 proteins are more sensitive to cisplatin, whereas cells knocked-out for IXR1, an HMG-domain gene, are 2-5 fold more resistant to cisplatin (McA'Nulty et al., 1996). Furthermore, the ability of cisplatin adducts to compete with hUBF has been shown in rRNA transcription assays, both *in vitro* (Zhai et al., 1998) and *in vivo* (Jordan and Carmo-Fonseca, 1998). Therefore, even though the complete mechanism of cisplatin in testicular cancer is thought to be even more complicated, involving the interplay of other cellular pathways (Cepeda et al., 2007), the repair shielding and transcription factor hijacking mechanisms are likely to be important contributors.

1.4.2 The vision – engineering programmable cytotoxins

Inspired by the mechanisms of cisplatin highlighted above, in the late 1990s, the Essigmann lab envisioned a design strategy for programmable cytotoxins: bifunctional agents comprised of a constant DNA alkylating moiety (a warhead) and a variable protein interacting moiety (ligand) that can be tailored to recognize cancer specific proteins (Essigmann et al., 2001). These compounds would alkylate DNA non-specifically, and in normal cells, these adducts would be readily repaired. However, in cancer cells expressing significant amounts of the target protein, the repair of the adducts would be impeded by the binding of the cancer specific protein to the molecule adducted to DNA. Furthermore, just like the cisplatin adducts, the DNA adducts of the proposed compounds would compete with the natural ligand for the target protein, diverting it from its normal cellular function and leading to additional cytotoxicity.

The choice for the DNA alkylating moiety was an aniline mustard, derived from chlorambucil. The reasoning behind this choice was the moderate toxicity of chlorambucil, the ease of incorporation into a synthetic scheme and bioavailability considerations (Rink et al., 1996). Another warhead derived from cisplatin was also considered; however, incorporation of a platinum cation into a large organic molecule might impede the molecule's ability to cross the cellular membrane. Nevertheless, a compound with a cisplatin derived

warhead was eventually synthesized and shown to have properties consistent with the mechanism proposed (Kim et al., 2009).

For a protein interacting moiety, a ligand for the estrogen receptor (ER) was initially chosen. It has been known for decades that a significant number of breast and ovarian cancers express high levels of the ER (Fernö et al., 1990). Being a transcription factor, the ER localizes in the nucleus, where it would have increased chances of interacting with DNA adducts formed by the compound and would shield them from being readily repaired. Additionally, given that each adduct represents a potential decoy binding site for the ER, the normal function of the steroid receptor will also be affected. Since receptor antagonism is a well established chemotherapeutic modality, an agent displaying an ER ligand could also squelch ER driven transcription in ER positive tumor cells, as well as block repair (Rink et al., 1996; Essigmann et al., 2001).

1.4.3 The proof of principle – the phenyl-indole compounds

The first compound synthesized featured the 2-(4'-hydroxyphenyl)-3-methyl-5-hydroxy-indole (2PI) moiety as a ligand for ER and the chlorambucil-derived 4-(3-aminopropyl)-N,N-(2-chloroethyl)-aniline warhead, linked together by a 15 atom long alkyl chain functionalized with a secondary amine and a carbamate (Figure 1.5 A)(Rink et al., 1996). For control purposes, another compound was synthesized using the 2-(4'-hydroxyphenyl)-3-methyl-indole moiety as the ligand. The subtle difference between the two ligands (one hydroxyl group) was introduced to drastically lower the affinity for the ER in the control compound. The lead compound was called 2PI-C6NC2 and the control compound was 2PI(OH)-C6NC2.

The linker design emerged from careful experimentation that balanced three distinct requirements: 1) the linker should allow binding to the ER; 2) the linker should not introduce unnecessary hydrophobicity in the molecule, while also being synthetically accessible; 3) the linker should be stable when exposed to intracellular enzymes. The first requirement dictated the length of the hydrophobic chain attached to the ligand, while the third requirement dictated the use of the carbamate and the amine functional groups. The secondary amine also

addressed the second requirement, because it was expected to be positively charged at physiological pH and thus assist with the solubility and the affinity of the molecule for a negatively charged DNA backbone. Systematic variation of the length of each segment of the linker yielded the C6NC2 structure as optimal for ER binding (Figure 1.6).

The 2PI-C6NC2 compound was shown to have a significant binding affinity towards the ER (7.1 relative binding affinity (RBA) compared to ER's natural ligand β -estradiol). Additionally, 2PI-C6NC2 could alkylate DNA *in vitro* generating piperidine-labile N7 guanine adducts. Furthermore, a DNA oligonucleotide modified with 2PI-C6NC2 retained a modest affinity towards the ER (RBA = 0.5) (Rink et al., 1996). The *in vivo* results proved very encouraging. The toxicity of 2PI-C6NC2 was determined in two breast cancer cell lines: MCF-7 which is ER positive, and MDA-MB-231, which is ER negative. These cell lines allowed us to test whether the presence of ER contributed to differential toxicity. Indeed, the MCF-7 cells were more sensitive to 2PI-C6NC2 than MDA-MB-231; as expected, the cell lines were equally sensitive to agents that do not interact with the ER, such as chlorambucil, and the control compound 2PI(OH)-C6NC2, which has an ER affinity 70-fold less than the lead compound (Rink et al., 1996). This result strongly implicated the ER as a modulating factor in the toxicity of 2PI-C6NC2.

1.4.4 E2-7 α – optimizing a compound targeted towards ER

Encouraged by the proof of principle highlighted by the 2PI-C6NC2 compound, a second generation of ER interacting compounds was designed, in which attempts were made to improve each aspect of the molecule: the ER affinity, the linker properties and the warhead.

To optimize the binding towards ER, a new compound was designed using β -estradiol as the ligand portion, while keeping the rest of the molecule identical to the first generation 2PI-C6NC2 compound. The linker was attached at the 7 α position of the steroid ring, in accordance with the published studies of β -estradiol derivatives that maintain a high affinity for ER when substituted at the 7 α position (Bowler et al., 1989; DaSilva and van Lier, 1990). Due to the new ligand, identical to the natural ER ligand, the new compound (named E2-7 α ,

Figure 1.5 B) showed a significantly improved ER affinity (RBA = 30 to 45 compared to β -estradiol) (Mitra et al., 2002); as mentioned before, the 2PI-C6NC2 has an RBA of 7.1 (Rink et al., 1996). It was also shown that E2-7 α alkylates a DNA oligo *in vitro*, forming a significant number of piperidine-labile adducts. These adducts could also bind the ER ligand binding domain (LBD), as demonstrated by a gel-shift assay; β -estradiol could compete away the shifts. Using the same two cell lines as before, it was shown that E2-7 α toxicity is noticeably enhanced by the presence of the ER, the ER positive MCF-7 cells being significantly more sensitive than the ER negative MDA-MD-231 cells (Mitra et al., 2002).

To optimize the linker properties, a series of compounds were synthesized that explored the type and number of functional groups present in the linker, while keeping constant the six carbon alkyl chain connecting to the estradiol moiety and the chlorambucil derived warhead (Sharma et al., 2004). The compounds made featured the following functional groups in the linker: one secondary amine group, two secondary amine groups, one amide group, two amide groups, one guanidine, one carbamate and one secondary amine and one guanidine (Figure 1.7). For comparison, E2-7 α compound, also included in Figure 1.7, features one secondary amine and one carbamate in its linker. The lengths of the linkers counted from the estradiol ring to the aniline ring varied between 11 and 16 atoms total. All of these compounds were tested for their affinity to the ER, DNA reactivity and cytotoxicity in cell lines. Far from being intuitive, the results highlighted the subtle interplay between all parts of the molecule and the crucial importance of the linker. The presence of one or two secondary amine groups in the linker positively correlated with the compound's solubility, ability to react with DNA and toxicity (Sharma et al., 2004). While all compounds had good affinities for the ER (RBA between 9 and 46), the linker flexibility seemed to influence the ER binding the most. The more rigid linkers (such as those with the single amide, the carbamate alone and the guanidine alone) are likely limiting the number of conformations available for the linker, which limits the interactions of the molecule with the surface of the ER and thus might negatively affect binding (Sharma et al., 2004). The original compound (E2-7 α) was found to have the best ER affinity (RBA = 45, in this assay), but the monoamine linker compound was almost as good (RBA = 44). In terms of toxicity, only E2-7 α , the monoamine and diamine linker compounds showed significantly higher toxicity than chlorambucil. These

three compounds also showed *in vivo* selective toxicity for the ER positive cell line MCF-7 versus the MDA-MB231 ER negative cell line, with E2-7 α being slightly more selective than the amine compounds. The investigation concluded that the parent compound had a linker that allowed the best compromise between ER affinity, DNA reactivity, and selective toxicity (Sharma et al., 2004).

Finally, a different warhead was explored in combination with the estradiol ligand and the linker featuring an amine and a carbamate (Kim et al., 2009). The new warhead was derived from *cis*-dichloroethylenediammineplatinum(II), by substitution on the carbon chain of the ethylenediammine (Figure 1.5 C). The resulting compound, [6-(2-amino-ethylamino)-hexyl]-carbamic acid 2-[6-(7 α -estra-1,3,5,(10)-triene)-hexylamino]-ethyl ester platinum(II) dichloride ((Est-en)PtCl₂) (Figure 1.5 C) had all the intended properties: it had good affinity for the ER, reacted with DNA, and was selectively toxic against ER positive cell lines. The ER affinity was measured to have an RBA of 28, which is somewhat less than the ER affinity of E2-7 α . In terms of toxicity, the platinum compound was less toxic when compared with E2-7 α ; however, it had good selective toxicity for the ER positive cell lines, including the ER positive CAOV3 ovarian cancer cell line (Kim et al., 2009).

Taken together, all the optimization experiments confirmed E2-7 α as the lead candidate in the class of ER targeted compounds, and highlighted the great flexibility of the programmable cytotoxins design approach. The ER dependent mechanism of E2-7 α is currently being investigated in several breast and ovarian cancer cell lines, in an effort to advance the compound in preclinical and eventually clinical trials (Gopal, 2009).

1.5 11 β -Dichloro – an androgen receptor targeted compound

1.5.1 Physico-chemical properties

Given the success of the ER targeted compounds, a new class of compounds was proposed that would take advantage of another nuclear steroid receptor that is overexpressed in certain cancers: the androgen receptor (AR). The AR was shown to be highly expressed in many prostate cancers (Marcelli and Cunningham, 1999). Given the high incidence of prostate cancer – highest incidence and second highest rate of mortality in men (Jemal et al., 2008) (Figure 1.1) – the design of an effective agent targeting prostate cancer constitutes an important scientific challenge. The programmable cytotoxin paradigm seemed like a promising way to address this challenge.

The choice for an AR ligand was 17 β -hydroxy-estra Δ 4(5), 9(10)-3-one, a moiety inspired from the synthetic steroid RU-486, which possesses a significant affinity for the AR (Fuhrmann et al., 2000). Studies on RU-486 and related compounds indicated that the 11 β position on the sterol ring system would be the least disruptive to AR binding, and thus, it was chosen as the place of attachment for the linker. Given that the ligand binding domain of AR has a high similarity to the ER ligand binding domain, the same linker found in the E2-7 α molecule was chosen, hoping that the properties of the C6NC2 linker that allowed ER binding would also favor the AR binding. The complete compound (called 11 β -dichloro¹, Figure 1.8 A) closely resembled E2-7 α , except for the different steroid moiety and the attachment point on the steroid (Marquis et al., 2005). Furthermore, two related compounds were synthesized to test the contribution of DNA damage to the overall mechanism. One of the compounds, called 11 β -dimethoxy (Figure 1.8 B) was identical to 11 β -dichloro, except the chlorines on the chloroethyl arms of the mustard have been replaced by methoxy groups. Given that the methoxy group is a very poor leaving group, the reactivity of the mustard is

¹ IUPAC name: 2-(6-((8S,11S,13S,14S,17S)-17-hydroxy-13-methyl-3-oxo-2,3,6,7,8,11,12,13,14,15,16,17 dodecahydro-1H-cyclopenta[a]phenanthren-11-yl)hexylamino)ethyl 3-(4-(bis(2-chloroethyl)amino)phenyl)propylcarbamate

essentially abolished and thus, the resulting molecule cannot alkylate DNA. The other related compound synthesized, called 11 β -monochloro (Figure 1.8 C) had only one chlorine atom replaced with a methoxy group. 11 β -monochloro can still form DNA mono-adducts, yet it is unable to form DNA crosslinks. A comparison between 11 β -dichloro and 11 β -monochloro could indicate the importance of crosslinks in the mechanism of toxicity.

The affinity for the AR was benchmarked against R1881, a synthetic androgen with one of the highest affinities for AR of all known ligands. Both 11 β -dichloro and 11 β -dimethoxy show good affinity for the AR (RBA = 11.3 and 18.3, respectively) when compared with the R1881 (Marquis et al., 2005). However, when compared with dihydrotestosterone (DHT), the best natural AR ligand, the RBA values would be 2- to 3-fold higher, because the synthetic androgen R1881 has 2- to 3- times higher affinity for the AR than DHT (Zhao et al., 1999).

In vitro, 11 β -dichloro displayed a good reactivity towards DNA oligonucleotides, generating mostly piperidine-labile N7 guanine adducts, N3 adenine adducts and guanine-guanine crosslinks. Additionally, the adducts maintained a measurable, albeit lower affinity towards AR (RBA = 0.22 compared to R1881). As expected, under the same conditions, 11 β -dimethoxy was not able to modify DNA (Marquis et al., 2005).

1.5.2 Toxicological properties

The most impressive feature of 11 β -dichloro is its potent toxicity against cancer cells in cell culture. The first experiments to test this property employed the AR positive prostate cancer LNCaP cell line. Treatment with 11 β -dichloro at concentrations of 5 μ M and higher induced apoptosis in LNCaP cells, as suggested by the morphological changes (cells rounding up and detaching from the plate) and confirmed by apoptosis markers such as Annexin V staining, poly-ADP ribose polymerase (PARP) cleavage and DNA fragmentation (Marquis et al., 2005). Interestingly, the cell cycle distribution of the LNCaP cells treated with 11 β -dichloro did not change, in spite of significant cell death suggested by the subG1 population, indicating that 11 β -dichloro toxicity may be cell cycle independent. However, the control compound, 11 β -dimethoxy, showed very little toxicity and did not show any of the apoptosis

markers that were induced by 11 β -dichloro. Although 11 β -dimethoxy induced some morphological changes, they were transient and cells recovered their initial appearance by 24 hours after treatment. One notable aspect about 11 β -dimethoxy was its ability to cause G1 arrest, as indicated by the cell cycle analysis (Marquis et al., 2005).

In vivo studies with 11 β -dichloro produced even more exciting results. Nude mice bearing LNCaP xenograft tumors were treated with 11 β -dichloro or with vehicle alone, using a daily dose of 30 mg/kg in a 5 days/week, 7 week long regimen. By the last day, the treatment with 11 β -dichloro showed an impressive 90% reduction in tumor growth compared with vehicle treated controls (Figure 1.9). More significantly, the overall toxicity to the treated mice was minimal, the treated animals having experienced a mean weight loss of only 9.7% (Marquis et al., 2005).

Encouraged by the promising effects of 11 β -dichloro on LNCaP xenografts, the biodistribution of the compound and the nature and quantity of DNA adducts formed was investigated in mice (Hillier et al., 2006). For these studies, a ¹⁴C labeled version of the molecule was prepared; small levels of radioactivity were then detected using the highly sensitive technique accelerator mass spectrometry (AMS). It was found that 11 β -dichloro has a good biodistribution in the mouse and that it reaches the xenograft tumor in quantities sufficient to cause a significant number of DNA adducts. Interestingly, a much greater number of DNA adducts was detected in liver cells, although, at the therapeutically effective dose, none of the four commonly used hepatotoxicity markers were affected (Hillier et al., 2006). This finding suggests that the level of DNA damage may not always correlate with toxicity; other factors such as cell specific proteins and metabolism may play important roles. The result was consistent with the intended design mechanism, which predicted that 11 β -dichloro adducts would be significantly more toxic in the AR positive LNCaP tumors, because of a repair shielding-like mechanism.

Unfortunately, recent experiments have seriously challenged the possibility of AR modulating 11 β -dichloro toxicity, at least in certain *in vitro* models. Initial data suggested the involvement of the AR consistent with a repair shielding mechanism, because the AR

positive cell lines (such as LNCaP and MDA453) were found to be more sensitive to 11 β -dichloro than AR negative cell lines (PC3 and DU145) in growth inhibition assays. However, a recent experiment comparing two isogenic cell lines derived from the PC3 cell line (one line expressing the AR, the other one AR negative) found no differential sensitivity to 11 β -dichloro (Figure 1.10). This result casts significant doubt over the role of the AR in modulating 11 β -dichloro toxicity in a repair shielding type of mechanism (Proffitt, 2009).

11 β -Dichloro was found to be significantly more toxic than the simpler mustard chlorambucil in all of the 60 cancer cell lines routinely used by the NCI (National Cancer Institute) to test candidate compounds for cancer chemotherapy. Moreover, the toxicity showed no significant correlation with the level of AR transcript present in each cell line (Croy, RG, personal communication). Such clear-cut data suggest that the mechanism of toxicity of 11 β -dichloro involves serendipitous properties beyond the compound's intended features.

Nevertheless, 11 β -dichloro is more than just a non-specific toxic compound because it does display a large degree of selectivity towards tumor cells *in vivo*. In addition to the compound's ability to prevent growth of LNCaP xenografts, 11 β -dichloro was also shown to be exceptionally effective against HeLa xenografts (Hillier, 2005). The regimen used in this experiment was similar to the one used for LNCaP xenografts, namely 30 mg/kg of compound daily, 5 days/week. However, because of the faster growth rate of HeLa cells in the vehicle treated controls, the experiment had to be stopped after 3 weeks. Nevertheless, by the last day of treatment, the 11 β -dichloro treatment had inhibited the growth of HeLa tumors by more than 90% compared with the vehicle treated controls (Figure 1.11).

An even more puzzling finding came from a structure-activity study that attempted to create a better control compound for the DNA alkylation property of 11 β -dichloro. Two new compounds resembling 11 β -dichloro were synthesized: one (11 β -phenyl, Figure 1.12 A) had the entire aniline mustard warhead replaced with a simple phenyl group; the other (11 β -dipropyl, Figure 1.12 B) had the chlorines on the mustard replaced with methyl groups. These compounds were not characterized in detail, but preliminary data were gathered about their toxicity against HeLa cells and solubility. 11 β -Phenyl is not very toxic in cell culture, a

finding consistent with the important role in toxicity played by the functional mustard. However, 11 β -dipropyl is just as toxic as 11 β -dichloro. Furthermore, their experimentally determined water/octanol partition coefficient (logP), a measure of solubility, is exactly the same, in accord with models that attribute about the same hydrophobicity to the chlorine in organic compounds as to a methyl group (Hillier, SM, 2006, personal communication). This unexpected finding suggests that the molecular structure of 11 β -dichloro, which is essentially identical to the structure of 11 β -dipropyl (the methyl group and the chlorine atoms have similar molecular sizes) may recognize a specific cellular target and trigger toxicity through an unknown pathway that does not require covalent modification.

1.5.3 Investigating the mechanism of toxicity of 11 β -dichloro

The toxicological properties of 11 β -dichloro, both *in vivo* and *in vitro*, have indicated the compound's great potential as a chemotherapeutic. However, considering all the unexpected properties and findings, it became apparent that the toxicity mechanism of 11 β -dichloro is significantly more complicated than the one intended by design.

This work constitutes a systematic investigation of the AR independent mechanism of toxicity of 11 β -dichloro. The toxicity will first be studied in *S. cerevisiae* (the budding yeast), by interrogating the complete single-gene knockout mutant library, with the goal of finding phenotypic classes of mutants particularly sensitive or resistant to our compound. In Chapter 2, the screening protocols and the most important results that emerged from the yeast genomic phenotyping are presented. Interestingly, a significant group of the mutants sensitive to 11 β -dichloro are missing genes encoding proteins that localize either in the mitochondria or the ribosomes. These findings suggest toxicity modulating pathways in addition to DNA damage. The complete list of yeast mutants sensitive to 11 β -dichloro is included in Appendix A. Additionally, several other yeast experiments that may contribute to some insights into the mechanism of toxicity in yeast are included in Appendix B. The most prominent yeast findings are then used as starting points for a mechanistic investigation in HeLa cells, an AR negative human cancer cell line. Chapter 3 analyzes the cellular responses to 11 β -dichloro related to the induction of reactive oxygen species (ROS) – a novel and

original finding of the current work. Finally, in Chapter 4, we investigate the induction of the unfolded protein response (UPR) in HeLa cells and other cellular responses, in an attempt to integrate additional 11β -dichloro properties reported by our coworkers. A detailed mechanism of action is postulated and several future directions are proposed.

1.6 Figures

<i>Figure 1.1 Predicted cancer incidence and mortality for 2008</i>	<i>43</i>
<i>Figure 1.2 The structures of nitrogen mustards currently used in clinic</i>	<i>44</i>
<i>Figure 1.3 Cisplatin and related compounds</i>	<i>45</i>
<i>Figure 1.4 Proposed mechanisms for cisplatin toxicity in testicular cancer</i>	<i>46</i>
<i>Figure 1.5 The ER binding compound based on programmable cytotoxins paradigm.....</i>	<i>47</i>
<i>Figure 1.6 A rational investigation of linker dimensions for ER binding optimization</i>	<i>48</i>
<i>Figure 1.7 A series of ER targeted compounds with variable linker functionalities.....</i>	<i>49</i>
<i>Figure 1.8 Compounds designed to target the AR in prostate cancer.....</i>	<i>50</i>
<i>Figure 1.9 The effect of 11β-dichloro on LNCaP tumor xenografts on nude mice</i>	<i>51</i>
<i>Figure 1.10 The effect of 11β-dichloro on the isogenic tumor cell lines AR1 and AR9.....</i>	<i>52</i>
<i>Figure 1.11 The effect of 11β-dichloro on HeLa tumor xenografts on nude mice</i>	<i>53</i>
<i>Figure 1.12 Comparison of 11β derivatives in terms of solubility and toxicity</i>	<i>54</i>

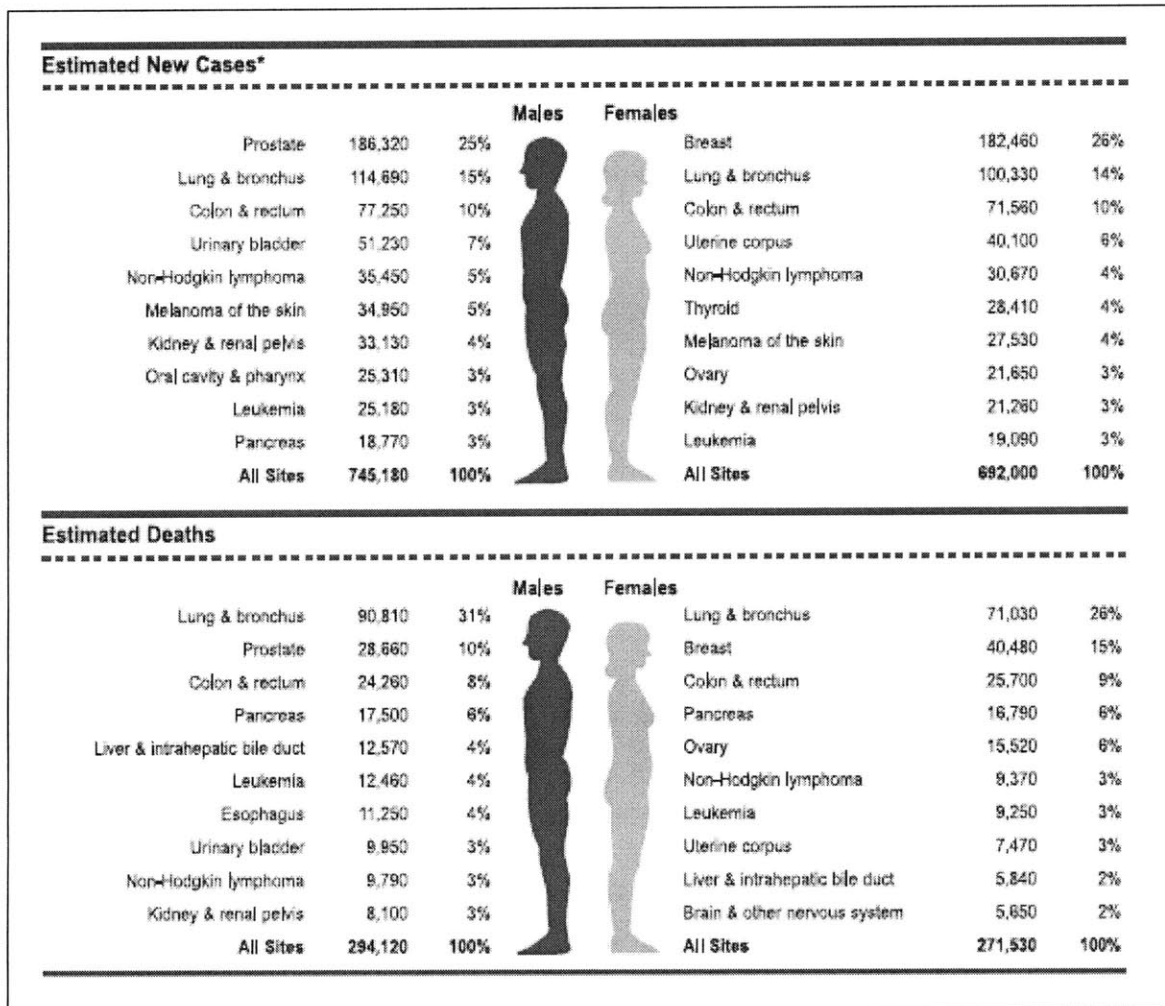


Figure 1.1 Predicted cancer incidence and mortality for 2008

Prostate cancer and breast cancer are the cancers with the highest incidence for men and women, respectively. However, the cancer with total highest mortality is lung cancer. (adapted from (Jemal et al., 2008))

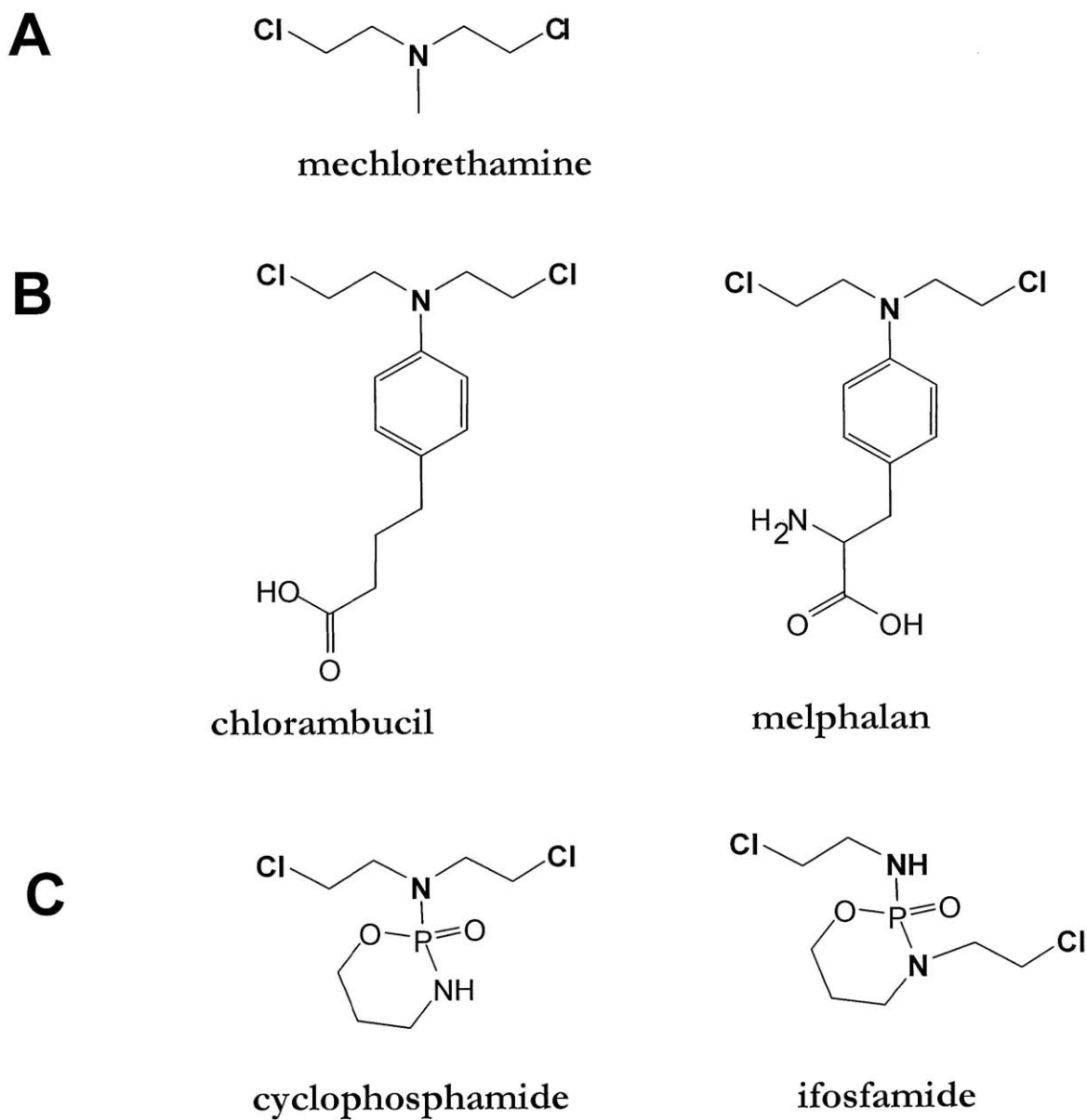
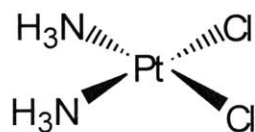
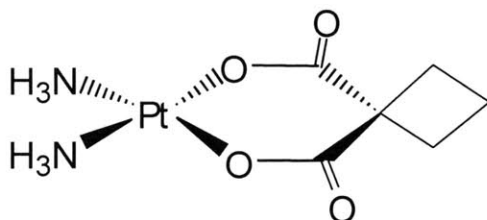


Figure 1.2 The structures of nitrogen mustards currently used in clinic

Mechlorethamine (A) is a very reactive compound. To limit its reactivity and side-effects and to improve its stability, the mustard nitrogen was attached to electron withdrawing groups such as an aromatic ring (B) or a phosphorus (C). In fact, the compounds in the C series are so stable that they need metabolic activation before they become reactive.

A

cisplatin



carboplatin

B

transplatin

Figure 1.3 Cisplatin and related compounds

Cisplatin and its analog, carboplatin (A) have shown remarkable efficacy in clinic, especially in testicular cancer. The trans isomer – transplatin (B) is also reactive and can form DNA crosslinks; however, transplatin is therapeutically ineffective.

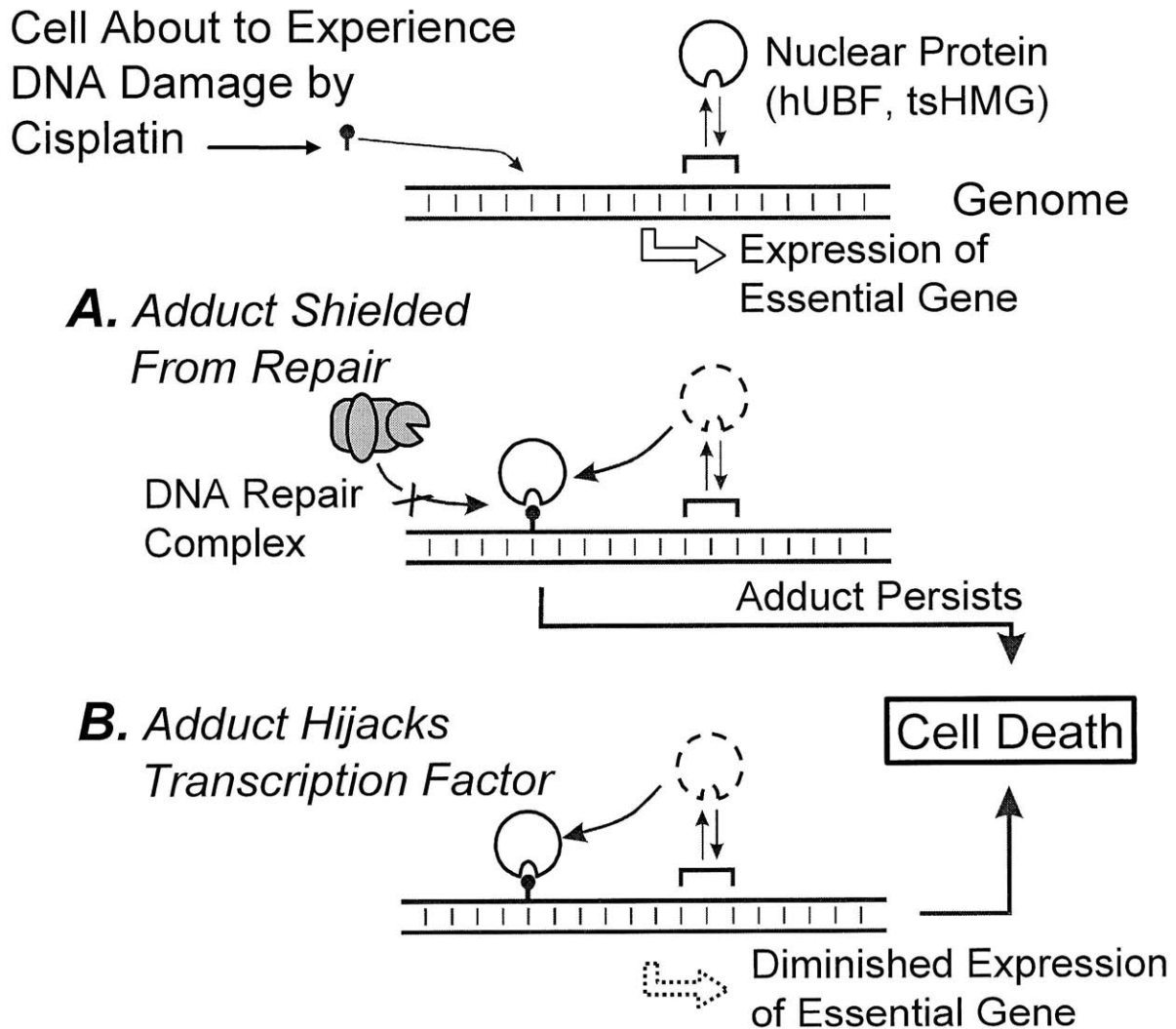


Figure 1.4 Proposed mechanisms for cisplatin toxicity in testicular cancer

1,2 DNA crosslinks are the major DNA damage product of cisplatin. Two mechanisms that explain the enhanced toxicity of these adducts have been proposed. The first mechanism, “repair shielding” (A) is based on the observation that cancer cell specific proteins can bind the adducts and shield them from the cellular repair machinery, thus increasing their lifetime and toxicity. The second mechanism, “transcription factor hijacking” (B) is based on the observation that some of the proteins with high affinity for adducts are also transcription factors; their binding to adducts titrates them away from their cellular function, which when reduced, leads to toxicity.

(adapted from (Essigmann et al., 2001)

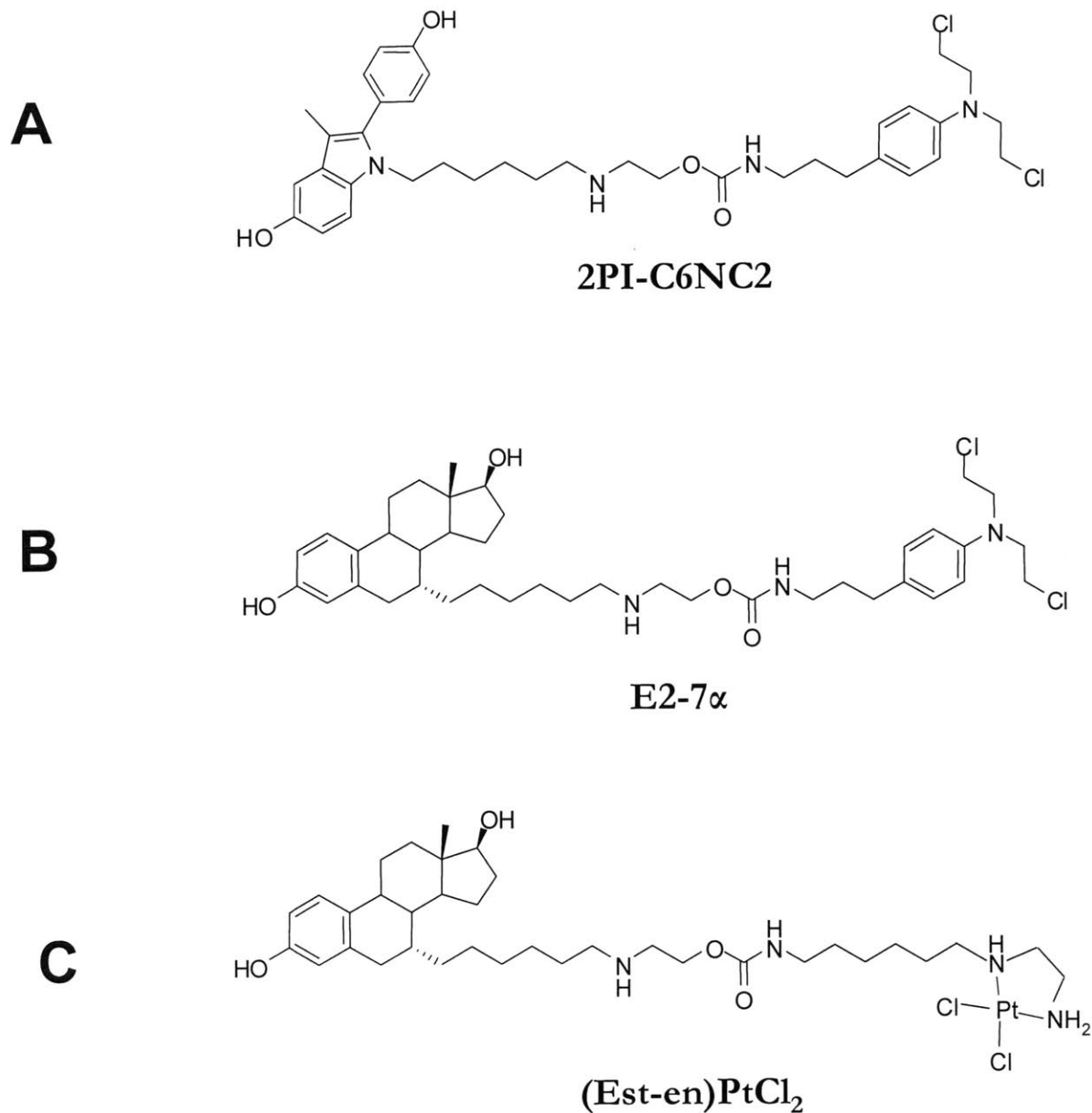
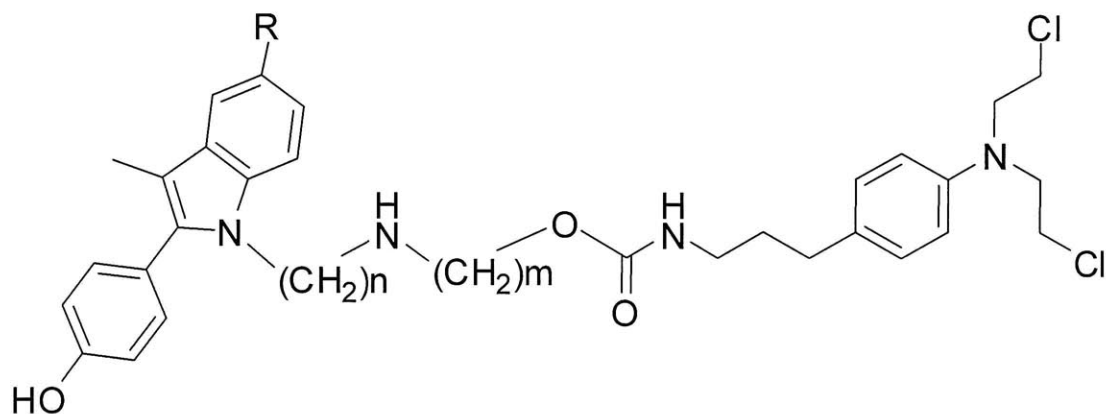


Figure 1.5 The ER binding compound based on programmable cytotoxins paradigm

This figure illustrates the flexibility of the programmable cytotoxins approach. The first compound synthesized (2PI-C6NC2) (A) displayed only modest ER binding. By changing the ligand to a 7 α substituted estradiol, the affinity for ER was significantly improved. (compound B – E2-7 α). To vary the reactivity and specificity, the aniline mustard warhead was replaced with a ethylene diamine – cisplatin warhead (C).

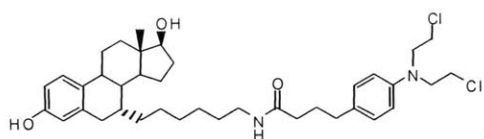
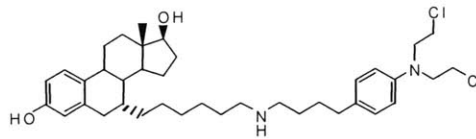
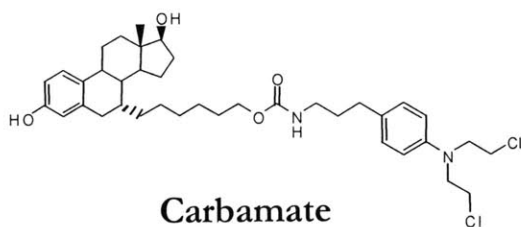
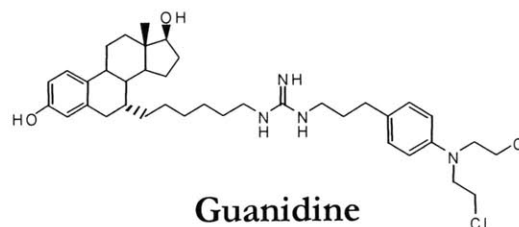
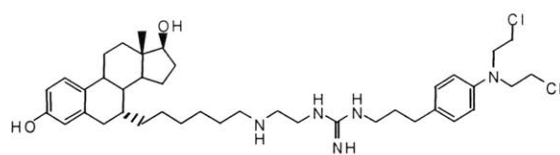
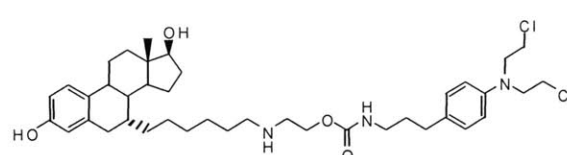
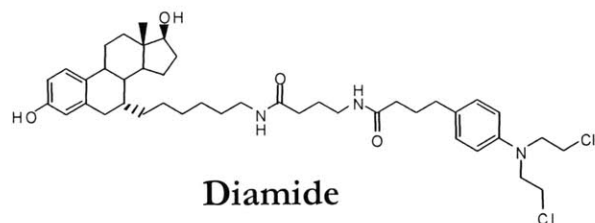
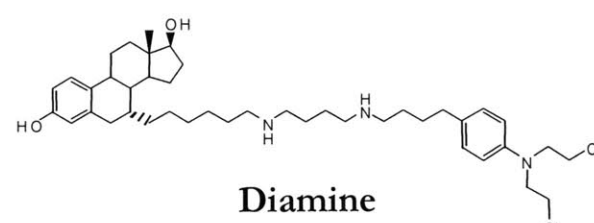


Mustard	m	n	R	RBA
2PI-C3NC3	3	3	OH	0
2PI-C5-NC3	3	5	OH	0.6
2PI-C6NC2	2	6	OH	7.1
2PI(OH)-C6NC2	2	6	H	0.1

Figure 1.6 A rational investigation of linker dimensions for ER binding optimization

Several 2-phenyl-indole compounds have been synthesized to optimize the linker features for improved ER binding.

(adapted from (Rink et al., 1996))

**Amide****Amine****Carbamate****Guanidine****Amine Guanidine****E2-7 α (Amine Carbamate)****Diamide****Diamine****Figure 1.7** A series of ER targeted compounds with variable linker functionalities

To optimize the linker, a series of compounds was synthesized that incorporate the same warhead and ER ligand, but vary the number and type of functional groups in the linker part of the molecule.

(adapted from (Sharma et al., 2004))

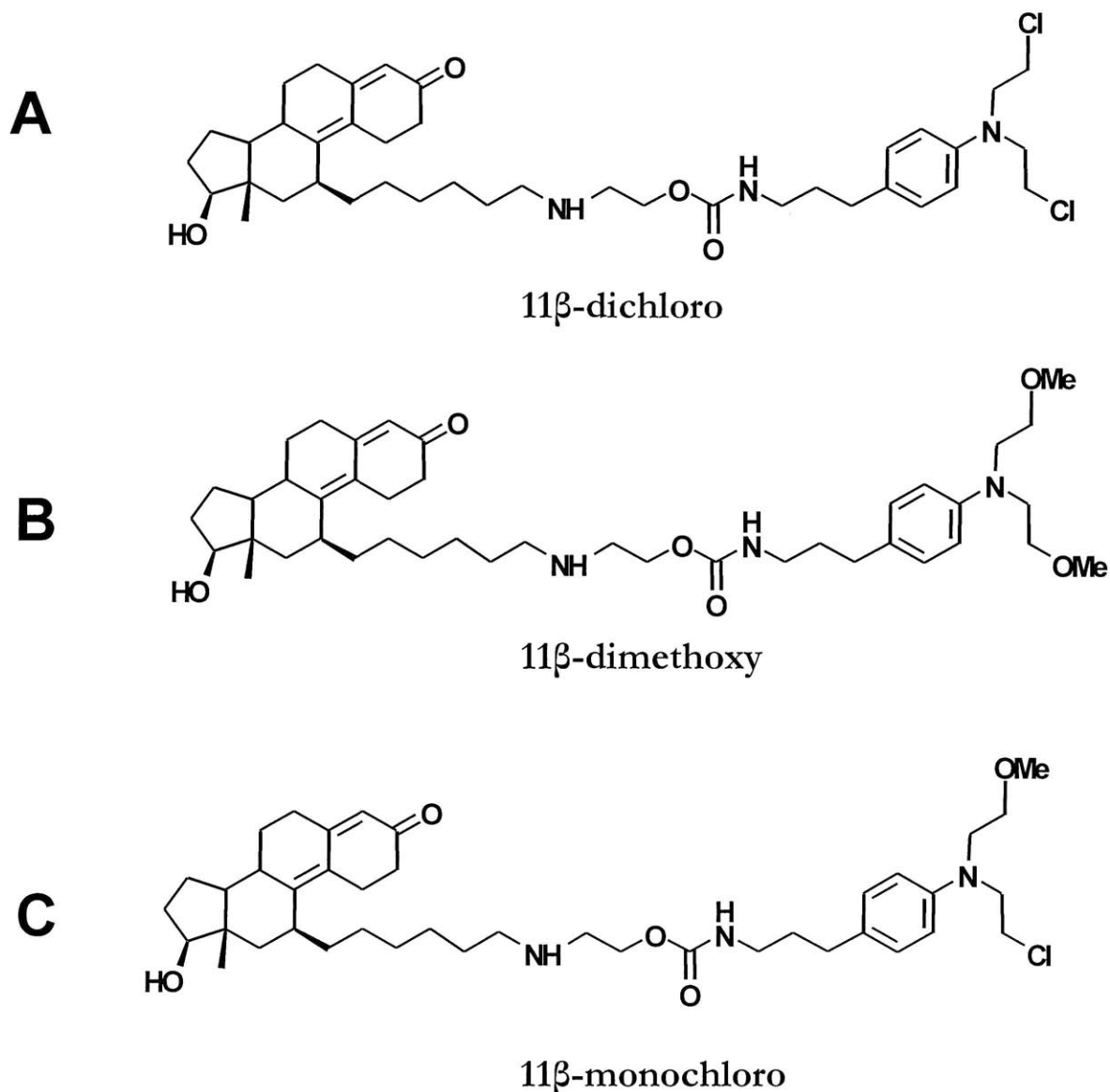


Figure 1.8 Compounds designed to target the AR in prostate cancer

The lead compound, 11 β -dichloro (A) is an aniline mustard tethered by a C₆NC₂ linker to an estradienone moiety that can interact with AR. Two additional compounds have been made to control for the ability to damage DNA, and the type of DNA damage. Compound B (11 β -dimethoxy) cannot damage DNA. Compound C (11 β -monochloro) can form monoadducts, but cannot form DNA crosslinks.

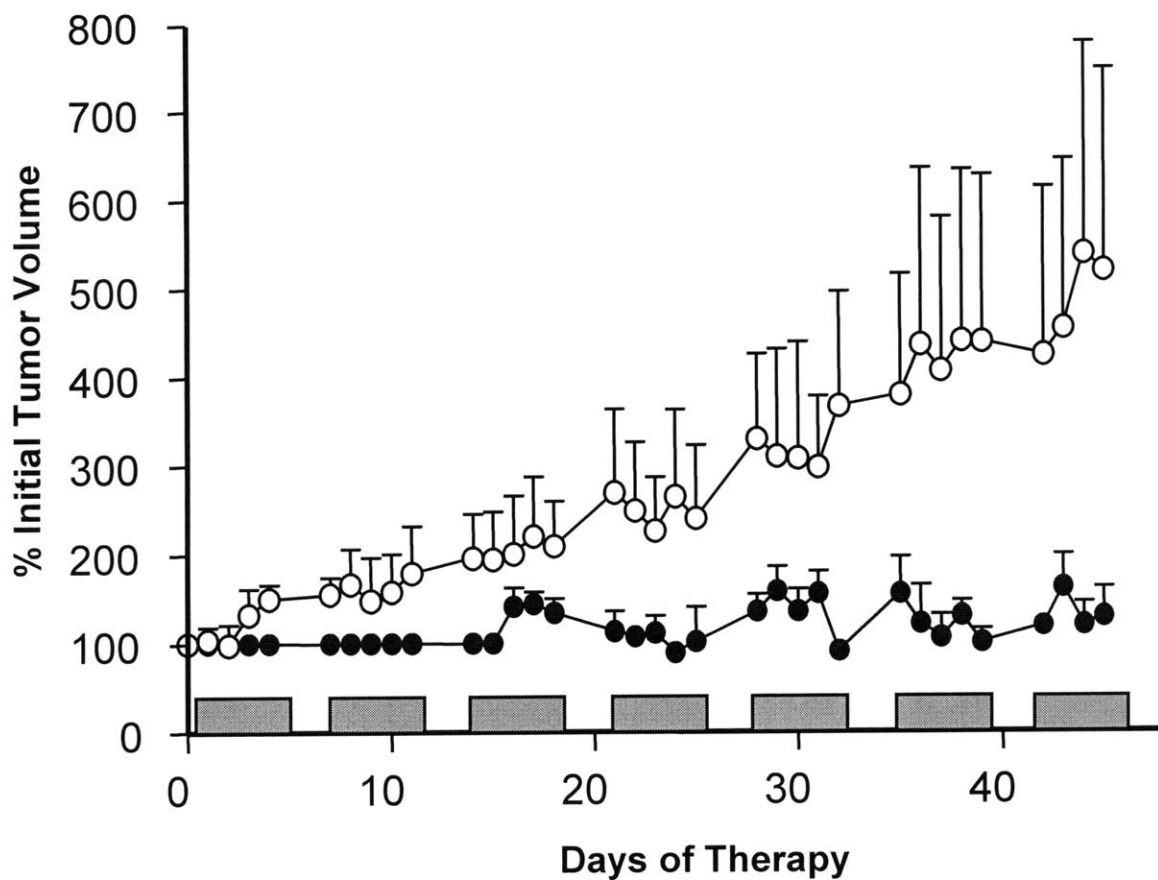


Figure 1.9 The effect of 11β -dichloro on LNCaP tumor xenografts on nude mice

The gray bars indicate the treatment regimen (5 days/week, 2 days recovery). Mice received 30mg/kg IP injection with 11β -dichloro (treated group - closed circles) or vehicle alone (open circles).

(adapted from (Hillier, 2005))

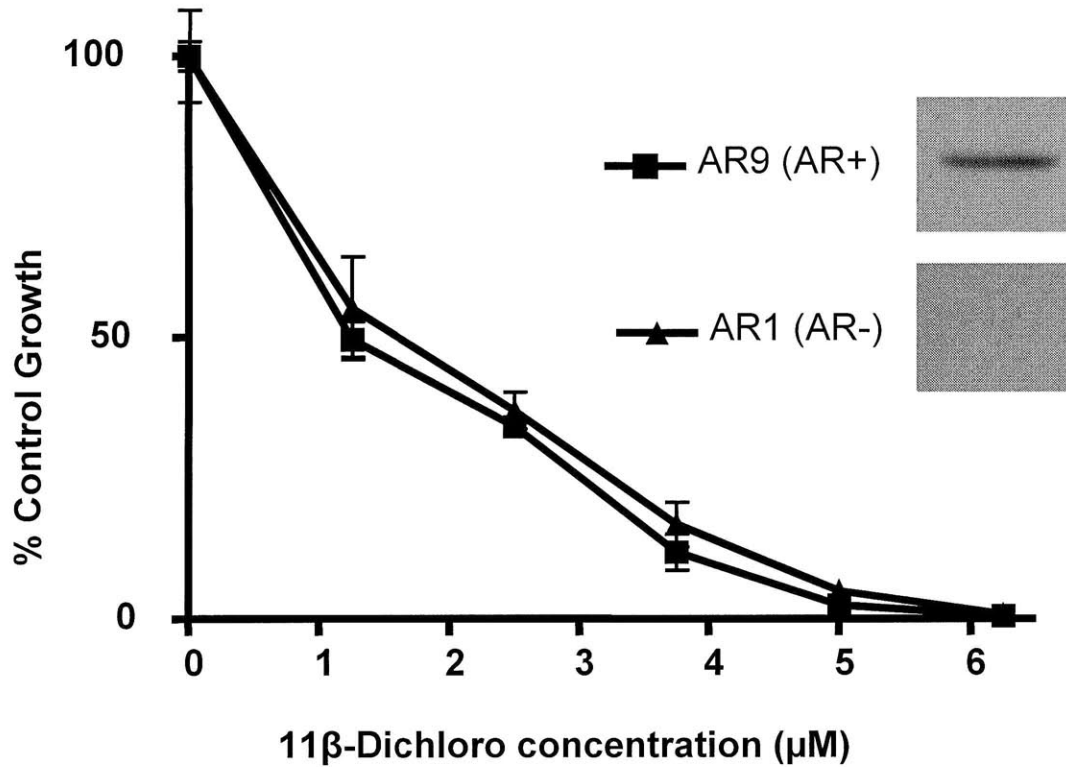


Figure 1.10 The effect of 11β-dichloro on the isogenic tumor cell lines AR1 and AR9

The involvement of the AR protein was investigated in the isogenic pair of PC3 derived cell lines AR1 and AR9. The AR9 cell line expresses the androgen receptor (AR), whereas the AR1 cell line does not. The insets show the AR protein band as seen by immunoblotting. The AR protein expressed in the AR9 strain is functional and, in the presence of its natural ligand (dihydrotestosterone), can bind to androgen response elements in the genome. However, the presence of the AR protein is not required for the growth of the AR9 cells. The cells have been exposed for 48 hours to the doses indicated, then counted with a Coulter counter. (adapted from Proffitt, 2009)

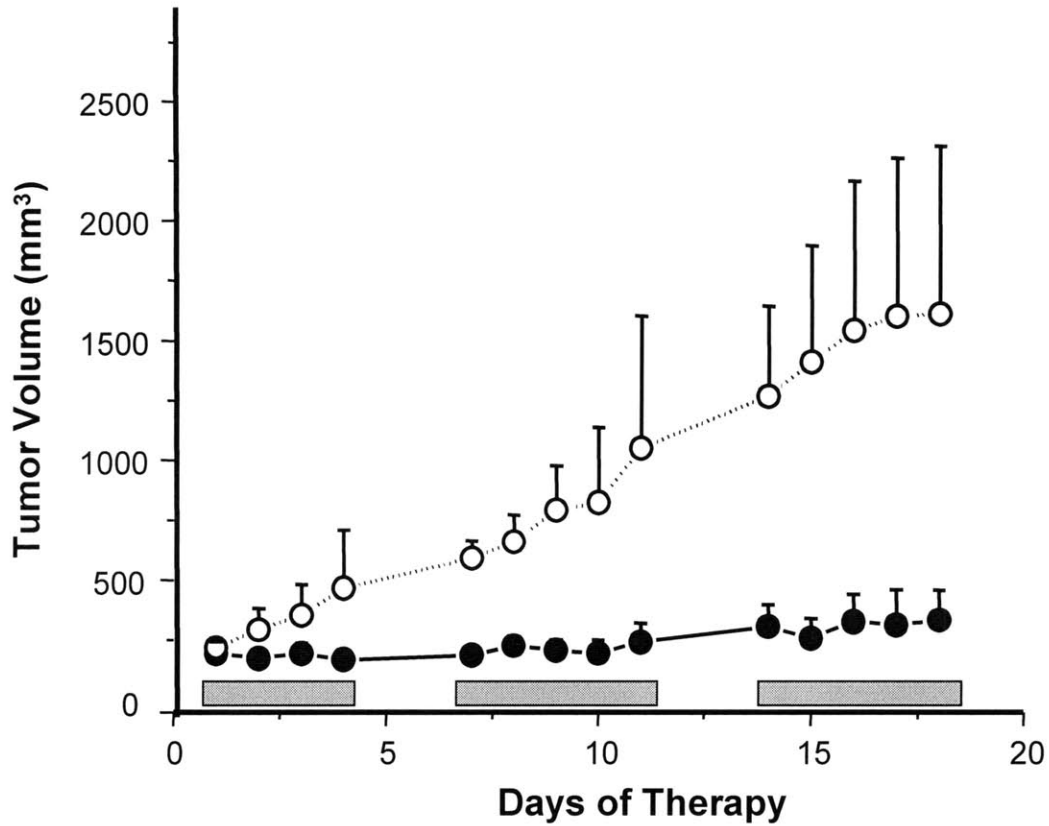
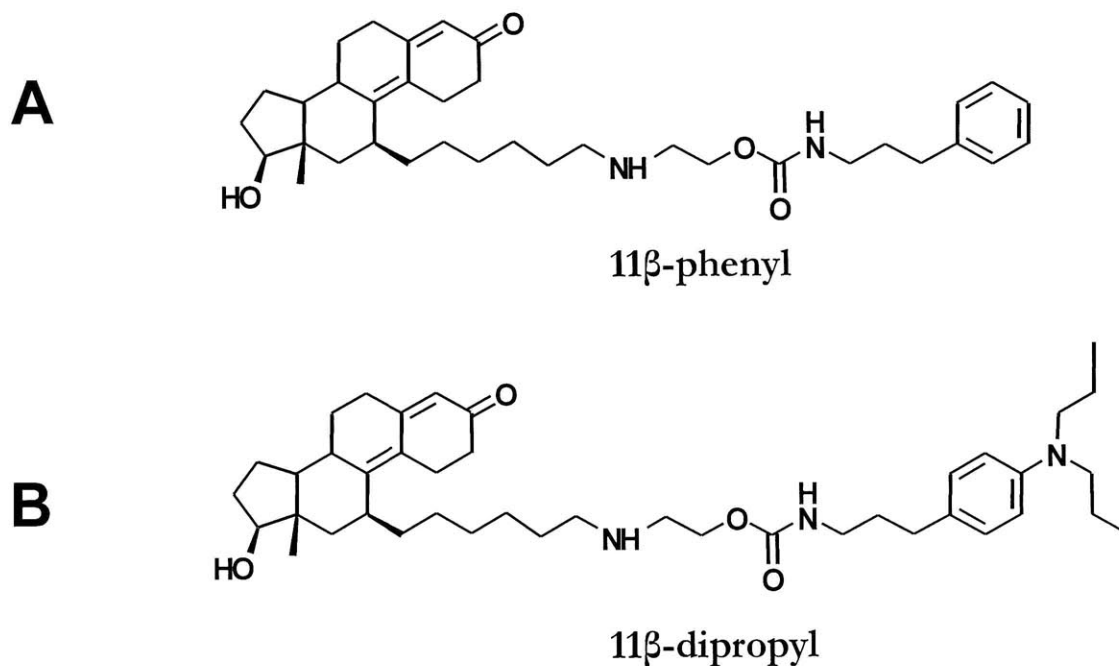


Figure 1.11 The effect of 11β -dichloro on HeLa tumor xenografts on nude mice

The gray bars indicate the treatment regimen (5 days/week, 2 days recovery). Mice received 30mg/kg IP injection with 11β -dichloro (treated group - closed circles) or vehicle alone (open circles).

(adapted from Hillier, 2005)



Compound	Experimental logP	Toxicity against HeLa cells (IC ₅₀ , μ M)
11β-dichloro	5.05	5
11β-monochloro	4.67	8
11β-dimethoxy	4.07	13
11β-phenyl	4.22	15
11β-dipropyl	5.04	< 5

Figure 1.12 Comparison of 11 β derivatives in terms of solubility and toxicity

Two more compounds have been synthesized, to elucidate the role of the warhead in 11 β -dichloro's toxicity: 11 β -phenyl (A) and 11 β -dipropyl (B). The table displays the values of the water/octanol partition coefficient (logP) and the IC₅₀ value measured in a growth inhibition at 24 hours for HeLa cells.

(adapted from Marquis & Hillier, 2005, personal communication)

1.7 References

- Albertini, R. J., Nicklas, J. A., O'Neill, J. P., and Robison, S. H. (1990). In vivo somatic mutations in humans: measurement and analysis. *Annu. Rev. Genet* 24, 305-326.
- American Cancer Society (2008). *Cancer Facts and Figures*.
- Bancroft, D., Lepre, C., and Lippard, S. (1990). Pt-195 NMR kinetic and mechanistic studies of cis-diamminedichloroplatinum and trans-diamminedichloroplatinum(II) binding to DNA. *J.Am.Chem.Soc* 112, 6860-6871.
- Bange, J., Zwick, E., and Ullrich, A. (2001). Molecular targets for breast cancer therapy and prevention. *Nat. Med* 7, 548-552.
- Baselga, J. (2001). Herceptin alone or in combination with chemotherapy in the treatment of HER2-positive metastatic breast cancer: pivotal trials. *Oncology* 61 *Suppl* 2, 14-21.
- Beckman, R. A., and Loeb, L. A. (2006). Efficiency of carcinogenesis with and without a mutator mutation. *Proc. Natl. Acad. Sci. U.S.A* 103, 14140-14145.
- Bedard, P. L., de Azambuja, E., and Cardoso, F. (2009). Beyond trastuzumab: overcoming resistance to targeted HER-2 therapy in breast cancer. *Curr Cancer Drug Targets* 9, 148-162.
- Bielas, J. H., Loeb, K. R., Rubin, B. P., True, L. D., and Loeb, L. A. (2006). Human cancers express a mutator phenotype. *Proc. Natl. Acad. Sci. U.S.A* 103, 18238-18242.
- Bos, J. L. (1989). ras oncogenes in human cancer: a review. *Cancer Res* 49, 4682-4689.
- Bowler, J., Lilley, T. J., Pittam, J. D., and Wakeling, A. E. (1989). Novel steroidal pure antiestrogens. *Steroids* 54, 71-99.
- Boyle, P., and Levin, B. (2008). *World Cancer Report (WHO-IARC)*.
- Cepeda, V., Fuertes, M. A., Castilla, J., Alonso, C., Quevedo, C., and Pérez, J. M. (2007). Biochemical mechanisms of cisplatin cytotoxicity. *Anticancer Agents Med Chem* 7, 3-18.
- Cervantes, R. B., Stringer, J. R., Shao, C., Tischfield, J. A., and Stambrook, P. J. (2002). Embryonic stem cells and somatic cells differ in mutation frequency and type. *Proc. Natl. Acad. Sci. U.S.A* 99, 3586-3590.
- Colvin, M., Brundrett, R. B., Kan, M. N., Jardine, I., and Fenselau, C. (1976). Alkylating properties of phosphoramidate mustard. *Cancer Res* 36, 1121-1126.

Chapter 1

- DaSilva, J. N., and van Lier, J. E. (1990). In vivo evaluation of 7 alpha-[11-(4-[125I]iodophenoxy)undecyl]-17 beta-estradiol: a potential vector for therapy of adrenal and estrogen receptor-positive cancers. *J. Steroid Biochem. Mol. Biol* 37, 77-83.
- Dronkert, M. L., and Kanaar, R. (2001). Repair of DNA interstrand cross-links. *Mutat. Res* 486, 217-247.
- Essigmann, J. M., Rink, S. M., Park, H. J., and Croy, R. G. (2001). Design of DNA damaging agents that hijack transcription factors and block DNA repair. *Adv Exp Med Biol* 500, 301-13.
- Fernö, M., Borg, A., Johansson, U., Norgren, A., Olsson, H., Rydén, S., and Sellberg, G. (1990). Estrogen and progesterone receptor analyses in more than 4,000 human breast cancer samples. A study with special reference to age at diagnosis and stability of analyses. Southern Swedish Breast Cancer Study Group. *Acta Oncol* 29, 129-135.
- Fichtinger-Schepman, A. M., van Oosterom, A. T., Lohman, P. H., and Berends, F. (1987). cis-Diamminedichloroplatinum(II)-induced DNA adducts in peripheral leukocytes from seven cancer patients: quantitative immunochemical detection of the adduct induction and removal after a single dose of cis-diamminedichloroplatinum(II). *Cancer Res* 47, 3000-3004.
- Fouchet, M., Guittet, E., Cognet, J., Kozelka, J., Gauthier, C., LeBret, M., Zimmermann, K., and Chottard, J. (1997). Structure of a nonanucleotide duplex cross-linked by cisplatin at an ApG sequence. *J. Biol. Inorg. Chem* 2, 83-92.
- Fuhrmann, U., Hess-Stumpp, H., Cleve, A., Neef, G., Schwede, W., Hoffmann, J., Fritzemeier, K. H., and Chwalisz, K. (2000). Synthesis and biological activity of a novel, highly potent progesterone receptor antagonist. *J. Med. Chem* 43, 5010-5016.
- Gelasco, A., and Lippard, S. J. (1998). NMR solution structure of a DNA dodecamer duplex containing a cis-diammineplatinum(II) d(GpG) intrastrand cross-link, the major adduct of the anticancer drug cisplatin. *Biochemistry* 37, 9230-9239.
- Gopal, S. (2009). Mechanistic Investigation of an Anticancer Agent that Damages DNA and Interacts with the Estrogen Receptor. PhD Thesis, Massachusetts Institute of Technology.
- Greenman, C., Stephens, P., Smith, R., Dalgliesh, G. L., Hunter, C., Bignell, G., Davies, H., Teague, J., Butler, A., Stevens, C., et al. (2007). Patterns of somatic mutation in human cancer genomes. *Nature* 446, 153-158.
- Haber, D. A., and Settleman, J. (2007). Cancer: drivers and passengers. *Nature* 446, 145-146.

Chapter 1

- Hanahan, D., and Weinberg, R. A. (2000). The hallmarks of cancer. *Cell* 100, 57-70.
- Hede, K. (2005). Which came first? Studies clarify role of aneuploidy in cancer. *J. Natl. Cancer Inst* 97, 87-89.
- Hillier, S. M., Marquis, J. C., Zayas, B., Wishnok, J. S., Liberman, R. G., Skipper, P. L., Tannenbaum, S. R., Essigmann, J. M., and Croy, R. G. (2006). DNA adducts formed by a novel antitumor agent 11beta-dichloro in vitro and in vivo. *Mol Cancer Ther* 5, 977-84.
- Hillier, S. M. (2005). Novel Genotoxins that Target Estrogen Receptor- and Androgen Receptor- Positive Cancers: Identification of DNA Adducts, Pharmacokinetics, and Mechanism. PhD Thesis, Massachusetts Institute of Technology.
- Huang, J. C., Zamble, D. B., Reardon, J. T., Lippard, S. J., and Sancar, A. (1994). HMG-domain proteins specifically inhibit the repair of the major DNA adduct of the anticancer drug cisplatin by human excision nuclease. *Proc Natl Acad Sci U S A* 91, 10394-8.
- Hurley, L. H. (2002). DNA and its associated processes as targets for cancer therapy. *Nat. Rev. Cancer* 2, 188-200.
- Jabbour, E., Cortes, J., and Kantarjian, H. (2009). Treatment selection after imatinib resistance in chronic myeloid leukemia. *Target Oncol* 4, 3-10.
- Jemal, A., Siegel, R., Ward, E., Hao, Y., Xu, J., Murray, T., and Thun, M. J. (2008). Cancer statistics, 2008. *CA Cancer J Clin* 58, 71-96.
- Jordan, P., and Carmo-Fonseca, M. (1998). Cisplatin inhibits synthesis of ribosomal RNA in vivo. *Nucleic Acids Res* 26, 2831-2836.
- Kartalou, M., and Essigmann, J. M. (2001). Recognition of cisplatin adducts by cellular proteins. *Mutat Res* 478, 1-21.
- Kim, E., Rye, P. T., Essigmann, J. M., and Croy, R. G. (2009). A bifunctional platinum(II) antitumor agent that forms DNA adducts with affinity for the estrogen receptor. *J. Inorg. Biochem* 103, 256-261.
- Leng, M., and Brabec, V. (1994). DNA adducts of cisplatin, transplatin and platinum-intercalating drugs. *IARC Sci. Publ*, 339-348.
- Loeb, L. A., Bielas, J. H., and Beckman, R. A. (2008). Cancers exhibit a mutator phenotype: clinical implications. *Cancer Res* 68, 3551-3557; discussion 3557.
- Lohrisch, C., and Piccart, M. (2001). HER2/neu as a predictive factor in breast cancer. *Clin. Breast Cancer* 2, 129-135; discussion 136-137.

Chapter 1

- Marcelli, M., and Cunningham, G. R. (1999). Hormonal signaling in prostatic hyperplasia and neoplasia. *J Clin Endocrinol Metab* *84*, 3463-8.
- Marquis, J. C., Hillier, S. M., Dinaut, A. N., Rodrigues, D., Mitra, K., Essigmann, J. M., and Croy, R. G. (2005). Disruption of gene expression and induction of apoptosis in prostate cancer cells by a DNA-damaging agent tethered to an androgen receptor ligand. *Chem Biol* *12*, 779-87.
- Masters, J. R. W., and Köberle, B. (2003). Curing metastatic cancer: lessons from testicular germ-cell tumours. *Nat Rev Cancer* *3*, 517-25.
- McA'Nulty, M. M., Whitehead, J. P., and Lippard, S. J. (1996). Binding of Ixr1, a yeast HMG-domain protein, to cisplatin-DNA adducts in vitro and in vivo. *Biochemistry* *35*, 6089-99.
- McHugh, P. J., Spanswick, V. J., and Hartley, J. A. (2001). Repair of DNA interstrand crosslinks: molecular mechanisms and clinical relevance. *Lancet Oncol* *2*, 483-490.
- Meijerman, I., Beijnen, J. H., and Schellens, J. H. M. (2008). Combined action and regulation of phase II enzymes and multidrug resistance proteins in multidrug resistance in cancer. *Cancer Treat. Rev* *34*, 505-520.
- Mitra, K., Marquis, J. C., Hillier, S. M., Rye, P. T., Zayas, B., Lee, A. S., Essigmann, J. M., and Croy, R. G. (2002). A rationally designed genotoxin that selectively destroys estrogen receptor-positive breast cancer cells. *J Am Chem Soc* *124*, 1862-3.
- Nojima, K., Hochegger, H., Saberi, A., Fukushima, T., Kikuchi, K., Yoshimura, M., Orelli, B. J., Bishop, D. K., Hirano, S., Ohzeki, M., et al. (2005). Multiple repair pathways mediate tolerance to chemotherapeutic cross-linking agents in vertebrate cells. *Cancer Res* *65*, 11704-11711.
- O'Brien, S. G., Guilhot, F., Larson, R. A., Gathmann, I., Baccarani, M., Cervantes, F., Cornelissen, J. J., Fischer, T., Hochhaus, A., Hughes, T., et al. (2003). Imatinib compared with interferon and low-dose cytarabine for newly diagnosed chronic-phase chronic myeloid leukemia. *N. Engl. J. Med* *348*, 994-1004.
- O'Connor, R. (2007). The pharmacology of cancer resistance. *Anticancer Res* *27*, 1267-1272.
- Parsons, D. W., Jones, S., Zhang, X., Lin, J. C., Leary, R. J., Angenendt, P., Mankoo, P., Carter, H., Siu, I., Gallia, G. L., et al. (2008). An integrated genomic analysis of human glioblastoma multiforme. *Science* *321*, 1807-1812.
- Perry, M. (2001). *The Chemotherapy Source Book* 3rd ed. (Philadelphia: Lippincott).

Chapter 1

- Pil, P. M., and Lippard, S. J. (1992). Specific binding of chromosomal protein HMG1 to DNA damaged by the anticancer drug cisplatin. *Science* 256, 234-237.
- Pollard, P. J., and Ratcliffe, P. J. (2009). Cancer. Puzzling patterns of predisposition. *Science* 324, 192-194.
- Povirk, L. F., and Shuker, D. E. (1994). DNA damage and mutagenesis induced by nitrogen mustards. *Mutat. Res* 318, 205-226.
- Proffitt, K. D. (2009). Mechanistic Investigation of an Anticancer Agent that Damages DNA and Interacts with the Androgen Receptor. PhD Thesis, Massachusetts Institute of Technology.
- Rappeneau, S., Baeza-Squiban, A., Jeulin, C., and Marano, F. (2000). Protection from cytotoxic effects induced by the nitrogen mustard mechlorethamine on human bronchial epithelial cells in vitro. *Toxicol. Sci* 54, 212-221.
- Ries, L. A. G., Melbert, D., Krapcho, M., Mariotto, A., Miller, B. A., Feuer, E. J., Clegg, L., Horner, M. J., Howlader, N., Eisner, M. P., et al. (2009). SEER cancer statistics review, 1975-2005. National Cancer Institute, Bethesda, MD. *XXV 1-12*. Available at: http://seer.cancer.gov/csr/1975_2005/, based on November 2007 SEER data submission, posted to the SEER web site, 2008.
- Rink, S. M., Yarema, K. J., Solomon, M. S., Paige, L. A., Tadayoni-Rebek, B. M., Essigmann, J. M., and Croy, R. G. (1996). Synthesis and biological activity of DNA damaging agents that form decoy binding sites for the estrogen receptor. *Proc Natl Acad Sci U S A* 93, 15063-8.
- Sharma, U., Marquis, J. C., Nicole Dinaut, A., Hillier, S. M., Fedeles, B., Rye, P. T., Essigmann, J. M., and Croy, R. G. (2004). Design, synthesis, and evaluation of estradiol-linked genotoxicants as anti-cancer agents. *Bioorg Med Chem Lett* 14, 3829-33.
- Sharom, F. J. (2008). ABC multidrug transporters: structure, function and role in chemoresistance. *Pharmacogenomics* 9, 105-127.
- Sliwkowski, M. X., Lofgren, J. A., Lewis, G. D., Hotaling, T. E., Fendly, B. M., and Fox, J. A. (1999). Nonclinical studies addressing the mechanism of action of trastuzumab (Herceptin). *Semin. Oncol* 26, 60-70.
- Sporn, M. B. (1997). The war on cancer: a review. *Ann. N. Y. Acad. Sci* 833, 137-146.
- Stratton, M. R., Campbell, P. J., and Futreal, P. A. (2009). The cancer genome. *Nature* 458, 719-724.

Chapter 1

- Takahara, P. M., Rosenzweig, A. C., Frederick, C. A., and Lippard, S. J. (1995). Crystal structure of double-stranded DNA containing the major adduct of the anticancer drug cisplatin. *Nature* *377*, 649-652.
- Treiber, D. K., Zhai, X., Jantzen, H. M., and Essigmann, J. M. (1994). Cisplatin-DNA adducts are molecular decoys for the ribosomal RNA transcription factor hUBF (human upstream binding factor). *Proc Natl Acad Sci U S A* *91*, 5672-6.
- Trimmer, E. E., and Essigmann, J. M. (1999). Cisplatin. *Essays Biochem* *34*, 191-211.
- Trimmer, E. E., Zamble, D. B., Lippard, S. J., and Essigmann, J. M. (1998). Human testis-determining factor SRY binds to the major DNA adduct of cisplatin and a putative target sequence with comparable affinities. *Biochemistry* *37*, 352-362.
- Zamble, D. B., and Lippard, S. J. (1995). Cisplatin and DNA repair in cancer chemotherapy. *Trends Biochem. Sci* *20*, 435-439.
- Zamble, D. B., Mikata, Y., Eng, C. H., Sandman, K. E., and Lippard, S. J. (2002). Testis-specific HMG-domain protein alters the responses of cells to cisplatin. *J. Inorg. Biochem* *91*, 451-462.
- Zhai, X., Beckmann, H., Jantzen, H. M., and Essigmann, J. M. (1998). Cisplatin-DNA adducts inhibit ribosomal RNA synthesis by hijacking the transcription factor human upstream binding factor. *Biochemistry* *37*, 16307-16315.
- Zhao, X. Y., Boyle, B., Krishnan, A. V., Navone, N. M., Peehl, D. M., and Feldman, D. (1999). Two mutations identified in the androgen receptor of the new human prostate cancer cell line MDA PCa 2a. *J. Urol* *162*, 2192-2199.

CHAPTER 2

Investigating the Mechanism of Toxicity of the Anticancer Agent 11 β -Dichloro in *Saccharomyces cerevisiae* by Genomic Phenotyping

2.1 Introduction

Chemotherapy represents one of the most important cancer treatments available today. Often used as an adjuvant following surgery or radiation therapy, chemotherapy is targeted at the remaining cells in the primary tumor and possible metastases. In certain non-resectable cancers (such as blood cancers), as well as in advanced metastatic cancers, chemotherapy is currently the main line of treatment (Perry, 2001). Unfortunately, most chemotherapeutic agents in use today are not very specific; they cause significant toxicity to healthy tissues thus eliciting a plethora of side-effects that often limit their effectiveness and decrease considerably the quality of life of the cancer patients. Given these considerations, the development of better, more specific chemotherapeutics remains an important scientific challenge.

However, certain chemotherapy regimens have been remarkably successful in clinic. Specifically, combination treatments containing cisplatin have achieved a cure rate of more than 95% against testicular cancers (Masters and Köberle, 2003; Ries et al., 2009). The key ingredient in such regimens, cisplatin, has been the subject of a large number of mechanistic studies. One theory suggests that cisplatin may achieve its high effectiveness by taking advantage of tumor specific proteins (Kartalou and Essigmann, 2001). Inspired by the proposed cisplatin mechanism, the Essigmann lab developed the concept of programmable cytotoxins – antineoplastic DNA-damaging agents tailored for specific cancers (Essigmann et al., 2001). The result was a series of compounds that could both alkylate DNA and bind to steroid receptors such as the estrogen receptor (ER) or the androgen receptor (AR). Given that the ER and the AR are often overexpressed in certain breast (Fernö et al., 1990), and prostate cancers (Marcelli and Cunningham, 1999) respectively, these steroid receptors constitute legitimate cancer-specific targets.

One of these compounds, called 11 β -dichloro² (Figure 2.1 A), which was designed to interact with the AR, displays a potent *in vivo* anti-tumor activity in mice, while being well tolerated

² IUPAC name: 2-(6-((8S,11S,13S,14S,17S)-17-hydroxy-13-methyl-3-oxo-2,3,6,7,8,11,12,13,14,15,16,17 dodecahydro-1H-cyclopenta[a]phenanthren-11-yl)hexylamino)ethyl 3-(4-(bis(2-chloroethyl)amino)phenyl)propylcarbamate

by animals (Marquis et al., 2005). However, the compound is also effective against tumors that do not express AR, much more so than simpler nitrogen mustards (Chapter 1). Such findings suggested that an additional mechanism of toxicity may be operating and prompted the current investigation. To identify the cellular pathways affected by 11 β -dichloro, we interrogated a complete yeast genomic single gene knock-out mutant library. We hoped that by comparing the yeast phenotypic profile of 11 β -dichloro with the profiles of other compounds, important clues about the mechanism of toxicity would emerge. Based on these clues, we subsequently would be able to formulate and test hypotheses in cancer cell lines. In fact, characterizing the complete mechanism of toxicity is an essential step for the eventual advancing of 11 β -dichloro in preclinical and clinical trials.

The most commonly used experimental system for studying anticancer agents is human cancer cell lines. While they are the closest model for the disease, given that they are derived from the cells that had evolved and caused cancer in a person, they also pose significant challenges for the study of fundamental mechanisms of cancer and finding of molecular therapeutic targets. These challenges arise primarily from the complexity of the human genome, further complicated in cancer cells by additional mutations and chromosomal rearrangements (Hede, 2005). Moreover, each human cancer cell line comes from a different individual, containing a very different collection of inherited traits and acquired passenger and driver mutations (Greenman et al., 2007). Such genotypic differences make any large scale genomic analysis very difficult to do and interpret.

The scientific literature has shown that fundamental cancer problems are often solved more effectively in model organisms rather than cancer cell lines. Among the many models, the budding yeast *Saccharomyces cerevisiae* continues to play an important role in the study of cancer (Hartwell, 2004; Bjornsti, 2002; Menacho-Márquez and Murguía, 2007). Although a simple eukaryote, the yeast uses the same fundamental mechanisms of cell division and control of genomic fidelity (e.g. DNA repair, cell cycle checkpoints) as higher eukaryotes. It is therefore no surprise that most of these yeast genes have mammalian homologues. In fact,

a large number of mammalian genes and gene functions have been identified by homology with yeast (Hartwell, 2004).

More recent studies have suggested that the study of yeast can play an important role in developing cancer therapeutics (Bjornsti, 2002; Menacho-Márquez et al., 2007). The main advantages of the yeast are its genetic tractability and flexibility. Not only is the yeast genome sequenced and well-annotated, but we also have available the complete single gene knockout library (such as the one constructed by the *S. cerevisiae* Genome Deletion Project), and a large number of genetic interaction data in databases such as GRID (General Repository for Interaction Datasets) and SGD (Saccharomyces Genome Database). Additionally, yeast is a robust and versatile organism requiring significantly simpler culture condition compared with mammalian cells, and being easily manipulated genetically.

The availability of the yeast complete single gene knockout library started a new era of research on target validation and mechanisms of drug action (Giaever, 2003; Outeiro and Giorgini, 2006). This new approach, coined by the Samson lab “genomic phenotyping” (Begley et al., 2002) provides complementary data to other genomic investigations such as transcriptional profiling. However, unlike transcriptional profiling, which rarely indicates the gene products that confer resistance to a given agent (Birrell et al., 2002), genomic phenotyping often pinpoints the pathways responsible for modulating the toxicity of a given agents. Additionally, genomic phenotyping can provide valuable information about all the targets of a drug, including mechanistic clues about the unintended or off-target effects (Kemmer et al., 2009; Ericson et al., 2008). In most cases, yeast genomic phenotyping studies indicate the genetic factors that confer increased sensitivity or resistance to a particular agent; these factors are usually closely related to the mechanism of action of the agent. For example, mutants lacking genes involved in various DNA repair processes are often very sensitive to DNA damaging agents, suggesting that the DNA repair pathways are important modulators of the toxicity of the DNA damaging agents (Lee et al., 2005).

The yeast single gene knock-out mutant library was designed for a massively parallel screening protocol (Winzeler et al., 1999). Each mutant incorporates two unique DNA

barcodes, flanked by priming regions common for all mutants. Using PCR amplification and hybridization on a DNA array, the relative numbers of each mutant in a pooled population can be determined. The pooled population can then be exposed to various agents or environmental factors to determine their genomic phenotype. After such a treatment, the growth of the mutants highly sensitive to the agent examined will be affected; therefore their proportion in the pooled population will change significantly (Giaever et al., 2002).

The pooled population approach is very convenient, yet it is not very sensitive (Begley et al., 2004). It only allows good identification of the mutants most affected by the treatment condition. Additionally, it requires microarrays to analyze the pooled population, and at the time when the experiments described herein were set up, these were prohibitively expensive. Furthermore, the pooled population method assumes that the yeast mutants grow independently of each other in the same culture tube, and ignores any possible crosstalk that might be occurring between different yeast mutants. Therefore, we opted for a very labor intensive method in which each mutant is grown and characterized separately. The model for this approach has been described by (Begley et al., 2002), where it was shown that by characterizing mutants' sensitivities one at a time, for multiple doses, the dynamic range of the assay increases significantly, yielding quantitative and reproducible data.

Unfortunately, the original method described by Begley et al, 2002 did not work well with 11 β -dichloro. The method involves creation of drug plates, which are agar dishes in which the test compound has been dissolved in the agar medium before pouring. A number of reasons such as low solubility, high reactivity and biophysical interactions with the medium (adsorption) have been invoked to explain why the 11 β -dichloro drug plates had no effect on the yeast growth in preliminary studies. In Appendix B, we include some experimental results that might explain why these initial experiments failed. Therefore, we developed a new approach that combines the method of Begley et al, 2002 with an older protocol commonly used for testing reactive compounds (McHugh et al., 1999) and with a spectrophotometric method of quantifying yeast growth in microplates (Simon et al., 2000). Preliminary results indicated that our new approach is adequately sensitive, and although

very labor intensive, it works well for assessing the sensitivity of yeast mutants to 11 β -dichloro.

The current Chapter describes the treatment of the complete single-gene knockout mutant yeast library with 11 β -dichloro and a high level analysis of the results. We shall focus on the properties of the whole group of mutants we identified as sensitive to 11 β -dichloro, exploring how this compound compares in terms of gene ontology (GO) functions, processes and localization with other DNA-damaging agents. We shall also highlight several of the pathways that seem involved in modulating toxicity of 11 β -dichloro in yeast. However, because our goal is to identify valuable leads to testable hypotheses in human cancer cell lines, we will focus less on the specific mechanism of toxicity in yeast, and more on how the yeast data can help design subsequent experiments that explore the features of the mechanism relevant for 11 β -dichloro's toxicity against cancer cell lines.

2.2 Materials and Methods

2.2.1 Reagents

Compounds 11 β -dichloro and 11 β -dimethoxy were synthesized using previously reported schemes (Marquis et al., 2005). Stock solutions (10 mM) were prepared in anhydrous DMSO (Sigma).

2.2.2 Yeast cell lines and culture

The *Saccharomyces cerevisiae* yeast genomic library, consisting of the parental strain BY4741 and 4841 non-lethal single gene knock-out haploid mutants was kindly provided by Professor Leona Samson, and manufactured by Research Genetics of Carlsbad, CA. The parental strain (BY4741 transformed with the pYE13g plasmid to achieve G418 resistance) was kindly supplied by Dr. Thomas Begley and Professor Leona Samson. The yeast strains are the exact strains used in the Begley et al, 2004 study. The strains were kept as glycerol stocks frozen at -80°C. When needed, each strain was inoculated into YPD rich medium supplemented with 200 μ g/mL G418 antibiotic (Invitrogen) and grown overnight ($OD_{600} > 2.0$). This starter culture was then used to inoculate the cultures for treatments. The YPD (yeast extract, peptone, dextrose) rich medium was prepared as follows: 20 g peptone and 10 g yeast extract (BD Biosciences) were dissolved in 0.8 L of doubly-distilled H₂O (ddH₂O) and autoclaved at 120°C, 20 psi for 25 minutes. The medium was allowed to cool down to room temperature, then 200 mL of a 20% filter-sterilized solution of D-glucose were added. The G418 antibiotic was also added at this time, if needed.

2.2.3 Survival analysis

Yeast cells were inoculated using a 96-pin replicator tool from frozen master plates into 150 μ L liquid YPD supplemented with G418 antibiotic and grown at 30°C for 36 hours. These saturated cultures were then used to inoculate an exponential culture for treatment, also in 150 μ L liquid YPD (with G418) and grown at 30°C for 12 hours. Cell concentration

was determined using a SpectraMax 250 multiwell plate spectrophotometer (Molecular Devices, Sunnyvale, CA, USA), which has been previously calibrated with cell stocks of known cell density, as determined with a haemocytometer (Neubauer Improved, Marienfeld, Germany). Cells were pelleted in a Sorvall Instruments RC-3B swing-bucket refrigerated centrifuge at 2000 rpm for 5 minutes and the supernatant was removed by vacuum aspiration. The cells were then resuspended in PBS (phosphate-buffered saline pH = 7.4) at a concentration of 2×10^7 cells/mL, yielding a PBS cell stock that was used for aliquoting cells into each drug treatment condition.

The toxicant solutions were prepared fresh before each experiment by mixing the corresponding amount of agent stock (in 100% DMSO) with PBS and additional DMSO so that final concentration of DMSO is 0.5% (v/v) in all samples. The solutions were then aliquoted into a fresh 96-well flat-bottom plate, 130 μ L per well. 20 μ L of the PBS cell stock solution were then added to each well, for a total reaction volume of 150 μ L. In each reaction well, the yeast cell density was 2.5×10^6 cells/mL. Each strain at each compound concentration was tested in triplicate. The plates were sealed with Breath-EZ air-permeable membranes (USA Scientific, Ocala, FL, USA), mixed on a MicroPlate Genie (USA Scientific), and incubated at 30°C and 300 rpm agitation for 4 hours. After incubation, cells were pelleted, washed once with PBS (150 μ L/well) and then resuspended in 200 μ L/well fresh YPD (without antibiotic). The plates were sealed again with Breath-EZ membranes and incubated at 30°C and 300 rpm agitation for 12 hours. At this point, plates were carefully homogenized on the MicroPlate Genie and OD₆₀₀ spectrophotometer readings were taken to determine the extent of growth in each well.

2.2.4 Library screening approach

Each library plate was replicated from the frozen stocks into a fresh 96 well master plate containing YPD medium supplemented with G418 antibiotic. Each plate had 6 empty wells in which control strains were inoculated from frozen stocks. The control strains were BY4741 (WT), Δ COX9, Δ ERG6, Δ REV1, chosen based on preliminary studies. Δ COX9,

Δ ERG6 mutants are highly sensitive to 11 β -dichloro treatment and serve as positive controls. Δ REV1 mutant was chosen as a typical mutant sensitive to DNA damaging agents; however, it is not sensitive to 11 β -dichloro and could serve as a negative control. The master plate was grown at 30°C to stationary phase and then replicated again into a submaster plate, which was then grown to exponential phase. The treatment and survival analysis was then carried out as described above.

2.2.5 Statistical analysis

All results are expressed as mean +/- standard deviation. The significance of the difference between two different populations was calculated using Student's t-test for unpaired, heteroscedastic populations. P values less than 0.05 were considered significant. The GO term enrichment statistics were done using the GO Slim Mapper and GO Term Finder tools available at the Saccharomyces Genome Database (SGD) website (www.yeastgenome.org).

2.3 Experimental Results

2.3.1 Validation of the spectrophotometric quantitation of cell growth

We established that the SpectraMax 250 spectrophotometer gives a good linear correlation ($R^2 > 0.99$) between the OD_{600} of a 200 μ L yeast cell suspension in a well of a flat-bottom 96-well microplate (Corning Inc., Corning, NY, USA) and the cell density in the well (Figure 2.2). The different cell densities were obtained by diluting a concentrated (3×10^8 cells/mL) stock of wild-type cells. The resulting curve also indicates the dynamic range of the assay; based on the spectrophotometer linear range, we can accurately detect up to 50 fold differences in cell densities, which corresponds to 1.7 orders of magnitude on a \log_{10} scale or about 6 orders of magnitude on a \log_2 scale. The \log_2 of relative differences will be used to construct a volcano plot in section 2.3.3. However, it is important to remember that the curve in Figure 2.2 only measures the ability of the instrument to distinguish between different cell densities. Some of the high densities of cells shown on the curve may not be actually reached by cells growing the microplate wells.

Our assay is based on quantifying the growth extent of the yeast cells. It was therefore important to test how the relative growth rate is affected by the initial concentration of viable cells, and when the cells reach their saturation point and stop growing. Dilutions of an initial stock (2×10^7 cells/mL) of wild-type cells were made, washed with PBS and then incubated in YPD for 8, 12 and 14 hours. We found that the relative growth extent is independent of the initial density of the cells (Figure 2.3) at 8 and 12 hours. The cell densities (measured by OD_{600} readings) after 8, 12 and 14 hours of growth are proportional to the initial cell densities; therefore, a difference in seeding density, difference that in an actual experiment could be due to differential sensitivity to toxicants, would translate into a proportional growth difference. We also found that the 12 hour growth makes use of the maximum dynamic range available in the experimental conditions. Longer incubations cause the cells that started with higher initial densities to stop growing when they reach $OD_{600} \approx 0.850$. When cells reach saturation, small differences in the initial number of yeast cells will not be detected any

longer. Based on these observations, we chose the 2×10^7 cells/mL density as the treatment density for the cells, and the 12 hour time point as the data collection time point. These experimental conditions are optimized for detecting sensitive mutants, i.e., mutants that grow slower when exposed to the toxicant, compared to when grown untreated. However, these conditions are not ideal for detecting resistant mutants, i.e., mutants that grow faster when exposed to the toxicant. To detect resistant mutants, smaller growth intervals (e.g. 8 hours) can be used. Our analysis, however, focused on identifying only the mutants sensitive to 11 β -dichloro.

2.3.2 Choosing and characterizing the control strains

An initial set of 455 mutants (about one 10th of the entire library) was selected for preliminary testing. These mutants were selected to correspond to a random group of genes spanning all the gene ontology (GO) functions. We also included a selected group of mutants that showed high sensitivity to MMS (methyl methane sulfonate) and 4NQO (4-nitro-quinoline oxide) alkylating agents based on published data (Begley et al., 2004). The rationale was that mutants sensitive to alkylating agents (especially the bulky 4NQO) are likely to be sensitive to 11 β -dichloro, which is also a potent DNA alkylator. However, the experimental results showed that very few of the chosen mutants sensitive to 4NQO and MMS were in fact sensitive to 11 β -dichloro. Nevertheless, this initial screen did identify two very sensitive mutants, Δ ERG6 and Δ COX9. From the mutants that show very little sensitivity to 11 β -dichloro, but are very sensitive to MMS and 4NQO, we chose Δ REV1 as a negative control.

The control strains were then used to validate our method by comparing it to the standard colony forming assay (CFA) for yeast cells (McHugh et al., 1999). The exposure to 11 β -dichloro was done in the 96-well format as described in Materials and Methods, but after washing with PBS, the cells were analyzed by the two methods in parallel. The results confirmed that our method can produce comparable results with the CFA (Figure 2.4). At a semi-quantitative level, both methods indicate that the Δ ERG6 and Δ COX9 mutants are significantly more sensitive to 11 β -dichloro than the WT or Δ REV1 strains. However, given

the smaller dynamic range of our method, we do not detect the difference in sensitivity between Δ ERG6 and Δ COX9 at the 40 μ M dose; this difference is nevertheless revealed by the more sensitive method, CFA. We conclude that our method might not be suitable for distinguishing between mutants of different grades of high sensitivity; however, the treatment with one single dose of the compound may be enough to identify semi-quantitatively the mutants significantly sensitive to 11 β -dichloro.

To select the treatment dose of our agent, we exposed our control strains to a number of different doses. There were significant concerns about the poor solubility of 11 β -dichloro in PBS during the treatment of the cells, given that the compound has a water/octanol partition coefficient (log P) of 5.05 (Hillier, 2005). However, the experimental results clearly show that for the range of concentrations used (10-20 μ M), the sensitive mutants (Δ ERG6, Δ COX9) exhibit a dose response to 11 β -dichloro (Figure 2.5). The dose response curves indicate that the formulation of 11 β -dichloro in the experimental conditions is sufficient for generating quantitative and reproducible data, irrespective of the exact nature of the compound's interaction with the PBS vehicle (solution versus suspension). Figure 2.5 indicates that the dose of 20 μ M 11 β -dichloro would be a good choice, because it provides a good differential toxicity between the WT strain and the sensitive control strain, yet it has also a slight effect on the growth extent of the WT strain.

2.3.3 Screening the complete single gene knockout mutant yeast library

The entire library consisting of 4841 single-gene knockout mutants was screened for phenotypic changes following exposure to a dose of 20 μ M 11 β -dichloro for 4 hours. The extent of growth for each mutant after exposure to 11 β -dichloro or after exposure to vehicle was quantified after 12 hours and used to calculate a simple metric of sensitivity, percentage relative growth, which we define as the percentage ratio between the growth extent in the treated condition and the growth extent in the control (untreated) condition. The data was binned in 1% intervals and used to construct a sensitivity histogram of the whole collection of mutants (Figure 2.6). By using the variance across the biological triplicates in both the treated and untreated conditions, significance values (p-values) were calculated and used to

delineate different groups of mutants (Table 2.1). The p-values illustrate the robustness of our method; even for very small changes in relative growth, we often recorded a highly significant p-value. This phenomenon is likely due to spectrophotometric quantitation of growth, which yields very small standard deviations for each data point.

Another way to display the sensitivity of the entire library is to use a volcano plot (Figure 2.7). Each data point corresponds to one mutant, positioned on the graph according to its relative growth and p-value. The X-axis shows the relative growth, expressed as a \log_2 fold change (LFC). A value of 0 corresponds to no-change (relative growth = 100%). Negative values indicate a decrease in the quantity measured. For example, LFC = -1 indicates a change of $1/2$ ($2^{(-1)} = 1/2$), corresponding to relative growth = 50%. Likewise, LFC = -2 corresponds to a relative growth of 25% ($2^{(-2)} = 1/4$). All the mutants with negative LFC values are displayed in red. Since most single-gene knockout yeast mutants have a diminished ability to withstand toxic insults such as 11 β -dichloro, most of the points will be red, depicting a decrease in relative growth. If the mutants grow better when treated with 11 β -dichloro, compared with vehicle treated only, their LFC is positive, corresponding to a relative growth greater than 100%. The LFC positive points are displayed in green. As the Figure shows, very few of the data points are green. The Y-axis of the graph indicates the significance of the data, in terms of the p-value. For better visualization, the base-ten logarithm of the p-value is plotted. In our experimental setup, the p-value represents the probability that the change in the growth ability of one yeast mutant is due to chance and not to the 11 β -dichloro treatment. Therefore, the lower the p-value is, the higher the significance of the measured effect. The volcano plot in Figure 2.7 highlights the fact that most of the mutants displaying low relative growth (low LFC values) also have very low p-values, indicating these mutants as the most sensitive group. Accordingly, we chose the cut-off points at LFC < -1 (corresponding to 50% or less relative growth) and p-value < 0.001, yielding a group of 848 mutants we called sensitive to 11 β -dichloro (Figure 2.8). Other levels of cutoff and their corresponding number of mutants are highlighted in Table 2.2. The complete list of the genes knocked out in the mutants sensitive to 11 β -dichloro, including a brief description of the function of each gene, and the sensitivity of the corresponding knockout mutant to other DNA-damaging agents, is provided in Appendix A.

2.3.4 The GO localization, processes and functions of mutants sensitive to 11 β -dichloro

Having identified a group of mutants sensitive to 11 β -dichloro, we wanted to investigate the specific cellular pathways that are affected in these mutants. The most general approach is to use gene ontology (GO) mining tools to determine if the genes knocked out in the corresponding mutants in our group are associated with specific GO terms. The GO system classifies each gene in terms of the cellular localization (GO component), cellular process (GO process) and cellular function (GO function) of the protein encoded by that gene. Given the diverse and overlapping functions of many proteins, a gene is often associated with several GO terms in each category. Additionally, the GO classifications are hierarchical, meaning that once a gene is associated with a GO term, it also receives the GO terms of its hierarchical parents. For example, if a protein localizes in the mitochondrial membrane, it is classified with the GO component term “mitochondrial membrane”. However, the GO term “mitochondrial membrane” denotes a subgroup of all the proteins that localize in the mitochondria (GO component term “mitochondrion”). Likewise, proteins that localize in the mitochondria are a subgroup of all the proteins in the cell (GO component term “intracellular”). Therefore, the mitochondrial membrane protein will be associated not only with the GO term “mitochondrial membrane”, but also with “mitochondrion” and “intracellular”.

The GO system nomenclature allows us to find the specific GO terms that describe the genes knocked out in the mutants we identified as sensitive to 11 β -dichloro. However, a more informative approach is to inquire whether among all the GO terms associated with our collection of mutants, there are certain GO terms that appear more often in our collection than they do in the whole genomic library. Such terms would indicate components, processes or functions that are more highly represented in our collection than on average in the whole genomic library, suggesting that these components, processes or functions are related to the mechanism of toxicity of 11 β -dichloro. Given that we are interrogating knockout mutants,

the cellular pathways and processes associated with the missing genes denote, in fact, pathways that modulate the resistance of the yeast cells to our compound.

By employing the GO Term Mapper tool from the SGD website, we obtained the GO components, GO functions and GO processes that are significantly enriched in the collection of genes corresponding to the group of mutants most sensitive to 11 β -dichloro (Table 2.3 – 2.5). The results were quite unexpected. The GO component terms indicate that a large portion of the proteins, encoded by the genes knocked out in our collection of mutants sensitive to 11 β -dichloro, localize in the mitochondria. Several GO terms associated with mitochondrial localization, such as “mitochondrion”, “mitochondrial inner membrane”, “mitochondrial matrix” and “mitochondrial envelope” are significantly enriched in our collection of genes (Table 2.3). Another clustering site, highly represented, is the ribosome. Interestingly, the GO component analysis does not find enrichment for other cellular compartments, such as the nucleus. Given that 11 β -dichloro is a DNA-damaging agent, mutants lacking genes involved in DNA repair were expected to be very sensitive to 11 β -dichloro; the proteins corresponding to the genes involved in DNA repair would most often localize in the nucleus. However, our data indicates that the nucleus is not a significantly enriched GO component term, suggesting that among the mutants sensitive to 11 β -dichloro, there may not be a large number of mutants knocked out for genes encoding proteins that localize in the nucleus. The GO processes and functions identified for the 11 β -dichloro sensitive mutants provide similar insights. Among the GO processes (Table 2.4), we recognize several associated with mitochondria, such as “aerobic respiration”, “generation of metabolites and energy”, and “energy derivation by oxidation of compounds”. Processes associated with ribosomes are also well represented, such as “macromolecule biosynthetic process” and “translation”. The GO processes do contain several that are associated with DNA damage and repair, such as “telomere maintenance” and “chromosome organization and biogenesis”, although the last term could also refer to the mitochondrial DNA, in addition to the nuclear DNA. Unlike the GO processes, the GO functions refer to specific classes of protein functions, rather than entire cellular pathways. The five GO functions significantly enriched in our dataset reinforce the previous observations; they are exclusively mitochondrial or ribosomal functions (Table 2.5).

2.3.5 Common mutants between most sensitive mutants to 11 β -dichloro and most sensitive mutants to other DNA alkylating agents

The analysis of the GO terms suggested that both the mitochondria and the ribosomes may play important functions in modulating the sensitivity of the yeast cells to 11 β -dichloro; at the same time, the analysis indicated that given the absence of a large number of proteins that localize in the nucleus, and the absence of enriched processes and functions related to DNA repair, DNA damage might not be the central mechanism of toxicity of 11 β -dichloro in yeast cells. To investigate more closely how the putative effects of 11 β -dichloro on DNA translate into phenotyping data, we compared the collection of mutants sensitive to 11 β -dichloro with collections of mutants sensitive to other DNA damaging agents. Specifically, we investigated how many of the mutants we identified as sensitive to 11 β -dichloro are also sensitive to methylmethane sulfonate (MMS), tert-butyl peroxide (TBP), 4-nitro-quinoline oxide (4NQO) and ultra-violet light (UV), using literature reported data (Begley et al., 2004).

The results indicate that there is a significant overlap between the mutants sensitive to 11 β -dichloro and the mutants sensitive to the 4 DNA-damaging agents tested by Begley et al. (Table 2.6). Even more intriguing, the proportion of mutants in our collection that are also sensitive to one of the other 4 DNA-damaging agents is significantly higher than the proportion of the same kind of sensitive mutants in the entire library. The most impressive enrichments happen in the cases of 4NQO (26.9% of mutants in the 11 β -dichloro sensitive group compared to 17.3% in the entire library) and UV light (13.7% of the 11 β -dichloro sensitive group compared to 6.1% in the entire library). However, the fraction of MMS and TBP sensitive mutants is also enriched in the 11 β -dichloro group (38.2% versus 30.0% for MMS, and 14.0% versus 9.4% for TBP). We then performed the same analysis but with only the top most sensitive mutants in the 11 β -dichloro group. Among the top 351 mutants most sensitive to 11 β -dichloro (corresponding to a cutoff LFC < -2), the proportion of 4NQO and UV sensitive mutants increases even more (for 4NQO, 31.5% versus 17.3%, and for UV 18.5% versus 6.1%). For an even more stringent cutoff (LFC < -3), which comprises only 142 mutants, the high proportion of 4NQO and UV sensitive mutants is maintained (Table

2.6). All these data suggest that the putative 11 β -dichloro-induced DNA damage has similarities to the cell stress and damage induced by 4NQO, a bulky alkylating agent and UV light, a DNA crosslinking agent. However, the mutants sensitive to both 11 β -dichloro and another DNA damaging agent may also be mutants critically impaired in dealing with most environmental stresses and hence, they would be sensitive to many different agents. Supporting evidence for this hypothesis comes from the proportion of mutants sensitive to all four agents tested by Begley et al. Only a relatively small number of mutants (27) from the entire library were found sensitive to all four agents (Begley et al., 2004). Of these, 11 are also sensitive to 11 β -dichloro, which corresponds to a twofold enrichment (1.30% in the 11 β -dichloro group versus 0.56% in the entire library).

2.3.6 The GO localization, processes and functions of mutants uniquely sensitive to 11 β -dichloro

Despite the good overlap between the mutants sensitive to 11 β -dichloro and one of the four DNA damaging agents from the Begley et al., 2004 study, a large proportion of the mutants sensitive to 11 β -dichloro are uniquely sensitive to our agent. The last column in Table 2.6 indicates that over 40% of the mutants sensitive 11 β -dichloro, at every cutoff level, are insensitive to MMS, 4NQO, TBP or UV radiation, suggesting that the mechanism of toxicity of 11 β -dichloro may involve an additional pathway, independent of DNA damage. We explored the nature of this additional pathway or pathways by reiterating the GO term cluster analysis on the subgroup of mutants sensitive to 11 β -dichloro but insensitive to MMS, 4NQO, TBP or UV. This subgroup is comprised of 373 genes (44% of 848 total sensitive mutants, Table 2.6). Interestingly, the results are very similar to the one observed in the previous GO analysis; the GO terms related to mitochondria and ribosomes are significantly enriched (Tables 2.7-2.9). In fact, the majority of the GO component and GO process terms refer to mitochondria or ribosomes. These data suggest that mitochondrial and ribosomal function play a key role in modulating the toxicity of 11 β -dichloro in a manner that is DNA damage independent.

2.4 Discussion

The goal of this study was to develop a better understanding of the cellular targets of 11 β -dichloro, a novel anti-tumor agent that has shown very good efficacy both *in vivo* and *in vitro* (Marquis et al., 2005; Hillier et al., 2006). Although this compound contains by design an estradienone moiety that allows it to bind to the androgen receptor (AR), experimental evidence has shown that 11 β -dichloro can also be very toxic against cell lines that do not express the AR (Hillier, 2005). Given the likely possibility that 11 β -dichloro utilizes several mechanisms of toxicity, we attempted to capture a genomic snapshot of the toxicity profile of our agent, by interrogating the complete, single gene knockout mutants yeast library.

As a model organism, the yeast *Saccharomyces cerevisiae* has been successfully employed to characterize mechanism of toxicity of many DNA damaging compounds (Lee et al., 2005; Begley et al., 2004). The versatility of this simple eukaryote combined with the large amount of available genomic and functional information make *S. cerevisiae* a standard development tool and test bed for many pharmaceuticals, including chemotherapeutic agents (Menacho-Márquez et al., 2007; Armour and Lum, 2005). In particular, the availability of the single gene knockout mutant library is very useful, because it allows generation of phenotypic data, inaccessible through other genomic high-throughput methods such as transcriptional profiling.

Although several approaches of interrogating the yeast genomic mutant library existed, none were suited perfectly for 11 β -dichloro. Given the poor solubility of our compound, we were limited at a relatively low maximal dose, and therefore needed a very sensitive method. The approach described by Begley et al., 2002 gave the best sensitivity but required the compound to be stable and soluble in the YPD-agar medium. Preliminary experiments showed that the Begley et al. method could work after certain modifications. In an attempt to minimize the amount of compound used (11 β -dichloro is expensive to synthesize), we opted for a liquid culture spectrophotometric method for detecting growth (Simon et al., 2000), and small volume, individual well treatments for the drug exposure. PBS was chosen as a drug vehicle instead of rich medium, following example of other yeast treatments involving

nitrogen mustards (Brooks et al., 1999; McHugh et al., 1999). The resulting approach, albeit very labor intensive, proved to be successful at generating high-quality data about the sensitivities of different mutants to 11 β -dichloro.

The screening results showcased several interesting characteristics. As seen on the data histogram (Figure 2.6), most mutants show a small but measurable phenotype, their relative growth being between 60% and 90%. The volcano plot (Figure 2.7) indicates that a large number of these small effects are in fact significant, at the 0.05 and 0.01 level. This phenomenon is not entirely surprising, being a confirmation on the high sensitivity of the method. Moreover, the dose of 11 β -dichloro used was high enough to cause 10-20% growth inhibition in the WT strain, therefore, most other strains should be affected at a similar level. However, a substantial number of yeast mutant strains show much smaller relative growths, clustering in the left most tail of the histogram; these are the mutants highly sensitive to 11 β -dichloro. The p-values corresponding to the highly sensitive mutants are even lower, reflecting the increased mean difference, in addition to the treated and untreated variances of the samples.

Our choices for cutoffs were based on the distribution of the data; we considered that the responses of non-sensitive mutants to 11 β -dichloro would cluster together in a relatively tight distribution, whereas the sensitive mutants would end up far from the mean of such distribution, in an outlying tail. Other methods of screening only rank the mutants in an increasing order of sensitivity and use a p-value cutoff to distinguish between sensitive and non-sensitive mutants. Often times, such methods only identify accurately only the top-most sensitive mutants (Lee et al., 2005; Hillenmeyer et al., 2008). Given our good p-values for most of the mutants, we relied on the effect size to delineate the group of mutants sensitive to 11 β -dichloro. The twofold decrease in growth extent was very close to the point lying two standard deviations away from the mean of the entire data distribution (assumed to be lognormal) and thus it was chosen as the initial cutoff for sensitivity. More stringent cutoffs can be made to isolate the groups of topmost sensitive mutants (Table 2.2).

The GO analysis of the most sensitive mutants to 11 β -dichloro generated some unexpected results. Although 11 β -dichloro is a nitrogen mustard, capable of alkylating DNA both *in vitro*

and in cell culture (Marquis et al., 2005; Hillier et al., 2006), the DNA-damaging properties of 11 β -dichloro are not very apparent in yeast cells, according to the enriched GO terms corresponding to the genes knocked out in the mutants sensitive to our agent. If DNA damage played a prominent role in toxicity, we would have expected that a significant number of mutants lacking various DNA repair capabilities to be very sensitive to 11 β -dichloro. This is the case for many DNA alkylating agents, such as MMS, 4NQO (Begley et al., 2004), cisplatin or mechlorethamine (Lee et al., 2005), for which the GO term analysis clearly indicates an enrichment in terms related to DNA damage and repair, and the nuclear localization of the proteins involved in such pathways. Nevertheless, even for simpler DNA alkylating agents such as MMS, 4NQO or UV light, the GO terms related to DNA damage constitute only a small fraction of all the GO terms. Many other GO terms from other pathways are enriched for MMS, 4NQO and UV light (Begley et al., 2004). Curiously, the GO terms related to DNA damage, DNA repair or nuclear localization are absent from the GO term cluster analysis on the mutants sensitive to 11 β -dichloro. Instead, the GO terms we found enriched refer to mitochondrial and ribosomal function. An enrichment in GO terms associated with ribosomal function has been seen for other DNA damaging agents such as MMS and 4NQO, whereas an enrichment of GO terms associated with mitochondrial function has been seen in the case of UV light and 4NQO (Begley and Samson, 2004). However, the combination of GO terms associated with the group of mutants sensitive to 11 β -dichloro is rather unique; the absence of GO terms pointing to nuclear proteins and the large number of GO terms pointing to mitochondrial and ribosomal function constitute unexpected and important findings of our study.

Nevertheless, certain mutants lacking DNA repair capabilities are sensitive to 11 β -dichloro. In fact, a significant number of mutants sensitive to 11 β -dichloro are also sensitive to MMS, 4NQO and UV radiation (Table 2.6). By closely investigating these common mutants, we identified genes such as RAD17, RAD51, RAD52 and RAD55 whose deletion renders the cells sensitive to DNA damage. Such a finding corroborated the observation that over 40% of the mutants sensitive to 11 β -dichloro are not sensitive to any of the four agents tested by Begley et al (Table 2.6, last column) and suggests that 11 β -dichloro may have several distinct modes of toxicity. Some of these may involve DNA damage but others probably do not. The

GO analysis of the mutants uniquely sensitive to 11 β -dichloro highlighted almost exclusive enrichments in mitochondrial and ribosomal related GO terms, suggesting that mitochondrial and ribosomal functions may be key modulators of 11 β -dichloro toxicity, possibly in a DNA damage independent manner.

While our data suggest that mitochondrial function is an important modulator of 11 β -dichloro toxicity, it does not pinpoint the exact target of the compound in cells. One possible hypothesis is that mitochondria assist in diminishing the toxic effects of 11 β -dichloro, by either detoxifying reactive intermediates (such as reactive oxygen species), generating metabolic precursors necessary for repairing cellular damage caused by the compound, or by simply generating the energy necessary for the cell to fend off the toxic effects of the agent. This hypothesis implies that the main targets of 11 β -dichloro are outside the mitochondria. However, another possible theory is that 11 β -dichloro targets mitochondria directly. While certain mitochondrial functions (for example, respiration) may have been compromised by the knocked out gene in the sensitive mutant, other aspects of mitochondrial function may still be intact (for example, certain metabolic reactions), and thus, exposure to 11 β -dichloro may be the last straw that pushes the organelle over the edge, with toxic consequences for the cell. The involvement of ribosomal function as a toxicity modulator can also suggest several hypotheses about the mechanism of toxicity. While the mutants lacking proteins involved in ribosomal function are viable, their translational machinery may not be able to function properly during certain circumstances of cell stress. One instance when translation is tightly regulated in direct response to stress is the unfolded protein response pathway. We hypothesize that 11 β -dichloro may be generating unfolded proteins, triggering the UPR, which requires a selective translation of certain genes. Most of the mutants with impaired ribosomal function will thus be highly sensitive, unable to properly execute the UPR. Other more complicated scenarios are also possible, but it is likely that the mechanism of toxicity involves several different pathways, which contribute differentially, depending on the specific mutant. Our data highlight the complexities of the mechanism of 11 β -dichloro and provides a number of leads that can be investigated further.

2.5 Tables and Figures

Table 2.1	<i>The breakdown of mutants in the library according to their p-value</i>	91
Table 2.2	<i>The breakdown of mutants in the library according to their LFC value</i>	92
Table 2.3	<i>The GO component terms enriched in the subset of mutants sensitive to 11β-dichloro</i>	93
Table 2.4	<i>The GO process terms enriched in the subset of mutants sensitive to 11β-dichloro</i>	94
Table 2.5	<i>The GO function terms enriched in the subset of mutants sensitive to 11β-dichloro</i>	95
Table 2.6	<i>Common sensitive mutants between 11β-dichloro and other DNA damaging agents</i>	96
Table 2.7	<i>The GO component terms enriched in the subset of mutants uniquely sensitive to 11β-dichloro (372 mutants)</i>	97
Table 2.8	<i>The GO process terms enriched in the subset of mutants uniquely sensitive to 11β-dichloro (372 mutants)</i>	98
Table 2.9	<i>The GO function terms enriched in the subset of mutants uniquely sensitive to 11β-dichloro (372 mutants)</i>	99
Figure 2.1	<i>The chemical structures of interest</i>	83
Figure 2.2	<i>SpectraMax250 spectrophotometer calibration curve</i>	84
Figure 2.3	<i>Growth extent estimations for yeast cultures in microwell plates</i>	85
Figure 2.4	<i>Comparison between the liquid culture method and CFA method</i>	86
Figure 2.5	<i>The mutants ΔCOX9 and ΔERG6 exhibit a dose reponse to 11β-dichloro</i>	87
Figure 2.6	<i>The histogram of 11β-dichloro sensitivity of the entire library of mutants</i>	88
Figure 2.7	<i>Volcano plot of the entire data set depicting the sensitivity to 11β-dichloro</i>	89
Figure 2.8	<i>Selecting the sensitive mutants to 11β-dichloro</i>	90

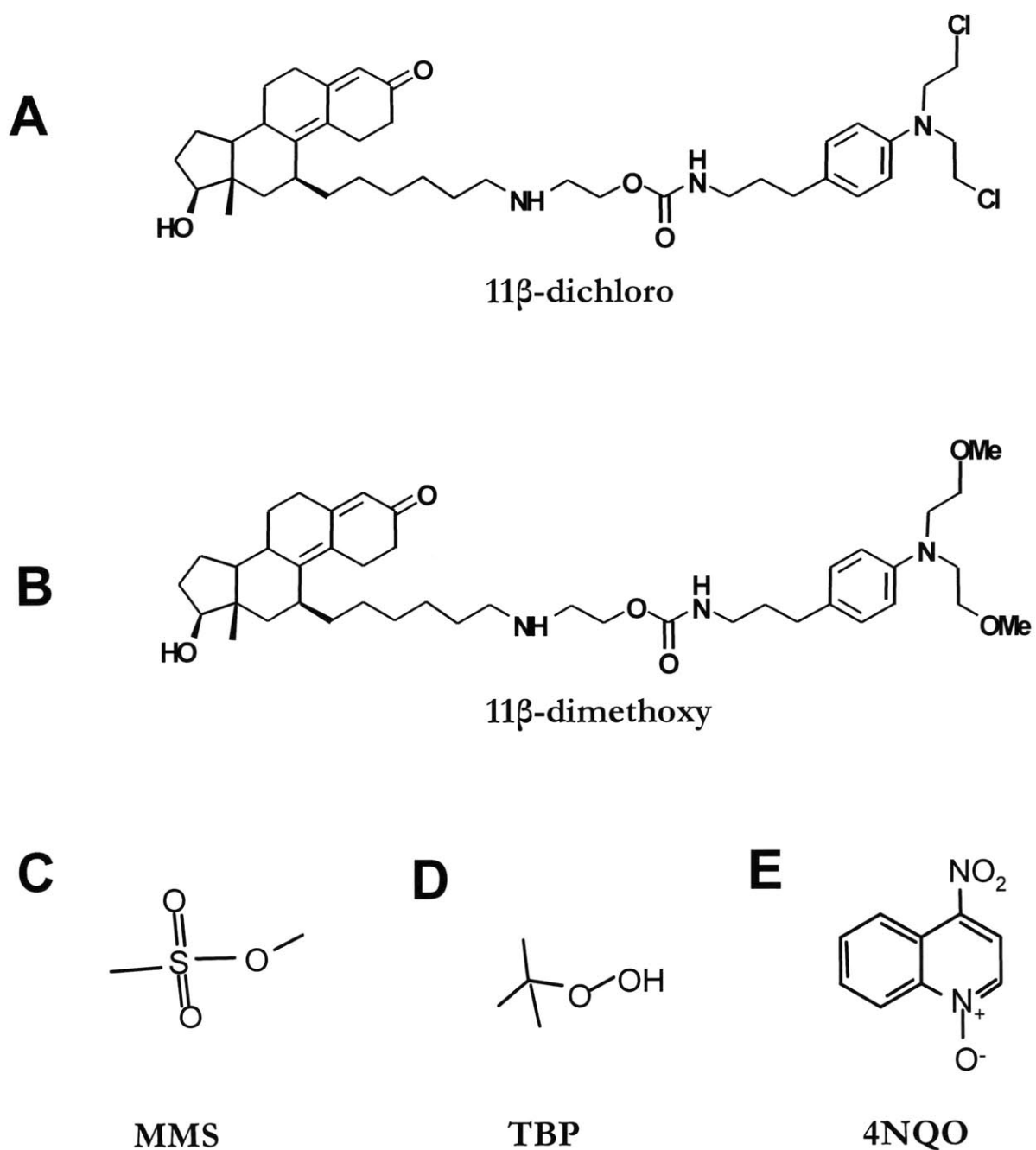


Figure 2.1 The chemical structures of interest

The chemical structures of the compounds used : 11 β -dichloro (A), 11 β -dimethoxy (B), methylmethanesulphonate (MMS) (C), tert-butyl peroxide (TBP)(D) and 4-nitroquinoline oxide (4NQO)(E).

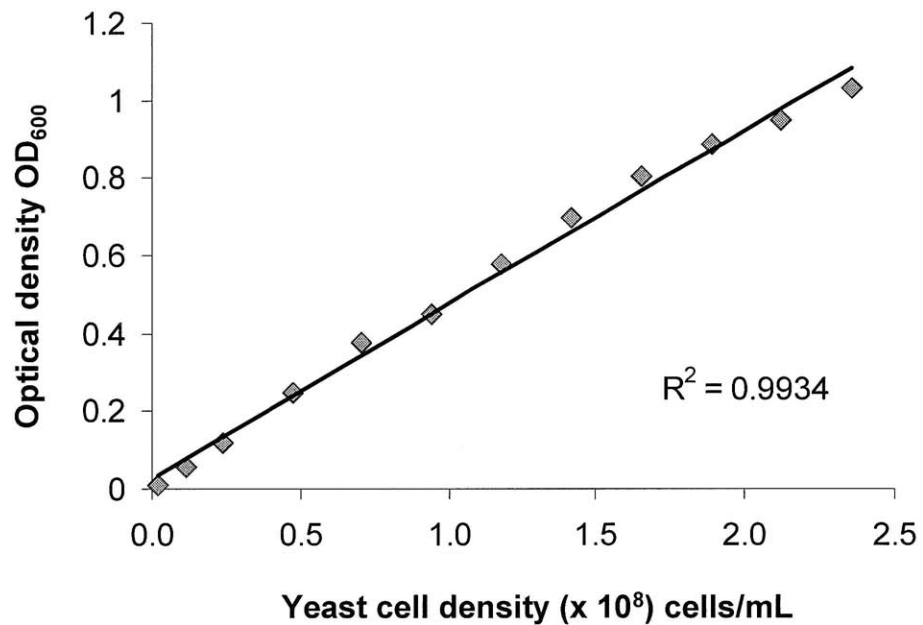


Figure 2.2 SpectraMax250 spectrophotometer calibration curve

The feasibility of using the optical density at 600 nm to measure yeast cell densities in the microplate wells was tested. A yeast cell stock of known density (determined with a haemocytometer) was diluted in microplate wells; the final volume of solution in each well was 200 μL . The data indicate a very good correlation between OD_{600} and cell density ($R^2 = 0.9934$).

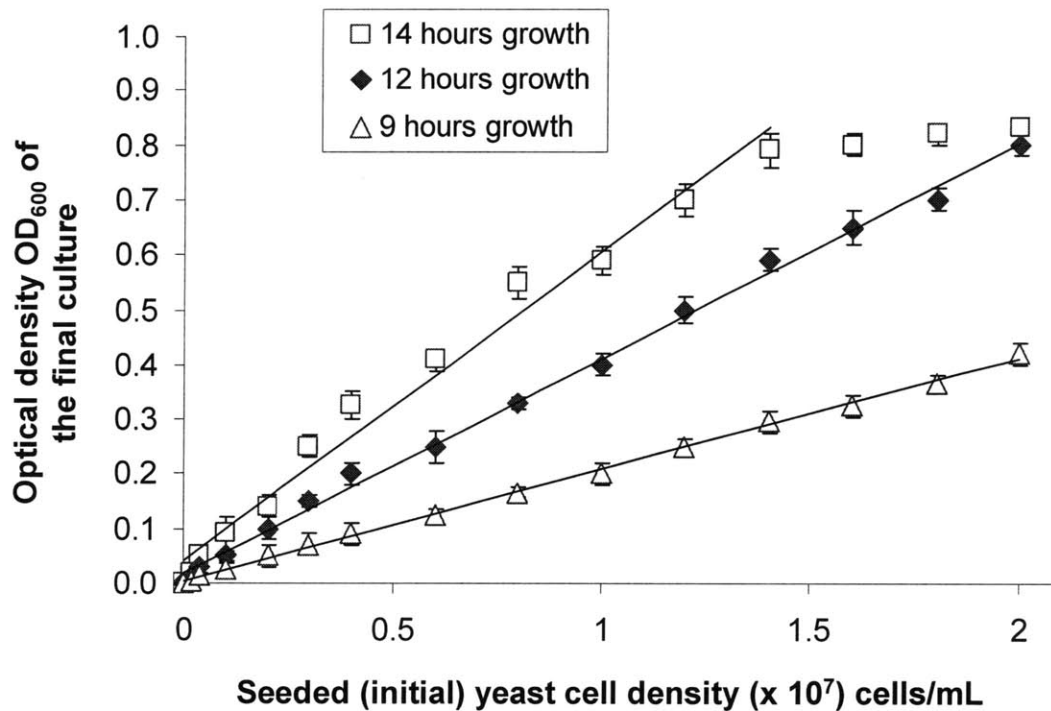


Figure 2.3 Growth extent estimations for yeast cultures in microwell plates

It was of interest to determine the time interval of growth after which an initial difference in cell density translates into a proportional difference in cell density after growth. This amounts to finding an interval of time in which the relative growth extent is essentially independent of the starting cell density. Yeast cells were seeded at concentrations ranging from 5×10^2 to 2×10^4 cells/ μ L and then grown for the indicated amount of time. The data indicate that for the cell densities analyzed, a 12 hour growth interval offers the most dynamic range, yielding a linear relationship between the initial seeding density and the final density of the culture. For longer growth intervals, cells at higher seeding densities reach saturation, and in those cases, OD measurements may underestimate the initial differences in seeding densities.

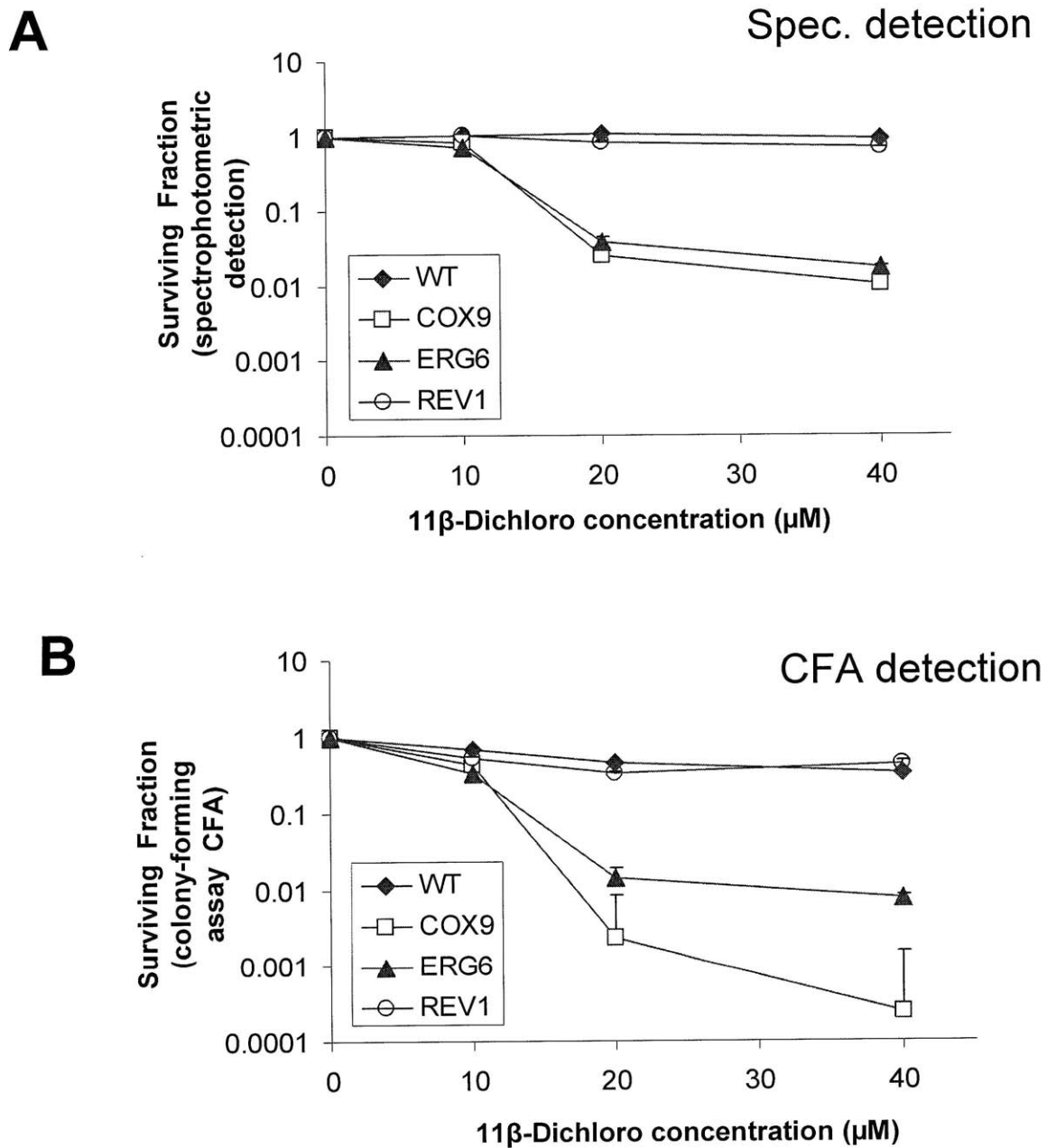


Figure 2.4 Comparison between the liquid culture method and CFA method

A comparison was made between the spectrophotometric method of quantifying sensitivity and the traditional colony-forming assay (CFA). Cells were treated in microwell plates for 4 hours, then analyzed by the two different methods. The spectrophotometric method (A) measures the extent of growth in the liquid culture directly in the 96-well plate. The CFA (B) involves spreading the cells onto media plates and counting the number of colonies that form within 60 hours. The data indicate that the two assays yield similar results, both methods recognizing the Δ COX9 and Δ ERG6 mutants as very sensitive to 11 β -dichloro.

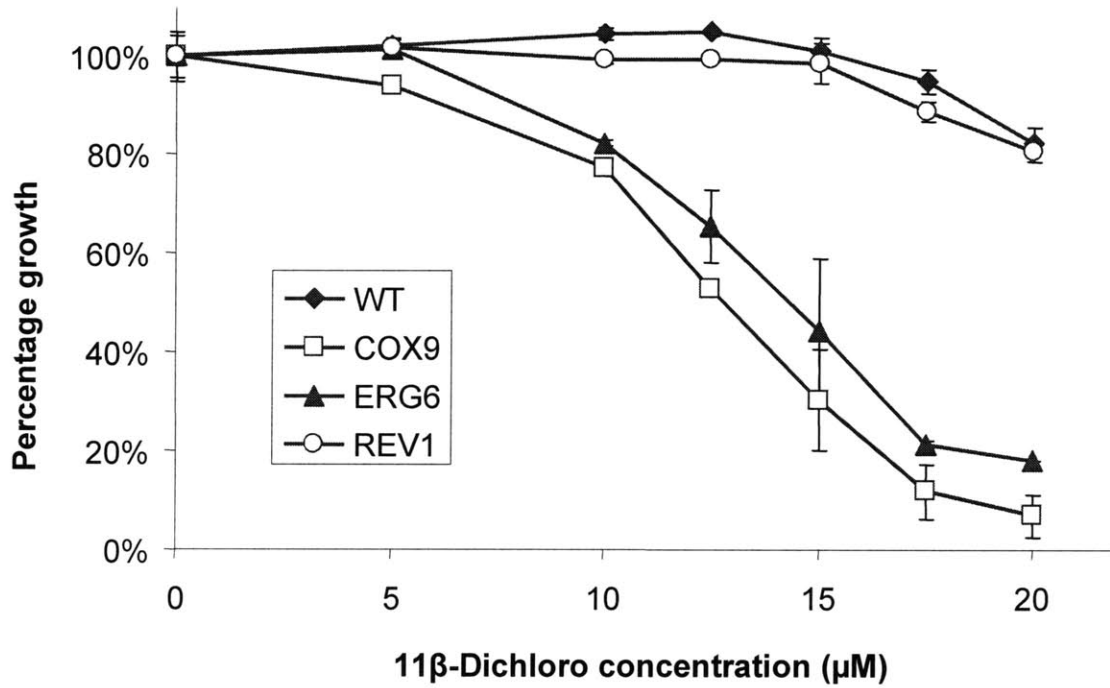


Figure 2.5 The mutants Δ COX9 and Δ ERG6 exhibit a dose response to 11β-dichloro

Yeast cells were exposed for 4 hours to the indicated 11β-dichloro, formulated in PBS with 0.5% DMSO. The data indicate that the sensitive mutants Δ COX9 and Δ ERG6 exhibit a dose response to 11β-dichloro.

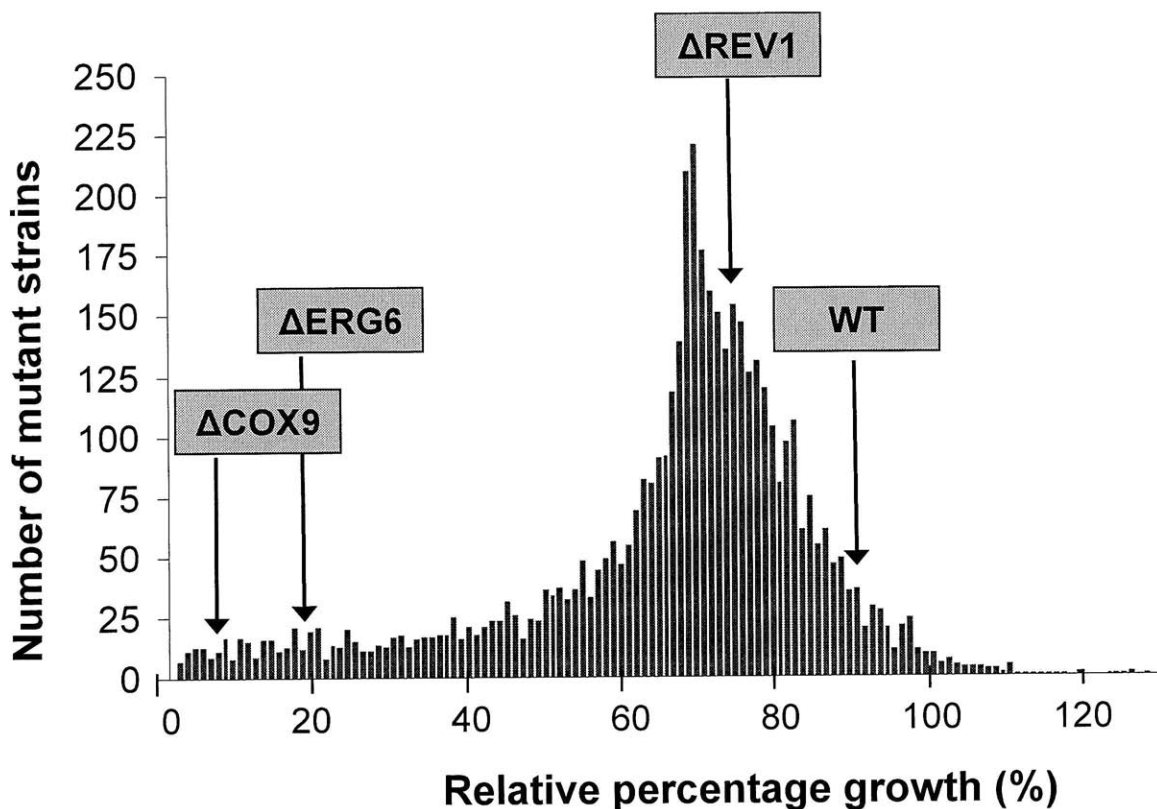


Figure 2.6 The histogram of 11 β -dichloro sensitivity of the entire library of mutants

For each mutant, the relative percentage growth was used as a measure of sensitivity to 11 β -dichloro treatment. The relative percentage growth was calculated as the percentage ratio of the growth of the strain after 11 β -dichloro exposure and the growth of the strain after the control exposure (to vehicle). The histogram was constructed by binning the mutants around each percentage point. The relative percentage growth of the control strains used in each plate (Δ COX9, Δ ERG6, Δ REV1 and WT) is indicated with arrows.

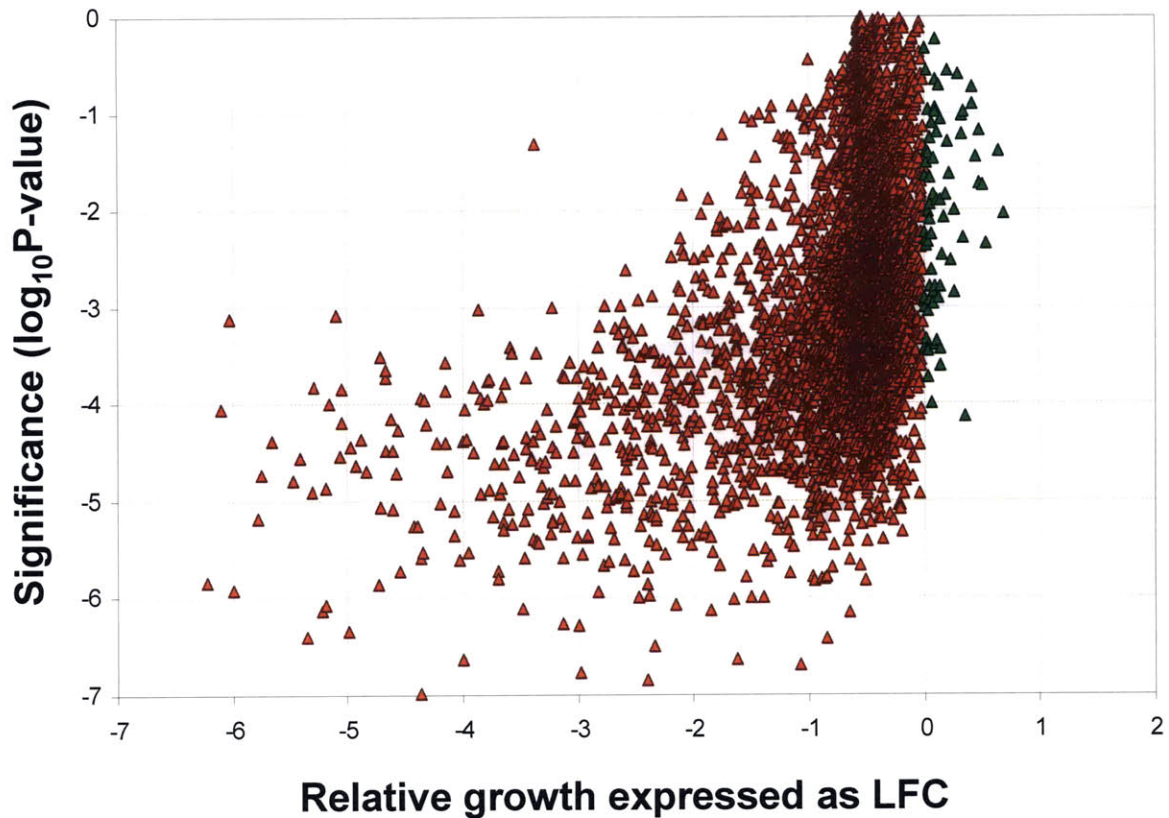


Figure 2.7 Volcano plot of the entire data set depicting the sensitivity to 11 β -dichloro

The measure of sensitivity employed, the relative growth, can be expressed as a log₂ fold-change (LFC) number. The red data points corresponding to negative LFC values, indicate that the growth has decreased compared to the control experiment. The green data points, corresponding to positive LFC values, indicate that growth has increased compared to the control experiment. Therefore, an LFC value of -1 correspond to a relative growth of 50%, an LFC value of -2 corresponds to a relative growth of 25%. The Y-axis measures the p-value associated with each data point; the lower the p-value, the more significant the relative growth measured on the X-axis. The plot highlights the fact most mutants are negatively affected by 11 β -dichloro treatment. However, for the majority of these mutants, their growth does not change by more than two fold (LFC = -1).

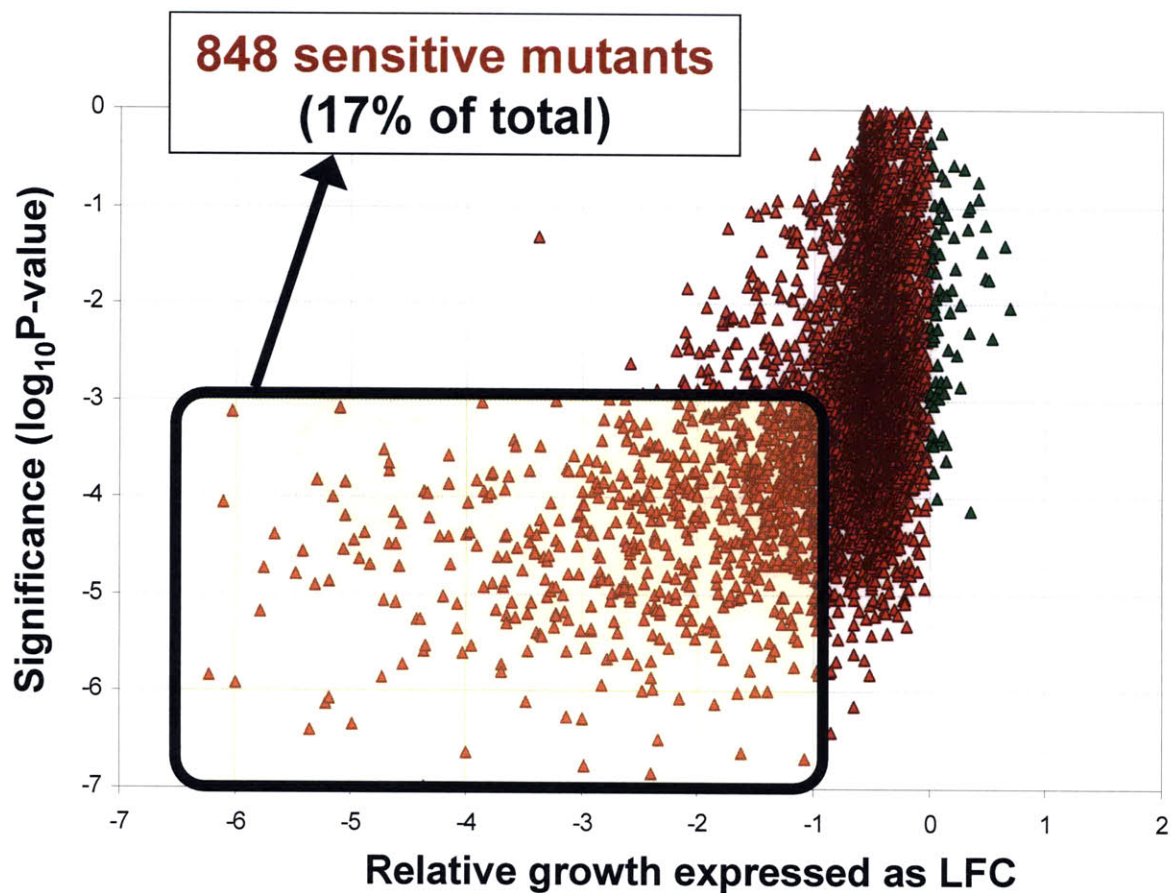


Figure 2.8 Selecting the sensitive mutants to 11 β -dichloro

The sensitive mutants were selected by employing the cutoffs $LFC < -1$ and $\log_{10}P\text{-value} < -3$. This yielded 848 sensitive mutants, as indicated, a number which amounts to 17% of the total mutants screened.

Significance (p-value)	# of mutants	% of the entire library
> 0.05	692	14.6%
< 0.05	4049	85.4%
< 0.01	3501	73.8%
< 0.001	2255	47.6%
< 10^{-4}	804	17.0%
< 10^{-5}	170	3.6%
< 10^{-6}	19	0.4%

Table 2.1 The breakdown of mutants in the library according to their p-value

The number of mutants was determined at each threshold of significance (p-value) and it was found that for most of the mutants in the library, the assay used finds a change in growth significant at the 0.05 level. Almost half of the mutants have a change significant at the 0.001 level.

LFC cutoff	Relative growth	# of mutants	% of the entire library
> 0	> 100%	72	1.5%
< 0	< 100%	4669	98.5%
< -1	< 50%	848	17.9%
< -2	< 25%	351	7.4%
< -3	< 12.5%	142	3.0%
< -4	< 6.25%	55	1.2%
< -5	< 3.12%	20	0.4%

Table 2.2 The breakdown of mutants in the library according to their LFC value

The number of mutants at each LFC level was determined and it was found that for most of the mutants in the library, the assay finds a decrease in growth (LFC < 0). Additionally, for the majority of mutants, the change in growth is less than a factor of two; only a small fraction (17%) have relative growths less than 50% (LFC < -1). This fraction was defined as the fraction of mutants sensitive to 11 β -dichloro.

GO Component	Cluster Freq.	Bkgr. Freq.	P-value
mitochondrion	29.2%	15.3%	5.49E-21
ribosomal subunit	10.0%	3.4%	1.69E-15
mitochondrial matrix	8.0%	2.3%	2.87E-15
organelle	70.7%	56.4%	2.72E-14
mitochondrial inner membrane	7.1%	2.3%	3.70E-11
membrane-bounded organelle	64.3%	51.6%	1.26E-10
mitochondrial envelope	9.8%	4.1%	3.22E-10
organelle inner membrane	7.1%	2.5%	4.37E-10
mitochondrial membrane	8.7%	3.5%	2.86E-09
mitochondrial ribosome	4.4%	1.2%	3.15E-09
small ribosomal subunit	4.8%	1.4%	3.53E-09
cytoplasm	63.6%	52.1%	1.12E-08
organelle envelope	11.4%	5.6%	3.90E-08
organelle membrane	15.4%	9.1%	1.92E-06
cytosolic ribosome	5.8%	2.4%	1.85E-05
protein complex	24.8%	17.7%	0.0001
macromolecular complex	31.2%	24.6%	0.00448

Table 2.3 The GO component terms enriched in the subset of mutants sensitive to 11 β -dichloro

The cluster frequency denotes the percentage of the genes associated with the GO term present in the subset sensitive to 11 β -dichloro. The background frequency denotes the percentage of the genes associated with the GO term from the entire library. The P-value denotes the significance of the observed difference in frequencies. The light gray cells indicate GO terms associated with mitochondrial localization. The dark gray indicate GO term associated with ribosomal localization.

GO Process	Cluster freq.	Bkgr. freq.	P-value
protein metabolic process	33.1%	21.7%	5.44E-11
telomere maintenance	9.2%	3.9%	1.40E-08
aerobic respiration	4.3%	1.2%	8.40E-08
generation of precursor metabolites and energy	6.4%	2.4%	2.14E-07
energy derivation by oxidation of organic compounds	5.3%	1.9%	6.00E-06
biosynthetic process	25.2%	17.6%	4.46E-05
protein complex assembly	4.6%	1.6%	4.73E-05
chromosome organization and biogenesis	13.4%	8.1%	0.00027
primary metabolic process	55.0%	46.6%	0.00108
phosphate metabolic process	6.1%	3.0%	0.00391
ubiquitin-dependent protein catabolic process via the multivesicular body pathway	1.3%	0.2%	0.00416
macromolecule biosynthetic process	17.2%	11.9%	0.00578
macromolecule metabolic process	47.8%	40.1%	0.00644
translation	14.4%	9.6%	0.00904
phosphorylation	4.7%	2.2%	0.01888
cellular component organization and biogenesis	37.7%	30.9%	0.02624
post-translational protein modification	9.0%	5.5%	0.04679
respiratory chain complex IV assembly	0.9%	0.1%	0.04848

Table 2.4 The GO process terms enriched in the subset of mutants sensitive to 11 β -dichloro

GO Function	Cluster freq.	Bkgr. freq.	P-value
structural constituent of the ribosome	9.80%	3.20%	6.11E-16
structural molecule activity	11.20%	4.90%	8.37E-11
monovalent inorganic cation transmembrane transporter activity	2.40%	0.80%	0.01128
hydrogen ion transmembrane transporter activity	2.30%	0.80%	0.01329
oxidoreductase activity, acting on the aldehyde or oxo group of donors, disulfide as acceptor	0.60%	0.10%	0.02575

Table 2.5 The GO function terms enriched in the subset of mutants sensitive to 11 β -dichloro

The cluster frequency denotes the percentage of the genes associated with the GO term present in the subset sensitive to 11 β -dichloro. The background frequency denotes the percentage of the genes associated with the GO term from the entire library. The P-value denotes the significance of the observed difference in frequencies. The light gray cells indicate GO terms associated with mitochondrial function. The dark gray indicate GO term associated with ribosomal function.

		DNA damaging agent				Unaffected by MMS, TBP, 4NQO, UV
		MMS	TBP	4NQO	UV	
Percentage of sensitive mutants	Entire library (4841 mutants)	30.0%	9.4%	17.3%	6.1%	56.8%
	11 β -dichloro LFC < -1 group (848 mutants)	38.2%	14.0%	26.9%	13.7%	44.2%
	11 β -dichloro LFC < -2 group (351 mutants)	37.6%	11.4%	31.3%	18.5%	42.5%
	11 β -dichloro LFC < -3 group (142 mutants)	32.4%	10.6%	31.0%	19.7%	43.0%

Table 2.6 Common sensitive mutants between 11 β -dichloro and other DNA damaging agents

This study investigated the overlap between groups of mutants sensitive to 11 β -dichloro and mutants sensitive to the DNA damaging agents MMS, TBP, 4NQO and UV radiation. The first row of the table shows the percentage of mutants from the entire library sensitive to the 4 DNA damaging agents listed at the top. The next rows ask the same question, but for the groups of mutants sensitive to 11 β -dichloro. The LFC < -1 group includes all the mutants considered sensitive to 11 β -dichloro. The LFC < -2 group includes only the top 351 mutants. The LFC < -3 group includes only the top 142 mutants sensitive to 11 β -dichloro. The right most column denotes the percentage of mutants from each group unaffected by MMS, 4NQO, TBP or UV. Interestingly, this number stays fairly constant in the 11 β -dichloro sensitive groups of mutants.

GO Component	Cluster Freq.	Bkgr. Freq.	P-value
mitochondrion	33.1%	15.3%	3.37E-11
mitochondrial part	18.0%	6.5%	6.57E-10
ribosomal subunit	11.3%	3.4%	1.78E-08
mitochondrial matrix	8.9%	2.3%	3.22E-07
mitochondrial inner membrane	8.3%	2.3%	7.35E-06
mitochondrial ribosome	5.6%	1.2%	9.48E-06
organelle inner membrane	8.3%	2.5%	2.49E-05
cytoplasmic part	53.0%	34.4%	5.25E-05
mitochondrial membrane	10.2%	3.5%	6.01E-05
organelle envelope	12.9%	5.6%	0.00015
small ribosomal subunit	5.4%	1.4%	0.0002
ribosome	11.8%	4.9%	0.00036
mitochondrial envelope	10.5%	4.1%	0.00095
intracellular organelle part	40.1%	25.3%	0.00118
large ribosomal subunit	5.9%	2.0%	0.00377
ribonucleoprotein complex	13.2%	6.3%	0.00645
mitochondrial large ribosomal subunit	3.2%	0.8%	0.00827

Table 2.7 The GO component terms enriched in the subset of mutants uniquely sensitive to 11 β -dichloro (372 mutants)

GO Process	Cluster freq.	Bkgr. freq.	P-value
translation	16.7%	9.6%	1.04E-11
aerobic respiration	6.2%	1.2%	2.54E-07
mitochondrial translation	6.5%	1.8%	5.39E-06
cellular respiration	6.5%	1.8%	5.39E-06
gene expression	28.5%	17.5%	1.59E-05
protein metabolic process	29.0%	21.7%	5.17E-05
cellular protein metabolic process	27.4%	17.2%	0.0001
macromolecule biosynthetic process	27.7%	11.9%	0.00017
biosynthetic process	34.7%	17.6%	0.00037
mitochondrion organization	9.7%	4.3%	0.00135
energy derivation by oxidation of organic compounds	7.0%	1.9%	0.00197
generation of precursor metabolites and energy	7.8%	2.4%	0.00245
biopolymer biosynthetic process	24.5%	16.0%	0.00464
maturation of SSU-rRNA	3.0%	0.7%	0.01037
cellular metabolic process	55.4%	45.0%	0.01122
ribosome biogenesis	5.9%	2.3%	0.01911
rRNA metabolic process	4.0%	1.3%	0.02423
rRNA processing	3.8%	1.1%	0.02833
macromolecule metabolic process	42.2%	40.1%	0.03748
metabolic process	56.2%	46.6%	0.04089

Table 2.8 The GO process terms enriched in the subset of mutants uniquely sensitive to 11 β -dichloro (372 mutants)

GO Function	Cluster freq.	Bkgr. freq.	P-value
structural constituent of ribosome	11.0%	3.2%	1.84E-08
structural molecule activity	11.8%	4.9%	4.73E-06

Table 2.9 The GO function terms enriched in the subset of mutants uniquely sensitive to 11 β -dichloro (372 mutants)

2.6 References

- Armour, C. D., and Lum, P. Y. (2005). From drug to protein: using yeast genetics for high-throughput target discovery. *Curr Opin Chem Biol* 9, 20-24.
- Begley, T. J., Rosenbach, A. S., Ideker, T., and Samson, L. D. (2002). Damage recovery pathways in *Saccharomyces cerevisiae* revealed by genomic phenotyping and interactome mapping. *Mol. Cancer Res* 1, 103-112.
- Begley, T. J., Rosenbach, A. S., Ideker, T., and Samson, L. D. (2004). Hot spots for modulating toxicity identified by genomic phenotyping and localization mapping. *Mol. Cell* 16, 117-125.
- Begley, T. J., and Samson, L. D. (2004). Network responses to DNA damaging agents. *DNA Repair (Amst.)* 3, 1123-1132.
- Birrell, G. W., Brown, J. A., Wu, H. I., Giaever, G., Chu, A. M., Davis, R. W., and Brown, J. M. (2002). Transcriptional response of *Saccharomyces cerevisiae* to DNA-damaging agents does not identify the genes that protect against these agents. *Proc. Natl. Acad. Sci. U.S.A* 99, 8778-8783.
- Bjornsti, M. A. (2002). Cancer therapeutics in yeast. *Cancer Cell* 2, 267-273.
- Brooks, N., McHugh, P. J., Lee, M., and Hartley, J. A. (1999). The role of base excision repair in the repair of DNA adducts formed by a series of nitrogen mustard-containing analogues of distamycin of increasing binding site size. *Anticancer Drug Des* 14, 11-18.
- Ericson, E., Gebbia, M., Heisler, L. E., Wildenhain, J., Tyers, M., Giaever, G., and Nislow, C. (2008). Off-target effects of psychoactive drugs revealed by genome-wide assays in yeast. *PLoS Genet* 4, e1000151.
- Essigmann, J. M., Rink, S. M., Park, H. J., and Croy, R. G. (2001). Design of DNA damaging agents that hijack transcription factors and block DNA repair. *Adv Exp Med Biol* 500, 301-13.
- Fernö, M., Borg, A., Johansson, U., Norgren, A., Olsson, H., Rydén, S., and Sellberg, G. (1990). Estrogen and progesterone receptor analyses in more than 4,000 human breast cancer samples. A study with special reference to age at diagnosis and stability of analyses. Southern Swedish Breast Cancer Study Group. *Acta Oncol* 29, 129-135.
- Giaever, G. (2003). A chemical genomics approach to understanding drug action. *Trends Pharmacol. Sci* 24, 444-446.

- Giaever, G., Chu, A. M., Ni, L., Connelly, C., Riles, L., Véronneau, S., Dow, S., Lucau-Danila, A., Anderson, K., André, B., et al. (2002). Functional profiling of the *Saccharomyces cerevisiae* genome. *Nature* 418, 387-391.
- Greenman, C., Stephens, P., Smith, R., Dalgliesh, G. L., Hunter, C., Bignell, G., Davies, H., Teague, J., Butler, A., Stevens, C., et al. (2007). Patterns of somatic mutation in human cancer genomes. *Nature* 446, 153-158.
- Hartwell, L. H. (2004). Yeast and cancer. *Biosci. Rep* 24, 523-544.
- Hede, K. (2005). Which came first? Studies clarify role of aneuploidy in cancer. *J. Natl. Cancer Inst* 97, 87-89.
- Hillenmeyer, M. E., Fung, E., Wildenhain, J., Pierce, S. E., Hoon, S., Lee, W., Proctor, M., St Onge, R. P., Tyers, M., Koller, D., et al. (2008). The chemical genomic portrait of yeast: uncovering a phenotype for all genes. *Science* 320, 362-365.
- Hillier, S. M., Marquis, J. C., Zayas, B., Wishnok, J. S., Liberman, R. G., Skipper, P. L., Tannenbaum, S. R., Essigmann, J. M., and Croy, R. G. (2006). DNA adducts formed by a novel antitumor agent 11beta-dichloro in vitro and in vivo. *Mol Cancer Ther* 5, 977-84.
- Hillier, S. M. (2005). Novel Genotoxins that Target Estrogen Receptor- and Androgen Receptor- Positive Cancers: Identification of DNA Adducts, Pharmacokinetics, and Mechanism. PhD Thesis, Massachusetts Institute of Technology.
- Kartalou, M., and Essigmann, J. M. (2001). Recognition of cisplatin adducts by cellular proteins. *Mutat Res* 478, 1-21.
- Kemmer, D., McHardy, L. M., Hoon, S., Rebérioux, D., Giaever, G., Nislow, C., Roskelley, C. D., and Roberge, M. (2009). Combining chemical genomics screens in yeast to reveal spectrum of effects of chemical inhibition of sphingolipid biosynthesis. *BMC Microbiol* 9, 9.
- Lee, W., St Onge, R. P., Proctor, M., Flaherty, P., Jordan, M. I., Arkin, A. P., Davis, R. W., Nislow, C., and Giaever, G. (2005). Genome-wide requirements for resistance to functionally distinct DNA-damaging agents. *PLoS Genet* 1, e24.
- Marcelli, M., and Cunningham, G. R. (1999). Hormonal signaling in prostatic hyperplasia and neoplasia. *J Clin Endocrinol Metab* 84, 3463-8.
- Marquis, J. C., Hillier, S. M., Dinaut, A. N., Rodrigues, D., Mitra, K., Essigmann, J. M., and Croy, R. G. (2005). Disruption of gene expression and induction of apoptosis in prostate cancer cells by a DNA-damaging agent tethered to an androgen receptor ligand. *Chem Biol* 12, 779-87.

- Masters, J. R. W., and Köberle, B. (2003). Curing metastatic cancer: lessons from testicular germ-cell tumours. *Nat Rev Cancer* 3, 517-25.
- McHugh, P. J., Gill, R. D., Waters, R., and Hartley, J. A. (1999). Excision repair of nitrogen mustard-DNA adducts in *Saccharomyces cerevisiae*. *Nucleic Acids Res* 27, 3259-3266.
- Menacho-Márquez, M., and Murguía, J. R. (2007). Yeast on drugs: *Saccharomyces cerevisiae* as a tool for anticancer drug research. *Clin Transl Oncol* 9, 221-228.
- Outeiro, T. F., and Giorgini, F. (2006). Yeast as a drug discovery platform in Huntington's and Parkinson's diseases. *Biotechnol J* 1, 258-269.
- Perry, M. (2001). *The Chemotherapy Source Book* 3rd ed. (Philadelphia: Lippincott).
- Ries, L. A. G., Melbert, D., Krapcho, M., Mariotto, A., Miller, B. A., Feuer, E. J., Clegg, L., Horner, M. J., Howlander, N., Eisner, M. P., et al. (2009). SEER cancer statistics review, 1975-2005. National Cancer Institute, Bethesda, MD. *XXV* 1-12. Available at: http://seer.cancer.gov/csr/1975_2005/, based on November 2007 SEER data submission, posted to the SEER web site, 2008.
- Simon, J. A., Szankasi, P., Nguyen, D. K., Ludlow, C., Dunstan, H. M., Roberts, C. J., Jensen, E. L., Hartwell, L. H., and Friend, S. H. (2000). Differential toxicities of anticancer agents among DNA repair and checkpoint mutants of *Saccharomyces cerevisiae*. *Cancer Res* 60, 328-333.
- Winzler, E. A., Shoemaker, D. D., Astromoff, A., Liang, H., Anderson, K., Andre, B., Bangham, R., Benito, R., Boeke, J. D., Bussey, H., et al. (1999). Functional characterization of the *S. cerevisiae* genome by gene deletion and parallel analysis. *Science* 285, 901-906.

CHAPTER 3

The Anticancer Agent 11 β -Dichloro Generates Reactive Oxygen Species in HeLa Cells

3.1 Introduction

Chemotherapy represents one of the most important cancer treatments available today. Often used as an adjuvant following surgery or radiation therapy, chemotherapy is among the few choices of treatments for advanced and metastatic cancers. Unfortunately, most current chemotherapeutic agents are not very specific; they cause significant toxicity to healthy tissues thus eliciting a plethora of side-effects that often limit their efficacy and decrease considerably the quality of life for cancer patients. Given these considerations, the development of more specific chemotherapeutics remains an important scientific challenge.

However, certain chemotherapeutics have shown in certain cancers a remarkable selectivity that make them very effective treatments. One such example is the spectacular effect of cisplatin against testicular cancer; regimens including cisplatin achieve a cure rate of more than 95% (Masters and Köberle, 2003; Ries et al., 2009). Mechanistic investigations have suggested that cisplatin may achieve its selectivity by taking advantage of tumor specific proteins (Kartalou and Essigmann, 2001). Inspired by the hypothetical cisplatin mechanisms, the Essigmann lab designed a series of compounds that would both alkylate DNA and bind to cancer-specific proteins.

One of these compounds, called 11 β -dichloro³, which was designed to interact with the androgen receptor (AR), displays a potent *in vivo* anti-tumor activity, while being well tolerated by animals (Marquis et al., 2005). Paradoxically, however, the compound is also very effective against tumors that do not express AR (Chapter 1). Moreover, *in vitro*, 11 β -dichloro is significantly more toxic than simpler nitrogen mustards in cell lines that do not express the AR (Chapter 1). All these findings suggest that an additional mechanism of toxicity may be operating and prompted the current investigation. Here we attempt to characterize the cellular responses to 11 β -dichloro in HeLa cells, a cell line that does not express the AR, in an effort to understand the additional cellular targets this compound might have and its additional mechanism(s) of toxicity. Such investigations constitute an essential

³ IUPAC name: 2-(6-((8S,11S,13S,14S,17S)-17-hydroxy-13-methyl-3-oxo-2,3,6,7,8,11,12,13,14,15,16,17 dodecahydro-1H-cyclopenta[a]phenanthren-11-yl)hexylamino)ethyl 3-(4-(bis(2-chloroethyl)amino)phenyl)propylcarbamate

step for the eventual advancement of 11 β -dichloro in preclinical and eventually into clinical trials.

Our mechanistic investigations focused on mitochondrial function. This direction was prompted by the results described in Chapter 2. In that work, a large scale phenotypic screen conducted on the complete single-gene knock-out mutant yeast library indicated that a large group of mutants with impaired mitochondrial function are particularly sensitive to 11 β -dichloro (Tables 2.3-2.5 and Tables 2.7-2.9). A second reason for focusing on mitochondrial function was the fact that mitochondrial DNA is often an additional and sometimes underestimated target of DNA alkylating drugs (Han et al., 2004).

The hallmark of impaired mitochondrial function is the generation of reactive oxygen species (ROS). In biological sciences, ROS commonly refers to the variety of highly reactive molecular species derived from molecular oxygen. They are often a normal byproduct of cell respiration; 2-4% of the total oxygen consumed by respiring cells is converted into ROS (Chow et al., 1999; Turrens, 2003). In small quantities, ROS may play some physiological roles; however, in high amounts, their effect is almost always deleterious. Given that ROS play important roles in inflammation, progression of diseases, cancer and aging, understanding the mechanisms involved in the generation and inactivation of ROS inside cells is an active area of research.

One of the main sources of ROS inside the cell is the mitochondrial electron transport chain (ETC), the complex molecular machinery involved in the reduction of molecular oxygen during the aerobic respiration. Inside complexes I, II and III of the ETC, highly reactive intermediates can occasionally react directly with molecular oxygen, generating the superoxide anion, the precursor to most other cellular ROS (Turrens, 2003). To counteract the high reactivity and toxicity of superoxide, cells have evolved the superoxide dismutases (SODs), specialized metalloenzymes capable of breaking down superoxide into molecular oxygen and hydrogen peroxide (Figure 3.1). While less reactive than superoxide, hydrogen peroxide can become toxic as well in the presence of transition metal ions when it can undergo a redox cycling known as “Fenton reaction,” generating the hydroxyl radical, the

most reactive ROS in biological systems. To circumvent the toxicity of hydrogen peroxide and to prevent the Fenton reaction, cells have evolved several pathways that utilize NADPH to reduce hydrogen peroxide to water (Figure 3.2). The main enzyme that detoxifies hydrogen peroxide in mitochondria is glutathione peroxidase (GPX), a glutathione dependent protein featuring a seleno-cysteine in its active site. GPX requires reduced glutathione to carry out the redox chemistry, the reaction rate depending on the concentration of reduced glutathione. A second enzyme, glutathione reductase (GR), then uses NADPH to regenerate reduced glutathione, enabling another cycle of redox chemistry. Finally, mitochondrial NADPH is generated by the NADP⁺ transhydrogenase, an enzyme that uses the NADH generated in the TCA cycle and the proton gradient of the mitochondrial inner membrane (Kowaltowski et al., 2001).

Increased generation of ROS from the mitochondrial ETC can be achieved either by partially inhibiting the electron flux through the ETC, which causes accumulation of reduced intermediaries, or by inhibiting the ATP synthase or adenine nucleotide translocase (ANT), key membrane complexes involved in transducing the proton gradient across the mitochondrial inner membrane into ATP generation. If the ATP production is impaired, the ETC will keep pumping protons and increasing the membrane potential until the gradient is too high. At this point, the ETC stalls leading to a similar accumulation of reduced intermediaries in the mitochondrial inner membrane, which then lead to an increased ROS production (Wallace, 2005).

Another mechanism that can increase generation of mitochondrial ROS is through uncoupling of the ETC from ATP production. If the proton gradient generated by the ETC is partially dissipated before it can be used by the ATP synthase, the cell will upregulate the ETC activity in order to maintain constant ATP production. A higher flux of electrons through the ETC will then generate a higher basal level of ROS (Leverve and Fontaine, 2001).

GSH levels are also crucial for maintaining the redox balance inside mitochondria and limiting the deleterious effects of ROS. Mitochondrial GSH, however, is not synthesized in

the mitochondria, but rather imported from the cytosol. As much as 15% of the total cellular GSH is found in the mitochondria (Lash, 2006). Moreover, there is no active mechanism for export of GSH from the mitochondria, which means that the mitochondrial GSH pool is relatively isolated from the fluctuations of the cytosolic GSH pool (Lash, 2006; Fernandez-Checa and Kaplowitz, 2005). The downside of such isolation is that the oxidized glutathione dimers (GSSG) are also trapped in the mitochondria. In the event that GSSG cannot be regenerated by GR, GSSG will accumulate in the mitochondria leading to impaired mitochondrial function (Sies et al., 1997). It is therefore possible to have mitochondrial toxicity even in the presence of sufficient cytosolic GSH. Moreover, accumulation of GSSG in the mitochondria may also be the reason that administration of soluble antioxidants such as N-acetyl L-cysteine (NAC), ascorbate (vitamin C) or even GSH may not always completely rescue mitochondrial function (Lash, 2006).

Our results described herein indicate that 11 β -dichloro generates a large amount of ROS in the cells, very soon after the onset of exposure. While ROS production has been occasionally listed among the cellular responses induced by nitrogen mustards currently used in the clinic, it has not been observed to be a primary response and usually it is only associated with the late stages of apoptosis or inflammation caused by cell death (Crater and Kannan, 2007). However, toxicity by ROS has been an important mechanism of several classes of chemotherapeutic compounds. Particularly, compounds that perturb mitochondrial function can induce apoptosis by generating ROS (Galluzzi et al., 2006). Moreover, this mechanism has been shown to exhibit selectivity for cancer cells that already have an increased level of ROS due to their accelerated and altered metabolism (Wallace, 2005).

Our results suggest that an additional mechanism of 11 β -dichloro involves generation of a large amount of ROS in the cell, predominantly H₂O₂. The source of the ROS is likely to be the mitochondrial ETC, a fact suggested by the significant perturbation of the mitochondrial membrane potential that can cause an increased electron flux through the respiratory chain. Additionally, our data indicate that mitochondrial GSH levels, but not cytosolic GSH levels are important in modulating 11 β -dichloro toxicity. The elevated ROS levels have widespread consequences in the cell such as the decrease in the cellular antioxidant pool and non-specific

damage to proteins, lipids and nucleic acids. Other cellular responses that may be caused by ROS, such as the increase in cytosolic calcium and the activation of the UPR (unfolded protein response) pathway will be discussed in Chapter 4. All the cellular changes due to ROS, together with changes induced by the previously documented DNA damaging properties of the compound (Hillier et al., 2006) may be important in the eventual activation of an apoptotic program and cell death.

3.2 Materials and Methods

3.2.1 Reagents

Compounds 11 β -dichloro and 11 β -dimethoxy were synthesized using previously reported schemes (Marquis et al., 2005). Stock solutions (10 mM) were prepared in anhydrous DMSO (Sigma). Vitamin E, NAC, BSO, chlorambucil, melphalan, mechlorethamine and crystal violet were purchased from Sigma-Aldrich (St.Louis, MO, USA). CM-H₂DCFDA, HPF, DHE, CMFDA, JC-1, calcein AM, molecular dyes were purchased from Molecular Probes (Invitrogen, Carlsbad, CA, USA). CTB reagent was from Promega (Madison, WI, USA).

3.2.2 Cell lines and culture

HeLa cells were obtained from American Type Culture Collection (Rockville, MD, USA) and maintained in minimal essential medium (MEM, Invitrogen) supplemented with 1 mM glutamax, 1% non-essential amino acids, 1 mM pyruvate (Invitrogen), and 10% fetal bovine serum (Hyclone, Logan, UT), in a humidified 5% CO₂/air atmosphere at 37°C. Cells were routinely passaged using TrypLE (Invitrogen) in P150 dishes (BD Biosciences) every three days at a seeding density of 2 \times 10⁶ cells/dish.

3.2.3 Assays for cell growth, cell viability and cytotoxicity

Colony formation assays were performed as previously reported (Marquis et al., 2005). Briefly, 1 \times 10³ cells per well were seeded in 6-well plates and incubated for 24 hours to allow cell attachment. Fresh media or drug solutions in media were then added to triplicate wells and incubated for 24 hours. Afterwards, fresh medium was added in each well and the plates were incubated for 3-5 days until colonies became clearly visible. The colonies were then fixed with a solution of water:methanol:acetic acid (4:5:1) for 10 minutes, stained with a 0.5% crystal violet solution in fixer for 15 minutes and manually counted. The surviving fraction was calculated as the fraction between the number of colonies in the treated and untreated wells. Growth inhibition assays were performed as follows. 1 \times 10⁵ cells were

seeded in 6-well plates and incubated for 24 hours to allow attachment. Fresh solution of media or drug-containing media were added to triplicate wells and incubated for the indicated amount of time. Afterwards, cells were washed once with PBS, detached using TrypLE (200 μ L/well) and resuspended in medium. The number of cells in each well was determined by counting aliquots in a Coulter Counter Z1 (Beckman Coulter, Miami, FL, USA) set for particle size higher than 10 μ m. The percentage growth inhibition was calculated as the number of cells in the treated wells divided by the number of cells in untreated wells times 100. Cell-titer blue (CTB) viability was determined as described in the manufacturer's instructions (Promega). Briefly, 2.5×10^3 cells/well were seeded in black/transparent bottom 96-well plates (Corning Inc., Corning, NY, USA) and incubated for 24 hours. Media were carefully aspirated by a flame-thinned Pasteur pipette and fresh media and drug containing media was added using a multichannel pipettor. After the incubation for the indicated times, 20 μ L of pre-warmed CTB reagent were added in low light to each well and mixed by gently tapping the sides of the plate. The plate was incubated an additional 2-4 hours and the fluorescent signal was recorded at excitation and emission (ex/em) 555/585 in a SpectraMax M5e spectrophotometer using the bottom-read feature. Every plate included wells with media only, from which the background fluorescence was determined and subtracted from all other fluorescence readings. The percentage viability was calculated as the ratio between the average signal in the treated wells and the average signal in the untreated control wells times 100.

3.2.4 Determination of intracellular ROS using flow cytometry

Cells were treated in 6-well plates, as described above, for the indicated amounts of time. The medium was then aspirated, replaced with a probe solution and incubated for 30 minutes. The fluorescent probes used were CM-H₂DCFDA (working concentration 5 μ M) for total ROS levels, HPF (working concentration 1 μ M) for hydroxyl radical levels and DHE (working concentration 0.5 μ M) for superoxide levels. After the incubation with the probe, the cells were trypsinized, resuspended in PBS and analyzed by flow cytometry in a FACSCanto II instrument. The flow cytometry protocol used a 488 nm laser for excitation and involved using front and side scatter to gate normal looking cells, and then quantifying

fluorescence in the green (FL1) channel for CM-H₂DCFDA and HPF, and in the red (FL3) channel for DHE.

3.2.5 Determination of the mitochondrial potential and reduced GSH

Mitochondrial inner membrane potential ($\Delta\Psi_m$) was determined using the mitochondrial specific dye JC-1 as described previously (Wagner et al., 2008). Briefly, cells were treated in the 96 well plates as described above and then incubated with 100 μ L/well JC-1 5 μ M solution in culture medium without phenol red for 2 hours. Wells were then washed once and refilled with PBS. Red and green fluorescence was determined at ex/em 530/580 and 488/530 respectively using the bottom-read and well-scan features of the SpectraMax M5e spectrophotometer. The red/green ratios were then used as a measure of the mitochondrial potential, calculating first the ratio for each well sub-area before averaging for the whole well and for all the biological replicates.

Cellular GSH levels were determined using the *in situ* probe CMFDA (Invitrogen) according to manufacturer's instructions. Briefly, cells were cultured and treated in 96 well plates as described above. Following medium removal, cells were then incubated with 100 μ L/well CMFDA 1 μ M solution in culture medium without phenol red for 1 hour. After two washes with PBS, wells were refilled with PBS and fluorescence was measured at ex/em 485/530 using the bottom-read and well-scan features of the SpectraMax M5e spectrophotometer. The fluorescence values in each well were normalized to the number of cells (determined by CTB, in a separate treatment) to yield the total cellular GSH levels.

3.2.6 Determination of H₂O₂, lipid peroxidation and cellular NADPH

Total cellular H₂O₂ was determined using the Quantichrom Peroxide Assay (Bioassay Systems (Hayward, CA, USA), an iron-xylenol orange based procedure, according to the manufacturer's instructions. Quantification of cellular ROS byproducts (lipid peroxidation) was done with the OxiSelect TBARS kit (Cell Biolabs, Inc., San Diego, CA) as described in the manufacturer's instructions. Total cellular NADPH content was assayed using the EnzyChrom NADP/NADPH assay (BioAssay Systems, Hayward, CA) according to the manufacturer's instructions. Briefly, 5×10^5 cells were seeded in P100 dishes and incubated

for 24 hours to allow cell attachment. Cells were then incubated with drug-containing media or control media for the indicated times, washed with ice-cold PBS, scraped and pelleted. Cell homogenization was accomplished with the alkaline NADPH extraction buffer on ice, followed by heating at 60°C for 7 minutes. Aliquots of each homogenate were then assayed for NADPH in the redox cycling reaction and for protein content using the Bradford reagent (Bio-Rad, Hercules, CA, USA). NADPH content was then calculated based on a NADPH calibration curve and normalized to protein levels.

3.2.7 Statistical analysis

All results are expressed as mean +/- standard deviation. The significance of the difference between two different populations was calculated using Student's t-test for unpaired, heteroscedastic populations. P values less than 0.05 were considered significant.

3.3 Experimental Results

3.3.1 11 β -Dichloro exhibits remarkable acute toxicity against HeLa cells *in vitro*, higher than simpler nitrogen mustards

We investigated the toxicity in 11 β -dichloro against HeLa cells *in vitro*, and compared it with other clinically approved nitrogen mustards chlorambucil, melphalan and mechlorethamine. In a colony forming assay (CFA), 11 β -dichloro ($IC_{50} = 2 \mu\text{M}$) was more toxic than melphalan. ($IC_{50} = 4 \mu\text{M}$) and chlorambucil ($IC_{50} > 5 \mu\text{M}$) (Figure 3.3 A). The same trend was true at 24 hours in a growth inhibition assay, where the number of viable cells was quantified using the CTB assay (see Materials and Methods) (Figure 3.3 B). The time frame needed to achieve a particular toxic effect was also investigated. We treated the cells with concentrations of 11 β -dichloro ranging from 4 to 12 μM and determined the number of viable cells remaining at various time points (3, 6 and 24 hours). Figure 3.4 A shows the percentage of cells remaining relative to the untreated controls at each time point. The number of viable cells was determined using CTB. We see that 11 β -dichloro acute toxicity increases rapidly with dose. In the conditions of the assay, at doses higher than 8 μM , more than 50% of the cells are killed within the first 6 hours of exposure. Also, we notice a threshold effect between the 4 and 6 μM doses. At 4 μM or below, in the conditions of this assay, the compound slows down the growth rate of the cells. However, for doses of 6 μM and higher, the number of viable cells remaining is much lower than the initial number of cells, indicating that a fraction of the cells have died. Given the acute toxicity of 11 β -dichloro, we were also interested in the persistence of the toxic effects. HeLa cells were exposed to 11 β -dichloro in separate experiments for 3, 6 and 24 hours. The 3 and 6 hour treatments were changed to fresh medium and returned to incubator allowing the cells to recover. Cell viability was determined for all conditions at 24 hours using the CTB assay. The results (Figure 3.4 B) show that for most doses, the toxicity achieved in 24 hours is in fact achieved as early as 6 hours. This suggests that for most doses, the first 6 hours of exposure to 11 β -dichloro are critical in deciding the cell fate. Therefore, we decided to investigate more closely the cellular changes that happen during this initial interval.

3.3.2 11 β -Dichloro exposure is accompanied by generation of ROS

We next investigated whether 11 β -dichloro is generating an ROS response and whether the ROS levels correlate with toxicity. HeLa cells were exposed to 11 β -dichloro for 6 hours and then stained with the ROS specific dye CM-H₂DCFDA (5- (and 6-)-chloromethyl-2',7'-dichlorodihydrofluorescein diacetate) (see Materials and Methods). Cells were then analyzed by flow cytometry (Figure 3.5). The results show that 11 β -dichloro is significantly increasing the ROS levels in a dose dependent manner, which correlates well with toxicity. Next, we investigated how soon after treatment the ROS response could be detected. In a time course experiment, we found that the ROS response occurs as early as 30 minutes after exposure to 8 μ M 11 β -dichloro (Figure 3.6 A). Next, we investigated the cellular distribution of the fluorescent signal. Figure 3.6 B shows how the bright green staining from CM-H₂DCFDA is distributed uniformly throughout the cell's body, suggesting at minimum the cytosolic presence of a reactive oxygen species. Given that the fluorescent form of the dye is not membrane permeable, had it formed inside an organelle, it would have remained there long enough to make the cell look speckled rather than uniformly dyed.

To confirm the presence of ROS, we did a direct assay for hydrogen peroxide (H₂O₂) in the cells treated with 11 β -dichloro. Hydrogen peroxide is one of the longest lived reactive oxygen species in the cell and it is also either a by-product or generator of other ROS. Being more stable than other ROS and a neutral molecule, H₂O₂ can easily diffuse through membranes (Wallace, 2005). Given the uniform fluorescent staining of the cells and the high intensity of the signal, we hypothesized that H₂O₂ is one of the main ROS generated by our compound. Indeed, an iron-xylenol orange based assay (Bioassay Systems) confirmed that hydrogen peroxide accumulates in cells during exposure to 5 μ M 11 β -dichloro (Figure 3.7 A& B).

We also looked for other ROS species, superoxide and hydroxyl radical, using the ROS specific dyes dihydroethidine (DHE) and 3'-(p-hydroxyphenyl) fluorescein (HPF) respectively, using similar flow cytometry experiments (see Materials and Methods). 11 β -

Dichloro was found not to increase the levels of superoxide (data not shown), but it does however, generate increasing levels of hydroxyl radical, in a dose dependent manner (Figure 3.8 A). To confirm further the presence of ROS and investigate whether these reactive species are eliciting a biological response, we looked for an increase in the lipid peroxidation biomarker, malondialdehyde (MDA), using a thiobarbituric acid assay. The results show an increase in lipid peroxidation consistent with the increased oxidative burden (Figure 3.8 B).

3.3.3 Antioxidants attenuate 11 β -dichloro toxicity

We next investigated the link between the ROS generation and 11 β -dichloro acute toxicity. First, we showed that we can markedly reduce the level of ROS in the cells by co-treating with the antioxidant N-acetyl L-cysteine (NAC). The cells were exposed to 11 β or 11 β + NAC (10 mM) for 3 hours and then the ROS levels were determined as above. NAC proved to be very effective at reducing the ROS close to baseline levels (Figure 3.9). Next, we co-treated HeLa cells with both water soluble (NAC, 20 mM) and lipid soluble (vitamin E, 100 μ M) antioxidants in an effort to ameliorate 11 β -dichloro toxicity by diminishing the ROS burden. Both antioxidants used had a significant effect in attenuating 11 β -dichloro toxicity measured at 24 hours in a CTB assay (Figure 3.10 A). To confirm further the reduction in toxicity due to the antioxidants, and to investigate whether this effect is temporary or long lasting, we compared in a clonogenic assay HeLa cells treated with 11 β -dichloro with or without 100 μ M vitamin E. The results (Figure 3.10 B) indicate that vitamin E is very potent in counteracting a large portion of 11 β -dichloro's toxicity. All these data together suggest an important link between the generation of ROS and the toxicity of our compound.

3.3.4 11 β -Dichloro depletes cellular NADPH and the free thiol pool

We next investigated the effects of 11 β -dichloro treatment on the cellular antioxidant pool. To determine the cellular NADPH levels, we used a glucose-6 phosphate dehydrogenase cycling reaction-based assay from BioAssay Systems (see Material and Methods). A 5 μ M dose of 11 β -dichloro was found to cause a striking reduction in cellular NADPH levels after 6 hours (Figure 3.11 A). To estimate reduced glutathione levels (GSH), we used the *in-situ* probe 5-chloromethylfluorescein diacetate (CMFDA) from Invitrogen, which binds reduced glutathione and other free thiols inside the cell. The cells were exposed to the indicated doses

of 11 β for 24 hours and then, in separate experiments, the levels of reduced free thiol (CMFDA fluorescence) and the viability (CTB) were determined. For each dose, the CMFDA fluorescent signal was normalized to the number of cells determined in the CTB assay to yield the relative free thiol (GSH) level per cell. The results indicate that the amount of free thiol (GSH) is significantly decreased in the cells exposed to 11 β -dichloro above 5 μ M (Figure 3.11 B).

3.3.5 Glutathione depletion sensitizes cells to 11 β -dichloro

The depletion of the antioxidant pool findings are in excellent agreement with the data showing large increases in the ROS levels, suggesting a mechanistic relationship between the two. To test this relationship, we inquired whether cells with lower levels of glutathione are more sensitive to 11 β -dichloro, hypothesizing that the toxicity is proportional to the ROS levels, which would be higher when less glutathione is available. Cellular GSH levels were reduced by pretreating with 100 μ M L- buthionine sulfoximine (BSO), a specific inhibitor of the γ -glutamyl cysteine synthetase, the rate limiting step in the biosynthesis of GSH. To achieve an increased sensitivity to 11 β -dichloro, however, cells had to be pretreated with BSO for 120 hours (Figure 3.12). The long pretreatment time is an unusual condition, suggesting that only a specific sub-fraction of the cellular GSH pool (for example, mitochondrial GSH) was involved in modulating 11 β -dichloro toxicity.

3.3.6 11 β -Dichloro treatment affects inner mitochondrial membrane polarization

Next, we looked to see if the mitochondrial membrane potential ($\Delta\Psi_m$) changes after 11 β -dichloro exposure and whether this change is associated with the generation of ROS. The mitochondrial specific dye, 5,5',6,6'-tetrachloro-1,1',3,3'-tetraethylbenzimidazol-carbocyanine iodide (JC-1) was utilized to evaluate $\Delta\Psi_m$ according to established protocols. JC-1 can easily diffuse inside cells and exhibits green fluorescence as a monomer. However, being a lipophilic cation, JC-1 accumulates specifically in the inner mitochondrial membrane, where

it forms bright red fluorescent J-aggregates. It has been shown that the ratio between the red and the green fluorescence of JC-1 is a good estimator of $\Delta\Psi_m$ (Reers et al., 1995). Figure 3.13 A shows that a 6 hour exposure to low doses ($<5 \mu\text{M}$) of 11 β -dichloro induces a hyperpolarization of the mitochondrial inner membrane. In treated cells, $\Delta\Psi_m$ increases by almost twofold compared to the untreated controls. This is an unexpected result. However, hyperpolarization of mitochondrial inner membrane has been reported for other cellular toxicants such as cisplatin – a DNA alkylator (Nowak, 2002) or bortezomib – a proteasome inhibitor (Ling et al., 2003).

Curiously, $\Delta\Psi_m$ measured at 24 hours after exposure to 11 β -dichloro shows a significant depolarization of the inner mitochondrial membrane, consistent with mitochondrial membrane permeabilisation and induction of apoptosis (Figure 3.13 B). Interestingly, the loss in $\Delta\Psi_m$ at 24 hours is detectable at doses that cause no significant loss in cell viability (measured by CTB), suggesting that mitochondrial membrane depolarization may be a required event that precedes apoptosis and cell death.

3.3.7 11 β -Dimethoxy displays cellular responses similar to 11 β -dichloro, but of lower magnitude

The cellular responses to 11 β -dichloro described so far may be ascribed to a separate toxicity mechanism, yet they are very similar to the generalized stress responses induced by other nitrogen mustards (Das et al., 2006) or DNA alkylators (Nowak, 2002). More specifically, we wanted to know whether the ROS induction and antioxidant depletion in the cell is dependent on the ability of 11 β -dichloro to alkylate substrates and damage DNA. To answer this question, we characterized the cellular responses to 11 β -dimethoxy, a compound identical to 11 β -dichloro except that the chloroethyl arms of the mustard have been replaced with methoxyethyl arms, rendering the compound unreactive towards nucleophiles.

Unable to damage DNA, 11 β -dimethoxy is significantly less toxic than 11 β -dichloro in a clonogenic bioassay (Figure 3.14 A). However, 11 β -dimethoxy does indeed show a measurable acute toxicity in a growth inhibition assay, achieving toxicity comparable to that

of 11 β -dichloro at doses about 3 times higher than those of 11 β -dichloro (Figure 3.14 B). We also found that 11 β -dimethoxy induces an ROS response at sub-lethal doses; however, the magnitude of the ROS response is smaller than for 11 β -dichloro (Figure 3.15 A). A dose of 10 μ M 11 β -dimethoxy generates an ROS signal comparable to the ROS signal generated by 5 μ M 11 β -dichloro. To investigate whether the ROS generated by 11 β -dimethoxy can impact the antioxidant pool, we measured the NADPH levels in a time course following exposure to 10 μ M 11 β -dimethoxy. As expected, 11 β -dimethoxy can lower NADPH levels; however, the extent of the effect is smaller than in the case of 11 β -dichloro (Figure 3.15 B). Finally, we investigated whether the toxicity of 11 β -dimethoxy (at doses of 10 μ M and higher) can be modulated by antioxidants. Co-treatments with 20 mM NAC and 100 μ M vitamin E exhibited significantly less toxicity when compared with 11 β -dimethoxy alone (Figure 3.16). Taken together, the properties of 11 β -dimethoxy suggest that in the case of 11 β -dichloro, the ROS induction and the related cellular responses are a consequence of the entire molecule, not just a reactive end. However, the presence of an aniline mustard moiety can significantly increase the overall toxicity of the compound.

3.4 Discussion

The goal of this study was to characterize the cellular responses to 11 β -dichloro, a novel anti-tumor agent that has shown very good efficacy both *in vivo* and *in vitro*. Although this compound contains by design an estradienone moiety that allows it to bind to androgen receptor, experimental evidence showed that 11 β -dichloro can also be very toxic against cell lines that do not express this steroid receptor (Hillier, 2005). Since the role of the androgen receptor in 11 β toxicity has been investigated elsewhere (Hillier et al., 2006; Proffitt, 2009), we focused on the androgen receptor independent mechanism, investigating the toxicity in HeLa cells, an AR negative cell line (Nelson-Rees et al., 1980).

Given that 11 β -dichloro is an aniline mustard derivative, we expected that an important aspect of its mechanism of toxicity may come from its ability to alkylate DNA. The DNA alkylating properties of 11 β -dichloro have already been characterized in detail (Hillier et al., 2006); however, compared with other aniline mustards used in clinic, at equimolar levels, 11 β -dichloro is much more potent (Figure 3.3 A). The clonogenic assay captures the ability of the compound to inhibit cell division; it does not tell us whether the seed cells have only been arrested or have undergone apoptosis. This is why we looked on a smaller time scale, using a growth inhibition assay (Figure 3.3 B). The time scale was chosen to be close to the doubling time of the HeLa cells (20 hours). Thus, cells exposed to a compound that causes mainly growth arrest will exhibit between 50 and 100% viability. However, if the compound causes cell death during this interval, the viability values will be below 50%. These assumptions are true only when the compound toxicity is not cell cycle specific. It has been shown (Marquis, JC personal communication) that 11 β -dichloro exposure does not affect significantly the cell cycle distribution of HeLa cells. Therefore, the viability values of less than 50% that we observe for doses of 11 β -dichloro higher than 5 μ M may be indicative of cell death. Phase-contrast microscopy examination of the cells revealed dramatic changes in cellular morphology, such as membrane blebbing and cell rounding, as well as significant cell detachment (anoikis). These morphological changes induced by 11 β -dichloro will be discussed in detail in Chapter 5. We employed the CTB assay to estimate viability; this assay takes into account the metabolic state of all cells, including detached cells. Careful

calibration experiments between the CTB assay, cell counting and other viability assays were done to ensure reproducibility and provide as correct as possible an interpretation of the results. A control experiment showed that CTB viability correlates very well with the number of attached cells remaining after treatment (Figure 3.17). Taken together, the microscopic observations and the CTB measurements suggest that the cells treated with 11 β -dichloro at doses higher than 5 μ M are indeed dying, not just arresting. The control compounds used (chlorambucil, melphalan, mechlorethamine) exert their toxicity mainly through DNA-damage mediated cell arrest (Roberts, 1980). The toxic effects of the control compounds in our experiments are consistent with literature reported values for IC₅₀ and toxicity kinetics (Detke et al., 1980; Rappeneau, Baeza-Squiban, Jeulin, et al., 2000; Frankfurt, 1987).

Also noteworthy, 11 β -dichloro toxicity happens on a fast timescale, at least for doses higher than 5 μ M (Figure 3.4), which suggests that an additional mechanism of toxicity might be operating besides or perhaps in conjunction with covalent DNA damage by 11 β -dichloro. The goal of this work was to characterize better this added-on mechanism. One important clue regarding the cellular pathways involved in this unknown mechanism came from a phenotypic screen of the entire single-gene knockout mutant yeast library (Chapter 2). The results of the yeast library investigation showed that a group of mutants that lacked a functional respiratory chain were particularly sensitive to 11 β -dichloro. Such data prompted us to investigate the effects of the compound on mitochondrial function in HeLa cells and led us to the discovery of the ROS induction.

ROS levels were determined using CM-H₂DCFDA, an ROS specific probe that can easily diffuse across the cell membrane. Once inside the cell, cellular esterases cleave the acetyl groups yielding a charged species that cannot diffuse out of the cell and, hence, accumulates inside the cell. ROS can then convert the probe into a fluorescent compound by oxidation (Tsuchiya et al., 1994). However, given the multi-step mechanism involved, the CM-H₂DCFDA fluorescence does not always indicate the presence of ROS (Bonini et al., 2006; Ohashi et al., 2002), therefore great care was taken in the design of the experiments and choice of controls (Halliwell and Whiteman, 2004).

One confounding variable is differential uptake of the dye. If the probe is taken up in larger amounts in treated cells, after enough time, the basal level of ROS in the cells may be enough to trigger oxidation of the available dye and generate enhanced but artifactual fluorescence. We examined the dye accumulation in HeLa cells using the fluorescent probes Calcein AM and Celltracker Green (Invitrogen) and we found no significant accumulation in cells treated with 11 β -dichloro compared with untreated cells. Thus, we concluded that the significant increase in fluorescence is not due to increased accumulation of dye, but to increased levels of ROS in the treated cells.

Another possible complication of using fluorescein derived probes is that, in certain conditions, they may be able to generate ROS themselves, either through redox cycling or through photoactivation. Such phenomena have been shown to lead to confounding results (Bonini et al., 2006; LeBel et al., 1992). To address such concerns, we employed a protocol that minimizes the loading time of the dye to reduce the possibility of redox cycling, and we kept the cells in the dark to reduce light driven reactions. Additionally, we employed the minimal concentration of the dye necessary to achieve a good signal, which was often much lower than in other published protocols.

To confirm our CM-H₂DCFDA results, we utilized a different method to quantitate cellular H₂O₂ (Figure 3.7). The iron-xylenol orange based assay (BioAssay Systems) is used to measure levels of H₂O₂ in cell lysates in conditions in which most other short lived ROS species are no longer present (Hermes-Lima et al., 1995). The results were consistent with the previous findings, confirming that 11 β -dichloro generates significant levels of H₂O₂ in HeLa cells.

We also investigated the generation of other ROS, such as superoxide and hydroxyl radical (HO \cdot) using more specific ROS probes. Hydroethidine has been employed for many years to specifically detect superoxide inside cells, because it reacts with superoxide but it is essentially unreactive towards hydrogen peroxide (Bindokas et al., 1996). The oxidized product becomes fluorescent only when it intercalates in DNA, allowing good retention times. Our results indicate that 11 β -dichloro treated cells do not generate more superoxide

than the untreated controls, suggesting that the mitochondrial ETC is not a direct target of our compound. However, we cannot rule out a mitochondrial origin for the ROS. It may be possible that MnSOD is not a rate limiting step in the ROS generation by 11 β -dichloro; therefore, superoxide never accumulates. Although we didn't detect superoxide, we were able to detect the hydroxyl radical using the HO \cdot specific probe HPF (Figure 3.8 A). The increase in HO \cdot is consistent with the increase in H₂O₂, HO \cdot being generated from H₂O₂. To further confirm the generation of HO \cdot , we measured the levels MDA, a marker of lipid peroxidation caused by HO \cdot (Figure 3.8 B) and found that they are also increased significantly after treatment with 11 β -dichloro.

Another way to investigate the nature of ROS generated in the cells is to see whether the ROS can be modulated by specific antioxidants. The data so far indicates that H₂O₂ is the major ROS generated; therefore we attempted to enhance the ability of the cell to deal with increased levels of H₂O₂. One common antioxidant used against H₂O₂ is N-acetyl cysteine (NAC), which acts as a precursor in the biosynthesis of GSH (Santangelo, 2003). As explained earlier, GSH is essential for the detoxification of H₂O₂ by GPX; by increasing the levels of GSH (and the ability to regenerate GSH), the cell should be able to detoxify larger amounts of H₂O₂. Indeed, by co-treating the cells with 11 β -dichloro and 10 mM NAC, the level of ROS detected by CM-H₂DCFDA is significantly reduced (Figure 3.9).

Another important class of antioxidants is the family of tocopherol derivatives, the most well known being α -tocopherol (vitamin E). Vitamin E is a liposoluble compound that plays a key role in modulating redox chemistry in the cell. Given its solubility, vitamin E accumulates in cell membranes, especially in the mitochondrial inner membrane where it acts as a radical sink, preventing propagation of radical states to the lipids and breaking the redox cycles that can generate more radicals (Ham and Liebler, 1995). By quenching the radical states, vitamin E prevents the initial stages of ROS generation. However, if present at too high a level, it may disturb membrane structure and inhibit electron transport through mitochondrial ETC (Wang and Quinn, 1999). For this reason, vitamin E rarely acts as a stoichiometric reagent, being present in cells at much lower levels than other water soluble antioxidants such as vitamin C and GSH. Thus, the regeneration of vitamin E from its radical state requires

reducing equivalents, which are usually provided by coenzyme Q (in the ETC) vitamin C or even GSH (Chow et al., 1999; Chow, 1991).

We employed both NAC and vitamin E as adjuvants to inquire whether antioxidants can modulate 11 β -dichloro toxicity. In a growth inhibition assay, co-treatment with 10 mM NAC or 100 μ M vitamin E significantly reduced the toxicity of our compound (Figure 3.10 A). Moreover, vitamin E can also significantly improve long term viability as measured in a clonogenic assay (Figure 3.11B). These results suggest that ROS may play a role in 11 β -dichloro toxicity. As it is the case with many co-treatment experiments, interactions between the active compound and the antioxidants outside the cell may obscure or change their effect inside the cell. NAC especially, has been shown to react with nitrogen mustards and cisplatin outside the cell, diminishing the effective dose that reaches the cells (De Flora et al., 1995; Rappeneau, Baeza-Squiban, Marano, et al., 2000; Rappeneau, Baeza-Squiban, Jeulin, et al., 2000). However, in the case of 11 β -dichloro, preliminary studies show that the reaction with NAC or GSH in medium proceeds relatively slowly, at a rate comparable to the rate of hydrolysis. It has been estimated that no more than 10% of 11 β -dichloro reacted with GSH in the first 6 hours of incubation (Morton, CI, personal communication). Such a change is insufficient to explain the significant difference in toxicity that we observe. In the case of vitamin E, there is no reported direct reaction with aniline mustards. However, we investigated whether vitamin E changes the solubility of 11 β -dichloro and found that for doses of 11 β -dichloro less than 10 μ M, the effective concentration of the compound (determined using ¹⁴C-labeled 11 β -dichloro) in the presence of 100 μ M vitamin E is reduced by only 10-15%. Such a small effect cannot explain the observed large difference in toxicity. These considerations are by no means exhaustive; ultimately, the co-treatment experiments constitute a necessary piece of evidence that ROS play a role in 11 β -dichloro toxicity, but they are by no means sufficient. However, had we found that the antioxidants do not significantly influence 11 β -dichloro toxicity, we might have had stronger reasons to doubt the involvement of ROS.

Generation of significant levels of ROS inside the cell can perturb the cellular antioxidant pool. As highlighted in Figure 3.2, large amounts of H₂O₂ will directly influence the cellular

levels of GSH and NADPH. Indeed, we found that levels of NADPH are severely affected by a 5 μM dose of 11 β -dichloro. Total cellular NADPH drops to about 20% of untreated controls 6 hours after exposure, suggesting a significant redox imbalance triggered perhaps by a burst of H_2O_2 (Figure 3.11 A). It is also noteworthy that the lowest levels of NADPH occur about 6 hours after exposure, because as seen in Figure 3.4 B, the majority of toxicity is due to the first 6 hours of exposure. The fact that NADPH levels eventually return to normal by 24 hours is consistent with the dose investigated; 5 μM causes about 50% growth inhibition at 24 hours, being thus a sub-lethal dose.

Analysis of cellular free thiol and GSH levels has been done using the CMFDA probe (Invitrogen). Despite its relatively high background (Hedley and Chow, 1994), this probe has shown to be useful in certain situations to estimate cellular GSH levels (Lantz et al., 2001; Coates and Tripp, 1995). However, since CMFDA binds rather non-specifically to all free thiols (for example, cysteine) in addition to GSH (Sebastià et al., 2003), we interpreted the CMFDA data only as semi-quantitative estimations of cellular GSH levels. Nevertheless, the dose dependent significant drop in the CMFDA signal measured at 24 hours (Figure 3.11 B) is still informative, because it indicates a decrease in the total free thiol concentration in the cell, a fact consistent with the generation of an ROS burst and extensive oxidative stress. However, given the semi-quantitative nature of the assay, we shall not comment on the specific GSH levels.

Addition of antioxidants was shown to diminish 11 β -toxicity (Figure 3.10). To investigate further the link between ROS and toxicity, we attempted to enhance 11 β -dichloro toxicity by diminishing the cellular antioxidant pools. One established assay is the use of L-buthionine sulfoximine (BSO) to lower cellular GSH levels (Griffith and Meister, 1979). BSO is a specific inhibitor of γ -glutamyl cysteine synthetase, the rate limiting step in the biosynthesis of GSH. The mechanism of BSO relies on the high turnover rate of GSH, an important fraction of cellular GSH being used for conjugation and hence, excreted (Griffith and Meister, 1979). In HeLa cells, a treatment of 100 μM BSO for 24 hours has been reported to diminish cellular GSH by 75-85% compared with untreated controls (Vos et al., 1984). However, HeLa cells pretreated with 100 μM BSO for 24 hours did not show a significant

increase in sensitivity to 11 β -dichloro (data not shown). Interestingly, pretreatment with BSO for 120 hours (2 passages) did render the cells significantly more sensitive to 11 β -dichloro (Figure 3.13). A possible explanation for these results may come from the non-uniform distribution of GSH pool inside the cell. As explained above, the mitochondrial GSH pool is relatively isolated from the cytosolic GSH; mitochondria can easily import GSH, but their levels of GSH equilibrate rather slowly with the cytosolic GSH (Griffith and Meister, 1985). It has actually been shown that BSO quickly reduces the cytosolic GSH, but incubations of several days are required to affect the mitochondrial GSH significantly (Griffith, 1982). Given these considerations, our results would imply that mitochondrial GSH levels (and not the cytosolic GSH) are responsible for modulating 11 β -dichloro toxicity, adding support to the hypothesis that mitochondria might be the source of the ROS associated with the compound's toxicity.

Mitochondrial inner membrane potential is an important indicator of the physiological state of the cell; dramatic changes in the membrane potential have been shown to be indicative of toxicity and may be an integral part of cell death mechanisms such as apoptosis (Lemasters et al., 1999). Given the previous results suggesting links between 11 β -dichloro toxicity and mitochondrial function, we closely examined whether exposure to 11 β -dichloro impacts the inner mitochondrial membrane potential. Using the established JC-1 ratiometric method of estimating inner mitochondrial membrane potential, $\Delta\Psi_m$, we found that exposure to 11 β -dichloro increases $\Delta\Psi_m$ in a dose and time dependent manner (Figure 3.13 A).

Hyperpolarization of mitochondrial inner membrane has been reported not only for certain DNA alkylators such as cisplatin (Nowak, 2002), but also for other classes of toxicants such as the proteasome inhibitor bortezomib (Ling et al., 2003). In all cases, the hyperpolarization has been associated with an increase in ROS. Our data are consistent with the hypothesis that increased mitochondrial potential generates an increased level of ROS in the cell. They do not, however, reveal the specific mechanism by which 11 β -dichloro perturbs $\Delta\Psi_m$ and generates ROS. Interestingly, at 24 hours after treatment, $\Delta\Psi_m$ drops in a dose dependent manner, a finding suggestive of the induction of a cell death program (Figure 3.13 B). A large body of literature has shown that depolarization of mitochondrial membrane can be caused by formation of mitochondrial membrane permeability pores that allow the release of

cytochrome c in the cytosol and activate the apoptosis pathway (Lemasters et al., 1999). Our data suggest that mitochondrial depolarization may be an important step that precedes cell death, given that some depolarization is detected even at sub-lethal doses (Figure 3.13 B).

Finally, we investigated the connection between the 11 β -dichloro's ability to alkylate substrates and the ROS response it generates. Nitrogen mustards and other alkylating compounds have been reported to induce numerous cellular stress responses, including ROS (Nowak, 2002; Rappeneau, Baeza-Squiban, Jeulin, et al., 2000; Boldogh et al., 2003). However, in the case of 11 β -dichloro, we hypothesized that the ROS response might be independent of its ability to damage DNA. To address this possibility, we studied the cellular responses induced by 11 β -dimethoxy, a derivative of our lead compound that cannot react with DNA. Confirming previous reports, 11 β -dimethoxy is significantly less toxic than 11 β -dichloro, as determined by a clonogenic assay (Figure 3.14 A) and a 24 hour growth inhibition assay quantified by CTB (Figure 3.14 B). However, 11 β -dimethoxy can induce ROS in a range of doses similar to that of 11 β -dichloro (Figure 3.15 A); a 6 hour exposure to 10 μ M 11 β -dimethoxy generates almost as much ROS as an equivalent exposure to 5 μ M 11 β -dichloro. Moreover, a dose of 10 μ M 11 β -dimethoxy has a significant impact on NADPH levels at 6 hours, in a similar fashion with 11 β -dichloro (Figure 3.15 B). Even more importantly, the antioxidants NAC and vitamin E can diminish 11 β -dimethoxy toxicity (Figure 3.16), indicating that ROS may play an important role in the toxicity of 11 β -dimethoxy, at least for the doses investigated. The effect of antioxidants on 11 β -dimethoxy toxicity is actually more compelling than the corresponding effect on 11 β -dichloro, because in the case of 11 β -dimethoxy, no drug-inactivating reactions are expected to occur outside the cell. All these properties of 11 β -dimethoxy suggest the possibility that in the case of 11 β -dichloro, the bulk of ROS response is not dependent on the aniline mustard reactivity, but on the general structure of the compound that includes the steroid moiety and the linker. Consequently, the enhanced toxicity of 11 β -dichloro may be due to its ability to act on several distinct targets: 11 β -dichloro can damage DNA but can also induce ROS.

Taken together, the data presented in this chapter demonstrates that 11 β -dichloro induces a significant level of ROS in HeLa cells. Additionally, the data hint to the possibility that ROS

may contribute to 11 β -dichloro toxicity. As for the origin of ROS, mitochondrial ETC might be a likely candidate. More experimental investigations are needed to pinpoint the exact source of ROS and the role played by ROS in the overall mechanism of toxicity of 11 β -dichloro.

3.5 Figures

<i>Figure 3.1 ROS sources in the mitochondria</i>	<i>129</i>
<i>Figure 3.2 The detoxification of ROS inside the mitochondrial matrix.....</i>	<i>130</i>
<i>Figure 3.3 11β-Dichloro exhibits remarkable acute and chronic toxicity.</i>	<i>131</i>
<i>Figure 3.4 11β-Dichloro exhibits significant acute toxicity.....</i>	<i>132</i>
<i>Figure 3.5 11β-Dichloro induces a robust ROS response in a dose dependent manner....</i>	<i>133</i>
<i>Figure 3.6 11β-Dichloro induces ROS in a time dependent manner.....</i>	<i>134</i>
<i>Figure 3.7 11β-Dichloro induces hydrogen peroxide accumulation in HeLa cells.</i>	<i>135</i>
<i>Figure 3.8 11β-Dichloro induces hydroxyl radical formation and lipid peroxidation.</i>	<i>136</i>
<i>Figure 3.9 The antioxidant NAC reduces ROS levels in 11β-dichloro treated cells.</i>	<i>137</i>
<i>Figure 3.10 Co-treatment with antioxidants ameliorates 11β-dichloro toxicity.</i>	<i>138</i>
<i>Figure 3.11 11β-Dichloro exposure diminishes the cellular antioxidant pool.....</i>	<i>139</i>
<i>Figure 3.12 GSH depletion increases sensitivity to 11β-dichloro.....</i>	<i>140</i>
<i>Figure 3.13 11β-Dichloro exposure affects mitochondrial membrane potential.</i>	<i>141</i>
<i>Figure 3.14 11β-Dimethoxy is much less toxic than 11β-dichloro.....</i>	<i>142</i>
<i>Figure 3.15 11β-Dimethoxy induces ROS and lowers cellular NADPH levels.....</i>	<i>143</i>
<i>Figure 3.16 11β-Dimethoxy toxicity is ameliorated by antioxidants.....</i>	<i>144</i>
<i>Figure 3.17 Comparison between cell counting and the CTB assay.....</i>	<i>145</i>

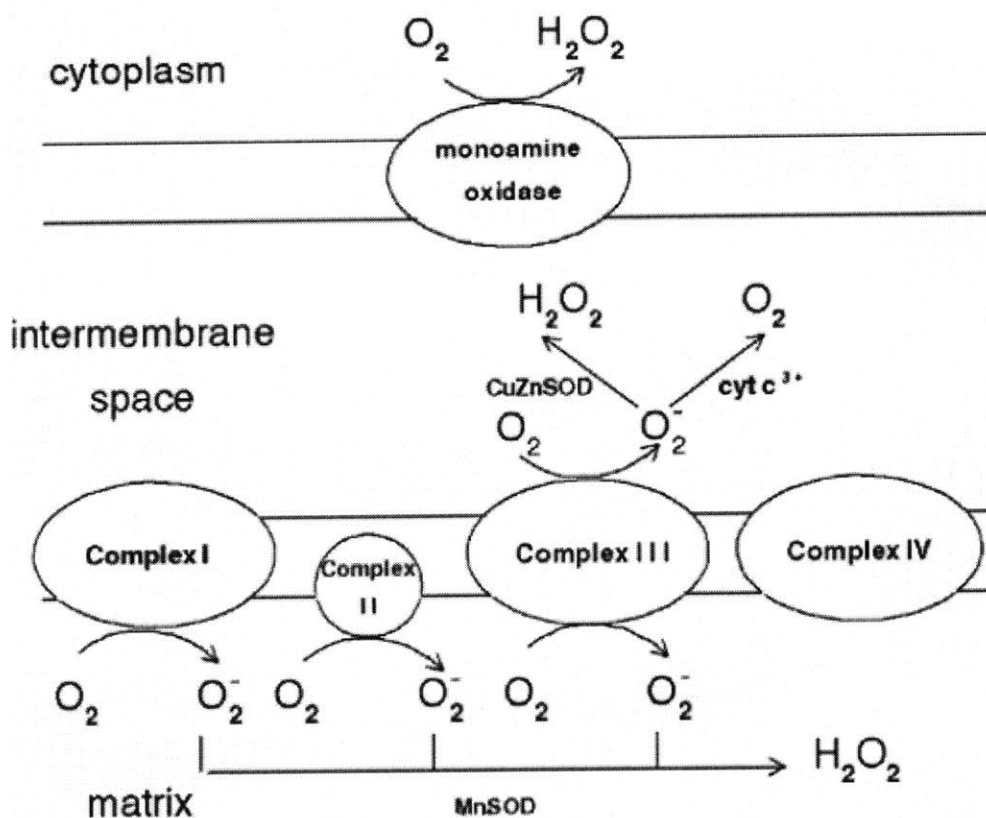


Figure 3.1 ROS sources in the mitochondria

Along the mitochondrial inner membrane, complexes I, II and III may contain intermediates capable of reducing O_2 to superoxide. When the superoxide is released in the matrix, it is quickly converted to H_2O_2 by the mitochondrial SOD (MnSOD). The superoxide released in the intermembrane space (or in the cytosol) is detoxified either by the cytosolic SOD (CuZnSOD) or by cytochrome c. In the latter case, cytochrome c can transport the reducing electrons to complex IV without generating any other ROS. Another source of H_2O_2 in the mitochondria is the monoamine oxidase, an enzyme in the outer mitochondrial membrane. (This figure was adapted from (Turrens, 2003)).

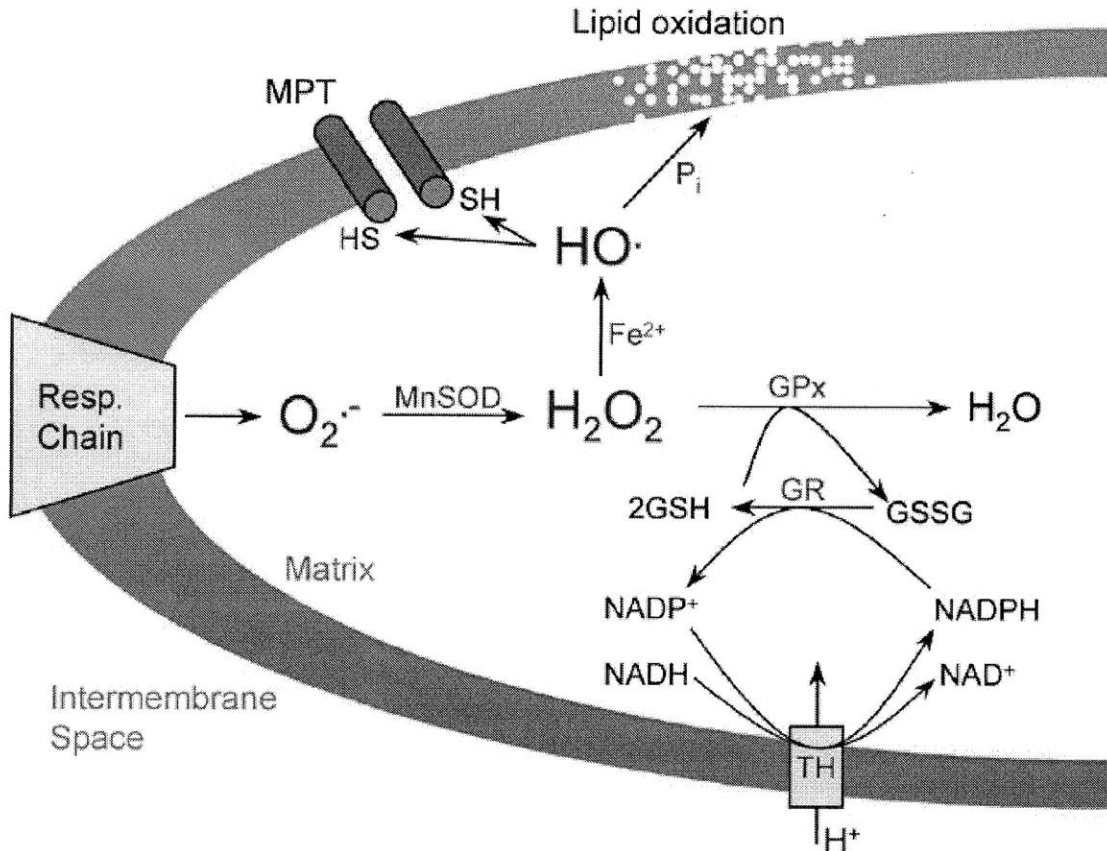


Figure 3.2 The detoxification of ROS inside the mitochondrial matrix

The superoxide generated from the ETC is converted by MnSOD into H_2O_2 . H_2O_2 is detoxified by glutathione peroxidase (GPX) in a GSH dependent reaction. GSH is then regenerated by the glutathione reductase (GR), in a NADPH dependent manner. Finally, NADPH is regenerated from NADH by the transhydrogenase (TH) using the membrane proton gradient. If H_2O_2 accumulates in high quantities, in the presence of reduced iron centers, it can generate $HO\cdot$, a highly reactive species that can cause lipid damage and activate mitochondrial permeability transition (MPT) by oxidizing the sulphur side chains of certain membrane proteins and locking them together into a membrane permeability pore. (This figure was adapted from (Kowaltowski et al., 2001)).

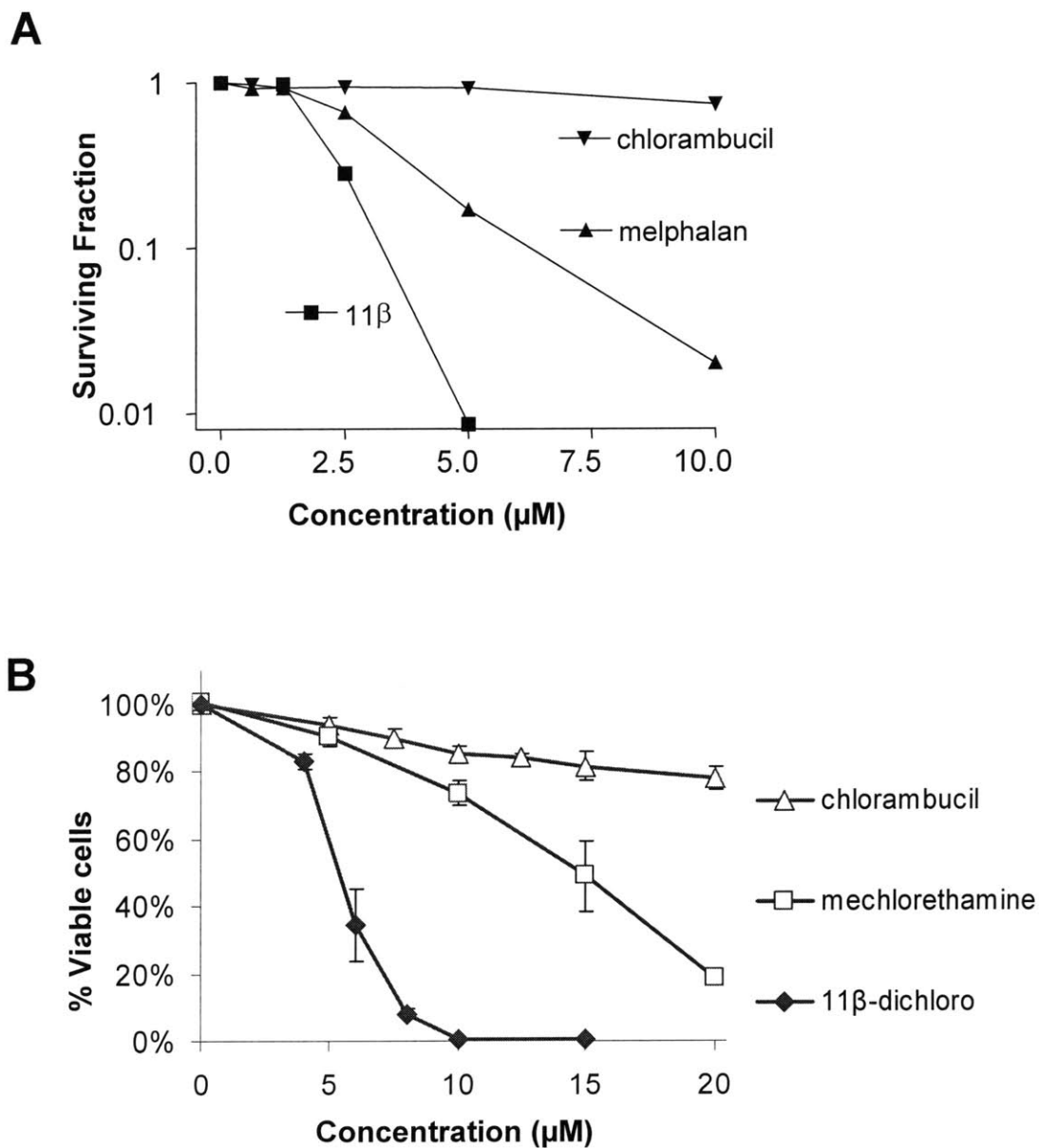


Figure 3.3 11β-Dichloro exhibits remarkable acute and chronic toxicity.

Direct comparison of 11β-dichloro with simpler nitrogen mustards in a clonogenic assay (A) and in a growth inhibition assay measured by CTB (B) highlights the remarkable toxicity of 11β-dichloro.

(The graph in part A was adapted from Croy, RG, 2005, personal communication).

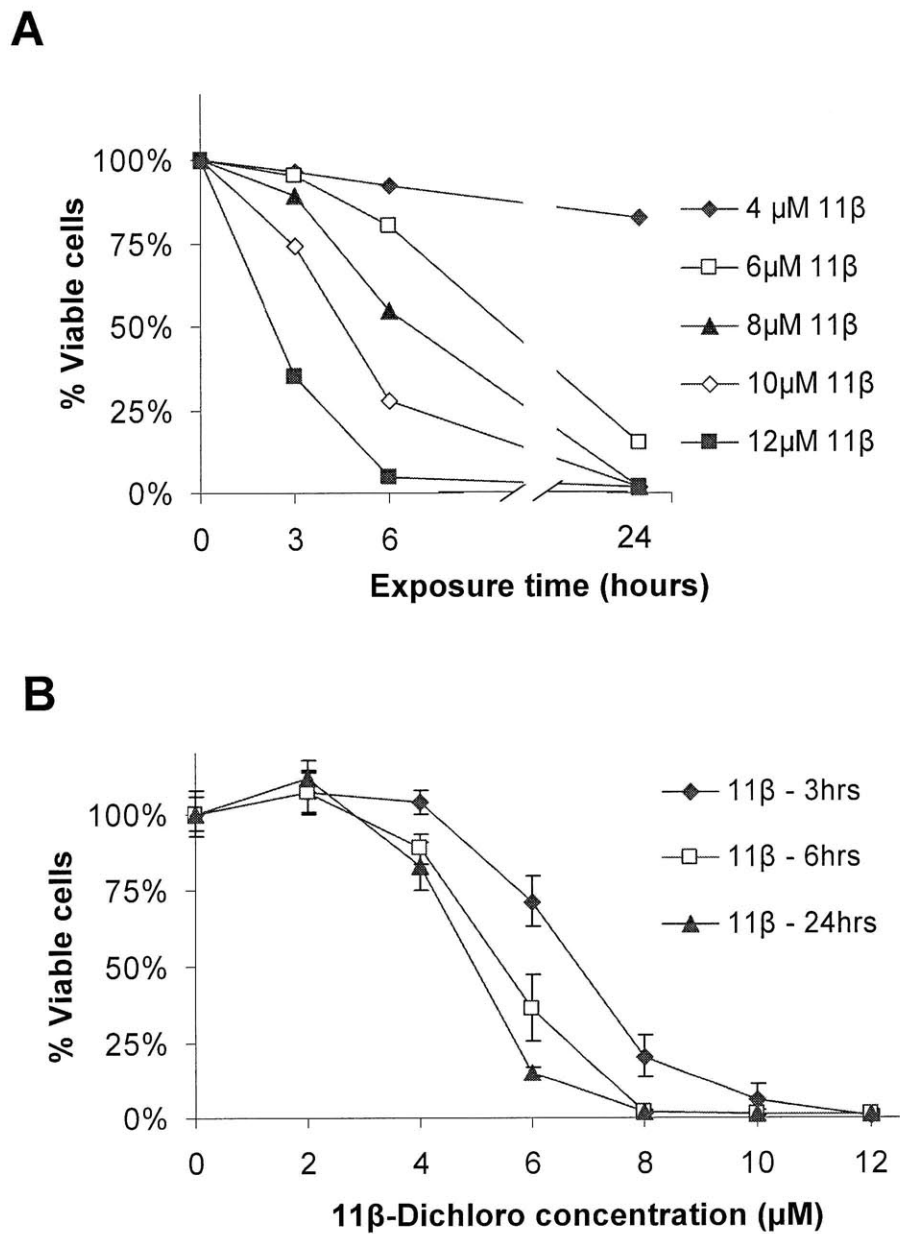


Figure 3.4 11 β -Dichloro exhibits significant acute toxicity

A growth inhibition assay shows that the cell number drops in a dose and time dependent manner (A). In a recovery assay (B), cells are treated for shorter amounts of time (3, 6hrs) then left to recover in regular medium. Their viability is measured at 24hrs (CTB) and compared with the viability of cells exposed continuously for 24hrs.

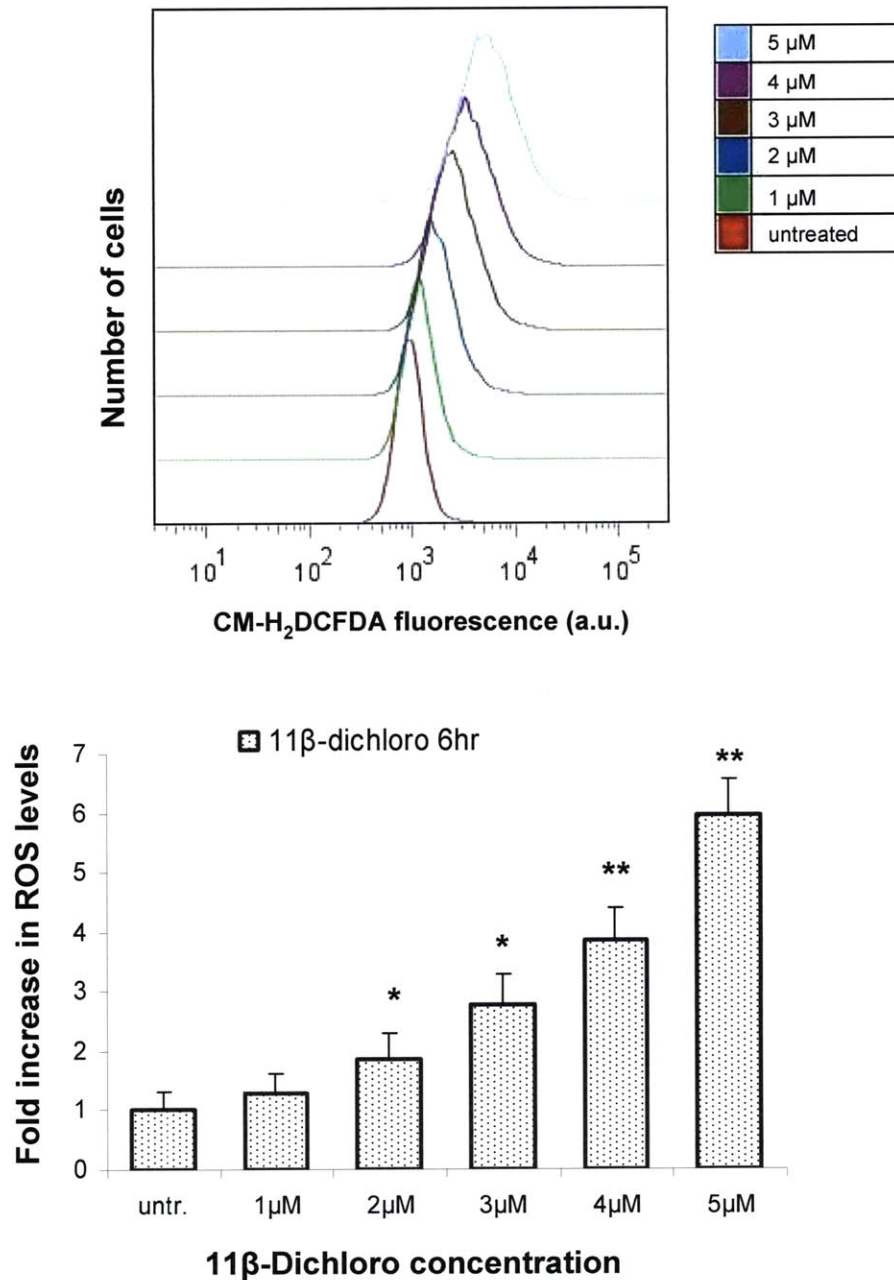


Figure 3.5 11β-Dichloro induces a robust ROS response in a dose dependent manner.

The top of the Figure displays typical flow cytometry traces of cells stained with ROS dye CM-H₂DCFDA; the bars at the bottom represent the median value of each peak, normalized to the untreated; the error bars are the standard deviation from 3 separate samples.

* signifies $p < 0.05$ compared with the untreated. ** signifies $p < 0.01$.

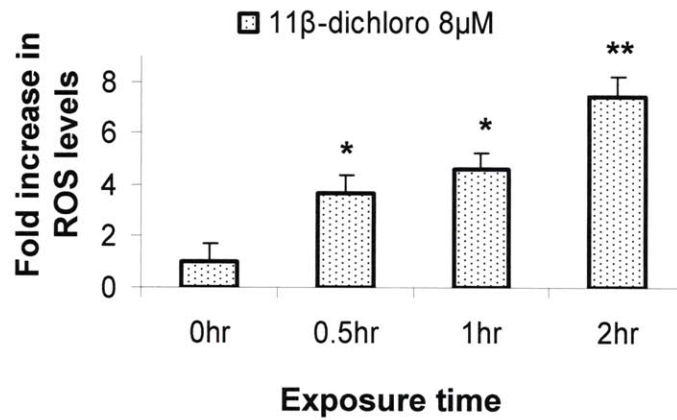
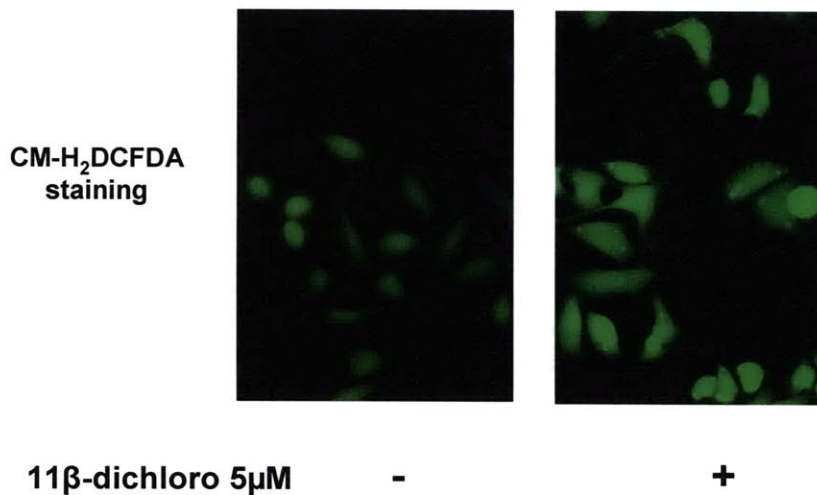
A**B**

Figure 3.6 11β-Dichloro induces ROS in a time dependent manner.

The ROS levels were determined in HeLa cells exposed to 8 μM 11β-dichloro for the indicated amounts of time. Each bar represents the median of the flow cytometry peak; the error bars are the standard deviations of 3 separate samples (A). Staining with CM-H₂DCFDA makes 11β-dichloro treated cells visibly brighter, as seen under a fluorescence microscope (B). The dye does not speckle the cells, accumulating rather uniformly.

* signifies $p < 0.05$ compared with the untreated. ** signifies $p < 0.01$.

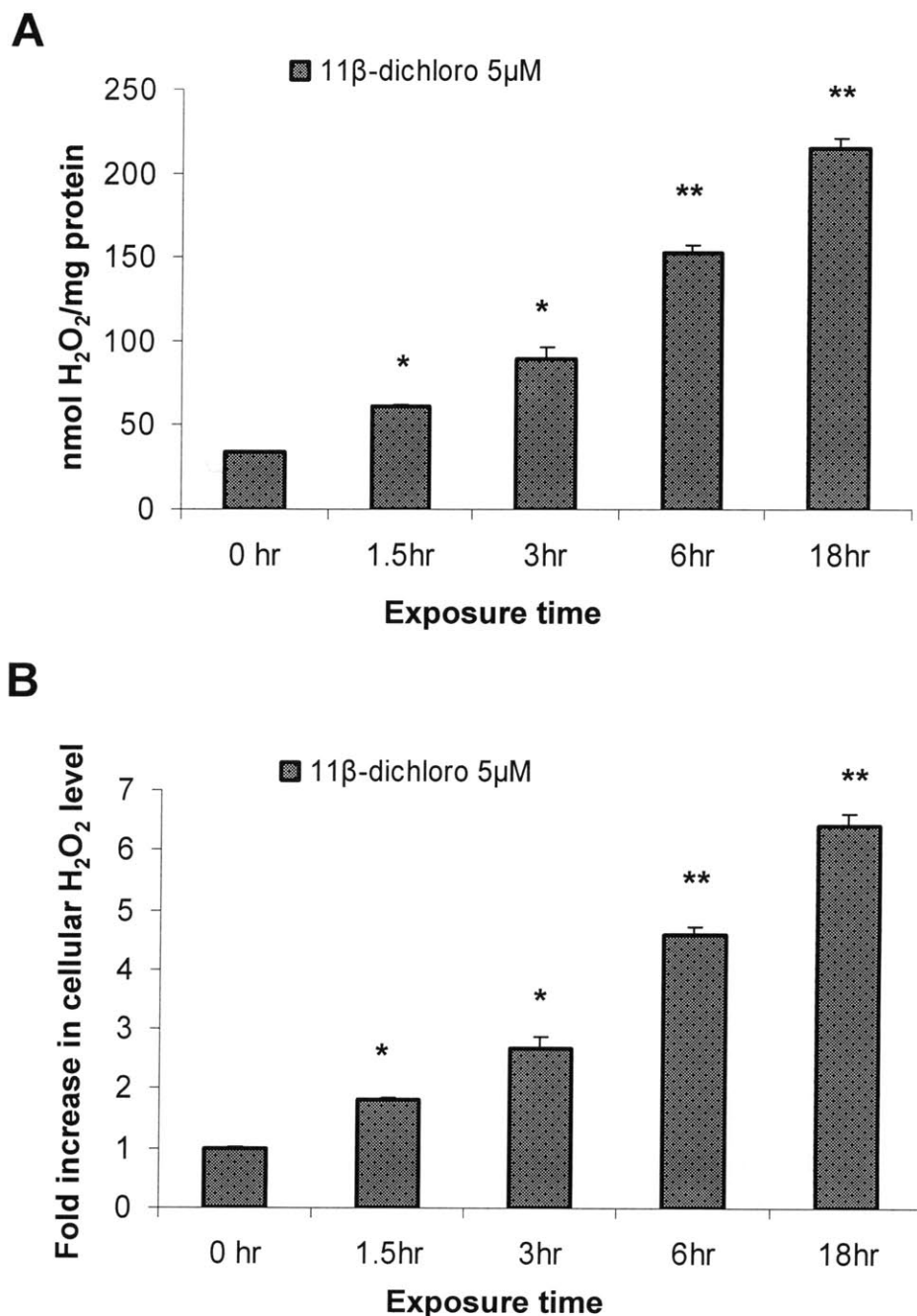


Figure 3.7 11 β -Dichloro induces hydrogen peroxide accumulation in HeLa cells.

A time course with 5 μ M 11 β -dichloro shows increasing accumulation of H₂O₂ in the cell, as measured with an iron-xylenol orange based kit. The bars represent amounts of H₂O₂ calculated as nmoles H₂O₂/mg protein in the cell lysate (A) or the same values normalized to the untreated (B). The error bars are standard deviations of 3 independent samples.

* signifies $p < 0.05$ compared with the untreated. ** signifies $p < 0.01$.

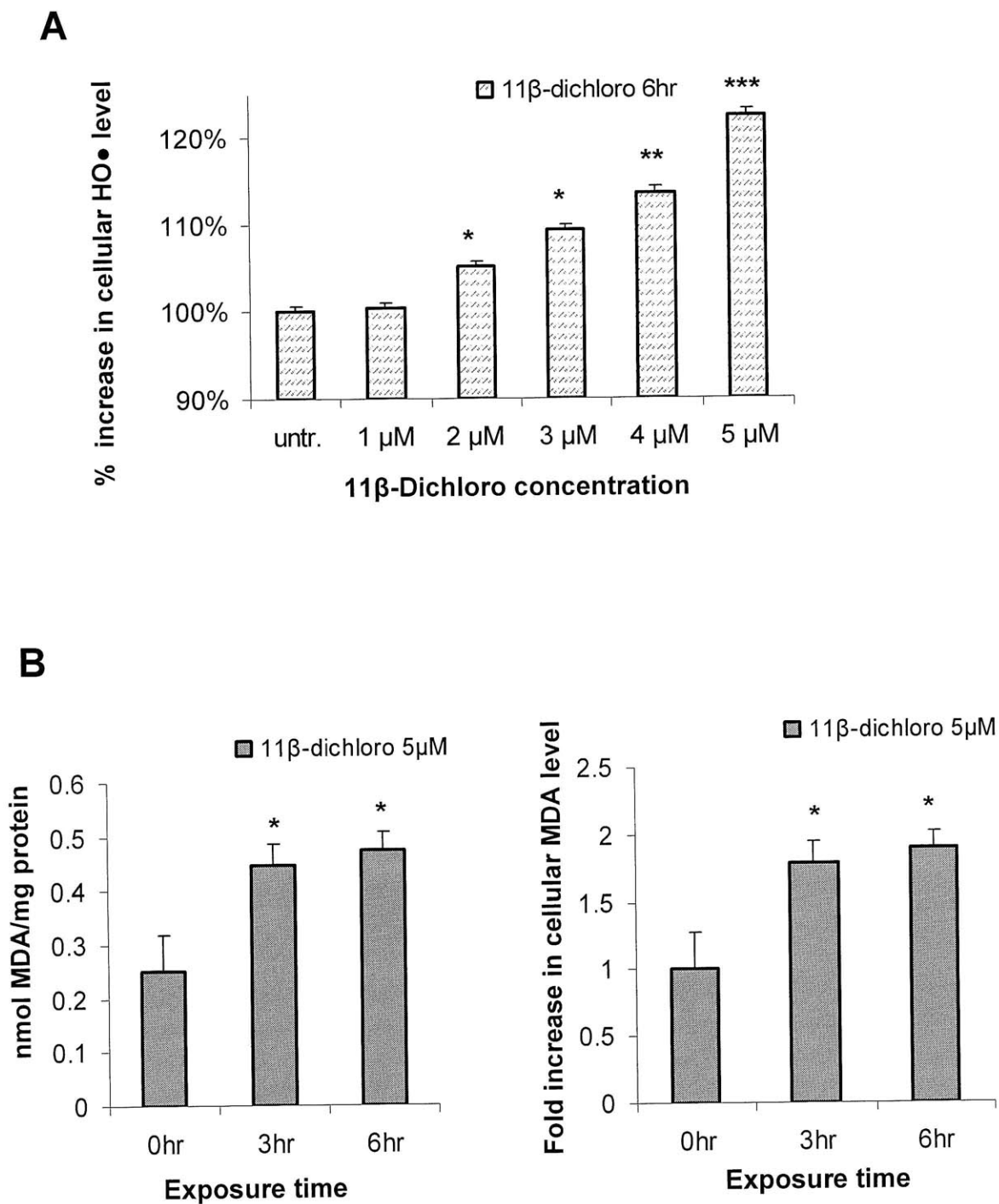


Figure 3.8 11β-Dichloro induces hydroxyl radical formation and lipid peroxidation.

11β-dichloro causes a significant increase in HO• generation as determined by flow cytometry with the HO• specific dye, HPF (A). 11β-dichloro at 5 μM causes accumulation of MDA, a lipid peroxidation marker. The bars represent amounts of MDA expressed as nmol MDA/mg protein in the cell lysate (B, left) or normalized to untreated (B, right).

* signifies $p < 0.05$ compared with the untreated. ** signifies $p < 0.01$. *** signifies $p < 0.001$.

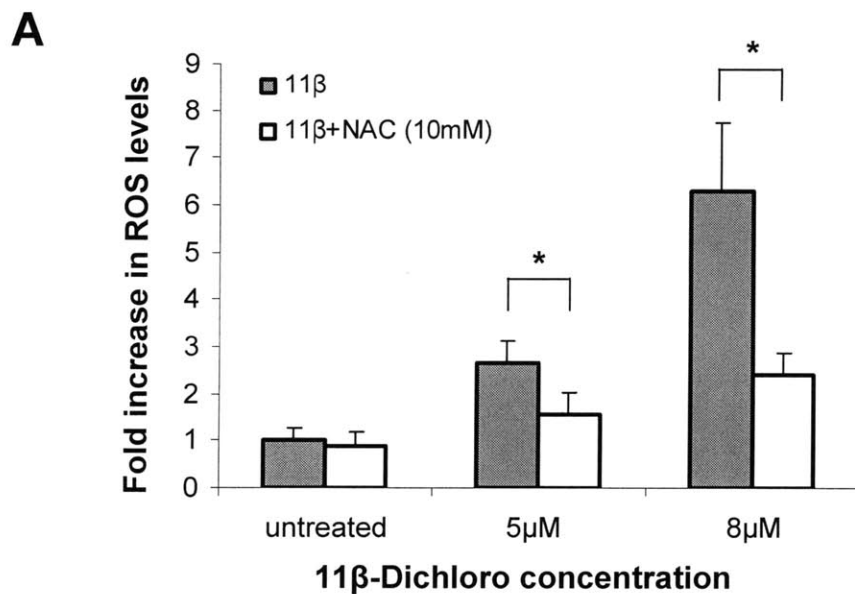


Figure 3.9 The antioxidant NAC reduces ROS levels in 11β-dichloro treated cells.

Cells co-treated with 11β-dichloro and NAC (10 mM) accumulate significantly less ROS than cells treated with 11β-dichloro alone.

* signifies $p < 0.05$ compared with the untreated. ** signifies $p < 0.01$.

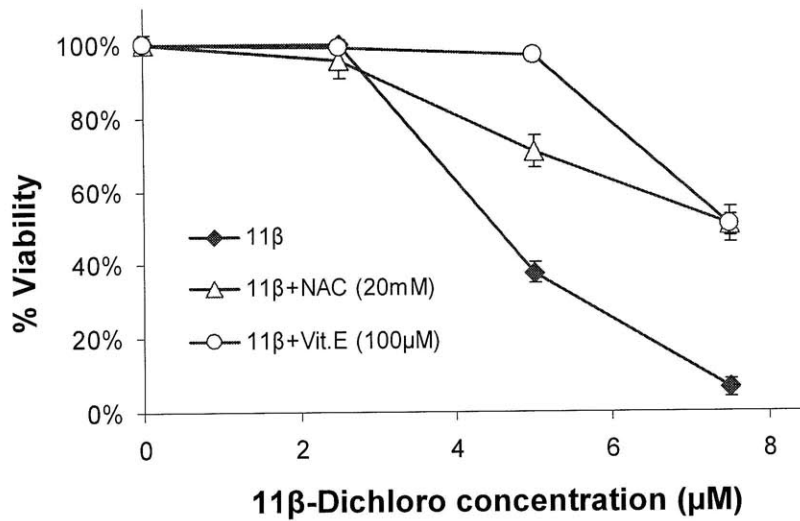
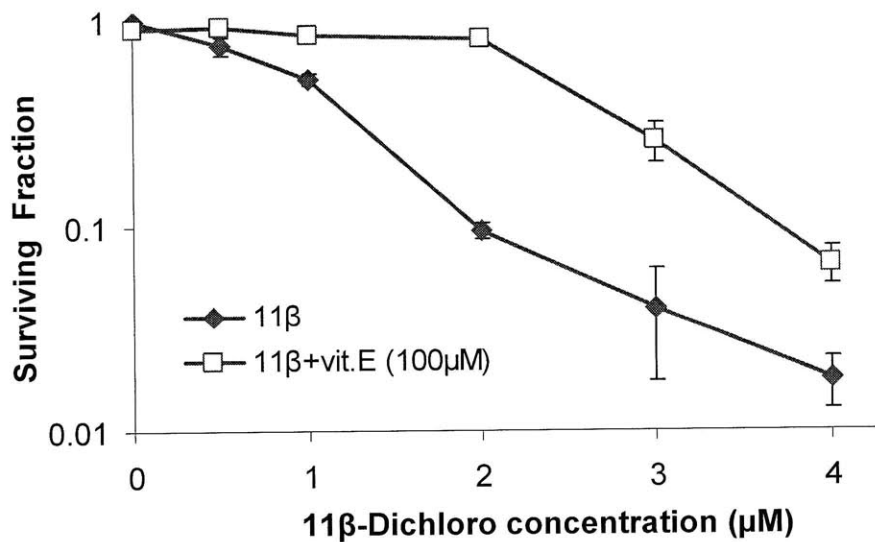
A**B**

Figure 3.10 Co-treatment with antioxidants ameliorates 11β-dichloro toxicity.

Co-treatment with NAC (20 mM) and vitamin E (100 μM) significantly diminishes 11β-dichloro toxicity as measured in a CTB assay at 24 hours (A). Vitamin E (100 μM) can drastically improve viability in a colony forming assay, after a 24 hour exposure to 11β-dichloro (B).

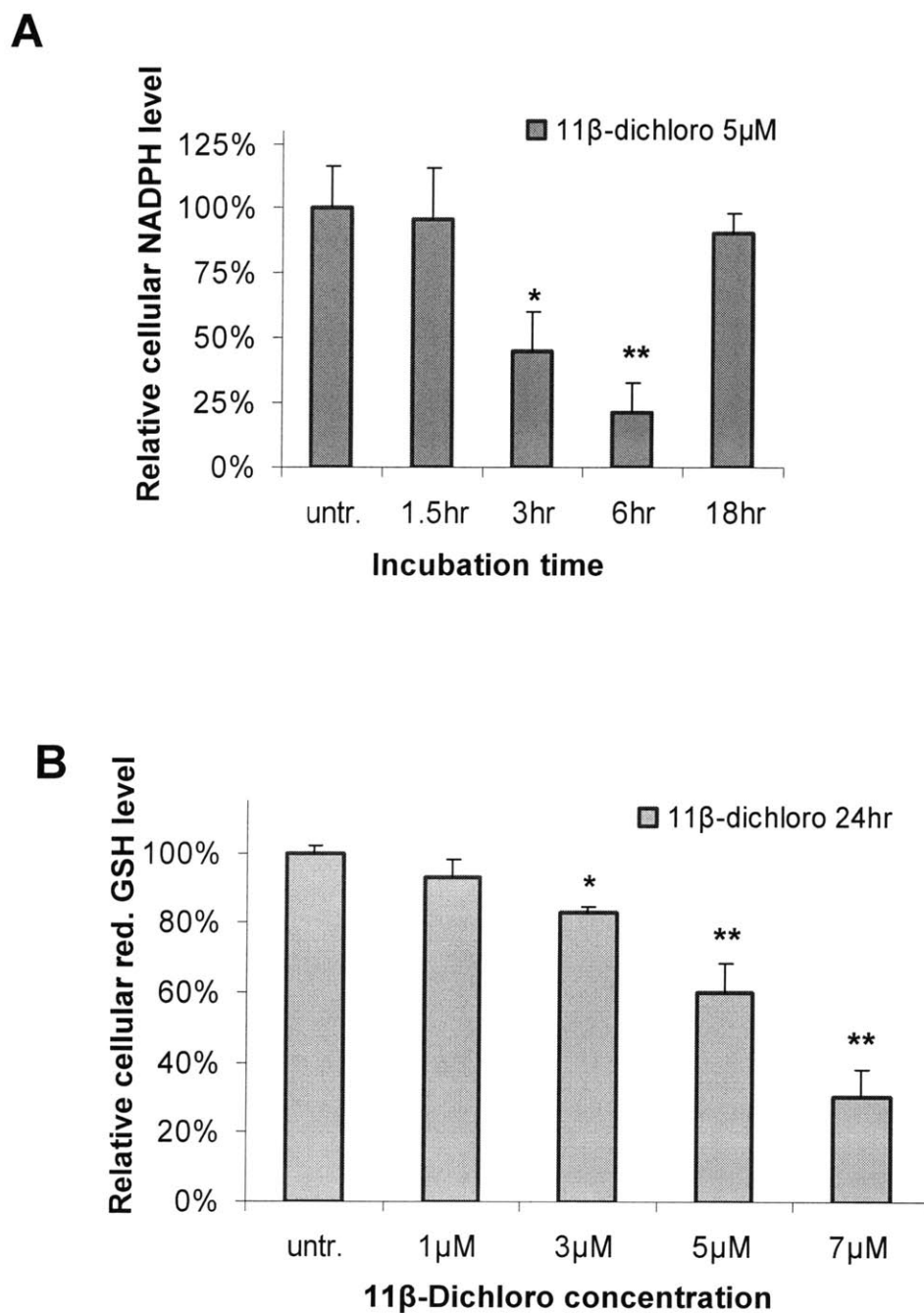


Figure 3.11 11β-Dichloro exposure diminishes the cellular antioxidant pool.

Cellular NADPH levels drop significantly following exposure to 5 μM 11β-dichloro (A). 11β-dichloro exposure diminishes cellular GSH levels in a dose dependent manner, as determined after 24 hours, using the *in situ* fluorescent probe CMFDA (B).

* signifies $p < 0.05$ compared with the untreated. ** signifies $p < 0.01$.

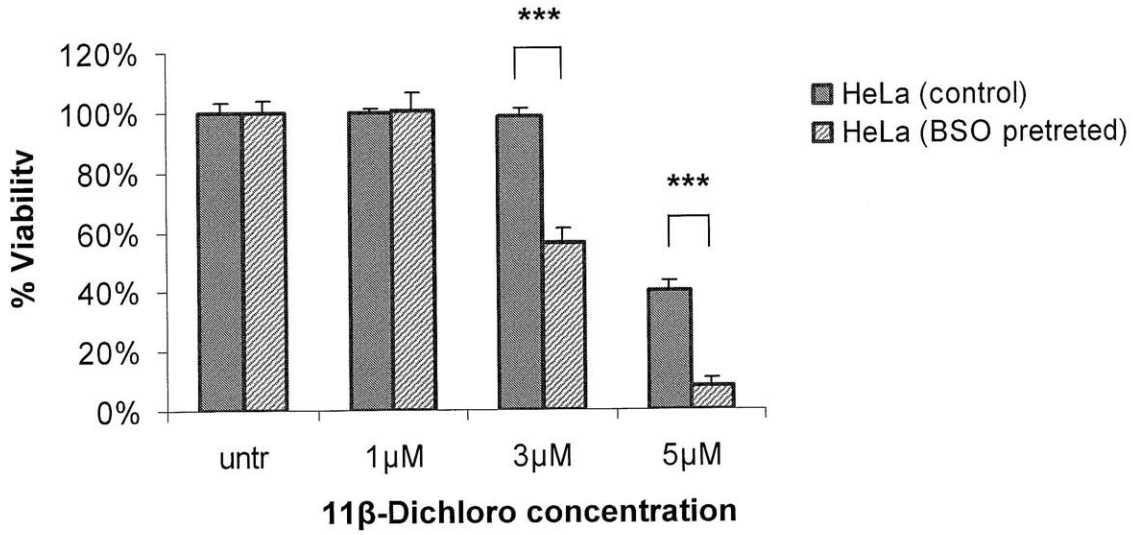


Figure 3.12 GSH depletion increases sensitivity to 11β-dichloro.

Pretreatment of HeLa cells with BSO (a GSH synthesis inhibitor) for 120 hours makes cells more sensitive to 11β-dichloro. Toxicity was measured with CTB after 24 hours exposure.

*** signifies $p < 0.001$.

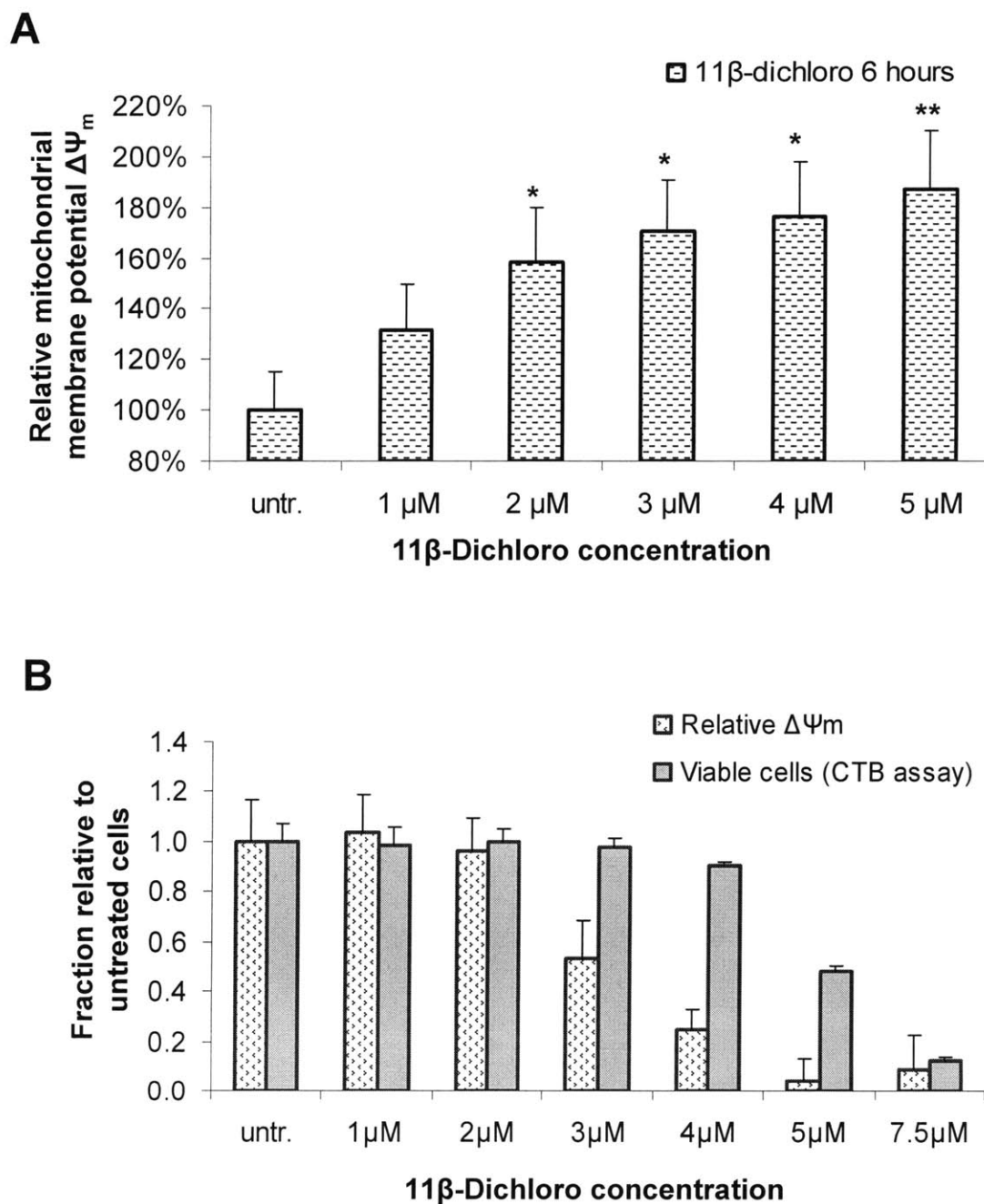


Figure 3.13 11 β -Dichloro exposure affects mitochondrial membrane potential.

A 6 hour exposure to 11 β -dichloro induces mitochondrial membrane hyper-polarization in a dose dependent manner (A). After 24 hours exposure, 11 β -dichloro causes mitochondrial membrane depolarization, at doses that do not cause a significant loss in cell viability (B). $\Delta\Psi_m$ was estimated from the red/green ratio of JC-1 fluorescence and normalized to the untreated.

* signifies $p < 0.05$ compared with the untreated. ** signifies $p < 0.01$.

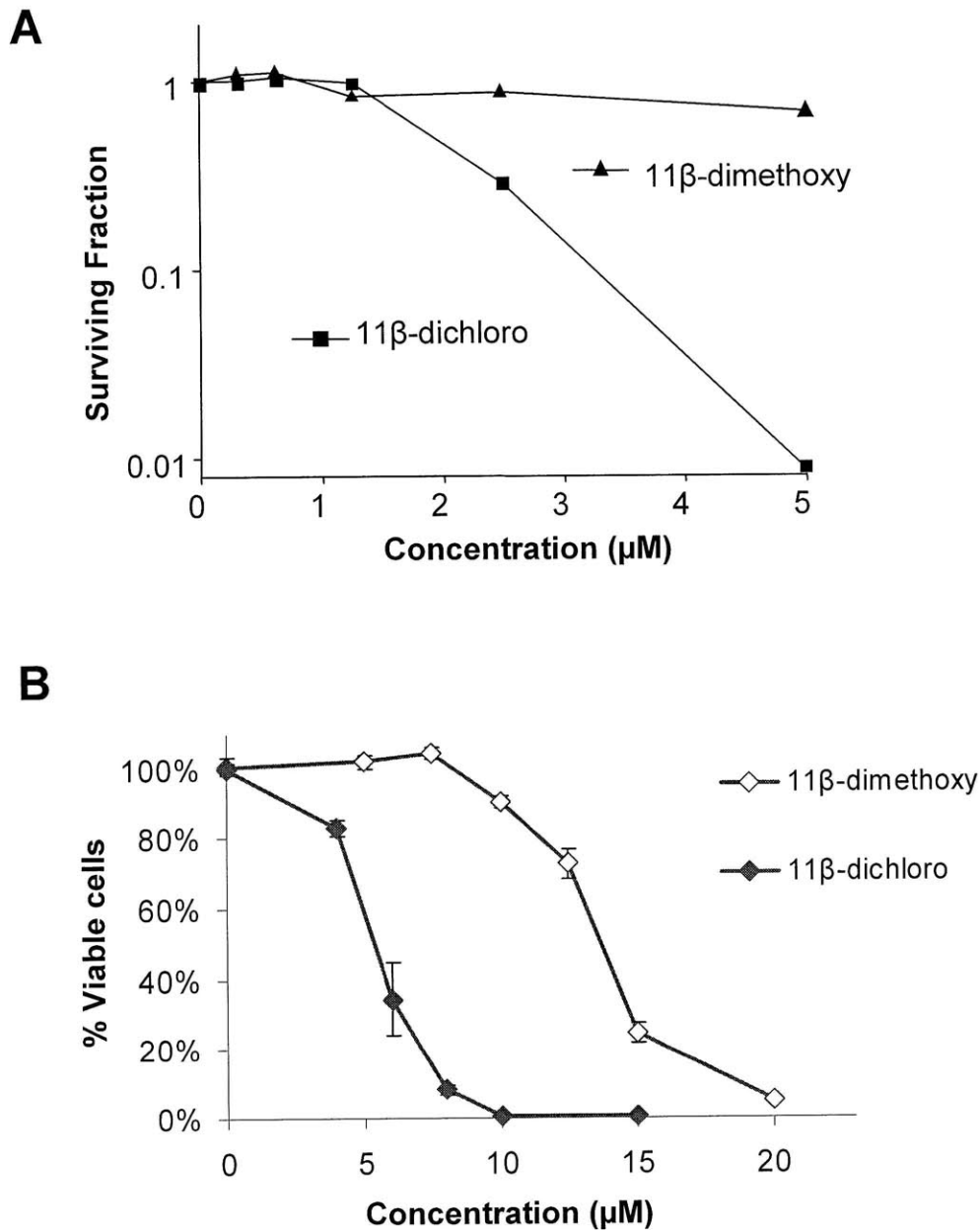


Figure 3.14 11β-Dimethoxy is much less toxic than 11β-dichloro.

11β-Dimethoxy does not display significant toxicity below 5 µM, in a clonogenic assay, whereas 11β-dichloro has an IC₅₀ of about 2 µM (A). 11β-Dimethoxy does show a measurable toxicity at 24 hours in a growth inhibition assay (measured with CTB), but it requires doses 2-3 times higher to achieve comparable toxicity with 11β-dichloro (B). (The graph in part A was adapted from Croy, RG, 2005, personal communication).

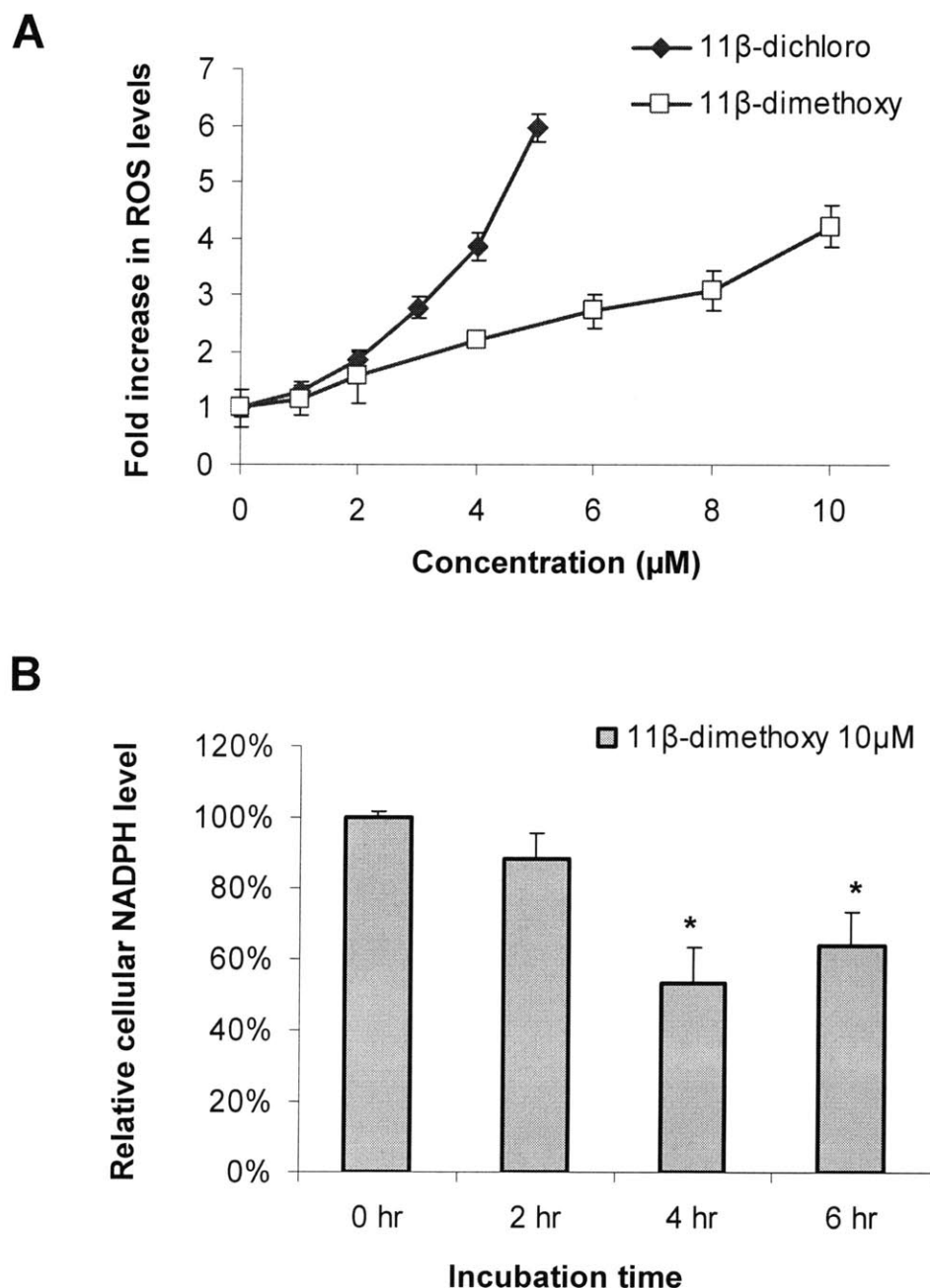


Figure 3.15 11 β -Dimethoxy induces ROS and lowers cellular NADPH levels.

11 β -Dimethoxy induces ROS, as measured with flow cytometry using the CM-H₂DCFDA probe. However, 11 β -dimethoxy achieves levels of ROS comparable with 11 β -dichloro only at concentrations twice as high (A). A dose of 10 μM 11 β -dimethoxy can lower significantly the cellular NADPH levels after 4 hours of exposure (B).

* signifies $p < 0.05$ compared with the untreated.

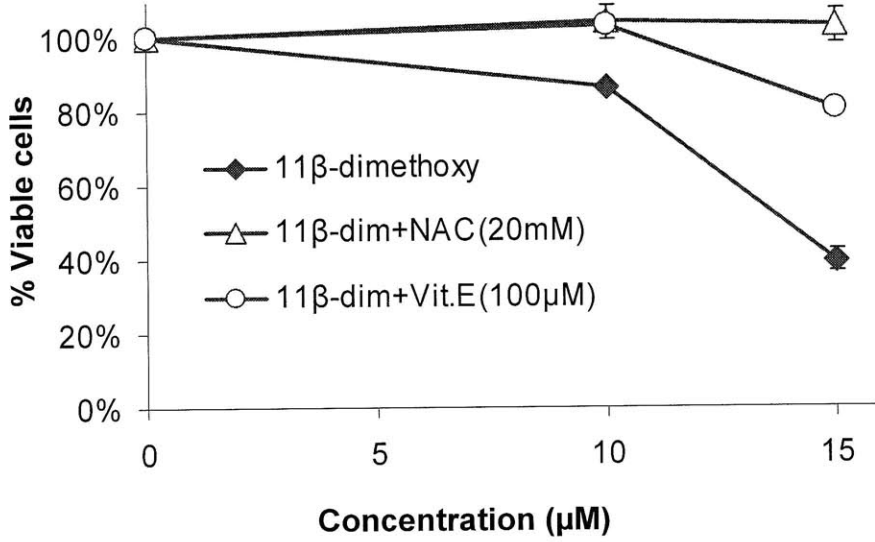


Figure 3.16 11β-Dimethoxy toxicity is ameliorated by antioxidants

Co-treatment with NAC (20 mM) and vitamin E (100 µM) significantly diminishes 11β-dimethoxy toxicity measured in a CTB assay at 24 hours.

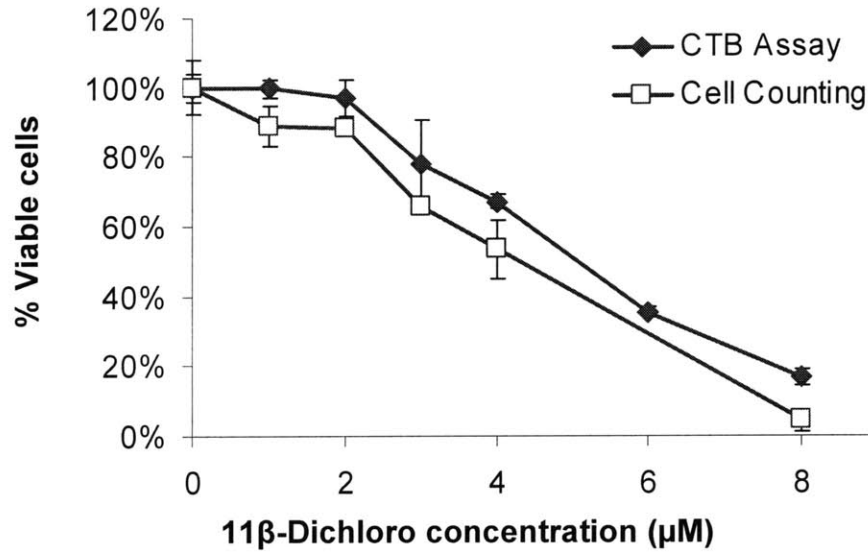


Figure 3.17 Comparison between cell counting and the CTB assay

HeLa cells have been seeded at the same density in either 96-well plates or 6-well plates. Then, the cells have been treated with the indicated concentrations of 11β-dichloro for 24 hours. The cells in the 96-well plates have been analyzed using the CTB assay, while the cells in the 6-well plates have been counted with a Coulter Counter (see Materials and Methods). The results indicate that both methods yield very similar results, providing experimental support for the use of CTB viability values as an estimate of the number of remaining attached cells after exposure to 11β-dichloro.

3.6 References

- Bindokas, V. P., Jordán, J., Lee, C. C., and Miller, R. J. (1996). Superoxide production in rat hippocampal neurons: selective imaging with hydroethidine. *J. Neurosci* *16*, 1324-1336.
- Boldogh, I., Roy, G., Lee, M. S., Bacsi, A., Hazra, T. K., Bhakat, K. K., Das, G. C., and Mitra, S. (2003). Reduced DNA double strand breaks in chlorambucil resistant cells are related to high DNA-PKcs activity and low oxidative stress. *Toxicology* *193*, 137-152.
- Bonini, M. G., Rota, C., Tomasi, A., and Mason, R. P. (2006). The oxidation of 2',7'-dichlorofluorescein to reactive oxygen species: a self-fulfilling prophesy? *Free Radic. Biol. Med* *40*, 968-975.
- Chow, C. K. (1991). Vitamin E and oxidative stress. *Free Radic. Biol. Med* *11*, 215-232.
- Chow, C. K., Ibrahim, W., Wei, Z., and Chan, A. C. (1999). Vitamin E regulates mitochondrial hydrogen peroxide generation. *Free Radic. Biol. Med* *27*, 580-587.
- Coates, A., and Tripp, E. (1995). Comparison of two fluorochromes for flow cytometric assay of cellular glutathione content in human malignant melanoma. *Melanoma Res* *5*, 107-111.
- Crater, J., and Kannan, S. (2007). Molecular mechanism of nitrogen mustard induced leukocyte(s) chemotaxis. *Med Hypotheses* *68*, 318-9.
- Das, G. C., Bacsi, A., Shrivastav, M., Hazra, T. K., and Boldogh, I. (2006). Enhanced gamma-glutamylcysteine synthetase activity decreases drug-induced oxidative stress levels and cytotoxicity. *Mol Carcinog* *45*, 635-47.
- De Flora, S., Cesarone, C. F., Balansky, R. M., Albini, A., D'Agostini, F., Bennicelli, C., Bagnasco, M., Camoirano, A., Scatolini, L., and Rovida, A. (1995). Chemopreventive properties and mechanisms of N-Acetylcysteine. The experimental background. *J. Cell. Biochem. Suppl* *22*, 33-41.
- Detke, S., Stein, J. L., and Stein, G. S. (1980). Influence of chlorambucil, a bifunctional alkylating agent, on DNA replication and histone gene expression in HeLa S3 cells. *Cancer Res* *40*, 967-974.
- Fernandez-Checa, J. C., and Kaplowitz, N. (2005). Hepatic mitochondrial glutathione: transport and role in disease and toxicity. *Toxicol. Appl. Pharmacol* *204*, 263-273.
- Frankfurt, O. S. (1987). Detection of DNA damage in individual cells by flow cytometric analysis using anti-DNA monoclonal antibody. *Exp. Cell Res* *170*, 369-380.

- Galluzzi, L., Larochette, N., Zamzami, N., and Kroemer, G. (2006). Mitochondria as therapeutic targets for cancer chemotherapy. *Oncogene* 25, 4812-30.
- Griffith, O. W. (1982). Mechanism of action, metabolism, and toxicity of buthionine sulfoximine and its higher homologs, potent inhibitors of glutathione synthesis. *J. Biol. Chem* 257, 13704-13712.
- Griffith, O. W., and Meister, A. (1979). Glutathione: interorgan translocation, turnover, and metabolism. *Proc. Natl. Acad. Sci. U.S.A* 76, 5606-5610.
- Griffith, O. W., and Meister, A. (1985). Origin and turnover of mitochondrial glutathione. *Proc. Natl. Acad. Sci. U.S.A* 82, 4668-4672.
- Griffith, O. W., and Meister, A. (1979). Potent and specific inhibition of glutathione synthesis by buthionine sulfoximine (S-n-butyl homocysteine sulfoximine). *J. Biol. Chem* 254, 7558-7560.
- Halliwell, B., and Whiteman, M. (2004). Measuring reactive species and oxidative damage in vivo and in cell culture: how should you do it and what do the results mean? *Br. J. Pharmacol* 142, 231-255.
- Ham, A. J., and Liebler, D. C. (1995). Vitamin E oxidation in rat liver mitochondria. *Biochemistry* 34, 5754-5761.
- Han, S., Espinoza, L. A., Liao, H., Boulares, A. H., and Smulson, M. E. (2004). Protection by antioxidants against toxicity and apoptosis induced by the sulphur mustard analog 2-chloroethylethyl sulphide (CEES) in Jurkat T cells and normal human lymphocytes. *Br J Pharmacol* 141, 795-802.
- Hedley, D. W., and Chow, S. (1994). Evaluation of methods for measuring cellular glutathione content using flow cytometry. *Cytometry* 15, 349-58.
- Hermes-Lima, M., Willmore, W. G., and Storey, K. B. (1995). Quantification of lipid peroxidation in tissue extracts based on Fe(III)xylene orange complex formation. *Free Radic. Biol. Med* 19, 271-280.
- Hillier, S. M., Marquis, J. C., Zayas, B., Wishnok, J. S., Liberman, R. G., Skipper, P. L., Tannenbaum, S. R., Essigmann, J. M., and Croy, R. G. (2006). DNA adducts formed by a novel antitumor agent 11beta-dichloro in vitro and in vivo. *Mol Cancer Ther* 5, 977-84.
- Hillier, S. M. (2005). Novel Genotoxins that Target Estrogen Receptor- and Androgen Receptor- Positive Cancers: Identification of DNA Adducts, Pharmacokinetics, and Mechanism. PhD Thesis, Massachusetts Institute of Technology.

Chapter 3

- Kartalou, M., and Essigmann, J. M. (2001). Recognition of cisplatin adducts by cellular proteins. *Mutat Res* 478, 1-21.
- Kowaltowski, A. J., Castilho, R. F., and Vercesi, A. E. (2001). Mitochondrial permeability transition and oxidative stress. *FEBS Lett* 495, 12-5.
- Lantz, R. C., Lemus, R., Lange, R. W., and Karol, M. H. (2001). Rapid reduction of intracellular glutathione in human bronchial epithelial cells exposed to occupational levels of toluene diisocyanate. *Toxicol. Sci* 60, 348-355.
- Lash, L. H. (2006). Mitochondrial glutathione transport: physiological, pathological and toxicological implications. *Chem. Biol. Interact* 163, 54-67.
- LeBel, C. P., Ischiropoulos, H., and Bondy, S. C. (1992). Evaluation of the probe 2',7'-dichlorofluorescein as an indicator of reactive oxygen species formation and oxidative stress. *Chem. Res. Toxicol* 5, 227-231.
- Lemasters, J. J., Qian, T., Bradham, C. A., Brenner, D. A., Cascio, W. E., Trost, L. C., Nishimura, Y., Nieminen, A. L., and Herman, B. (1999). Mitochondrial dysfunction in the pathogenesis of necrotic and apoptotic cell death. *J. Bioenerg. Biomembr* 31, 305-319.
- Leverve, X. M., and Fontaine, E. (2001). Role of substrates in the regulation of mitochondrial function in situ. *IUBMB Life* 52, 221-9.
- Ling, Y., Liebes, L., Zou, Y., and Perez-Soler, R. (2003). Reactive oxygen species generation and mitochondrial dysfunction in the apoptotic response to Bortezomib, a novel proteasome inhibitor, in human H460 non-small cell lung cancer cells. *J Biol Chem* 278, 33714-23.
- Marquis, J. C., Hillier, S. M., Dinaut, A. N., Rodrigues, D., Mitra, K., Essigmann, J. M., and Croy, R. G. (2005). Disruption of gene expression and induction of apoptosis in prostate cancer cells by a DNA-damaging agent tethered to an androgen receptor ligand. *Chem Biol* 12, 779-87.
- Masters, J. R. W., and Köberle, B. (2003). Curing metastatic cancer: lessons from testicular germ-cell tumours. *Nat Rev Cancer* 3, 517-25.
- Nelson-Rees, W. A., Hunter, L., Darlington, G. J., and O'Brien, S. J. (1980). Characteristics of HeLa strains: permanent vs. variable features. *Cytogenet Cell Genet* 27, 216-31.
- Nowak, G. (2002). Protein kinase C-alpha and ERK1/2 mediate mitochondrial dysfunction, decreases in active Na⁺ transport, and cisplatin-induced apoptosis in renal cells. *J Biol Chem* 277, 43377-88.

Chapter 3

- Ohashi, T., Mizutani, A., Murakami, A., Kojo, S., Ishii, T., and Taketani, S. (2002). Rapid oxidation of dichlorodihydrofluorescein with heme and hemoproteins: formation of the fluorescein is independent of the generation of reactive oxygen species. *FEBS Lett* *511*, 21-27.
- Proffitt, K. D. (2009). Mechanistic Investigation of an Anticancer Agent that Damages DNA and Interacts with the Androgen Receptor. PhD Thesis, Massachusetts Institute of Technology.
- Rappeneau, S., Baeza-Squiban, A., Jeulin, C., and Marano, F. (2000). Protection from cytotoxic effects induced by the nitrogen mustard mechlorethamine on human bronchial epithelial cells in vitro. *Toxicol. Sci* *54*, 212-221.
- Rappeneau, S., Baeza-Squiban, A., Marano, F., and Calvet, J. (2000). Efficient protection of human bronchial epithelial cells against sulfur and nitrogen mustard cytotoxicity using drug combinations. *Toxicol. Sci* *58*, 153-160.
- Reers, M., Smiley, S. T., Mottola-Hartshorn, C., Chen, A., Lin, M., and Chen, L. B. (1995). Mitochondrial membrane potential monitored by JC-1 dye. *Methods Enzymol* *260*, 406-17.
- Ries, L. A. G., Melbert, D., Krapcho, M., Mariotto, A., Miller, B. A., Feuer, E. J., Clegg, L., Horner, M. J., Howlader, N., Eisner, M. P., et al. (2009). SEER cancer statistics review, 1975-2005. National Cancer Institute, Bethesda, MD. *XXV 1-12*. Available at: http://seer.cancer.gov/csr/1975_2005/, based on November 2007 SEER data submission, posted to the SEER web site, 2008.
- Roberts, J. J. (1980). DNA repair mechanisms and cytotoxicity of antitumour alkylating agents and neutral platinum complexes. *Antibiot Chemother* *28*, 109-114.
- Santangelo, F. (2003). Intracellular thiol concentration modulating inflammatory response: influence on the regulation of cell functions through cysteine prodrug approach. *Curr. Med. Chem* *10*, 2599-2610.
- Sebastià, J., Cristòfol, R., Martín, M., Rodríguez-Farré, E., and Sanfeliu, C. (2003). Evaluation of fluorescent dyes for measuring intracellular glutathione content in primary cultures of human neurons and neuroblastoma SH-SY5Y. *Cytometry A* *51*, 16-25.
- Sies, H., Sharov, V. S., Klotz, L. O., and Briviba, K. (1997). Glutathione peroxidase protects against peroxynitrite-mediated oxidations. A new function for selenoproteins as peroxynitrite reductase. *J. Biol. Chem* *272*, 27812-27817.
- Tsuchiya, M., Suematsu, M., and Suzuki, H. (1994). In vivo visualization of oxygen radical-dependent photoemission. *Meth. Enzymol* *233*, 128-140.

Chapter 3

Turrens, J. F. (2003). Mitochondrial formation of reactive oxygen species. *J Physiol* 552, 335-44.

Vos, O., van der Schans, G. P., and Roos-Verhey, W. S. (1984). Effects of BSO and DEM on thiol-level and radiosensitivity in HeLa cells. *Int. J. Radiat. Oncol. Biol. Phys* 10, 1249-1253.

Wagner, B. K., Kitami, T., Gilbert, T. J., Peck, D., Ramanathan, A., Schreiber, S. L., Golub, T. R., and Mootha, V. K. (2008). Large-scale chemical dissection of mitochondrial function. *Nat Biotechnol* 26, 343-51.

Wallace, D. C. (2005). Mitochondria and cancer: Warburg addressed. *Cold Spring Harb Symp Quant Biol* 70, 363-74.

Wang, X., and Quinn, P. J. (1999). Vitamin E and its function in membranes. *Prog. Lipid Res* 38, 309-336.

CHAPTER 4

The Anticancer Agent 11 β -Dichloro Induces the Unfolded Protein Response in HeLa Cells

4.1 Introduction

The use of cytotoxic agents as chemotherapeutics has been commonplace for decades. Among the antineoplastic agents used, DNA damaging agents have been among the most versatile and most successful. The prime example is cisplatin, a DNA alkylator extremely effective against testicular cancer. Therapeutic regimens that include cisplatin have achieved cure rates of over 95% in testicular cancer (Masters and Köberle, 2003). Research on the cisplatin mechanism of toxicity has shown, however, that DNA damage is only one part of the puzzle; one theory is that the high effectiveness of cisplatin is due to the interaction of DNA adducts with tumor specific proteins (Kartalou and Essigmann, 2001). The studies on the mechanism of cisplatin have highlighted the complexity of the toxicity mechanisms of compounds effective in clinic, suggesting that successful therapeutics may require more than one target inside the cell. Given that for most cancers, there is no chemotherapeutic regimen of effectiveness comparable to the effectiveness of cisplatin-containing regimens for testicular cancer, the development of better and more specific antineoplastic agents remains an important scientific challenge.

Inspired by the one of the proposed cisplatin mechanism in testicular cancer, the Essigmann lab envisioned a design strategy for programmable cytotoxins: bifunctional agents comprised of a constant DNA alkylating moiety and a variable protein interacting moiety that can be tailored to recognize cancer specific proteins (Essigmann et al., 2001). One of these compounds, called 11 β -dichloro⁴ (Figure 4.1 A), was designed to interact with the androgen receptor (AR) – a protein overexpressed in many prostate cancers (Marcelli and Cunningham, 1999). 11 β -Dichloro displays a potent *in vivo* activity against xenograft tumors expressing AR, while being well tolerated by animals (Marquis et al., 2005). However, this potent activity is also observed against tumors that do not express AR. Moreover, *in vitro*, 11 β -dichloro is significantly more toxic than simpler nitrogen mustards against AR negative cell lines. All these findings suggest that an additional mechanism of toxicity may be operating and prompted the current investigation. The possibility of uncovering a novel

⁴ IUPAC name: 2-(6-((8S,11S,13S,14S,17S)-17-hydroxy-13-methyl-3-oxo-2,3,6,7,8,11,12,13,14,15,16,17 dodecahydro-1H-cyclopenta[a]phenanthren-11-yl)hexylamino)ethyl 3-(4-(bis(2-chloroethyl)amino)phenyl)propylcarbamate

mechanism of toxicity specific for cancer cells raised a lot of interest into the outcome of this research. Moreover, characterizing the complete mechanism of action is a necessary step for the eventual advancement of 11 β -dichloro in preclinical and clinical trials.

A large scale phenotypic screen conducted on the complete single-gene knock-out mutant yeast library indicated that mitochondrial function is an important factor that can modulate the toxicity of 11 β -dichloro (Chapter 2). When the yeast findings were investigated in HeLa cells – an AR independent cancer cell line, it was found that 11 β -dichloro induces a large amount of ROS in the cells, very soon after the onset of exposure. The induction of ROS correlates well with changes in the antioxidant pool of the cell and changes in mitochondrial function. Most notably, the mitochondrial inner membrane potential is significantly increased (Chapter 3). Additionally, the same responses, albeit of smaller magnitude were also caused by 11 β -dimethoxy (Figure 4.1 B), a defanged derivative of 11 β -dichloro that cannot alkylate DNA. These findings suggest that 11 β -dichloro has at least two independent targets inside the cell: one is DNA, the other is responsible for the induction of ROS.

Additional information on the toxicity mechanism of 11 β -dichloro came from the work of other people involved in the project. A complete transcriptional profile of cells exposed to 11 β -dichloro has been characterized (Proffitt, 2009), indicating that 11 β -dichloro activates stress response pathways such as unfolded protein response (UPR) and sterol biosynthesis. These experiments were carried out in LNCaP cells, an AR positive prostate cancer cell line chosen as a model for the intended 11 β -dichloro clinical targets. In this chapter we shall explore whether such transcriptional responses are specific to LNCaP cells, or they also happen in AR negative cells lines such as HeLa.

In mammalian cells, the UPR is a mechanism by which cells limit the accumulation of misfolded proteins in the endoplasmic reticulum (ER), the central site of synthesis for transmembrane and secreted proteins. Perturbation in the ER homeostasis can lead to the accumulation of unfolded proteins and protein aggregates, which are detrimental to the cell. The UPR coordinates the cellular effort in preventing further accumulation of unfolded proteins, in degrading and disposing of the aggregates and in restoring the ER homeostasis.

However, if the unfolded protein load is too high and the ER function cannot be restored, the UPR triggers the activation of a programmed cell death pathway (Kaufman et al., 2002). There are many factors that can generate ER stress; among the most common, we find : the disturbance in calcium homeostasis, oxidative stress, increased demand for secretory proteins which leads to increased demand for translation, nutrient deprivation and the presence of mutant or damaged proteins (Kaufman et al., 2002). The UPR acts in several different ways towards restoring the ER function. First, it upregulates the expressions of genes encoding proteins necessary for folding and ER homeostasis (e.g., calcium ATPases). Second, the UPR attenuates global translation levels, in an effort to limit the amount of proteins that need to be folded at one particular time (Prostko et al., 1993). However, the translation of certain UPR proteins is preferentially increased (Harding et al., 2000). Thirdly, the UPR activates master regulator genes (e.g. DDIT3) that integrate multiple stress signals and can trigger cell death if an activation threshold is reached (Oyadomari and Mori, 2004). At molecular levels, the UPR is controlled by the status of an ER chaperone, BiP (binding Ig protein), also known as GRP78 (glucose regulated protein 78). During normal ER function, BiP is inhibiting, by protein-protein interaction, a number of ER transmembrane proteins responsible for UPR activation. However, when increased levels of unfolded proteins accumulate in the ER, BiP is recruited to exert its chaperone function, dissociates from its targets and leads to UPR activation (Kaufman, 1999). The three UPR-activating proteins controlled by BiP are IRE1 (inositol requiring 1), PERK (PKR-like endoplasmic reticulum kinase) and ATF6 (activating transcription factor 6) (Mori, 2000). Each one of these proteins activates a particular aspect of the UPR. PERK is responsible for attenuating translation via phosphorylation of eIF2 α (eukaryotic translation initiation factor 2 α) and IRE1 is responsible for activating XBP1, which together with the activated ATF6 drive transcription of most of the genes involved in UPR. The mechanism of attenuating translation relies on the lower affinity of the phosphorylated eIF2 α for the ribosome; most mRNAs require the binding of eIF2 α to initiate translation. However, certain mRNAs can be translated without an initiation factor; their corresponding proteins will thus be preferentially translated during the UPR. One such protein preferentially translated is ATF4, a transcription factor important for upregulating other UPR-related genes (Kaufman et al., 2002). The activation of ATF6 occurs by proteolytic processing as follows. The ATF6 precursor in the ER membrane, once dissociated

from BiP, translocates to the Golgi apparatus via a coated vesicle. There, two site specific proteases S1P and S2P cleave the protein inside its transmembrane domain, liberating the active transcription factor on the cytosolic side (Ye et al., 2000). In the nucleus, ATF6 drives transcription of many UPR genes, including XBP1 (X-box binding protein 1), another key regulator of UPR (Lee et al., 2002). The mRNA for XBP1, which we'll denote XBP1p (precursor) encodes a truncated, non-functional protein. To become active, XBP1 needs to be processed by an activated ER membrane-resident ribonuclease IRE1. As indicated before, IRE1 becomes active after it dissociates from BiP. At this point, IRE1 can act on the precursor mRNA of XBP1 and specifically remove a short intron. This modification amounts to a translational frameshift that generates the longer, active XBP1 protein, denoted XBP1s (spliced). In its active form, XBP1 is a potent transcription factor, complementing ATF6 for the activation of UPR related genes.

When the ER stress is too extensive, the UPR can activate a cell death program. The molecular basis for this signal is thought to be DDIT3, a central gene in the UPR pathway. DDIT3 (DNA-damage inducible transcript 3), also known as CHOP or GADD153, is a transcription factor highly expressed during UPR (Oyadomari et al., 2004). The promoter region for DDIT3 features binding elements for transcription factors corresponding to each of the three main UPR signaling branches, suggesting that DDIT3 integrates signals from multiple pathways. ATF6, XBP1s and ATF4 are the main transcription factors controlling expression of DDIT3. The main function of the CHOP protein is to activate apoptosis in response to ER stress. In fact, CHOP expression is essential for UPR induced apoptosis; cells lacking CHOP are resistant to ER-stress induced cell death (Zinszner et al., 1998). The mechanism by which CHOP induces apoptosis is very complex and it involves in part transcriptional inhibition of the anti-apoptotic protein BCL-2 and the upregulation of a number of pro-apoptotic proteins. Some of these (e.g., Bax, Bak) are involved in releasing calcium from the ER; others are involved in negating the UPR efforts for controlling proper protein folding (e.g., GADD34, which upregulates translation); yet another set of proteins directly interact with the apoptosis machinery (DR5, TRB3) (Malhotra and Kaufman, 2007). It has also been shown that the stability of the CHOP protein is significantly enhanced by phosphorylation. A number of stress related kinases, such as JNK, ASK1 and the kinases

from p38 MAPK pathway are thought to phosphorylate CHOP, increase its stability and thus elicit an enhanced apoptotic effect (Oyadomari et al., 2004).

The sterol biosynthesis pathway is another pathway controlled from the ER and whose activation is often linked to ER stress (Colgan et al., 2007). The main role of the sterol biosynthesis pathway is to maintain the homeostasis of cholesterol in the cellular membranes. The mechanism of sensing the cholesterol levels in membranes and adjusting transcription accordingly is very complex. It involves a family of membrane bound transcription factors known as sterol responsive element-binding proteins (SREBPs) (Brown and Goldstein, 1997). These proteins are anchored in the ER membrane in an inactive form, in a complex with a cholesterol sensor membrane protein (SCAP) and an inhibitor membrane protein (INSIG). When cholesterol levels are adequate, the complex is stable and no transcription driven by SREBP occurs. However, when cholesterol levels drop, changes in the conformation of SCAP allows it to dissociate from INSIG (Sun et al., 2007). The SCAP-SREBP complex is then free to recruit other proteins, which will allow a vesicle containing the complex to bud off from ER and migrate to the Golgi apparatus. There, the S1P and S2P proteases (the same proteases responsible for the activation of ATF6) will cleave the full length SREBP, freeing up its cytosolic N-terminal domain, which is the active transcription factor (Horton et al., 2002; Goldstein et al., 2002). SREBP drives the expression of many genes involved in sterol biosynthesis, fatty acid biosynthesis but also genes involved in sterol and fatty acid import. Among the genes activated by SREBP, a notable few are : SREBP itself, INSIG1, HMGCS (HMG-CoA synthase), HMGCR (HMG-CoA reductase), SQLE (squalene epoxidase) and LDLR (LDL receptor) (Brown and Goldstein, 1999).

The current chapter brings together a list of additional experimental observations about the cellular responses to 11 β -dichloro, highlighting the results that are general and independent of the cell line used. An attempt is then made to formulate a comprehensive hypothesis about the mechanism of toxicity of 11 β -dichloro in HeLa cells. Finally, we shall discuss how this hypothesis fits all the currently available experimental evidence. A number of predictions are made about the likely mechanistic involvement of other cellular pathways and future experiments are suggested to test such predictions.

4.2 Materials and Methods

4.2.1 Reagents

Compounds 11 β -dichloro and 11 β -dimethoxy were synthesized using previously reported schemes (Marquis et al., 2005). Stock solutions (10 mM) were prepared in anhydrous DMSO (Sigma-Aldrich). Fluo-4 AM molecular dye was purchased from Molecular Probes (Invitrogen, Carlsbad, CA, USA). CTB reagent was from Promega (Madison, WI, USA). 3-methyl adenine (3meA) and acridine orange (AO) were from Sigma. Caspase inhibitor I (zVAD-fmk) was from Calbiochem (San Diego, CA, USA).

4.2.2 Cell lines and culture

HeLa cells were obtained from American Type Culture Collection (Rockville, MD, USA) and maintained in minimal essential medium (MEM, Invitrogen) supplemented with 1 mM glutamax, 1% non-essential amino acids, 1 mM pyruvate (Invitrogen), and 10% fetal bovine serum (Hyclone, Logan, UT), in a humidified 5% CO₂/ 95% air atmosphere at 37°C. Cells were routinely passaged using TrypLE (Invitrogen) in P150 dishes (BD Biosciences) every three days at a seeding density of 2×10^6 cells/dish.

4.2.3 Quantifying changes in cell size

HeLa cells were seeded in 6-well plates at a density of 1×10^5 cells per well and incubated for 24 hours to allow attachment. Fresh solution of media or drug-containing media were added to triplicate wells and incubated for 24 hours. Afterwards, cells were washed once with PBS, detached using TrypLE (200 μ L/well) and resuspended in fresh medium. The distribution of cell sizes in each well was determined by counting aliquots in a Multisizer 4 Coulter Counter (Beckman Coulter, Miami, FL, USA), with an active counting window set between 10 and 30 μ m. The data were analyzed in Microsoft Excel. The estimations of cell diameters were made based on the measured volumes, assuming that the cells have a spherical shape.

4.2.4 Determination of intracellular Ca⁺⁺ using flow cytometry

HeLa cells were seeded in 6-well plates at a density of 1×10^5 cells per well and incubated for 24 hours to allow attachment. Fresh solution of media or drug-containing media were added to triplicate wells and incubated for the indicated amounts of time. Afterwards, the medium was then aspirated, replaced with a Fluo-4 AM probe solution (final concentration 1 μ M in phenol-red free medium) and incubated for 30 minutes. After incubation with the probe, cells were washed once with PBS, detached using TrypLE (200 μ L/well), resuspended in fresh medium and analyzed by flow cytometry in a FACSCanto II instrument (BD Biosciences, Franklin Lakes, NJ, USA). The flow cytometry protocol used a 488 nm laser for excitation, involved using front and side scatter to gate normal looking cells, and then fluorescence in the green (FL1) channel was quantified. The data were acquired and analyzed with a FACSDiva software (BD Biosciences).

4.2.5 Determination of transcript levels using RT-PCR

HeLa cells were seeded in P100 dishes at a density of 1×10^6 cells per well and incubated for 24 hours to allow attachment. Fresh solution of media or drug-containing media were added to triplicate dishes and incubated for the indicated amounts of time. The cells were then washed in ice-cold PBS, detached by scrapping and pelleted using low g-force centrifugation. Total cellular RNA was isolated using the RNeasy mini columns (Qiagen, Valencia, CA, USA), employing QIAshredder columns for sample homogenization (Qiagen) and the optional on-column DNase digestion, according to manufacturer's instructions. The transcript levels of the genes of interest were analyzed using the Quantitect SYBR Green RT-PCR kit (Qiagen) at MIT BioMicro Center on MJ Research Real-Time PCR Machine. The RT-PCR reactions included for each gene a well with no reverse transcriptase (to control for DNA impurities in the isolated RNA), a well with no template (to rule out possible contamination) and a 6 point calibration curve spanning 5 orders of magnitude in RNA concentration. The curve was used to accurately determine the concentration of each

transcript, using the Opticon 3 software (MJ Research). The levels of each transcript were then normalized for each time point to the levels of GAPDH transcript. GAPDH is a highly expressed house-keeping gene. The sequences of the primers were as follows (Proffitt, 2009): *GAPDH* (based on accession NM_002046) Forward: ACA GTC AGC CGC ATC TTC TT, Reverse: GCC CAA TAC GAC CAA ATC C; *GDF15* Forward: GAG GTG CAA GTG ACC ATG TG, Reverse: GTG CAG GCT CGT CTT GAT CT; *DDIT3* Forward: GAG GTG CAA GTG ACC ATG TG, Reverse: GTG CAG GCT CGT CTT GAT CT; *HMGCS1* Forward: GCT CAG AGA GGA CAC CCA TC, Reverse: GCC GAG CGT AAG TTC TTC TG; *ATF3* Forward: CTA ACC TGA CGC CCT TTG TC, Reverse: TTG TTC TGG ATG GCA AAC CT; *TRIB3* Forward: TTA GGC AGG GTC TGT CCT GT, Reverse: GTA TGG ACC TGG GAT TGT GG; *INSIG1* Forward: TGA GAT GTC CCG AGA GAA GG, Reverse: TGG AGG TTG TAA CCC GAA AG; *CCNE2* Forward: TTG GCT ATG CTG GAG GAA GT , Reverse: CAA CTG TCCCCC TTT TCT GA ; *CCNG2* Forward: TGA GCT GCC AAC GAT ACC T , Reverse: GAT CAC TGG GAG GAG AGC TG . A method was also developed to identify the spliced form of XBP1, which we termed *XBPIs*. To identify specifically the spliced form, the forward primer was designed to anneal across the splice-site, on a sequence unique only to the spliced form that does not exist in the unspliced precursor of XBP1. The primers were as follows: *XBPIs* Forward: CTG AGT CCG CAG CAG GTG, Reverse: ACT GGG TCC AAG TTG TCC AG.

4.2.6 Determination of relative protein levels using Western blotting

Cells were harvested by scraping into media, washing with PBS, and subsequently lysing in RIPA buffer (Santa Cruz Biotechnology, Santa Cruz, CA) containing PMSF, sodium orthovanadate, and protease inhibitor cocktail at 0°C. Cellular debris was pelleted by centrifugation at 14,000 RPM in a bench top microcentrifuge, supernatants were collected, and protein quantified by Bradford dye binding assay (Bio-Rad Laboratories, Hercules, CA). Equal quantities of protein were electrophoretically separated on a 10% polyacrylamide gel in a miniProtean 3 machine (Bio-Rad) and transferred to Immobilon-P PVDF membrane (Millipore, Billerica, MA). Non-specific protein binding was blocked with 5% milk in Tris-buffered saline (0.1% Tween 20, 10 mM Tris (pH 7.4), 150 mM NaCl) and proteins were

detected by primary antibodies followed by horseradish peroxidase (HRP) conjugated secondary antibodies and chemiluminescent HRP substrate (Supersignal West; Pierce, Rockford, IL). Antibodies used were as follows: SREBP-1 (sc-13551, Santa Cruz), Insig-1 (sc-25124-R, Santa Cruz), β -actin (sc-1615R, Santa Cruz), and HRP-conjugated secondary antibodies (#7076, anti-mouse IgG; #7074 anti-rabbit IgG; Cell Signaling Technology, Danvers, MA).

4.2.7 Determination of cell viability in the presence of cell death inhibitors

Cell-titer blue (CTB) viability assay was employed according to the manufacturer's instructions (Promega). 2.5×10^3 cells/well were seeded in black/transparent bottom 96-well plates (Corning Inc., Corning, NY, USA) and incubated for 24 hours. Media were carefully aspirated by a flame-thinned Pasteur pipette and fresh media and drug containing media was added using a multichannel pipettor. To test the involvement of different forms of cell death, cells were treated with $1 \mu\text{M}$ β -dichloro alone, or co-treated with 3meA (2 mM final concentration) or zVAD-fmk (50 μM final concentration). After the incubation for the indicated times, 20 μL of pre-warmed CTB reagent were added in low light to each well and mixed by gently tapping the sides of the plate. The plate was incubated an additional 2-4 hours and the fluorescent signal was recorded at excitation and emission (ex/em) 555/585 in a SpectraMax M5e spectrophotometer using the bottom-read feature. Every plate included wells with media only, from which the background fluorescence was determined and subtracted from all other fluorescence readings. The percentage viability was calculated as the ratio between the average signal in the treated wells and the average signal in the untreated control wells times 100.

4.2.8 Determination of acidic cellular compartments using acridine orange staining

The amount of acidic cellular compartments (lysosomes) was quantified using the metachromatic dye acridine orange (AO) as described previously (Antunes et al., 2001). Briefly, cells were treated in the 96 well plates as described above and then incubated with 100 μ L/well AO 2 μ M solution in culture medium without phenol red for 15 minutes. Wells were then washed once and refilled with PBS. Red and green fluorescence was determined at ex/em 530/580 and 488/530 respectively using the bottom-read and well-scan features of the SpectraMax M5e spectrophotometer. The red/green ratios were then used as a measure of the total acidic compartment volume, calculating first the ratio for each well sub-area before averaging for the whole well and for all the biological replicates.

4.3 Experimental Results

4.3.1 11 β -Dichloro upregulates the expression of genes involved in the UPR response and sterol biosynthesis

Our initial question was whether 11 β -dichloro induces a transcription pattern in the AR negative cell line HeLa, similar to the one detected in LNCaP cells (Proffitt, 2009). To this end, we chose a number of genes in each of the important pathways found to be upregulated by exposure of LNCaP cells to 5 μ M 11 β -dichloro for 6 hours, namely UPR, sterol biosynthesis and several cell cycle genes. HeLa cells were exposed to 5 μ M 11 β -dichloro for 3 and 6 hours, the total RNA was isolated and used to investigate transcript levels of the genes of interest by RT-PCR. Table 5.1 shows the list of interrogated genes, the log₂ fold-change (LFC) in transcript levels in HeLa cells at 6 hours and the LFC reported by Proffitt in LNCaP cells at 6 hours. The data suggest that 11 β -dichloro is inducing similar transcriptional changes in the two cell lines. However, the transcriptional effects of 11 β -dichloro are somewhat higher in LNCaP cells than in HeLa cells, although the direction of change is generally the same. There are also a few differences. ATF3 is a transcript significantly induced in LNCaP cells after 11 β -dichloro treatment; ATF3 is however significantly repressed in HeLa cells. Also, at 6 hours, we do not detect an increase in the INSIG1 transcript levels in HeLa cells, whereas in LNCaP cells, at 6 hours, INSIG1 is significantly induced.

Another way to present the HeLa cells data is as a time course for each individual gene, a view that can inform about the timing of the upregulation, and some changes in the transcription pattern on a faster time scale (Figure 4.2). The time courses indicate the same trends for each of the genes investigated before. Notable is the transcriptional profile of INSIG1, a gene significantly induced at 3 hours, but not induced anymore at 6 hours. This pattern suggests faster changes in the transcription levels of INSIG1 (Figure 4.2 B).

The upregulation in the expression of DDIT3, a central effector of UPR pathway, XBP1s, GDF15 and TRB3 is indicative of 11 β -dichloro inducing the UPR pathway in HeLa cells

(Figure 4.2 A). Additionally, the upregulation of HMGCS1 and INSIG1 transcripts is suggestive of the compound's induction of the sterol biosynthesis pathway (Figure 4.2 B). Finally, the decreases in levels of CCNE2 (cyclin E2, a cyclin promoting cell cycle progression) and the increase levels of CCNG2 (cyclin G2, a cyclin inhibiting cell cycle progression) are consistent with the induction of a cell cycle arrest mechanism in HeLa cells (Figure 4.2 C).

4.3.2 11 β -Dichloro increases the levels of the SREBP protein

To confirm the activation of the sterol biosynthesis pathway, we investigated the changes occurring at the protein level in the main transcription factor SREBP (Sterol Response Element-Binding Protein) and one of the important regulators INSIG1. A time course following cells after exposure to 5 μ M 11 β -dichloro confirms that levels of SREBP protein are increasing (Figure 4.3 A). The protein levels of INSIG1 show a more complicated pattern : they decrease initially, a finding consistent with the role of Insig as an inhibitor of SREBP activation; then the levels of Insig1 protein increase, a finding consistent with the feedback loop of SREBP driving transcription of INSIG1 (Figure 4.3 B).

4.3.3 11 β -Dichloro causes an increase in cytosolic Ca⁺⁺

One of the central markers of UPR induction is the increase in cytosolic Ca⁺⁺. Additionally, high levels of cytosolic Ca⁺⁺ stimulate the induction of UPR. While the interplay between the cytosolic Ca⁺⁺ levels and the induction of UPR is a complex and only partially understood mechanism, given the induction of the UPR genes, we expected that Ca⁺⁺ levels would increase as a consequence of 11 β -dichloro exposure. To investigate this possibility, we monitored cytosolic Ca⁺⁺ levels in a time course following exposure to 8 μ M 11 β -dichloro, using the sensitive fluorescent probe Fluo-4 AM. The results indicate that cytosolic Ca⁺⁺ levels rise strikingly as early as 30 minutes after 11 β -dichloro exposure (Figure 4.4).

4.3.4 11 β -Dichloro causes an increase in cell size

Early in this study, an empirical observation has been made that cells exposed to low doses of 11 β -dichloro look larger when inspected under a phase-contrast microscope. Literature reports have associated increases in cell sizes with cation imbalance, perturbation in membrane integrity and also induction of UPR (Sriburi et al., 2004). We decided to quantitate this effect, which can constitute additional supporting evidence for UPR induction and the consequences of UPR in the cells. The HeLa cells were treated with low concentrations of 11 β -dichloro for 24 hours. After treatment, cell size measurements performed on a Multisizer 4 Coulter Counter revealed that doses of 11 β -dichloro of 3 μ M and lower cause a significant increase in the cell volume and cell diameter (Figure 4.5). The average diameter of the untreated cell is 20.2 μ m; after exposure to 3 μ M 11 β -dichloro for 24 hours, the average diameter becomes 24.2 μ m, a 24% increase in diameter, which corresponds to a 71% increase in cell volume and a 43% increase in cell surface area (assuming the cell is a perfect sphere).

4.3.5 11 β -Dichloro induces the proliferation of acidic compartments in the cell

Microscopical examination of HeLa cells treated with 11 β -dichloro also revealed an increased number of vesicles compared with untreated cells. To investigate the nature of these vesicles, the pH sensitive dye acridine orange (AO) was employed, according to established protocols (Antunes et al., 2001). Our results indicate that 11 β -dichloro induces an increase in the AO signal, in a dose dependant manner, suggesting an increase in the number or volume of lysosomes (Figure 4.6). Next, we were interested whether the increase in the lysosome-specific signal is indicative of autophagy – a mechanism of cell death where the cell utilizes the lysosomes to digest the cellular components (Gozuacik and Kimchi, 2004). Co-treatment with autophagy inhibitor 3-methyl adenine (3meA) showed no change in the AO signal (Figure 4.6) and no change in the cellular viability (Figure 4.7), suggesting that autophagy may not be an important cell death pathway activated by 11 β -dichloro. To investigate whether the caspases are involved in the cell death induced by 11 β -dichloro, we

Chapter 4

co-treated the cells with the pan-caspase inhibitor zVADfmk (carbobenzoxy-valyl-alanyl-aspartyl-[O-methyl]- fluoromethylketone). The results indicate that zVADfmk did not attenuate 11β -dichloro toxicity for any of the doses tested (Figure 4.7), suggesting that caspases may not be the only executors of the cell death signal induced by 11β -dichloro.

4.4 Discussion

The mechanism of toxicity of 11 β -dichloro has been investigated in AR positive cell lines such as LNCaP. One such study (Proffitt, 2009) characterized the complete transcriptional responses to subtoxic doses of 11 β -dichloro using microarray technology. Their results indicated that the 11 β -dichloro treatment is upregulating genes involved in pathways such as the unfolded protein response (UPR) and sterol biosynthesis. Additionally, 11 β -dimethoxy, a compound unable to damage DNA, has a transcriptional profile very similar with 11 β -dichloro, suggesting that the pathways induced are an indication of additional cellular targets, independent of DNA damage. We decided to investigate whether the induction of the UPR and sterol biosynthesis pathways by 11 β -dichloro is specific for LNCaP cells, or they are more general cellular responses that happen in other cancer cell lines, such as HeLa.

We used RT-PCR technique to investigate the transcriptional responses in HeLa cells exposed to 5 μ M 11 β -dichloro for 3 and 6 hours. From the large number of transcriptionally responsive genes in LNCaP cells, we selected a small subset that includes genes involved in the UPR, sterol biosynthesis and cell cycle regulation. For each pathway, we picked the genes whose expression is increased the most by 11 β -dichloro in LNCaP cells. For the cell cycle related genes, we picked one gene upregulated in LNCaP cells (CCNG2) and one gene downregulated in LNCaP cells (CCNE2) by 11 β -dichloro.

Our findings indicate that the transcriptional response of HeLa cells to 11 β -dichloro exposure is very similar to that of LNCaP cells (Table 5.1). The levels of most transcripts investigated changed in the same direction in both cell lines; however, the HeLa cells transcriptional responses are somewhat smaller than those of LNCaP cells, a finding likely due to intrinsic differences between the two cell lines. We also have noted one difference : the ATF3 gene is significantly induced in LNCaP cells, but significantly repressed in HeLa.cells.

Based on the transcriptional data, we have good evidence that 11 β -dichloro induces the UPR in HeLa cells. One way in which cells activate the UPR pathway is through the XBP1 (X-box

binding protein 1). The mRNA of this protein exists in the cytosol as an inactive precursor. When unfolded proteins accumulate in the endoplasmic reticulum (ER), the IRE1 α protein present in the ER membrane becomes activated. The cytosolic end of IRE1 α has an endoribonuclease activity that can perform an unconventional splicing on the XBP1 precursor. The spliced form of XBP1, denoted XBP1s, can then be translated into the XBP1 protein, a transcription factor that can activate transcription of UPR related genes. We used primers specific for XBP1s that would not amplify the inactive, unspliced version of XBP1 and we found that the level of XBP1s mRNA is increased about 5 fold after exposure to 5 μ M 11 β -dichloro for 6 hours.

One of the most important UPR genes transcribed by XBP1 is DDIT3 (DNA-damage inducible transcript 3), considered a central regulator of the UPR response. DDIT3 (also known as CHOP or GADD153) integrates signals from multiple pathways being one of the most induced transcripts as a response to ER stress (Oyadomari et al., 2004). A transcription factor itself, DDIT3 drives expression of genes involved in overcoming the ER stress. However, higher levels of DDIT3 can activate a cell death program, by inhibiting the transcription of the anti-apoptotic protein BCL-2. In fact, high induction of DDIT3 often denotes severe ER stress and a commitment to apoptosis (Kim et al., 2008). We see a considerable induction of DDIT3 in HeLa cells treated with 11 β -dichloro, which suggests that UPR could play an important role in triggering cell death. Additional support to this hypothesis comes from the other UPR genes upregulated by our compound. TRB3 and GDF15 are both genes downstream of DDIT3, their activation also contributing to apoptosis. Two important functions have been identified for TRB3: 1) it stabilizes the DDIT3 protein, and in doing so, it upregulates its own expression (Ohoka et al., 2005); 2) it inhibits the activation of the pro-mitotic Akt kinase, which is part of the mTOR pathway (Du et al., 2003). Activation of TRB3 has been associated with both autophagy and apoptosis; it has also been shown to play a role in the mechanism of toxicity of several anticancer compounds (Dieterle et al., 2009; Salazar et al., 2009).

GDF15 (growth differentiation factor 15, also known as NAG-1(non-steroidal anti-inflammatory drug-activated gene 1) is another gene whose expression has been associated

with pro-apoptotic and antitumorigenic effects. GDF15 is highly induced not only by anti-inflammatory drugs such as aspirin, but also by many natural products shown to have anticancer activities, such as resveratrol (Baek et al., 2002), indole-3-carbinol (Lee et al., 2005), diallyldisulfide (Bottone et al., 2002), linoleic acid (Lee et al., 2006) and genistein (Wilson et al., 2003). Interestingly, most of these natural products have also antioxidant properties, although the antioxidant properties are not associated with GDF15 induction. The pro-apoptotic properties of GDF15 are associated with the induction of p53; in p53 null cells, GDF15 is not highly induced. All these observations provide a plausible explanation for why GDF15 is induced to much higher levels in LNCaP cells, which are p53 positive, compared to HeLa cells, which are p53 negative. The p53 null phenotype of HeLa cells is due to the expression of the HPV E6 protein, an ubiquitin ligase that ubiquitinates p53 and targets it for degradation (Singh et al., 2007). Therefore, inducing apoptosis in HeLa cells cannot depend on the activity of p53. The lower induction of DDIT3 and GDF15 by 11 β -dichloro treatment in HeLa cells compared with LNCaP cells may be a consequence of the different p53 status.

Our RT-PCR data suggest 11 β -dichloro is also inducing the sterol biosynthesis pathway in HeLa cells, the pathway responsible for maintaining the cholesterol homeostasis in the cell. We detected the activation of the SREBP pathway, both at the transcriptional level (HMGCS, INSIG1, Figure 4.2 B) and at the protein level (SREBP, INSIG1, Figure 4.3 A&B). The INSIG1 protein levels variation (they drop initially, then they recover) is consistent with a proposed mechanism of INSIG regulating the activation of SREBP by negative feedback (Gong et al., 2006). It has been shown that the INSIG protein unbound to SCAP is quickly degraded. However, SREBP drives the transcription of the INSIG gene, so the transcript level of INSIG will increase. Therefore, the activation of the SREBP pathway causes both a drop in the protein levels and an increase in the INSIG mRNA levels (Gong et al., 2006), a pattern that we observe in our results.

The activation of the sterol biosynthesis pathway is not very surprising, in the context of ER stress. Compounds such as thapsigargin that cause ER stress and induce UPR have also been shown to induce the SREBP pathway (Lee and Ye, 2004; Colgan et al., 2007). The mechanism is thought to involve an accelerated proteolytic degradation of INSIG1 protein,

due to the overall lower translation levels dictated by the UPR. Moreover, activation of SREBP by ER stress does not depend on the cholesterol levels (Lee et al., 2004). Our studies indicate a significant drop in INSIG1 protein levels only 1.5 hours after exposure to 11 β -dichloro (Figure 4.3 B), a result consistent with activation of the SREBP pathway via UPR.

One important consequence of the UPR induction is an increase in cytosolic calcium, which then has pleiotropic effects on the cell, including activation of a cell death program (Malhotra et al., 2007). Given that protein folding reactions and chaperones in the ER require high concentration of calcium, the ER constitutes the main storage calcium compartment of the cell. It is believed that the increase in cytosolic calcium during UPR is caused by a release of calcium from the ER (Malhotra et al., 2007). The mechanism of such release is not fully characterized but some evidence implicates proteins from the BCL-2 family. Similar to the mechanisms described for mitochondria, the proteins BAX (BCL-2 associated X protein) and BAK (BCL-2 antagonist killer) oligomerize on the ER membrane to form pores that would allow calcium to leak out (Scorrano et al., 2003). The activity of pro-apoptotic BAX and BAK proteins is counteracted by the presence of BCL-2 protein. However, in UPR, BCL-2 is inhibited at the transcriptional level by DDIT3, thus derepressing BAK and BAX (Zong et al., 2003). Presumably, BAX and BAK can also act at the level of the mitochondria, where they stabilize a mitochondrial membrane transition pore that allows release of cytochrome c and triggers caspase-dependent apoptosis. However, ER stress can also activate caspases in a mitochondrial-independent manner: the high cytosolic calcium activates the calcium-dependent protease m-calpain, which subsequently cleaves and activates caspase-12, an ER resident caspase (Nakagawa and Yuan, 2000). Our results indicate that 11 β -dichloro induces a significant increase in cytosolic calcium levels, which start increasing as early as 30 minutes after an exposure to an 8 μ M dose. The increase in cytosolic calcium is consistent with the presence of ER stress and UPR, and may play a key role in the 11 β -dichloro induced apoptosis.

One more piece of evidence about the UPR is provided by the changes in the size of the cells exposed to 11 β -dichloro. The general understanding is that the accumulation of unfolded proteins in the ER leads to activation of UPR that, at least initially, induces many genes

involved in ER function and, thus, stimulates ER biogenesis (Yoshida et al., 2003). Consequentially, the ER increases in size which then leads to an increase in the overall cell size. Several studies have shown that constitutive activation of proteins responsible for triggering the UPR such as XBPs and ATF6 α leads to ER biogenesis and a significant increase in cell size (Bommiasamy et al., 2009; Sriburi et al., 2004). In the case of XBPs overexpression in NIH-3T3 fibroblasts, the authors report a 44% increase in the cell surface area (Sriburi et al., 2004). Our results show that a dose of 3 μ M 11 β -dichloro induces a 43% increase in cell surface area in HeLa cells after 24 hours (Figure 4.5), suggesting that a similar mechanism involving UPR and ER biogenesis may be activated. However, higher doses of 11 β -dichloro negate this effect, indicating that increased ER biogenesis is not activated anymore. This finding may be consistent with the different operational levels of the UPR. When low to moderate ER stress is induced, UPR is aimed at restoring ER homeostasis and thus, ER biogenesis is stimulated. Yet, when the ER stress is severe, UPR is aimed at committing the cell to a programmed cell death pathway, by upregulating the pro-apoptotic DDIT3 (Oyadomari et al., 2004).

4.5 Conclusions and Future Directions

Taking all the available evidence together, we hypothesize that the unknown, additional mechanism of toxicity of 11 β -dichloro involves the interplay between the UPR and oxidative stress. Each one of these cellular responses (UPR, oxidative stress) has the potential of inducing apoptosis on its own; however, the high level of crosstalk between these pathways suggests that they are closely related. In fact, protein misfolding, ER stress and the generation of ROS are intimately intertwined phenomena (Malhotra et al., 2007).

Increased ROS levels can induce ER stress by several mechanisms. One possibility is that ROS damage proteins, especially their oxidation sensitive thiol bonds, causing them to misfold. Accumulation of misfolded proteins in the ER leads to ER stress and UPR activation. Alternatively, ROS can induce an increase in cytosolic calcium by inactivating ER membrane Ca⁺⁺ATPases responsible for maintaining high calcium concentrations in the ER. When calcium levels drop in the ER, misfolded proteins start to accumulate and trigger the UPR (Malhotra et al., 2007).

Conversely, ER stress can induce oxidative stress. One consequence of UPR is increased cytosolic calcium, which can stimulate mitochondrial ROS in several ways: 1) calcium can stimulate the tricarboxylic acid (TCA) cycle in the mitochondria, leading to increased O₂ consumption and ROS production; 2) calcium can stimulate nitric oxide synthase, which generates NO that inhibits complex IV of the electron transport chain(ETC), thus generating ROS from complex III; 3) calcium can also stimulate the formation of a permeability transition pore, which with release cytochrome c from mitochondria, thereby stopping the ETC at complex III and thus increasing ROS; additionally, the transition pore may lead to leakage of mitochondrial GSH, contributing to more ROS generation (Malhotra et al., 2007).

ER stress can also induce ROS in a mitochondrial independent manner. As the site of protein folding and disulfide bond formation, the ER lumen is an inherently oxidating environment. Unlike the cytosol, where the ratio between reduced glutathione (GSH) and oxidized

glutathione (GSSG) is over 50:1, inside the ER, this ratio is close to 1:1, to facilitate the formation of disulfide bonds. Protein disulfide isomerase (PDI), one of the important ER resident proteins that assists in folding, catalyzes the formation of disulfide bonds by transferring two electrons from the substrate to its active site. It is believed that these electrons end up reducing molecular oxygen, but the exact mechanism is poorly understood. Another player involved in this process is ERO1 (ER oxidoreductin 1), a flavin dependent protein thought to assist in electron transfer from PDI to molecular oxygen (Tu and Weissman, 2004). The interplay between PDI, ERO1 and certain thiol-rich proteins is thought to generate ROS inside ER, through a futile cycle mechanism that depletes GSH (Malhotra et al., 2007). Nevertheless, more studies are needed to confirm this mechanism as a significant source of ROS in the ER.

More experiments are needed to determine the initial cellular target of 11 β -dichloro. So far, we have seen that 11 β -dichloro induces an early generation of ROS and an early increase in the cytosolic calcium levels. The question remains about which response happens first and whether the two responses are causally related. More studies modulating the levels of calcium should provide additional insight into the toxicity mechanism of 11 β -dichloro. We can investigate whether chelating agents such as BAPTA and EGTA that can be used to specifically sequester calcium, can ameliorate 11 β -dichloro toxicity, by diminishing the extent of UPR induction. It would also be interesting to investigate the effect of such agents on ROS generation. The opposite effect can be achieved with ionophores (ionomycin, A23187) that increase the cytosolic calcium, by abrogating intracellular gradients. If cytosolic calcium plays a key role in the toxicity of 11 β -dichloro, co-treatment with ionophores should render the cells more sensitive. Other experiments could address the involvement of UPR in the overall toxicity. If UPR is an important contributor to toxicity, we might expect that by using chemical inhibitors towards key UPR effectors, or by knocking down the transcript levels of DDIT3 or XBP1s, we would see a decrease in sensitivity towards 11 β -dichloro.

One possible mechanism of toxicity of 11 β -dichloro may involve the following steps (Figure 4.8). Initially, the compound interacts with the mitochondria and increases generation of

ROS by mildly uncoupling the respiratory chain from the ATP synthase. Increased ROS levels start depleting the antioxidant pool of the cell; as more and more glutathione is oxidized, more NADPH is consumed to regenerate GSH. Additionally, ROS perturb the activity of Ca^{++} ATPases which maintain the homeostasis of Ca^{++} in the cell, leading to an increase in cytosolic calcium. The high cytosolic calcium acts as a general stress response messenger activating UPR and contributing to the collapse of the mitochondrial membrane potential. Additionally, high calcium activates mitochondrial calpains which trigger cell death either by releasing the apoptosis inducing factor (AIF) or by activating caspases.

Let us examine how the experimental data fit the model proposed. We postulate that mitochondria may be one of the important initial targets of 11 β -dichloro, based on the physico-chemical properties of the compound and the responses it elicits in the cell. 11 β -dichloro is a cationic amphiphile, being at the same time very lipophilic ($\log P = 5.05$ as calculated by (Hillier, 2005)) and positively charged at physiological pH due to the secondary amino group. Many cationic amphiphilic compounds (e.g., tamoxifen, paraquat, chlorpromazine) have been reported to accumulate in the mitochondrial inner membrane (Novgorodov et al., 2005), because of its special composition (essentially no cholesterol, high content of cardiolipin and negatively charged phospholipids) and its high membrane potential created by the proton gradient generated by the electron-transport chain (Galluzzi et al., 2006). Moreover, we postulate that 11 β -dichloro exhibits protonophoric properties in the mitochondrial membrane: it slowly uncouples the mitochondrial respiration from the mitochondrial ATP synthase by shuttling protons from the intermembrane space into the mitochondrial matrix but without blocking the respiratory chain, in a similar fashion with that of established protonophores such as 2,4-dinitrophenol (Leverve and Fontaine, 2001). One possible consequence of transporting protons across the mitochondrial membrane is an increase in the mitochondrial respiration, which leads to an increased mitochondrial NADH consumption, increased electron flux through the respiratory chain and finally increased ROS production. Additionally, the increased NADH consumption can diminish the available reducing equivalents necessary for regenerating NADPH via the mitochondrial NADP⁺ transhydrogenase. Reduced levels of mitochondrial NADPH then contribute to more ROS generation (Kowaltowski et al., 2001).

Another possible consequence of protonophoric compounds is the reduction in mitochondrial ATP generation. We did not see a substantial decrease in the cellular ATP levels following 11 β -dichloro exposure. However, it has been shown that many transformed cells, including HeLa cells produce most of their ATP through glycolysis, and not through the mitochondrial ATP synthase. Therefore, changes in mitochondrial ATP generation may not significantly affect the overall ATP pool (Wallace, 2005; Ramanathan et al., 2005). Moreover, protonophoric uncoupling does not always lead to impaired mitochondrial ATP production, the outcome depending on the metabolic state of the cell (Leverve et al., 2001).

Experimental approaches that test the protonophoric abilities of compounds have been well documented (Holmuhamedov et al., 2004). We can employ some of these techniques to test the properties of 11 β -dichloro, both *in vitro* and in isolated mitochondria. Additionally, we can also measure the effect of the compound on isolated mitochondria, in terms of ROS induction, changes in the mitochondrial membrane potential and metabolites accumulation. Nevertheless, while 11 β -dichloro behaving as a protonophore is an attractive hypothesis, other explanations may be possible. Careful studies in isolated mitochondria may reveal whether a more specific target (e.g., one of the ETC complexes) is involved.

Our data indicate that 11 β -dichloro generates high levels of hydrogen peroxide (Chapter 3). As explained in Chapter 3, the initial mitochondrial ROS is the superoxide anion. Using the superoxide specific probe DHE, we investigated whether the cellular superoxide levels change after exposure to 11 β -dichloro and we found no significant increase. A possible explanation for the absence of an increase in detected superoxide may come from the fact that HeLa cells (and cancer cells in general) express high levels of mitochondrial superoxide dismutase (MnSOD) (Pani et al., 2000), which is very effective at converting superoxide into hydrogen peroxide. The bottleneck in detoxifying mitochondrial ROS is thought to be hydrogen peroxide, which requires the activity of glutathione peroxidase, GPX. While MnSOD does not require any cofactors, GPX requires reduced glutathione, GSH, whose regeneration depends on the glutathione reductase and the NADPH levels (Kowaltowski et al., 2001). A decrease in the NADPH levels will diminish the available reduced glutathione,

which in turn will diminish the effectiveness of GPX at reducing hydrogen peroxide, and hence, lead to increased levels of hydrogen peroxide in the cell. Our data (Chapter 3 Figures 3.5-3.10) is consistent with this interpretation. We detect increasing levels of hydrogen peroxide (Figures 3.5-3.7), increasing levels of hydroxyl radical -the toxic byproduct of hydrogen peroxide and increased lipid oxidation due to the hydroxyl radical (Figure 3.8). Moreover, co-treatments with antioxidants ameliorate 11 β -dichloro toxicity (Figure 3.10), suggesting a mechanistic link between the generation of ROS and the cellular fate.

One consequence of increased ROS burden in the cell is oxidative damage to proteins in the form of altered disulfide bonds patterns (Kowaltowski et al., 2001). Erroneous disulfide bonds lead to changes in protein folding and consequently to changes in protein function. Among the proteins prone to inactivation by increased ROS levels are calcium ATPases, which maintain calcium homeostasis in the cell by actively pumping calcium out of the cytosol and into organelles (ER, mitochondria) or outside the cell (Malhotra et al., 2007). Inactivation of the calcium ATPases can cause a significant increase in the cytosolic calcium, consistent with our experimental data (Figure 4.4).

One notable class of calcium ATPases is sarco-endoplasmic reticulum calcium ATPases (SERCA), which maintain the high calcium concentration in the ER needed for proper folding of certain classes of proteins (Meldolesi and Pozzan, 1998). We postulate that through generation of ROS, 11 β -dichloro can diminish the activity of certain SERCA, triggering the increases in cytosolic calcium. The perturbation in SERCA activity leads to insufficient calcium in the ER, one important cause for increased protein misfolding events. Additional protein misfolding and damage can also be generated by the direct action of ROS. When the misfolded proteins reach a threshold level, the UPR response pathway is activated. We have shown in Figure 4.2 that the transcripts of key proteins involved in UPR response XBP1-cleaved and CHOP as well as downstream transcripts controlled by CHOP such as GDF15 and TRB3 are highly upregulated following exposure to 11 β -dichloro. Additionally, ATF3, a repressor of CHOP expression is being transcriptionally downregulated. CHOP (DDIT3, GADD153) is a central regulator of the UPR pathway. It is one of the highest induced genes in ER stress because it integrates signals from multiple stress-sensing

pathways (Oyadomari et al., 2004). The CHOP protein has a pro-apoptotic function, inhibiting BCL-2. Lower levels of BCL-2 derepress Bak and Bax proteins, which can then stimulate formation of mitochondrial permeability transition pores that lead to release of mitochondrial proteins and apoptosis. Although the UPR pathway has an initial purpose of reestablishing ER function, it can lead to apoptosis if the ER stress is too severe. High induction of CHOP often denotes severe ER stress and a commitment to apoptosis (Kim et al., 2008). As mentioned before, the involvement of UPR in modulating the toxicity of the compound can be easily tested, by inhibiting or knocking down key proteins such as CHOP or TRB3, which should lead to increased resistance to 11 β -dichloro. Additionally, overexpression of BCL-2 should also increase the resistance of the cells to the compound, implicating the Bax/Bak proteins as important effectors of the death signal.

CHOP activity is also modulated via the p38 MAPK (mitogen activated protein kinase) pathway. When phosphorylated by p38, CHOP becomes a more active transcription factor, exerting an enhanced pro-apoptotic activity (Oyadomari et al., 2004). The contribution of p38 to CHOP activation might provide an attractive explanation of how the DNA damage generated by 11 β -dichloro enhances the overall toxicity by synergistically activating the same pro-apoptotic pathways. The p38 MAPK pathway is critically involved in regulating cell cycle arrest following DNA damage by blocking both the G1/S and the G2/M transitions, in a p53 independent manner (Thornton and Rincon, 2009). Supporting evidence that p38 signaling is indeed induced during 11 β -dichloro exposure is the increased transcript levels of cyclin G2, a p53 independent cell cycle inhibitor (Figure 4.2 C). We are interested in a p53 independent pathway, because HeLa cells are essentially p53 negative, due to the expression of the E6 HPV protein, which targets p53 protein for proteosomal degradation (Singh et al., 2007). In the absence of DNA damage, the activation of the p38 MAPK pathway will be less prominent and hence, the phosphorylation of CHOP will happen to a lesser extent, even though CHOP transcript levels might still be induced. 11 β -Dimethoxy, the variant of the 11 β molecule that cannot alkylate DNA, exhibits cellular responses consistent with this hypothesis. Just like 11 β -dichloro, 11 β -dimethoxy increases ROS levels in the cell, reduces the antioxidant pool and upregulates the transcription of genes involved in the UPR pathway (Proffitt, 2009). However, all the cellular responses to 11 β -dimethoxy are of smaller

magnitude than those to 11 β -dichloro, at an equimolar dose. The most striking difference between the two compounds is in toxicity, 11 β -dimethoxy being significantly toxic to HeLa cells only above 15 μ M. We propose that the difference in toxicity between the two compounds comes from the ability of 11 β -dichloro to damage DNA, therefore highly activating p38 MAPK pathway, which subsequently phosphorylates CHOP. Hence, CHOP, integrating signals coming from several pathways rather than just one, reaches a pro-apoptotic threshold sooner.

Other MAPK pathways involving kinases such as ERK (extracellular-signal regulated kinase), MEK (MAPK/ERK kinase) and JNK (c-Jun N-terminal kinase) are often activated during UPR and may play important roles in modulating the cellular response to ER stress (Chang and Karin, 2001; Sekine et al., 2006; Yoshida, 2007; Szegezdi et al., 2006). The use of chemical inhibitors, such as U0126 for MEK, and SB203580 for p38 MAPK (Joo et al., 2007), SP600125 for JNK (Nieminen et al., 2006) as well as siRNA experiments should clarify which of these pathways are crucial in modulating the toxicity of 11 β -dichloro.

Another important consequence of high cytosolic calcium is the activation of calcium dependent cysteine proteases – calpains. While calpains may play a number of physiological roles important for cell survival, a lot of which are not well understood, we argue that a widespread activation of calpains is one of the death inducing process after 11 β -dichloro exposure. In fact, cell death due to calpain activation has been shown to be a consequence of high ROS generation in certain cells, especially when the ROS production happens at the mitochondrial level (Smith et al., 2008). Calpains can relay the cell death message by activating caspases (Nakagawa et al., 2000), or activate cell death in a manner that is caspase independent. Calpain-triggered cell death involves proteolytic cleavage of apoptosis-inducing factor (AIF), a mitochondrial membrane protein related to the activity of respiratory complex I. Once activated, AIF translocates to the nucleus and activates the transcription of genes involved in a death program independent of caspases (Oka et al., 2008). We have some preliminary evidence that caspases may not play a critical role in 11 β -dichloro triggered cell death (Figure 4.7). The pan-caspase inhibitor zVADfmk does not ameliorate the toxicity of 11 β -dichloro at any dose, suggesting that caspases do not play an exclusive role in the death

program. However, these data can also be misleading; the use of caspase inhibitors has been shown to induce other forms of cell death such as necrosis and autophagy (Vandenabeele et al., 2006). More careful experiments that specifically monitor the levels and activation status of individual caspases, specifically caspase-8, caspase-9 and caspase-3 are required to completely characterize the contribution of caspase-dependent apoptosis to the cell death induced by 11 β -dichloro in HeLa cells. Autophagy, another form of cell death, involving self digestion of cellular components inside autophagosomes (Gozuacik et al., 2004), has also been considered. However, the autophagy-specific inhibitor 3meA has no effect on the lysosomal expansion induced by 11 β -dichloro (Figure 4.6) and no effect on the toxicity induced by 11 β -dichloro (Figure 4.7). These data suggest that 11 β -dichloro does not induce autophagy in HeLa cells; however, more detailed experiments may be needed to completely rule out autophagy and to find an explanation for the increased acidic compartment proliferation.

Finally, in the light of the proposed mechanism, we can speculate why 11 β -dichloro is very effective against xenograft tumors, while being relatively non-toxic to the animals. Given the amphiphilic properties of 11 β -dichloro, we postulated that the compound may accumulate preferentially in the mitochondrial inner membrane because of the inner membrane composition and high membrane potential. It has been shown that cancer cells' mitochondria have higher mitochondrial membrane potential than normal cells, therefore they might accumulate 11 β -dichloro in their mitochondria faster than normal tissues, and up to a higher local concentration (Galluzzi et al., 2006). Moreover, cancer cells have a higher basal ROS level that acts both as a mutagenic factor and a proliferative stimulus (Pelicano et al., 2003). However, a higher basal ROS level would make cancer cells more susceptible than normal cells to significant increases in ROS levels, a property that 11 β -dichloro might be exploiting.

Given its potent antitumor effect displayed in mouse xenograft models, yet without an overwhelming systemic toxicity, 11 β -dichloro constitutes an intriguing scientific challenge. Our studies suggest that the mechanism of toxicity of 11 β -dichloro is multifaceted, involving perturbations in several distinct cellular compartments such as DNA, ER and mitochondria. The cellular effects of DNA damage, ER stress and mitochondrial function disruption are

Chapter 4

likely synergizing towards the observed remarkable toxicity of 11 β -dichloro.

4.6 Tables & Figures

<i>Table 4.1</i>	<i>Relative transcription levels of certain genes in LNCaP and HeLa cells.....</i>	<i>181</i>
<i>Figure 4.1</i>	<i>The structures of 11β-dichloro and 11β-dimethoxy.....</i>	<i>182</i>
<i>Figure 4.2</i>	<i>11β-Dichloro induces transcription of genes involved in UPR, sterol biosynthesis and cell cycle arrest in HeLa cells</i>	<i>183</i>
<i>Figure 4.3</i>	<i>11β-Dichloro upregulates the protein levels of SREBP and Insig1</i>	<i>184</i>
<i>Figure 4.4</i>	<i>11β-Dichloro exposure increases the cytosolic calcium</i>	<i>185</i>
<i>Figure 4.5</i>	<i>11β-Dichloro exposure induces changes in cell size</i>	<i>186</i>
<i>Figure 4.6</i>	<i>11β-Dichloro induces accumulation of acidic vesicles</i>	<i>187</i>
<i>Figure 4.7</i>	<i>The effect of cell death inhibitors 3meA and zVAD-fmk on the 11β-dichloro induced toxicity.</i>	<i>188</i>
<i>Figure 4.8</i>	<i>The hypothetical mechanisms of toxicity of 11β-dichloro</i>	<i>189</i>

	Gene name	HeLa	LNCaP
Genes involved in UPR	DDIT3	1.73	3.20 [†]
	XBP1s	2.32	3.17 [†]
	GDF15	1.66	2.91 [†]
	TRB3	1.94	2.32 [†]
	ATF3	-1.15	1.38 [†]
Genes involved in cholesterol biosynthesis	HMGCoS	1.22	1.32 [†]
	INSIG1	-0.38	2.50 [#]
Genes involved in cell cycle arrest	CyclinG2	1.64	1.71 [#]
	CyclinE2	-3.42	-1.50 [#]

Table 4.1 Relative transcription levels of certain genes in LNCaP and HeLa cells

The values in the table are log₂ fold-change (LFC) in transcript levels in cells treated with 5 μM 11β-dichloro for 6 hours in the indicated cell line, compared to cells treated with DMSO vehicle only. Positive values indicate an increase in the transcript levels; negative values represent a reduction in transcript levels. Values marked with (†) have been obtained in RT-PCR experiments in LNCaP cells; values marked with (#) have been obtained from the microarray analysis (Proffit, 2009).

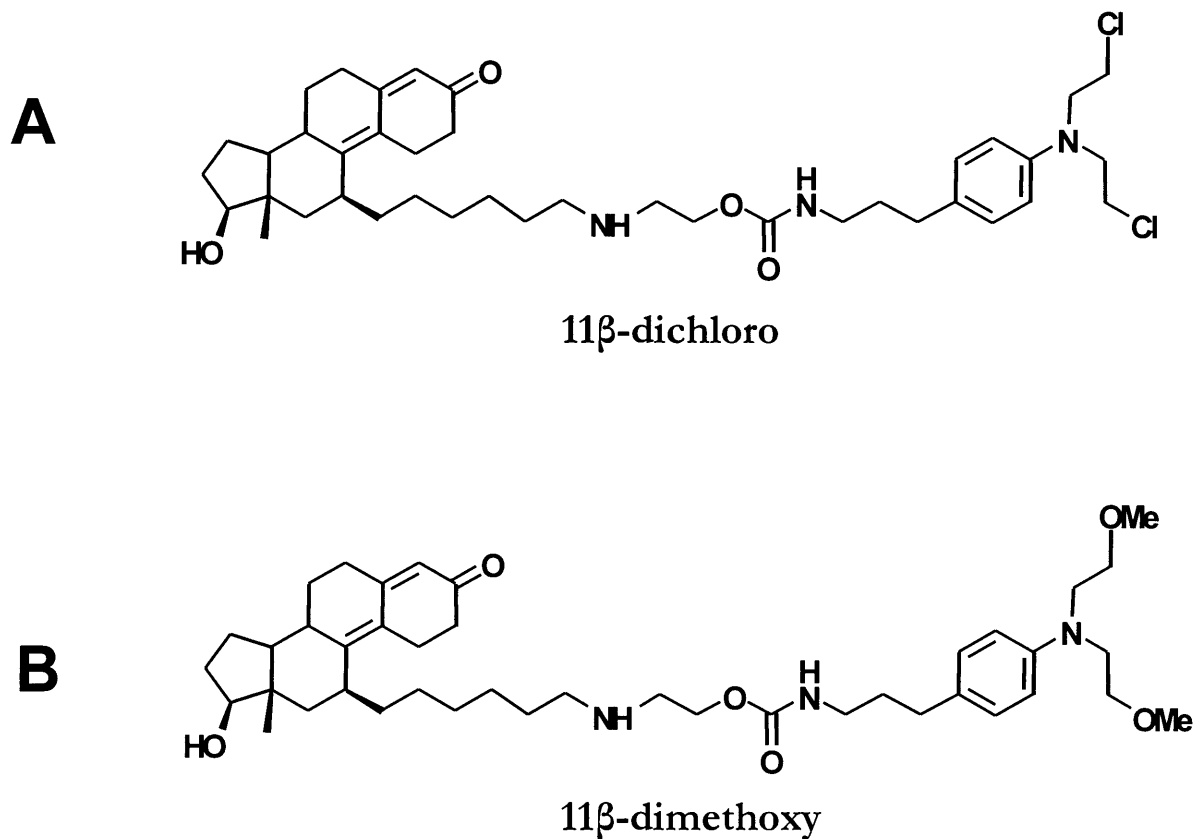


Figure 4.1 The structures of 11 β -dichloro and 11 β -dimethoxy

The lead compound of our investigation, 11 β -dichloro (A) features a steroid ligand tethered to an aniline mustard. The control compound 11 β -dimethoxy (B) has the chlorine atoms of the mustard replaced with methoxy groups, thereby inhibiting its ability to alkylate DNA.

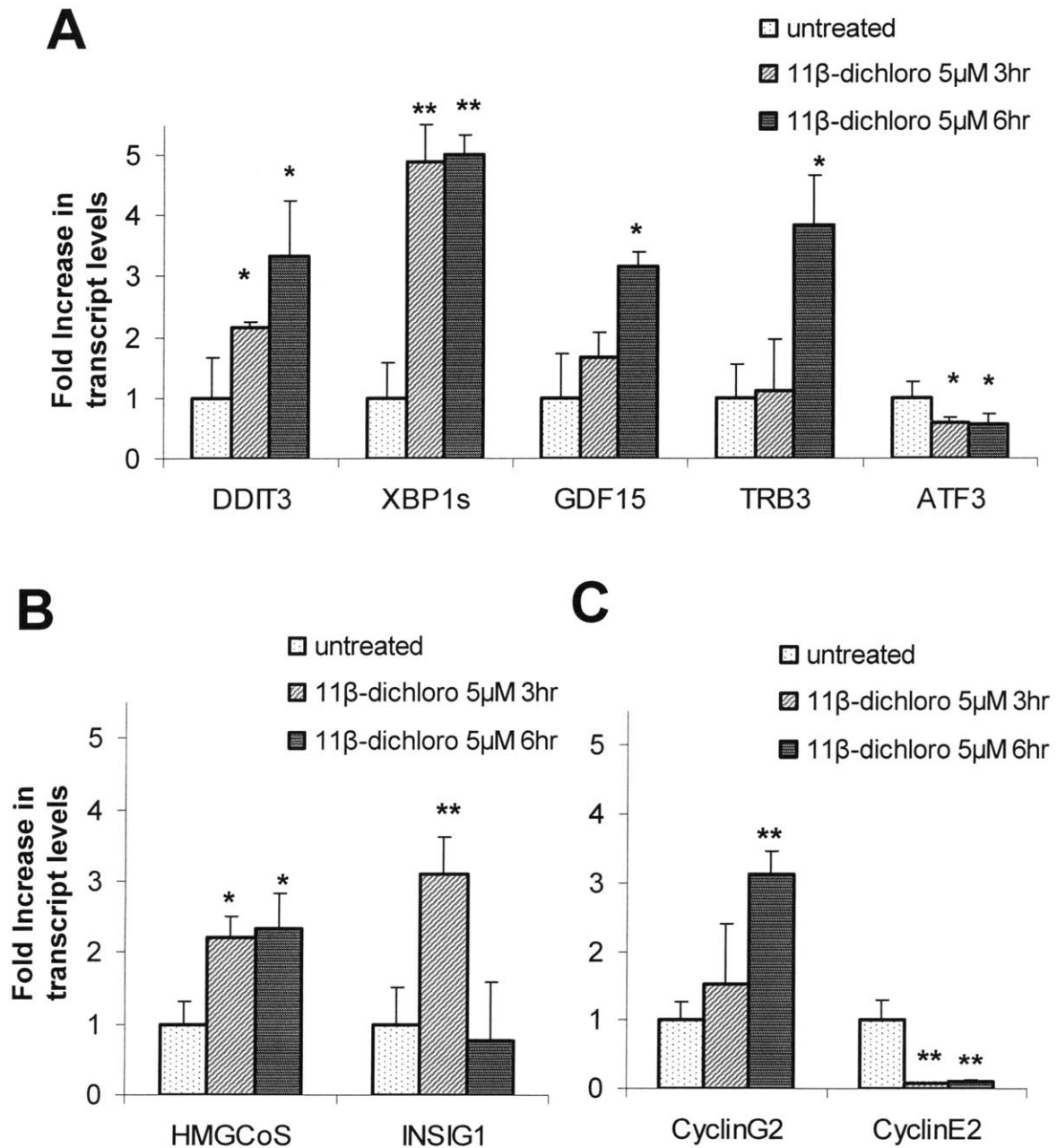
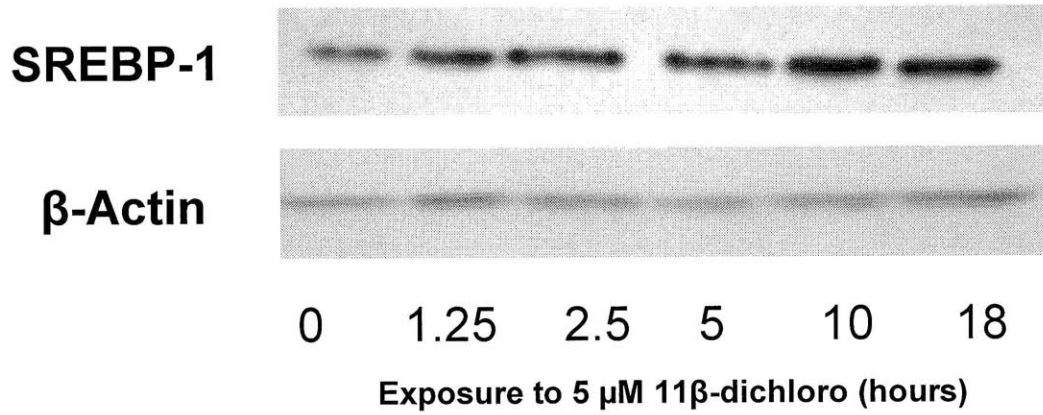


Figure 4.2 11β-Dichloro induces transcription of genes involved in UPR, sterol biosynthesis and cell cycle arrest in HeLa cells

RT-PCR experiments performed on RNA extracted from HeLa cells treated with 5 μM 11β-dichloro for 3 and 6 hours indicate that genes involved in UPR(A), sterol biosynthesis (B) and cell cycle regulation (C) are highly modified at transcriptional level.

* signifies $p < 0.05$ compared with the untreated. ** signifies $p < 0.01$

A



B

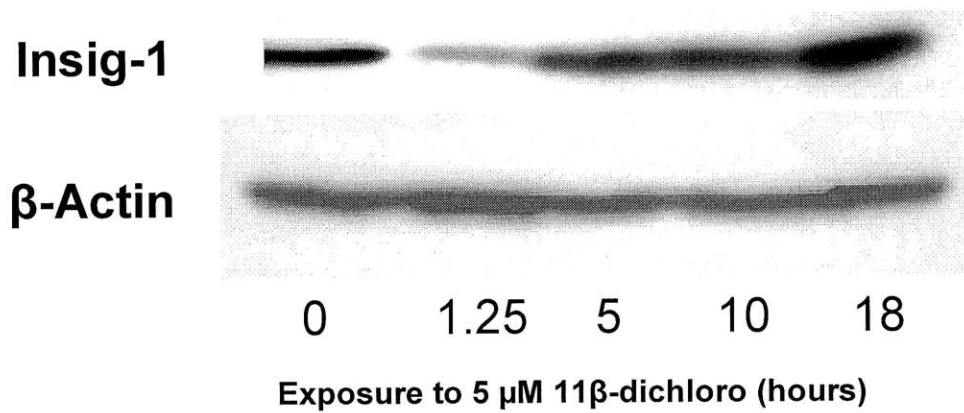


Figure 4.3 11 β -Dichloro upregulates the protein levels of SREBP and Insig1

Western blot analysis reveals that a dose of 5 μ M 11 β -dichloro has a notable effect on protein levels of SREBP (A) and Insig1 (B), key regulators of sterol biosynthesis pathway.

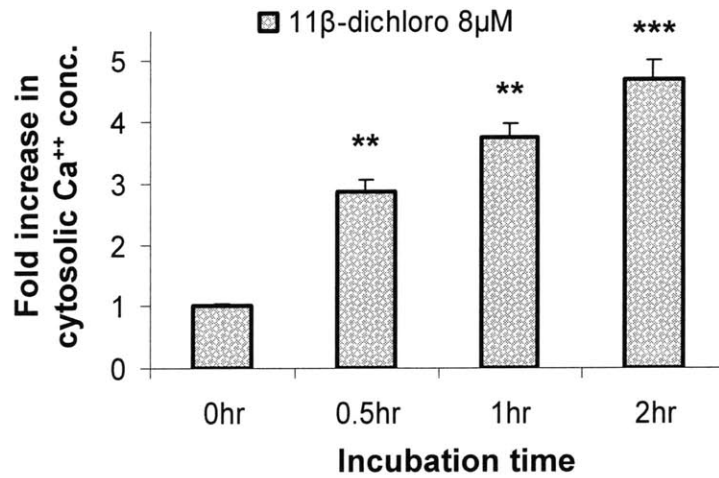


Figure 4.4 11β-Dichloro exposure increases the cytosolic calcium

Exposure of HeLa cells to a dose of 8 μM 11β-dichloro induces an early, significant increase in cytosolic calcium, as determined by flow cytometry with the calcium specific dye Fluo-4.

* signifies $p < 0.05$ compared with the untreated. ** signifies $p < 0.01$. *** signifies $p < 0.001$.

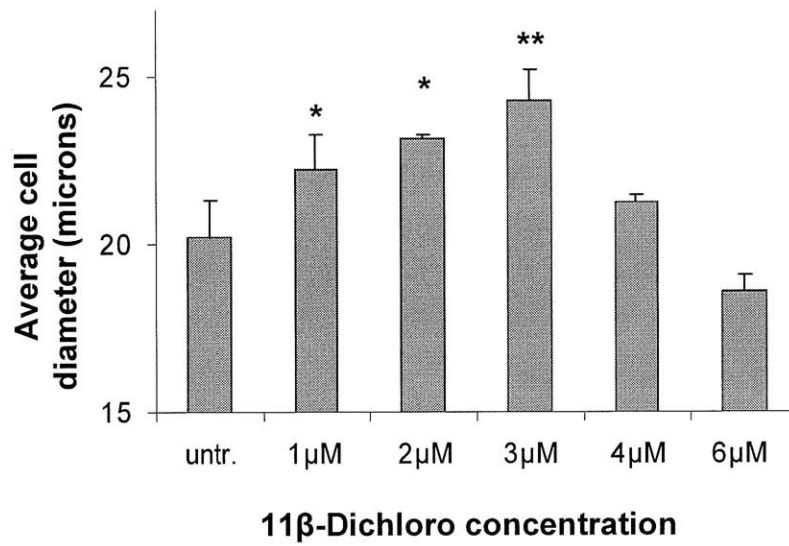


Figure 4.5 11β-Dichloro exposure induces changes in cell size

When HeLa cells are exposed to 11β-dichloro for 24 hours, their diameter increases in a dose dependent manner until 3 μM. For higher concentrations, the effect disappears.

* signifies $p < 0.05$ compared with the untreated. ** signifies $p < 0.01$.

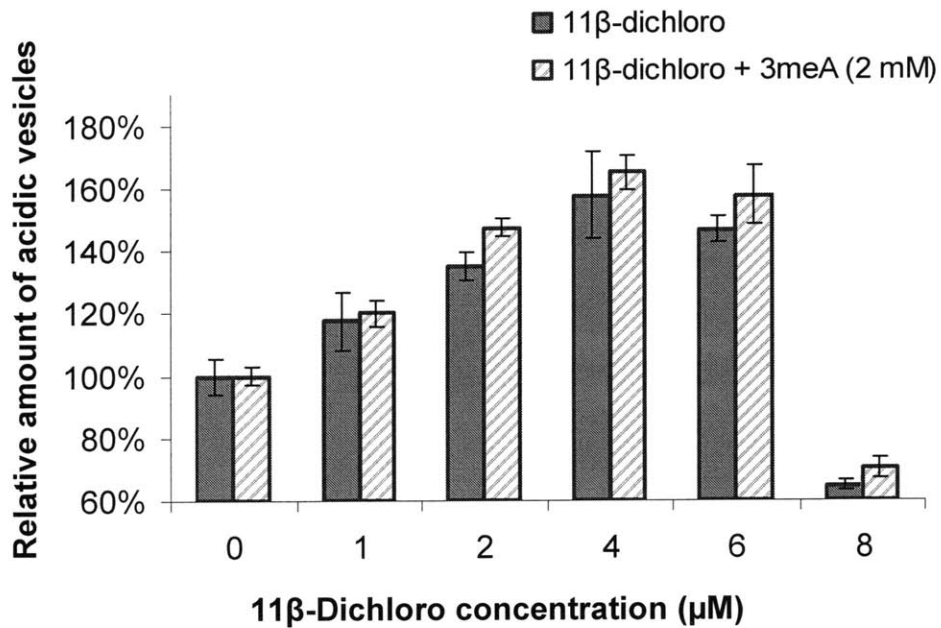


Figure 4.6 11β-Dichloro induces accumulation of acidic vesicles

HeLa cells were treated with 11β-dichloro, or co-treated with the autophagy inhibitor 3meA (2 mM) for 24 hours. Then, the relative amount of acidic vesicles was quantified using the metachromatic dye acridine orange. The results indicate that the acidic vesicles accumulate in a dose dependant manner. Co-treatment with 3meA does not change the effect, suggesting it might be autophagy independent.

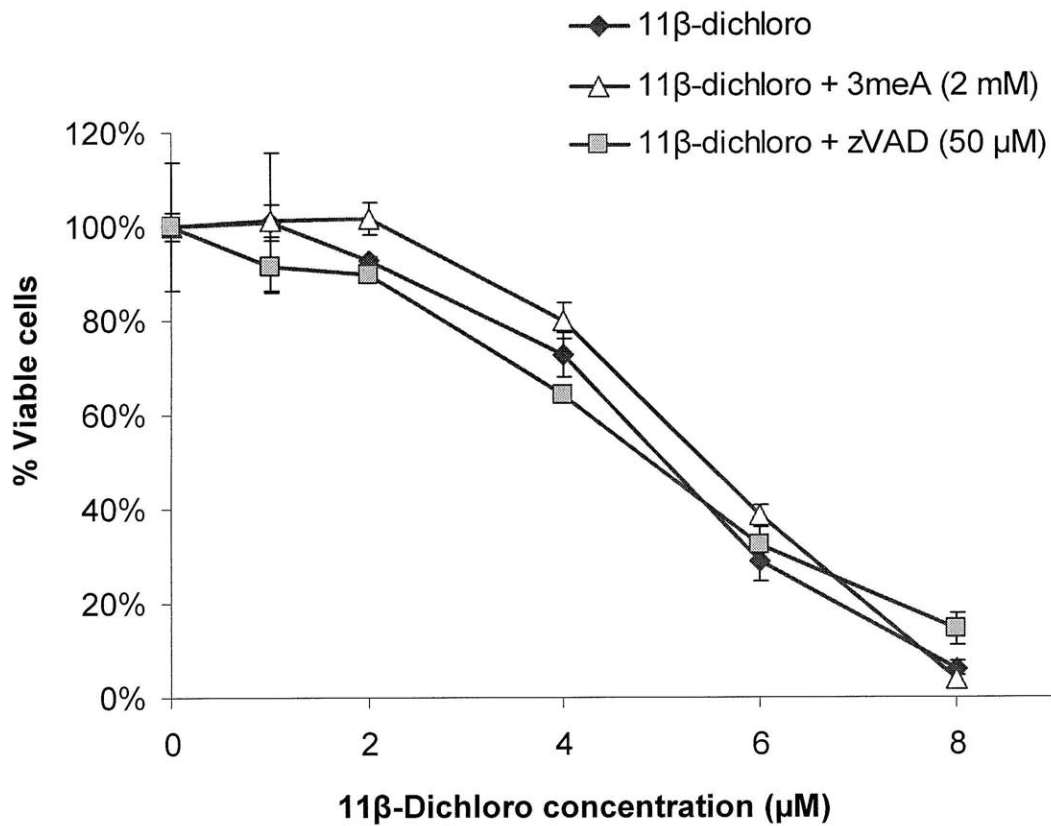


Figure 4.7 The effect of cell death inhibitors 3meA and zVAD-fmk on the 11β-dichloro induced toxicity.

HeLa cells were treated with 11β-dichloro or co-treated with autophagy inhibitor 3meA (2 mM) or pan-caspase inhibitor zVAD-fmk (50 μM) for 24 hours. There is no significant difference in the cell viability between the three conditions, which suggests that 11β-dichloro induces a mode of cell death that is autophagy- and caspase-independent.

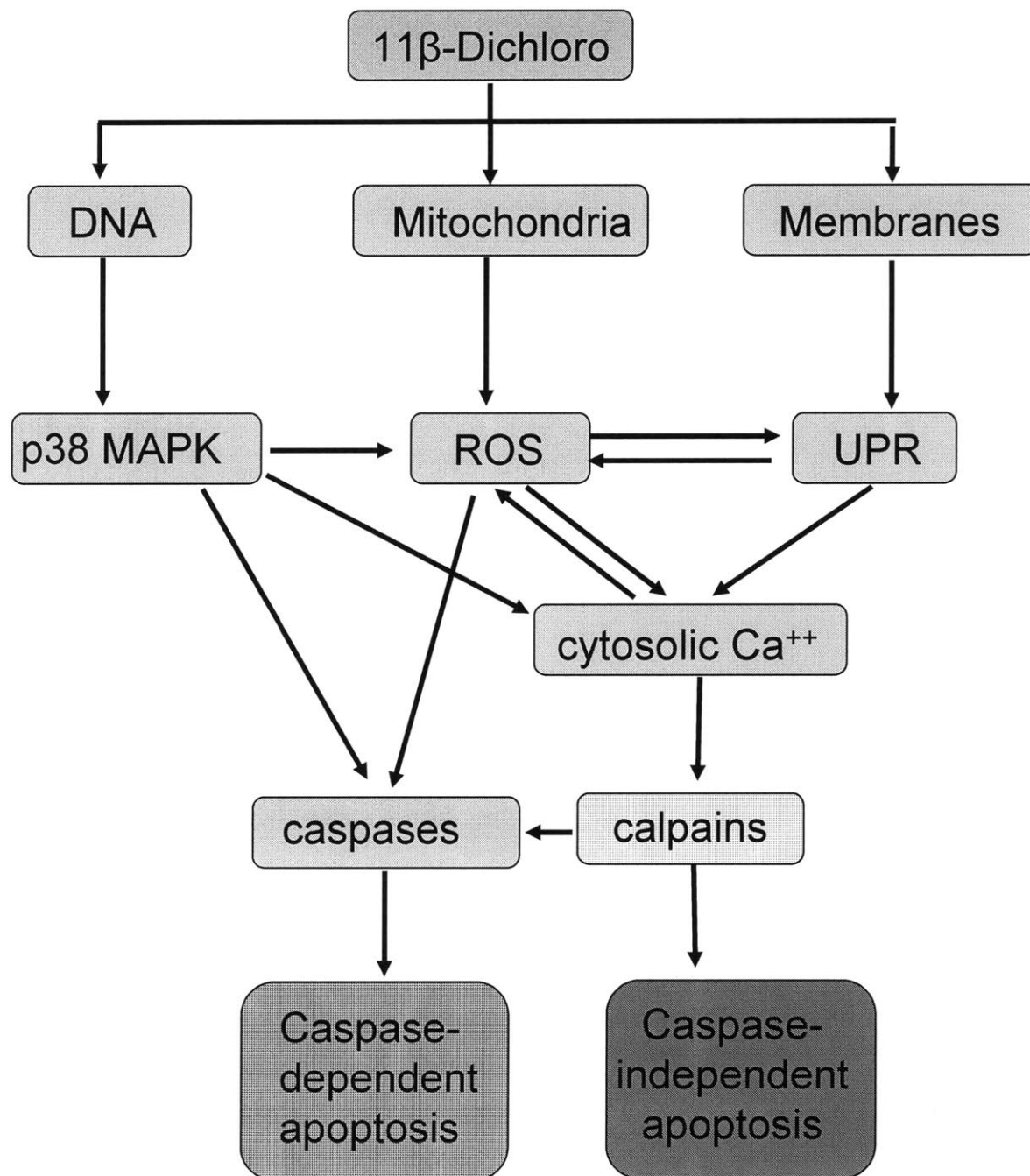


Figure 4.8 The hypothetical mechanisms of toxicity of 11 β -dichloro

Our data indicate that 11 β -dichloro toxicity involves the disruption of at least three different pathways: DNA, mitochondria, and cellular membranes. The potent toxicity of the compound may be due to the extensive crosstalk between these pathways, which converge on common cellular responses such as increased ROS and increased cytosolic calcium. From there, several different modes of cell death may be induced.

4.7 References

- Antunes, F., Cadenas, E., and Brunk, U. T. (2001). Apoptosis induced by exposure to a low steady-state concentration of H₂O₂ is a consequence of lysosomal rupture. *Biochem. J* 356, 549-555.
- Baek, S. J., Wilson, L. C., and Eling, T. E. (2002). Resveratrol enhances the expression of non-steroidal anti-inflammatory drug-activated gene (NAG-1) by increasing the expression of p53. *Carcinogenesis* 23, 425-434.
- Bommiasamy, H., Back, S. H., Fagone, P., Lee, K., Meshinchi, S., Vink, E., Sriburi, R., Frank, M., Jackowski, S., Kaufman, R. J., et al. (2009). ATF6 $\{\alpha\}$ induces XBP1-independent expansion of the endoplasmic reticulum. *J. Cell. Sci* 122, 1626-1636.
- Bottone, F. G., Baek, S. J., Nixon, J. B., and Eling, T. E. (2002). Diallyl disulfide (DADS) induces the antitumorigenic NSAID-activated gene (NAG-1) by a p53-dependent mechanism in human colorectal HCT 116 cells. *J. Nutr* 132, 773-778.
- Brown, M. S., and Goldstein, J. L. (1999). A proteolytic pathway that controls the cholesterol content of membranes, cells, and blood. *Proc. Natl. Acad. Sci. U.S.A* 96, 11041-11048.
- Brown, M. S., and Goldstein, J. L. (1997). The SREBP pathway: regulation of cholesterol metabolism by proteolysis of a membrane-bound transcription factor. *Cell* 89, 331-340.
- Chang, L., and Karin, M. (2001). Mammalian MAP kinase signalling cascades. *Nature* 410, 37-40.
- Colgan, S. M., Tang, D., Werstuck, G. H., and Austin, R. C. (2007). Endoplasmic reticulum stress causes the activation of sterol regulatory element binding protein-2. *Int. J. Biochem. Cell Biol* 39, 1843-1851.
- Dieterle, A., Orth, R., Daubrawa, M., Grotemeier, A., Alers, S., Ullrich, S., Lammers, R., Wesselborg, S., and Stork, B. (2009). The Akt inhibitor triciribine sensitizes prostate carcinoma cells to TRAIL-induced apoptosis. *Int. J. Cancer*. Available at: <http://www.ncbi.nlm.nih.gov/pubmed/19422047> [Accessed May 10, 2009].
- Du, K., Herzig, S., Kulkarni, R. N., and Montminy, M. (2003). TRB3: a tribbles homolog that inhibits Akt/PKB activation by insulin in liver. *Science* 300, 1574-7.
- Essigmann, J. M., Rink, S. M., Park, H. J., and Croy, R. G. (2001). Design of DNA damaging agents that hijack transcription factors and block DNA repair. *Adv Exp Med Biol* 500, 301-13.

Chapter 4

- Galluzzi, L., Larochette, N., Zamzami, N., and Kroemer, G. (2006). Mitochondria as therapeutic targets for cancer chemotherapy. *Oncogene* 25, 4812-30.
- Goldstein, J. L., Rawson, R. B., and Brown, M. S. (2002). Mutant mammalian cells as tools to delineate the sterol regulatory element-binding protein pathway for feedback regulation of lipid synthesis. *Arch. Biochem. Biophys* 397, 139-148.
- Gong, Y., Lee, J. N., Lee, P. C. W., Goldstein, J. L., Brown, M. S., and Ye, J. (2006). Sterol-regulated ubiquitination and degradation of Insig-1 creates a convergent mechanism for feedback control of cholesterol synthesis and uptake. *Cell Metab* 3, 15-24.
- Gozuacik, D., and Kimchi, A. (2004). Autophagy as a cell death and tumor suppressor mechanism. *Oncogene* 23, 2891-2906.
- Harding, H. P., Novoa, I., Zhang, Y., Zeng, H., Wek, R., Schapira, M., and Ron, D. (2000). Regulated translation initiation controls stress-induced gene expression in mammalian cells. *Mol. Cell* 6, 1099-1108.
- Hillier, S. M. (2005). Novel Genotoxins that Target Estrogen Receptor- and Androgen Receptor- Positive Cancers: Identification of DNA Adducts, Pharmacokinetics, and Mechanism. PhD Thesis, Massachusetts Institute of Technology.
- Holmuhamedov, E. L., Jahangir, A., Oberlin, A., Alex, Komarov, E., Colombini, M., and Terzic, A. (2004). Potassium channel openers are uncoupling protonophores: implication in cardioprotection. *FEBS Letters* 568, 167-170.
- Horton, J. D., Goldstein, J. L., and Brown, M. S. (2002). SREBPs: transcriptional mediators of lipid homeostasis. *Cold Spring Harb. Symp. Quant. Biol* 67, 491-498.
- Joo, J. H., Liao, G., Collins, J. B., Grissom, S. F., and Jetten, A. M. (2007). Farnesol-induced apoptosis in human lung carcinoma cells is coupled to the endoplasmic reticulum stress response. *Cancer Research* 67, 7929.
- Kartalou, M., and Essigmann, J. M. (2001). Recognition of cisplatin adducts by cellular proteins. *Mutat Res* 478, 1-21.
- Kaufman, R. J. (1999). Stress signaling from the lumen of the endoplasmic reticulum: coordination of gene transcriptional and translational controls. *Genes Dev* 13, 1211-1233.
- Kaufman, R. J., Scheuner, D., Schröder, M., Shen, X., Lee, K., Liu, C. Y., and Arnold, S. M. (2002). The unfolded protein response in nutrient sensing and differentiation. *Nat. Rev. Mol. Cell Biol* 3, 411-421.
- Kim, I., Xu, W., and Reed, J. C. (2008). Cell death and endoplasmic reticulum stress: disease relevance and therapeutic opportunities. *Nat Rev Drug Discov* 7, 1013-30.

- Kowaltowski, A. J., Castilho, R. F., and Vercesi, A. E. (2001). Mitochondrial permeability transition and oxidative stress. *FEBS Lett* 495, 12-5.
- Lee, J. N., and Ye, J. (2004). Proteolytic activation of sterol regulatory element-binding protein induced by cellular stress through depletion of Insig-1. *J. Biol. Chem* 279, 45257-45265.
- Lee, K., Tirasophon, W., Shen, X., Michalak, M., Prywes, R., Okada, T., Yoshida, H., Mori, K., and Kaufman, R. J. (2002). IRE1-mediated unconventional mRNA splicing and S2P-mediated ATF6 cleavage merge to regulate XBP1 in signaling the unfolded protein response. *Genes Dev* 16, 452-466.
- Lee, S., Kim, J., Yamaguchi, K., Eling, T. E., and Baek, S. J. (2005). Indole-3-carbinol and 3,3'-diindolylmethane induce expression of NAG-1 in a p53-independent manner. *Biochem. Biophys. Res. Commun* 328, 63-69.
- Lee, S., Yamaguchi, K., Kim, J., Eling, T. E., Safe, S., Park, Y., and Baek, S. J. (2006). Conjugated linoleic acid stimulates an anti-tumorigenic protein NAG-1 in an isomer specific manner. *Carcinogenesis* 27, 972-981.
- Leverve, X. M., and Fontaine, E. (2001). Role of substrates in the regulation of mitochondrial function in situ. *IUBMB Life* 52, 221-9.
- Malhotra, J. D., and Kaufman, R. J. (2007). The endoplasmic reticulum and the unfolded protein response. *Semin Cell Dev Biol* 18, 716-31.
- Marcelli, M., and Cunningham, G. R. (1999). Hormonal signaling in prostatic hyperplasia and neoplasia. *J Clin Endocrinol Metab* 84, 3463-8.
- Marquis, J. C., Hillier, S. M., Dinaut, A. N., Rodrigues, D., Mitra, K., Essigmann, J. M., and Croy, R. G. (2005). Disruption of gene expression and induction of apoptosis in prostate cancer cells by a DNA-damaging agent tethered to an androgen receptor ligand. *Chem Biol* 12, 779-87.
- Masters, J. R. W., and Köberle, B. (2003). Curing metastatic cancer: lessons from testicular germ-cell tumours. *Nat Rev Cancer* 3, 517-25.
- Meldolesi, J., and Pozzan, T. (1998). The endoplasmic reticulum Ca²⁺ store: a view from the lumen. *Trends Biochem Sci* 23, 10-4.
- Mori, K. (2000). Tripartite management of unfolded proteins in the endoplasmic reticulum. *Cell* 101, 451-454.
- Nakagawa, T., and Yuan, J. (2000). Cross-talk between two cysteine protease families. Activation of caspase-12 by calpain in apoptosis. *J. Cell Biol* 150, 887-894.

Chapter 4

- Nieminen, R., Lahti, A., Jalonen, U., Kankaanranta, H., and Moilanen, E. (2006). JNK inhibitor SP600125 reduces COX-2 expression by attenuating mRNA in activated murine J774 macrophages. *Int. Immunopharmacol* 6, 987-996.
- Novgorodov, S. A., Szulc, Z. M., Luberto, C., Jones, J. A., Bielawski, J., Bielawska, A., Hannun, Y. A., and Obeid, L. M. (2005). Positively charged ceramide is a potent inducer of mitochondrial permeabilization. *J Biol Chem* 280, 16096-105.
- Ohoka, N., Yoshii, S., Hattori, T., Onozaki, K., and Hayashi, H. (2005). TRB3, a novel ER stress-inducible gene, is induced via ATF4-CHOP pathway and is involved in cell death. *EMBO J* 24, 1243-55.
- Oka, S., Ohno, M., Tsuchimoto, D., Sakumi, K., Furuichi, M., and Nakabeppu, Y. (2008). Two distinct pathways of cell death triggered by oxidative damage to nuclear and mitochondrial DNAs. *EMBO J* 27, 421-432.
- Oyadomari, S., and Mori, M. (2004). Roles of CHOP/GADD153 in endoplasmic reticulum stress. *Cell Death Differ* 11, 381-9.
- Pani, G., Bedogni, B., Anzevino, R., Colavitti, R., Palazzotti, B., Borrello, S., and Galeotti, T. (2000). Deregulated manganese superoxide dismutase expression and resistance to oxidative injury in p53-deficient cells. *Cancer Res* 60, 4654-60.
- Pelicano, H., Feng, L., Zhou, Y., Carew, J. S., Hileman, E. O., Plunkett, W., Keating, M. J., and Huang, P. (2003). Inhibition of mitochondrial respiration: a novel strategy to enhance drug-induced apoptosis in human leukemia cells by a reactive oxygen species-mediated mechanism. *J Biol Chem* 278, 37832-9.
- Proffitt, K. D. (2009). Mechanistic Investigation of an Anticancer Agent that Damages DNA and Interacts with the Androgen Receptor. PhD Thesis, Massachusetts Institute of Technology.
- Prostko, C. R., Brostrom, M. A., and Brostrom, C. O. (1993). Reversible phosphorylation of eukaryotic initiation factor 2 alpha in response to endoplasmic reticular signaling. *Mol. Cell. Biochem* 127-128, 255-265.
- Ramanathan, A., Wang, C., and Schreiber, S. L. (2005). Perturbational profiling of a cell-line model of tumorigenesis by using metabolic measurements. *Proc Natl Acad Sci U S A* 102, 5992-7.
- Salazar, M., Carracedo, A., Salanueva, I. J., Hernández-Tiedra, S., Lorente, M., Egia, A., Vázquez, P., Blázquez, C., Torres, S., García, S., et al. (2009). Cannabinoid action induces autophagy-mediated cell death through stimulation of ER stress in human glioma cells. *J. Clin. Invest* 119, 1359-1372.

Chapter 4

- Scorrano, L., Oakes, S. A., Opferman, J. T., Cheng, E. H., Sorcinelli, M. D., Pozzan, T., and Korsmeyer, S. J. (2003). BAX and BAK regulation of endoplasmic reticulum Ca²⁺: a control point for apoptosis. *Science* *300*, 135-139.
- Sekine, Y., Takeda, K., and Ichijo, H. (2006). The ASK1-MAP kinase signaling in ER stress and neurodegenerative diseases. *Curr. Mol. Med* *6*, 87-97.
- Singh, M., Sharma, H., and Singh, N. (2007). Hydrogen peroxide induces apoptosis in HeLa cells through mitochondrial pathway. *Mitochondrion* *7*, 367-73.
- Smith, D. J., Ng, H., Kluck, R. M., and Nagley, P. (2008). The mitochondrial gateway to cell death. *IUBMB Life* *60*, 383-9.
- Sriburi, R., Jackowski, S., Mori, K., and Brewer, J. W. (2004). XBP1: a link between the unfolded protein response, lipid biosynthesis, and biogenesis of the endoplasmic reticulum. *J. Cell Biol* *167*, 35-41.
- Sun, L., Seemann, J., Goldstein, J. L., and Brown, M. S. (2007). Sterol-regulated transport of SREBPs from endoplasmic reticulum to Golgi: Insig renders sorting signal in Scap inaccessible to COPII proteins. *Proc. Natl. Acad. Sci. U.S.A* *104*, 6519-6526.
- Szegezdi, E., Logue, S. E., Gorman, A. M., and Samali, A. (2006). Mediators of endoplasmic reticulum stress-induced apoptosis. *EMBO Rep* *7*, 880-885.
- Thornton, T. M., and Rincon, M. (2009). Non-classical p38 map kinase functions: cell cycle checkpoints and survival. *Int J Biol Sci* *5*, 44-51.
- Tu, B. P., and Weissman, J. S. (2004). Oxidative protein folding in eukaryotes: mechanisms and consequences. *J. Cell Biol* *164*, 341-346.
- Vandenabeele, P., Vanden Berghe, T., and Festjens, N. (2006). Caspase inhibitors promote alternative cell death pathways. *Sci. STKE* *2006*, pe44.
- Wallace, D. C. (2005). Mitochondria and cancer: Warburg addressed. *Cold Spring Harb Symp Quant Biol* *70*, 363-74.
- Wilson, L. C., Baek, S. J., Call, A., and Eling, T. E. (2003). Nonsteroidal anti-inflammatory drug-activated gene (NAG-1) is induced by genistein through the expression of p53 in colorectal cancer cells. *Int. J. Cancer* *105*, 747-753.
- Ye, J., Rawson, R. B., Komuro, R., Chen, X., Davé, U. P., Prywes, R., Brown, M. S., and Goldstein, J. L. (2000). ER stress induces cleavage of membrane-bound ATF6 by the same proteases that process SREBPs. *Mol. Cell* *6*, 1355-1364.
- Yoshida, H. (2007). ER stress and diseases. *FEBS J* *274*, 630-658.

Chapter 4

- Yoshida, H., Matsui, T., Hosokawa, N., Kaufman, R. J., Nagata, K., and Mori, K. (2003). A time-dependent phase shift in the mammalian unfolded protein response. *Dev. Cell* *4*, 265-271.
- Zinszner, H., Kuroda, M., Wang, X., Batchvarova, N., Lightfoot, R. T., Remotti, H., Stevens, J. L., and Ron, D. (1998). CHOP is implicated in programmed cell death in response to impaired function of the endoplasmic reticulum. *Genes Dev* *12*, 982-995.
- Zong, W., Li, C., Hatzivassiliou, G., Lindsten, T., Yu, Q., Yuan, J., and Thompson, C. B. (2003). Bax and Bak can localize to the endoplasmic reticulum to initiate apoptosis. *J. Cell Biol* *162*, 59-69.

Chapter 4

APPENDIX A

**The Complete List of Yeast Mutants Sensitive to 11 β -
Dichloro**

Appendix A

A.1 Description

This appendix contains the entire list of the yeast mutants identified as sensitive to 11 β -dichloro. The table A.1 contains the following columns: ORF, gene symbol, a short description for each gene, the sensitivity to 11 β -dichloro as percentage relative growth (PRG), the sensitivity expressed as log₂ fold change (LFC), the p-value (p-val) and 4 additional fields containing the sensitivity scores to MMS, TBP, 4NQO and UV. The gene symbols and gene descriptions were retrieved from SGD (Saccharomyces Genome Database) in May 2009. The values for PRG, LFC and p-value were determined experimentally as described in Chapter 2. The sensitivity scores to MMS, TBP, 4NQO and UV were reproduced from the Begley et al., 2004 paper. Their significance is as follows: a score of 0 indicates no phenotype and hence no sensitivity. The higher the score (maximum is 30), the more sensitive the mutant to that damaging agent.

A.2 References

Begley, T. J., Rosenbach, A. S., Ideker, T., and Samson, L. D. (2004). Hot spots for modulating toxicity identified by genomic phenotyping and localization mapping. *Mol. Cell* 16, 117-125.

Appendix A

A.3 Table

Table A.1 The list of mutants sensitive to 11 β -dichloro

ORF	Gene	Description	PRG	LF C	p-val	M M S	T B P	4 N Q O	U V
YDR523C	SPS1	Putative protein serine/threonine kinase expressed at the end of meiosis and localized to the prospore membrane, required for correct localization of enzymes involved in spore wall synthesis	1.3%	-6.2	1E-06	0	0	0	4
YKL003C	MRP17	Mitochondrial ribosomal protein of the small subunit; MRP17 exhibits genetic interactions with PET122, encoding a COX3-specific translational activator	1.5%	-6.1	9E-05	0	0	0	0
YOL008W	COQ10	Coenzyme Q (ubiquinone) binding protein, functions in the delivery of Q6 to its proper location for electron transport during respiration; START domain protein with homologs in bacteria and eukaryotes	1.5%	-6.0	0.0008	4	0	0	0
YLR415C	N/A	Putative protein of unknown function; YLR415C is not an essential gene	1.6%	-6.0	1E-06	0	0	0	0
YGR102C	N/A	Putative protein of unknown function; transposon insertion mutant is salt sensitive and deletion mutant has growth defects; the authentic, non-tagged protein is detected in highly purified mitochondria in high-throughput studies	1.8%	-5.8	7E-06	0	0	0	0
YJL063C	MRPL8	Mitochondrial ribosomal protein of the large subunit	1.9%	-5.8	2E-05	0	0	0	0
YLR202C	N/A	Dubious open reading frame unlikely to encode a protein, based on available experimental and comparative sequence data; partially overlaps the verified ORF YLR201C; ORF contains a putative intron	2.0%	-5.7	4E-05	0	0	0	0
YOR125C	CAT5	Protein required for ubiquinone (Coenzyme Q) biosynthesis; localizes to the matrix face of the mitochondrial inner membrane in a large complex with ubiquinone biosynthetic enzymes; required for gluconeogenic gene activation	2.3%	-5.5	2E-05	0	0	0	0
YDL181W	INH1	Protein that inhibits ATP hydrolysis by the F1F0-ATP synthase; inhibitory function is enhanced by stabilizing proteins Stf1p and Stf2p; has similarity to Stf1p; has a calmodulin-binding motif and binds calmodulin in vitro	2.3%	-5.4	3E-05	0	0	8	0
YJL186W	MNN5	Alpha-1,2-mannosyltransferase, responsible for addition of the second alpha-1,2-linked mannose of the branches on the mannan backbone of oligosaccharides, localizes to an early Golgi compartment	2.4%	-5.4	4E-07	0	0	0	0
YLR204W	QRI5	Mitochondrial inner membrane protein, required for accumulation of spliced COX1 mRNA; may have an additional role in translation of COX1 mRNA	2.5%	-5.3	1E-05	0	0	0	0
YDR237 W	MRPL7	Mitochondrial ribosomal protein of the large subunit	2.5%	-5.3	0.0002	0	0	0	9

Appendix A

ORF	Gene	Description	PRG	LF C	p-val	M M S	T B P	4 N Q O	U V
YLR038C	COX12	Subunit VIb of cytochrome c oxidase, which is the terminal member of the mitochondrial inner membrane electron transport chain; required for assembly of cytochrome c oxidase but not required for activity after assembly; phosphorylated	2.7%	-5.2	7E-07	0	0	0	9
YLR201C	COQ9	Protein required for ubiquinone (coenzyme Q) biosynthesis and respiratory growth; localizes to the matrix face of the mitochondrial inner membrane in a large complex with ubiquinone biosynthetic enzymes	2.7%	-5.2	9E-07	0	0	0	0
YAL039C	CYC3	Cytochrome c heme lyase (holocytochrome c synthase), attaches heme to apo-cytochrome c (Cyc1p or Cyc7p) in the mitochondrial intermembrane space; human ortholog may have a role in microphthalmia with linear skin defects (MLS)	2.7%	-5.2	1E-05	4	0	0	0
YNL160W	YGP1	Cell wall-related secretory glycoprotein; induced by nutrient deprivation-associated growth arrest and upon entry into stationary phase; may be involved in adaptation prior to stationary phase entry; has similarity to Sps100p	2.8%	-5.2	0.0001	0	0	0	0
YPR100 W	MRPL51	Mitochondrial ribosomal protein of the large subunit	2.9%	-5.1	0.0008	0	0	0	0
YDR529C	QCR7	Subunit 7 of the ubiquinol cytochrome-c reductase complex, which is a component of the mitochondrial inner membrane electron transport chain; oriented facing the mitochondrial matrix; N-terminus appears to play a role in complex assembly	3.0%	-5.1	3E-05	0	0	0	1 1
YKL208W	CBT1	Protein involved in 5' end processing of mitochondrial COB, 15S_rRNA, and RPM1 transcripts; may also have a role in 3' end processing of the COB pre-mRNA; displays genetic interaction with cell cycle-regulated kinase Dbf2p	3.0%	-5.1	0.0001	4	0	0	0
YDR518 W	EUG1	Protein disulfide isomerase of the endoplasmic reticulum lumen, function overlaps with that of Pdi1p; may interact with nascent polypeptides in the ER	3.0%	-5.0	7E-05	0	0	0	0
YNR036C	MRPS1 2	Mitochondrial protein; may interact with ribosomes based on co-purification experiments; similar to E. coli and human mitochondrial S12 ribosomal proteins	3.1%	-5.0	5E-07	0	0	2	6
YNR041C	COQ2	Para hydroxybenzoate: polyprenyl transferase, catalyzes the second step in ubiquinone (coenzyme Q) biosynthesis	3.2%	-5.0	4E-05	0	0	0	0
YMR097C	MTG1	Peripheral GTPase of the mitochondrial inner membrane, essential for respiratory competence, likely functions in assembly of the large ribosomal subunit, has homologs in plants and animals	3.3%	-4.9	2E-05	0	0	0	0
YPL029W	SUV3	ATP-dependent RNA helicase, component of the mitochondrial degradosome along with the RNase Dss1p; the degradosome associates with the ribosome and mediates turnover of aberrant or unprocessed RNAs	3.4%	-4.9	4E-05	0	0	0	0

Appendix A

ORF	Gene	Description	PRG	LF C	p-val	M M S	T B P	4 N Q O	U V
YLR055C	SPT8	Subunit of the SAGA transcriptional regulatory complex but not present in SAGA-like complex SLIK/SALSA, required for SAGA-mediated inhibition at some promoters	3.5%	-4.8	2E-05	0	0	9	0
YCR071C	IMG2	Mitochondrial ribosomal protein of the small subunit	3.8%	-4.7	1E-06	0	0	0	0
YLR203C	MSS51	Nuclear encoded protein required for translation of COX1 mRNA; binds to Cox1 protein	3.8%	-4.7	9E-06	4	0	0	0
YLR407W	N/A	Putative protein of unknown function; YLR407W is not an essential gene	3.8%	-4.7	0.0003	0	0	7	0
YDR079 W	PET100	Chaperone that specifically facilitates the assembly of cytochrome c oxidase, integral to the mitochondrial inner membrane; interacts with a subcomplex of subunits VII, VIIa, and VIII (Cox7p, Cox9p, and Cox8p) but not with the holoenzyme	3.9%	-4.7	0.0002	0	0	0	0
YER110C	KAP123	Karyopherin beta, mediates nuclear import of ribosomal proteins prior to assembly into ribosomes and import of histones H3 and H4; localizes to the nuclear pore, nucleus, and cytoplasm; exhibits genetic interactions with RAI1	3.9%	-4.7	3E-05	0	0	0	0
YGR101 W	PCP1	Mitochondrial serine protease required for the processing of various mitochondrial proteins and maintenance of mitochondrial DNA and morphology; belongs to the rhomboid-GlpG superfamily of intramembrane peptidases	3.9%	-4.7	0.0002	0	0	0	0
YER169 W	RPH1	JmjC domain-containing histone demethylase which can specifically demethylate H3K36 tri- and dimethyl modification states; transcriptional repressor of PHR1; Rph1p phosphorylation during DNA damage is under control of the MEC1-RAD53 pathway	4.1%	-4.6	7E-05	0	0	0	0
YNL213C	N/A	Protein of unknown function; null mutant lacks mitochondrial DNA and cannot grow on glycerol; the authentic, non-tagged protein is detected in highly purified mitochondria in high-throughput studies	4.1%	-4.6	8E-06	0	0	0	6
YDR392 W	SPT3	Subunit of the SAGA and SAGA-like transcriptional regulatory complexes, interacts with Spt15p to activate transcription of some RNA polymerase II-dependent genes, also functions to inhibit transcription at some promoters	4.1%	-4.6	3E-05	1 0	0	1 9	0
YJL151C	SNA3	Integral membrane protein localized to vacuolar intraluminal vesicles, computational analysis of large-scale protein-protein interaction data suggests a possible role in either cell wall synthesis or protein-vacuolar targeting	4.2%	-4.6	2E-05	0	0	0	0
YER154 W	OXA1	Mitochondrial inner membrane insertase, mediates the insertion of both mitochondrial- and nuclear-encoded proteins from the matrix into the inner membrane, interacts with mitochondrial ribosomes; conserved from bacteria to animals	4.2%	-4.6	5E-05	0	0	0	8

Appendix A

ORF	Gene	Description	PRG	LF C	p-val	M M S	T B P	4 N Q O	U V
YGL143C	MRF1	Mitochondrial translation release factor, involved in stop codon recognition and hydrolysis of the peptidyl-tRNA bond during mitochondrial translation; lack of MRF1 causes mitochondrial genome instability	4.3%	-4.5	2E-06	0	0	0	0
YNL081C	SWS2	Putative mitochondrial ribosomal protein of the small subunit, has similarity to E. coli S13 ribosomal protein; participates in controlling sporulation efficiency	4.7%	-4.4	6E-06	0	0	2 6	0
YNL177C	MRPL22	Mitochondrial ribosomal protein of the large subunit	4.8%	-4.4	6E-06	0	0	0	0
YDR042C	N/A	Putative protein of unknown function; expression is increased in ssu72-ts69 mutant	4.8%	-4.4	3E-06	0	0	0	0
YPL139C	UME1	Negative regulator of meiosis, required for repression of a subset of meiotic genes during vegetative growth, binding of histone deacetylase Rpd3p required for activity, contains a NEE box and a WD repeat motif; homologous with Wtm1p, Wtm2p	4.8%	-4.4	0.0001	0	0	2	0
YDL063C	N/A	Putative protein of unknown function; green fluorescent protein (GFP)-fusion protein localizes to the cytoplasm and nucleus; predicted to be involved in ribosome biogenesis	4.9%	-4.4	1E-07	0	0	0	0
YBL045C	COR1	Core subunit of the ubiquinol-cytochrome c reductase complex (bc1 complex), which is a component of the mitochondrial inner membrane electron transport chain	4.9%	-4.3	3E-06	0	0	0	0
YDR507C	GIN4	Protein kinase involved in bud growth and assembly of the septin ring, proposed to have kinase-dependent and kinase-independent activities; undergoes autophosphorylation; similar to Kcc4p and Hsl1p	5.0%	-4.3	0.0001	0	0	0	0
YJL134W	LCB3	Long-chain base-1-phosphate phosphatase with specificity for dihydrosphingosine-1-phosphate, regulates ceramide and long-chain base phosphates levels, involved in incorporation of exogenous long chain bases in sphingolipids	5.0%	-4.3	6E-05	7	0	1 2	0
YDL068W	N/A	Dubious ORF unlikely to encode a protein, based on available experimental and comparative sequence data	5.3%	-4.2	4E-05	0	0	0	9
YNL096C	RPS7B	Protein component of the small (40S) ribosomal subunit, nearly identical to Rps7Ap; interacts with Kti11p; deletion causes hypersensitivity to zymocin; has similarity to rat S7 and Xenopus S8 ribosomal proteins	5.4%	-4.2	9E-06	7	0	0	0
YJL149W	N/A	Putative SCF ubiquitin ligase F-box protein; interacts physically with both Cdc53p and Skp1 and genetically with CDC34; similar to putative F-box protein YDR131C	5.6%	-4.2	0.0001	0	0	0	0
YLL018C-A	COX19	Protein required for cytochrome c oxidase assembly, located in the cytosol and mitochondrial intermembrane space; putative copper metallochaperone that delivers copper to cytochrome c oxidase	5.6%	-4.2	0.0003	2	0	0	0
YBL090W	MRP21	Mitochondrial ribosomal protein of the small subunit; MRP21 exhibits genetic interactions with mutations in the COX2 and COX3 mRNA 5'-untranslated leader sequences	5.7%	-4.1	4E-05	0	0	0	0

Appendix A

ORF	Gene	Description	PRG	LF C	p-val	M M S	T B P	4 N Q O	U V
YOR201C	MRM1	Ribose methyltransferase that modifies a functionally critical, conserved nucleotide in mitochondrial 21S rRNA	5.7%	-4.1	2E-05	0	0	2	0
YKL037W	AIM26	Putative protein of unknown function; null mutant is viable and displays elevated frequency of mitochondrial genome loss; null mutation confers sensitivity to tunicamycin and DTT	5.9%	-4.1	4E-06	0	3	6	0
YOR205C	N/A	Protein of unknown function; the authentic, non-tagged protein is detected in purified mitochondria in high-throughput studies	5.9%	-4.1	8E-06	0	0	0	0
YBR248C	HIS7	Imidazole glycerol phosphate synthase (glutamine amidotransferase: cyclase), catalyzes the fifth and sixth steps of histidine biosynthesis and also produces 5-aminoimidazole-4-carboxamide ribotide (AICAR), a purine precursor	6.1%	-4.0	2E-06	0	0	0	0
YMR031 W-A	N/A	Dubious open reading frame unlikely to encode a protein, based on available experimental and comparative sequence data; null mutant displays shortened telomeres; partially overlaps the uncharacterized ORF YMR031C	6.2%	-4.0	2E-07	2 4	0 0	1 0	0
YOR374 W	ALD4	Mitochondrial aldehyde dehydrogenase, required for growth on ethanol and conversion of acetaldehyde to acetate; phosphorylated; activity is K ⁺ dependent; utilizes NADP ⁺ or NAD ⁺ equally as coenzymes; expression is glucose repressed	6.3%	-4.0	4E-05	4	0	0	0
YDL033C	SLM3	tRNA-specific 2-thiouridylase, responsible for 2-thiolation of the wobble base of mitochondrial tRNAs; human ortholog is implicated in myoclonus epilepsy associated with ragged red fibers (MERRF)	6.3%	-4.0	9E-05	0	0	0	0
YCR003 W	MRPL32	Mitochondrial ribosomal protein of the large subunit	6.4%	-4.0	4E-05	0	0	2	0
YHR116 W	COX23	Mitochondrial intermembrane space protein that functions in mitochondrial copper homeostasis, essential for functional cytochrome oxidase expression; homologous to Cox17p	6.4%	-4.0	3E-06	0	0	0	0
YBR044C	TCM62	Protein involved in the assembly of the mitochondrial succinate dehydrogenase complex; putative chaperone	6.7%	-3.9	3E-05	4	0	0	0
YNL298W	CLA4	Cdc42p-activated signal transducing kinase of the PAK (p21-activated kinase) family, which also includes Ste20p and Skm1p; involved in septin ring assembly, vacuole inheritance, and cytokinesis; phosphorylates septins Cdc3p and Cdc10p	6.7%	-3.9	0.0002	7	0	1 2	0
YBR173C	UMP1	Short-lived chaperone required for correct maturation of the 20S proteasome; may inhibit premature dimerization of proteasome half-mers; degraded by proteasome upon completion of its assembly	6.9%	-3.9	0.0009	0	0	0	0

Appendix A

ORF	Gene	Description	PRG	LF C	p-val	M M S	T B P	4 N Q O	U V
YLR398C	SKI2	Ski complex component and putative RNA helicase, mediates 3'-5' RNA degradation by the cytoplasmic exosome; null mutants have superkiller phenotype of increased viral dsRNAs and are synthetic lethal with mutations in 5'-3' mRNA decay	7.0%	-3.8	0.0001	0	0	6	0
YGL012W	ERG4	C-24(28) sterol reductase, catalyzes the final step in ergosterol biosynthesis; mutants are viable, but lack ergosterol	7.0%	-3.8	1E-05	0	5	1 5	0
YPR116 W	N/A	Putative protein of unknown function; null mutation results in a decrease in plasma membrane electron transport	7.1%	-3.8	1E-04	0	0	1 3	0
YMR003 W	AIM34	Protein of unknown function; GFP-fusion protein localizes to the mitochondria; null mutant is viable and displays reduced frequency of mitochondrial genome loss	7.2%	-3.8	0.0002	0	0	9	0
YBL099W	ATP1	Alpha subunit of the F1 sector of mitochondrial F1F0 ATP synthase, which is a large, evolutionarily conserved enzyme complex required for ATP synthesis; phosphorylated	7.3%	-3.8	0.0001	1 5	0	6	9
YDL155W	CLB3	B-type cyclin involved in cell cycle progression; activates Cdc28p to promote the G2/M transition; may be involved in DNA replication and spindle assembly; accumulates during S phase and G2, then targeted for ubiquitin-mediated degradation	7.3%	-3.8	0.0002	1 4	0	9	7
YDR320C	SWA2	Auxilin-like protein involved in vesicular transport; clathrin-binding protein required for uncoating of clathrin-coated vesicles	7.4%	-3.8	1E-05	9	0	9	0
YJR113C	RSM7	Mitochondrial ribosomal protein of the small subunit, has similarity to E. coli S7 ribosomal protein	7.5%	-3.7	7E-06	9	0	0	0
YDR508C	GNP1	High-affinity glutamine permease, also transports Leu, Ser, Thr, Cys, Met and Asn; expression is fully dependent on Grr1p and modulated by the Ssy1p-Ptr3p-Ssy5p (SPS) sensor of extracellular amino acids	7.6%	-3.7	2E-05	2	0	1 0	0
YBR122C	MRPL36	Mitochondrial ribosomal protein of the large subunit; overproduction suppresses mutations in the COX2 leader peptide-encoding region	7.7%	-3.7	2E-06	7	0	1 2	0
YGR155 W	CYS4	Cystathionine beta-synthase, catalyzes the synthesis of cystathionine from serine and homocysteine, the first committed step in cysteine biosynthesis; mutations in the human ortholog cause homocystinuria	7.7%	-3.7	2E-06	4	3	0	0
YNR037C	RSM19	Mitochondrial ribosomal protein of the small subunit, has similarity to E. coli S19 ribosomal protein	7.8%	-3.7	1E-05	0	0	0	7
YBL002W	HTB2	Histone H2B, core histone protein required for chromatin assembly and chromosome function; nearly identical to HTB1; Rad6p-Bre1p-Lge1p mediated ubiquitination regulates transcriptional activation, meiotic DSB formation and H3 methylation	7.9%	-3.7	1E-05	0	0	0	0

Appendix A

ORF	Gene	Description	PRG	LF C	p-val	M M S	T B P	4 N Q O	U V
YJL120W	N/A	Dubious open reading frame unlikely to encode a protein, based on available experimental and comparative sequence data; partially overlaps the verified gene YJL121C/RPE1; deletion confers sensitivity to GSAO	7.9%	-3.7	4E-05	7	0	1 7	0
YGR257C	MTM1	Mitochondrial protein of the mitochondrial carrier family, involved in activating mitochondrial Sod2p probably by facilitating insertion of an essential manganese cofactor	7.9%	-3.7	0.0001	0	0	0	0
YBR228 W	SLX1	Subunit of a complex, with Slx4p, that hydrolyzes 5' branches from duplex DNA in response to stalled or converging replication forks; function overlaps with that of Sgs1p-Top3p	8.0%	-3.7	2E-05	0	0	0	0
YCR024C	SLM5	Mitochondrial asparaginyl-tRNA synthetase	8.0%	-3.7	4E-05	0	2	0	3
YLR079W	SIC1	Inhibitor of Cdc28-Clb kinase complexes that controls G1/S phase transition, preventing premature S phase and ensuring genomic integrity; phosphorylation targets Sic1p for SCF(CDC4)-dependent turnover; functional homolog of mammalian Kip1	8.0%	-3.7	6E-06	4	0	7	0
YOR303 W	CPA1	Small subunit of carbamoyl phosphate synthetase, which catalyzes a step in the synthesis of citrulline, an arginine precursor; translationally regulated by an attenuator peptide encoded by YOR302W within the CPA1 mRNA 5'-leader	8.0%	-3.6	5E-06	0	0	0	0
YLR061W	RPL22A	Protein component of the large (60S) ribosomal subunit, has similarity to Rpl22Bp and to rat L22 ribosomal protein	8.1%	-3.6	0.0002	0	2	0	0
YKL134C	40087	Mitochondrial intermediate peptidase, cleaves N-terminal residues of a subset of proteins upon import, after their cleavage by mitochondrial processing peptidase (Mas1p-Mas2p); may contribute to mitochondrial iron homeostasis	8.2%	-3.6	8E-06	0	0	6	2
YDR231C	COX20	Mitochondrial inner membrane protein, required for proteolytic processing of Cox2p and its assembly into cytochrome c oxidase	8.3%	-3.6	0.0004	0	0	0	0
YMR198 W	CIK1	Kinesin-associated protein required for both karyogamy and mitotic spindle organization, interacts stably and specifically with Kar3p and may function to target this kinesin to a specific cellular role; has similarity to Vik1p	8.4%	-3.6	0.0003	1 9	4	2 3	4
YOR035C	SHE4	Protein containing a UCS (UNC-45/CRO1/SHE4) domain, binds to myosin motor domains to regulate myosin function; involved in endocytosis, polarization of the actin cytoskeleton, and asymmetric mRNA localization	8.4%	-3.6	6E-06	7	2	0	0
YBR120C	CBP6	Mitochondrial translational activator of the COB mRNA; phosphorylated	8.5%	-3.6	3E-05	0	0	0	0
YBR226C	N/A	Dubious open reading frame unlikely to encode a protein, based on available experimental and comparative sequence data; partially overlaps the uncharacterized ORF YBR225W	8.7%	-3.5	2E-05	0	0	0	0
YOR221C	MCT1	Predicted malonyl-CoA:ACP transferase, putative component of a type-II mitochondrial fatty acid synthase that produces intermediates for phospholipid remodeling	8.9%	-3.5	3E-05	1 0	0	0	1 3

Appendix A

ORF	Gene	Description	PRG	LF C	p-val	M M S	T B P	4 N Q O	U V
YBR245C	ISW1	Member of the imitation-switch (ISWI) class of ATP-dependent chromatin remodeling complexes; ATPase that forms a complex with loc2p and loc4p to regulate transcription elongation, and a complex with loc3p to repress transcription initiation	9.0%	-3.5	8E-07	1 2	0	0	0
YPR067 W	ISA2	Protein required for maturation of mitochondrial and cytosolic Fe/S proteins, localizes to the mitochondrial intermembrane space, overexpression of ISA2 suppresses grx5 mutations	9.1%	-3.5	6E-06	4	0	0	0
YFL033C	RIM15	Glucose-repressible protein kinase involved in signal transduction during cell proliferation in response to nutrients, specifically the establishment of stationary phase; identified as a regulator of IME2; substrate of Pho80p-Pho85p kinase	9.1%	-3.5	3E-06	0	4	0	0
YDL049C	KNH1	Protein with similarity to Kre9p, which is involved in cell wall beta 1,6-glucan synthesis; overproduction suppresses growth defects of a kre9 null mutant; required for propionic acid resistance	9.1%	-3.5	3E-05	0	0	0	0
YDR194C	MSS116	DEAD-box protein required for efficient splicing of mitochondrial Group I and II introns; non-polar RNA helicase that also facilitates strand annealing	9.1%	-3.5	4E-05	0	0	0	5
YER083C	GET2	Subunit of the GET complex; involved in insertion of proteins into the ER membrane; required for the retrieval of HDEL proteins from the Golgi to the ER in an ERD2 dependent fashion and for meiotic nuclear division	9.1%	-3.5	0.0002	1 0	5	3 0	0
YJR090C	GRR1	F-box protein component of the SCF ubiquitin-ligase complex; involved in carbon catabolite repression, glucose-dependent divalent cation transport, high-affinity glucose transport, morphogenesis, and sulfite detoxification	9.3%	-3.4	8E-06	5	5	6	3
YNL280C	ERG24	C-14 sterol reductase, acts in ergosterol biosynthesis; mutants accumulate the abnormal sterol ignosterol (ergosta-8,14 dienol), and are viable under anaerobic growth conditions but inviable on rich medium under aerobic conditions	9.4%	-3.4	3E-05	9	0	0	0
YKR009C	FOX2	Multifunctional enzyme of the peroxisomal fatty acid beta-oxidation pathway; has 3-hydroxyacyl-CoA dehydrogenase and enoyl-CoA hydratase activities	9.4%	-3.4	3E-05	2	0	0	0
YKL155C	RSM22	Mitochondrial ribosomal protein of the small subunit; also predicted to be an S-adenosylmethionine-dependent methyltransferase	9.5%	-3.4	4E-05	0	0	0	0
YDL113C	ATG20	Sorting nexin family member required for the cytoplasm-to-vacuole targeting (Cvt) pathway and for endosomal sorting; has a Phox homology domain that binds phosphatidylinositol-3-phosphate; interacts with Snx4p; potential Cdc28p substrate	9.5%	-3.4	4E-06	0	0	0	0

Appendix A

ORF	Gene	Description	PRG	LF C	p-val	M M S	T B P	4 N Q O	U V
YLL045C	RPL8B	Ribosomal protein L4 of the large (60S) ribosomal subunit, nearly identical to Rpl8Ap and has similarity to rat L7a ribosomal protein; mutation results in decreased amounts of free 60S subunits	9.6%	-3.4	0.047	0	0	0	0
YJR074W	MOG1	Conserved nuclear protein that interacts with GTP-Gsp1p, which is a Ran homolog of the Ras GTPase family, and stimulates nucleotide release, involved in nuclear protein import, nucleotide release is inhibited by Yrb1p	9.7%	-3.4	6E-05	7	0	3	0
YOR289 W	N/A	Putative protein of unknown function; transcription induced by the unfolded protein response; green fluorescent protein (GFP)-fusion protein localizes to both the cytoplasm and the nucleus	9.7%	-3.4	4E-06	0	0	0	0
YDL146W	LDB17	Protein of unknown function; GFP-fusion protein localizes to the cell periphery, cytoplasm, bud, and bud neck; null mutant shows a reduced affinity for the alcian blue dye suggesting a decreased net negative charge of the cell surface	9.8%	-3.4	0.0003	0	0	0	0
YNL097C	PHO23	Probable component of the Rpd3 histone deacetylase complex, involved in transcriptional regulation of PHO5; C-terminus has similarity to human candidate tumor suppressor p33(ING1) and its isoform ING3	9.9%	-3.3	4E-06	4	0	1 6	0
YDL107W	MSS2	Peripherally bound inner membrane protein of the mitochondrial matrix involved in membrane insertion of C-terminus of Cox2p, interacts genetically and physically with Cox18p	10.0%	-3.3	5E-05	0	0	0	7
YBR003 W	COQ1	Hexaprenyl pyrophosphate synthetase, catalyzes the first step in ubiquinone (coenzyme Q) biosynthesis	10.0%	-3.3	2E-05	4	0	0	0
YJL130C	URA2	Bifunctional carbamoylphosphate synthetase (CPSase)-aspartate transcarbamylase (ATCase), catalyzes the first two enzymatic steps in the de novo biosynthesis of pyrimidines; both activities are subject to feedback inhibition by UTP	10.0%	-3.3	1E-05	0	0	0	0
YML013 W	UBX2	Protein involved in ER-associated protein degradation; proposed to coordinate the assembly of proteins involved in ERAD; contains a UBX (ubiquitin regulatory X) domain and a ubiquitin-associated (UBA) domain	10.2%	-3.3	2E-05	0	0	0	0
YER153C	PET122	Mitochondrial translational activator specific for the COX3 mRNA, acts together with Pet54p and Pet494p; located in the mitochondrial inner membrane	10.2%	-3.3	9E-06	0	0	0	8
YDR195 W	REF2	RNA-binding protein involved in the cleavage step of mRNA 3'-end formation prior to polyadenylation, and in snoRNA maturation; part of holo-CPF subcomplex APT, which associates with 3'-ends of snoRNA- and mRNA-encoding genes	10.2%	-3.3	7E-05	1 8	0	3 0	1 5

Appendix A

ORF	Gene	Description	PRG	LF C	p-val	M M S	T B P	4 N Q O	U V
YNL084C	END3	EH domain-containing protein involved in endocytosis, actin cytoskeletal organization and cell wall morphogenesis; forms a complex with Sla1p and Pan1p	10.3%	-3.3	3E-05	0	3	0	0
YMR067C	UBX4	UBX (ubiquitin regulatory X) domain-containing protein that interacts with Cdc48p	10.3%	-3.3	1E-05	4	2	0	0
YER103 W	SSA4	Heat shock protein that is highly induced upon stress; plays a role in SRP-dependent cotranslational protein-membrane targeting and translocation; member of the HSP70 family; cytoplasmic protein that concentrates in nuclei upon starvation	10.4%	-3.3	9E-05	0	0	0	0
YJL189W	RPL39	Protein component of the large (60S) ribosomal subunit, has similarity to rat L39 ribosomal protein; required for ribosome biogenesis; loss of both Rpl31p and Rpl39p confers lethality; also exhibits genetic interactions with SIS1 and PAB1	10.5%	-3.3	1E-05	0	5	2	0
YOR356 W	N/A	Mitochondrial protein with similarity to flavoprotein-type oxidoreductases; found in a large supramolecular complex with other mitochondrial dehydrogenases	10.6%	-3.2	5E-06	0	0	0	0
YDR477 W	SNF1	AMP-activated serine/threonine protein kinase found in a complex containing Snf4p and members of the Sip1p/Sip2p/Gal83p family; required for transcription of glucose-repressed genes, thermotolerance, sporulation, and peroxisome biogenesis	10.7%	-3.2	6E-06	0	0	0	0
YOR078 W	BUD21	Component of small ribosomal subunit (SSU) processosome that contains U3 snoRNA; originally isolated as bud-site selection mutant that displays a random budding pattern	10.7%	-3.2	1E-05	0	0	3	0
YKL087C	CYT2	Cytochrome c1 heme lyase, involved in maturation of cytochrome c1, which is a subunit of the mitochondrial ubiquinol-cytochrome-c reductase; links heme covalently to apocytochrome c1	10.7%	-3.2	4E-05	0	0	0	1 1
YLR382C	NAM2	Mitochondrial leucyl-tRNA synthetase, also has a direct role in splicing of several mitochondrial group I introns; indirectly required for mitochondrial genome maintenance	10.7%	-3.2	0.001	0	0	0	0
YLR139C	SLS1	Mitochondrial membrane protein that coordinates expression of mitochondrially-encoded genes; may facilitate delivery of mRNA to membrane-bound translation machinery	10.7%	-3.2	6E-06	0	0	0	0
YNL284C	MRPL10	Mitochondrial ribosomal protein of the large subunit; appears as two protein spots (YmL10 and YmL18) on two-dimensional SDS gels	10.9%	-3.2	3E-05	0	0	0	0
YEL045C	N/A	Dubious open reading frame unlikely to encode a protein based on available experimental and comparative sequence data; deletion gives MMS sensitivity, growth defect under alkaline conditions, less than optimal growth upon citric acid stress	10.9%	-3.2	6E-05	2	1 1	1 9	0

Appendix A

ORF	Gene	Description	PRG	LF C	p-val	M M S	T B P	4 N Q O	U V
YBR095C	RXT2	Subunit of the histone deacetylase Rpd3L complex; possibly involved in cell fusion and invasive growth	11.2%	-3.2	1E-05	6	0	1 0	0
YNL248C	RPA49	RNA polymerase I subunit A49	11.3%	-3.1	7E-06	0	0	7	9
YDR075 W	PPH3	Catalytic subunit of an evolutionarily conserved protein phosphatase complex containing Psy2p and the regulatory subunit Psy4p; required for cisplatin resistance; involved in activation of Gln3p	11.4%	-3.1	3E-06	1 9	0	7	0
YPL041C	N/A	Protein of unknown function involved in maintenance of proper telomere length	11.4%	-3.1	0.0002	4	0	1 2	1 0
YDL067C	COX9	Subunit VIIa of cytochrome c oxidase, which is the terminal member of the mitochondrial inner membrane electron transport chain	11.5%	-3.1	5E-07	0	0	0	4
YNL299W	TRF5	Poly (A) polymerase involved in nuclear RNA quality control based on: homology with Pap2p, genetic interactions with PAP2 mutants, physical interaction with Mtr4p (TRAMP subunit), and by direct assay; disputed role as a sigma DNA polymerase	11.5%	-3.1	2E-05	0	0	0	0
YOR200 W	N/A	Dubious open reading frame unlikely to encode a protein, based on available experimental and comparative sequence data; partially overlaps the verified ORF MRM1/YOR201c	11.6%	-3.1	0.0002	5	0	7	1 8
YML120C	NDI1	NADH:ubiquinone oxidoreductase, transfers electrons from NADH to ubiquinone in the respiratory chain but does not pump protons, in contrast to the higher eukaryotic multisubunit respiratory complex I; phosphorylated; homolog of human AMID	11.6%	-3.1	6E-06	0	0	0	0
YDL032W	N/A	Dubious open reading frame unlikely to encode a protein, based on available experimental and comparative sequence data; partially overlaps verified gene SLM3/YDL033C; YDL032W is not an essential gene	12.0%	-3.1	0.0003	2 7	0	0	0
YNR052C	POP2	RNase of the DEDD superfamily, subunit of the Ccr4-Not complex that mediates 3' to 5' mRNA deadenylation	12.2%	-3.0	1E-05	8	0	2 6	1 1
YDR136C	VPS61	Dubious open reading frame, unlikely to encode a protein; not conserved in closely related Saccharomyces species; 4% of ORF overlaps the verified gene RGP1; deletion causes a vacuolar protein sorting defect	12.2%	-3.0	3E-05	0	0	1 0	0
YNL236W	SIN4	Subunit of the RNA polymerase II mediator complex; associates with core polymerase subunits to form the RNA polymerase II holoenzyme; contributes to both positive and negative transcriptional regulation; dispensable for basal transcription	12.2%	-3.0	6E-05	8	0	3 0	0
YDL006W	PTC1	Type 2C protein phosphatase (PP2C); inactivates the osmosensing MAPK cascade by dephosphorylating Hog1p; mutation delays mitochondrial inheritance; deletion reveals defects in precursor tRNA splicing, sporulation and cell separation	12.3%	-3.0	2E-05	1 5	0	1 9	0

Appendix A

ORF	Gene	Description	PRG	LF C	p-val	M M S	T B P	4 N Q O	U V
YPL031C	PHO85	Cyclin-dependent kinase, with ten cyclin partners; involved in regulating the cellular response to nutrient levels and environmental conditions and progression through the cell cycle	12.3%	-3.0	7E-05	9	7	0	1 1
YLR328W	NMA1	Nicotinic acid mononucleotide adenylyltransferase, involved in pathways of NAD biosynthesis, including the de novo, NAD(+) salvage, and nicotinamide riboside salvage pathways	12.3%	-3.0	7E-05	0	0	0	0
YDL044C	MTF2	Mitochondrial matrix protein that interacts with an N-terminal region of mitochondrial RNA polymerase (Rpo41p) and couples RNA processing and translation to transcription	12.4%	-3.0	0.0002	0	0	0	2
YNL171C	N/A	Dubious open reading frame unlikely to encode a functional protein, based on available experimental and comparative sequence data	12.4%	-3.0	5E-05	1 5	0	3 0	0
YLR439W	MRPL4	Mitochondrial ribosomal protein of the large subunit	12.4%	-3.0	4E-06	0	0	0	0
YDR375C	BCS1	Protein of the mitochondrial inner membrane that functions as an ATP-dependent chaperone, required for the incorporation of the Rip1p and Qcr10p subunits into the cytochrome bc(1) complex; member of the CDC48/PAS1/SEC18 ATPase family	12.5%	-3.0	5E-07	0	0	0	0
YDL104C	QRI7	Putative metalloprotease, similar to O-sialoglycoprotein metalloproteinase from <i>P. haemolytica</i> ; the authentic, non-tagged protein is detected in highly purified mitochondria in high-throughput studies	12.5%	-3.0	9E-05	0	0	0	0
YBL080C	PET112	Protein required for mitochondrial translation; mutation is functionally complemented by a <i>Bacillus subtilis</i> ortholog	12.6%	-3.0	0.0001	0	0	0	0
YOR318C	N/A	Dubious open reading frame unlikely to encode a protein, based on available experimental and comparative sequence data; transcript is predicted to be spliced but there is no evidence that it is spliced in vivo	12.7%	-3.0	6E-05	0	0	0	0
YPL065W	VPS28	Component of the ESCRT-I complex (Stp22p, Srn2p, Vps28p, and Mvb12p), which is involved in ubiquitin-dependent sorting of proteins into the endosome; conserved C-terminal domain interacts with ESCRT-III subunit Vps20p	12.7%	-3.0	2E-07	2 2	2	0	0
YER178 W	PDA1	E1 alpha subunit of the pyruvate dehydrogenase (PDH) complex, catalyzes the direct oxidative decarboxylation of pyruvate to acetyl-CoA; phosphorylated; regulated by glucose	12.7%	-3.0	8E-05	1 0	0	1 2	0
YJL046W	AIM22	Putative lipoate-protein ligase A family member; null mutant is viable and displays reduced frequency of mitochondrial genome loss	12.8%	-3.0	3E-06	2 6	0	0	0
YOR158 W	PET123	Mitochondrial ribosomal protein of the small subunit; PET123 exhibits genetic interactions with PET122, which encodes a COX3 mRNA-specific translational activator	12.9%	-3.0	0.0002	0	0	0	0

Appendix A

ORF	Gene	Description	PRG	LF C	p-val	M M S	T B P	4 N Q O	U V
YBL007C	SLA1	Cytoskeletal protein binding protein required for assembly of the cortical actin cytoskeleton; interacts with proteins regulating actin dynamics and proteins required for endocytosis; found in the nucleus and cell cortex; has 3 SH3 domains	13.2%	-2.9	4E-05	0	0	0	0
YER016 W	BIM1	Microtubule-binding protein that together with Kar9p makes up the cortical microtubule capture site and delays the exit from mitosis when the spindle is oriented abnormally	13.2%	-2.9	4E-06	1 0	0	1 6	0
YOR338 W	N/A	Putative protein of unknown function; YOR338W transcription is regulated by Azf1p and its transcript is a specific target of the G protein effector Scp160p; identified as being required for sporulation in a high-throughput mutant screen	13.3%	-2.9	5E-06	0	0	0	0
YDL081C	RPP1A	Ribosomal stalk protein P1 alpha, involved in the interaction between translational elongation factors and the ribosome; accumulation of P1 in the cytoplasm is regulated by phosphorylation and interaction with the P2 stalk component	13.3%	-2.9	5E-05	8	0	0	0
YML032C	RAD52	Protein that stimulates strand exchange by facilitating Rad51p binding to single-stranded DNA; anneals complementary single-stranded DNA; involved in the repair of double-strand breaks in DNA during vegetative growth and meiosis	13.3%	-2.9	0.0002	2 0	0	2 0	1 0
YBR216C	YBP1	Protein required for oxidation of specific cysteine residues of the transcription factor Yap1p, resulting in the nuclear localization of Yap1p in response to stress	13.3%	-2.9	8E-06	0	5	0	0
YML010 W-A	N/A	Dubious ORF unlikely to encode a functional protein, based on available experimental and comparative sequence data; deletion mutation confers an increase in Ty1 transposition	13.3%	-2.9	1E-06	1 5	0	0	6
YER090 W	TRP2	Anthranilate synthase, catalyzes the initial step of tryptophan biosynthesis, forms multifunctional hetero-oligomeric anthranilate synthase:indole-3-glycerol phosphate synthase enzyme complex with Trp3p	13.4%	-2.9	4E-05	0	0	0	0
YPL002C	SNF8	Component of the ESCRT-II complex, which is involved in ubiquitin-dependent sorting of proteins into the endosome; appears to be functionally related to SNF7; involved in glucose derepression	13.4%	-2.9	0.0001	2 6	2	0	0
YDR322 W	MRPL35	Mitochondrial ribosomal protein of the large subunit	13.5%	-2.9	1E-05	0	0	1 8	0
YOR150 W	MRPL23	Mitochondrial ribosomal protein of the large subunit	13.6%	-2.9	0.0001	0	0	0	0
YKR055 W	RHO4	Non-essential small GTPase of the Rho/Rac subfamily of Ras-like proteins, likely to be involved in the establishment of cell polarity	13.6%	-2.9	0.0002	6	0	2 0	0

Appendix A

ORF	Gene	Description	PRG	LF C	p-val	M M S	T B P	4 N Q O	U V
YER119C -A	N/A	Dubious open reading frame, not conserved in closely related <i>Saccharomyces</i> species; deletion mutation blocks replication of Brome mosaic virus in <i>S. cerevisiae</i> , but this is likely due to effects on the overlapping gene SCS2	13.8%	-2.9	1E-04	0	0	0	0
YOR321 W	PMT3	Protein O-mannosyltransferase, transfers mannose residues from dolichyl phosphate-D-mannose to protein serine/threonine residues; acts in a complex with Pmt5p, can instead interact with Pmt1p in some conditions; target for new antifungals	13.8%	-2.9	3E-05	0	0	0	0
YDR175C	RSM24	Mitochondrial ribosomal protein of the small subunit	13.9%	-2.9	0.0001	0	0	9	0
YMR038C	CCS1	Copper chaperone for superoxide dismutase Sod1p, involved in oxidative stress protection; Met-X-Cys-X2-Cys motif within the N-terminal portion is involved in insertion of copper into Sod1p under conditions of copper deprivation	13.9%	-2.8	2E-05	7	0	2 3	0
YPR134 W	MSS18	Nuclear encoded protein needed for efficient splicing of mitochondrial COX1 α 5beta intron; mss18 mutations block cleavage of 5' exon - intron junction; phenotype of intronless strain suggests additional functions	14.0%	-2.8	2E-05	0	0	0	0
YDR241 W	BUD26	Dubious open reading frame, unlikely to encode a protein; not conserved in closely related <i>Saccharomyces</i> species; 1% of ORF overlaps the verified gene SNU56; diploid mutant displays a weak budding pattern phenotype in a systematic assay	14.1%	-2.8	1E-06	0	0	0	0
YFL033C	RIM15	Glucose-repressible protein kinase involved in signal transduction during cell proliferation in response to nutrients, specifically the establishment of stationary phase; identified as a regulator of IME2; substrate of Pho80p-Pho85p kinase	14.1%	-2.8	4E-05	0	4	0	0
YBR200 W	BEM1	Protein containing SH3-domains, involved in establishing cell polarity and morphogenesis; functions as a scaffold protein for complexes that include Cdc24p, Ste5p, Ste20p, and Rsr1p	14.1%	-2.8	1E-05	1 7	0	0	0
YJL003W	COX16	Mitochondrial inner membrane protein, required for assembly of cytochrome c oxidase	14.1%	-2.8	0.0004	0	0	0	0
YNL309W	STB1	Protein with a role in regulation of MBF-specific transcription at Start, phosphorylated by Cln-Cdc28p kinases in vitro; unphosphorylated form binds Swi6p and binding is required for Stb1p function; expression is cell-cycle regulated	14.2%	-2.8	0.0001	0	0	0	0
YJL207C	LAA1	AP-1 accessory protein; colocalizes with clathrin to the late-Golgi apparatus; involved in TGN-endosome transport; physically interacts with AP-1; similar to the mammalian p200; may interact with ribosomes; YJL207C is a non-essential gene	14.2%	-2.8	0.0006	0	0	0	0

Appendix A

ORF	Gene	Description	PRG	LF C	p-val	M M S	T B P	4 N Q O	U V
YKL057C	NUP120	Subunit of the Nup84p subcomplex of the nuclear pore complex (NPC), required for even distribution of NPCs around the nuclear envelope, involved in establishment of a normal nucleocytoplasmic concentration gradient of the GTPase Gsp1p	14.3%	-2.8	5E-06	1 5	0	2 6	7
YPL106C	SSE1	ATPase that is a component of the heat shock protein Hsp90 chaperone complex; binds unfolded proteins; member of the heat shock protein 70 (HSP70) family; localized to the cytoplasm	14.4%	-2.8	0.0002	1 0	0	4	0
YGR063C	SPT4	Protein involved in the regulating Pol I and Pol II transcription, pre-mRNA processing, kinetochore function, and gene silencing; forms a complex with Spt5p	14.5%	-2.8	2E-06	8	0	6	0
YJL079C	PRY1	Protein of unknown function	14.5%	-2.8	2E-06	0	0	0	0
YOR376 W	N/A	Dubious open reading frame unlikely to encode a protein, based on available experimental and comparative sequence data; YOR376W is not an essential gene.	14.6%	-2.8	1E-05	4	0	0	0
YIL110W	MNI1	Putative S-adenosylmethionine-dependent methyltransferase of the seven beta-strand family; deletion mutant exhibits a weak vacuolar protein sorting defect, enhanced resistance to caspofungin, and is synthetically lethal with MEN mutants	14.7%	-2.8	0.0011	5	0	4	6
YGL105W	ARC1	Protein that binds tRNA and methionyl- and glutamyl-tRNA synthetases (Mes1p and Gus1p), delivering tRNA to them, stimulating catalysis, and ensuring their localization to the cytoplasm; also binds quadruplex nucleic acids	14.8%	-2.8	4E-05	0	0	0	5
YFL018C	LPD1	Dihydrolipoamide dehydrogenase, the lipoamide dehydrogenase component (E3) of the pyruvate dehydrogenase and 2-oxoglutarate dehydrogenase multi-enzyme complexes	14.8%	-2.8	9E-06	0	0	0	0
YOR199 W	N/A	Dubious open reading frame unlikely to encode a protein, based on available experimental and comparative sequence data	15.0%	-2.7	0.0001	0	0	2 2	0
YDR347 W	MRP1	Mitochondrial ribosomal protein of the small subunit; MRP1 exhibits genetic interactions with PET122, encoding a COX3-specific translational activator, and with PET123, encoding a small subunit mitochondrial ribosomal protein	15.1%	-2.7	2E-06	0	0	0	0
YFL025C	BST1	GPI inositol deacylase of the ER that negatively regulates COPII vesicle formation, prevents production of vesicles with defective subunits, required for proper discrimination between resident ER proteins and Golgi-bound cargo molecules	15.1%	-2.7	1E-05	0	4	0	0
YPL161C	BEM4	Protein involved in establishment of cell polarity and bud emergence; interacts with the Rho1p small GTP-binding protein and with the Rho-type GTPase Cdc42p; involved in maintenance of proper telomere length	15.1%	-2.7	9E-05	4	8	1 5	9

Appendix A

ORF	Gene	Description	PRG	LF C	p-val	M M S	T B P	4 N Q	U V
YLR048W	RPS0B	Protein component of the small (40S) ribosomal subunit, nearly identical to Rps0Ap; required for maturation of 18S rRNA along with Rps0Ap; deletion of either RPS0 gene reduces growth rate, deletion of both genes is lethal	15.1%	-2.7	5E-06	0	3	0	0
YGR240C	PFK1	Alpha subunit of heterooctameric phosphofructokinase involved in glycolysis, indispensable for anaerobic growth, activated by fructose-2,6-bisphosphate and AMP, mutation inhibits glucose induction of cell cycle-related genes	15.4%	-2.7	6E-05	0	0	1 2	0
YDR432 W	NPL3	RNA-binding protein that promotes elongation, regulates termination, and carries poly(A) mRNA from nucleus to cytoplasm; required for pre-mRNA splicing; dissociation from mRNAs promoted by Mtr10p; phosphorylated by Sky1p in the cytoplasm	15.5%	-2.7	4E-06	1 8	0	2 6	2 2
YJR144W	MGM10 1	Protein involved in mitochondrial genome maintenance; component of the mitochondrial nucleoid, required for the repair of oxidative mtDNA damage	15.5%	-2.7	4E-05	1 6	0	0	8
YPL148C	PPT2	Phosphopantetheine:protein transferase (PPTase), activates mitochondrial acyl carrier protein (Acp1p) by phosphopantetheinylation	15.6%	-2.7	1E-05	9	0	0	0
YOR342C	N/A	Putative protein of unknown function; green fluorescent protein (GFP)-fusion protein localizes to the cytoplasm and the nucleus	15.6%	-2.7	1E-05	0	0	0	0
YIL098C	FMC1	Mitochondrial matrix protein, required for assembly or stability at high temperature of the F1 sector of mitochondrial F1F0 ATP synthase; null mutant temperature sensitive growth on glycerol is suppressed by multicopy expression of Odc1p	15.7%	-2.7	0.0006	4	9	0	0
YMR263 W	SAP30	Subunit of a histone deacetylase complex, along with Rpd3p and Sin3p, that is involved in silencing at telomeres, rDNA, and silent mating-type loci; involved in telomere maintenance	15.7%	-2.7	0.0001	0	0	1 5	0
YDL116W	NUP84	Subunit of the nuclear pore complex (NPC), forms a subcomplex with Nup85p, Nup120p, Nup145p-C, Sec13p, and Seh1p that plays a role in nuclear mRNA export and NPC biogenesis	15.8%	-2.7	0.0002	2 2	0	3 0	1 8
YEL024W	RIP1	Ubiquinol-cytochrome-c reductase, a Rieske iron-sulfur protein of the mitochondrial cytochrome bc1 complex; transfers electrons from ubiquinol to cytochrome c1 during respiration	15.9%	-2.6	0.0005	4	0	0	0
YPL259C	APM1	Mu1-like medium subunit of the clathrin-associated protein complex (AP-1); binds clathrin; involved in clathrin-dependent Golgi protein sorting	16.1%	-2.6	0.001	4	0	0	0
YOL085C	N/A	Dubious open reading frame unlikely to encode a protein, based on experimental and comparative sequence data; partially overlaps the dubious gene YOL085W-A	16.1%	-2.6	4E-05	4	0	0	0

Appendix A

ORF	Gene	Description	PRG	LF C	p-val	M M S	T B P	4 N Q O	U V
YDR350C	ATP22	Mitochondrial inner membrane protein required for assembly of the F0 sector of mitochondrial F1F0 ATP synthase, which is a large, evolutionarily conserved enzyme complex required for ATP synthesis	16.2%	-2.6	1E-05	0	0	0	0
YBL044W	N/A	Putative protein of unknown function; YBL044W is not an essential protein	16.2%	-2.6	1E-05	0	0	0	0
YLR021W	IRC25	Component of a heterodimeric Poc4p-Irc25p chaperone involved in assembly of alpha subunits into the 20S proteasome; may regulate formation of proteasome isoforms with alternative subunits under different conditions	16.3%	-2.6	0.0001	0	0	0	0
YKL048C	ELM1	Serine/threonine protein kinase that regulates cellular morphogenesis, septin behavior, and cytokinesis; required for the regulation of other kinases; forms part of the bud neck ring	16.3%	-2.6	3E-05	8	0	1 5	0
YDR056C	N/A	Putative protein of unknown function; green fluorescent protein (GFP)-fusion protein localizes to the endoplasmic reticulum; YDR056C is not an essential protein	16.4%	-2.6	0.0004	0	0	0	0
YPL157W	TGS1	Trimethyl guanosine synthase, conserved nucleolar methyl transferase that converts the m(7)G cap structure of snRNAs, snoRNAs, and telomerase TLC1 RNA to m(2,2,7)G; also required for ribosome synthesis and nucleolar morphology	16.4%	-2.6	0.0004	0	0	0	0
YDL185W	TFP1	Subunit A of the eight-subunit V1 peripheral membrane domain of the vacuolar H ⁺ -ATPase; protein precursor undergoes self-catalyzed splicing to yield the extein Tfp1p and the intein Vde (PI-SceI), which is a site-specific endonuclease	16.4%	-2.6	3E-05	0	0	1 6	0
YJL184W	GON7	Protein proposed to be involved in the modification of N-linked oligosaccharides, osmotic stress response, telomere uncapping and elongation, transcription; component of the EKC/KEOPS protein complex with Kae1p, Cgi121p, Pcc1p, and Bud32p	16.5%	-2.6	9E-05	1 2	0	2 3	3
YBR069C	TAT1	Amino acid transport protein for valine, leucine, isoleucine, and tyrosine, low-affinity tryptophan and histidine transporter; overexpression confers FK506 and FTY720 resistance	16.5%	-2.6	0.0007	0	0	0	0
YOR270C	VPH1	Subunit a of vacuolar-ATPase V0 domain, one of two isoforms (Vph1p and Stv1p); Vph1p is located in V-ATPase complexes of the vacuole while Stv1p is located in V-ATPase complexes of the Golgi and endosomes	16.5%	-2.6	3E-06	4	9	0	0
YNL071W	LAT1	Dihydrolipoamide acetyltransferase component (E2) of pyruvate dehydrogenase complex, which catalyzes the oxidative decarboxylation of pyruvate to acetyl-CoA	16.6%	-2.6	0.0024	2 0	0	1 6	3

Appendix A

ORF	Gene	Description	PRG	LF C	p-val	M M S	T B P	4 N Q O	U V
YIL125W	KGD1	Component of the mitochondrial alpha-ketoglutarate dehydrogenase complex, which catalyzes a key step in the tricarboxylic acid (TCA) cycle, the oxidative decarboxylation of alpha-ketoglutarate to form succinyl-CoA	16.7%	-2.6	2E-05	0	0	0	0
YNL229C	URE2	Nitrogen catabolite repression transcriptional regulator that acts by inhibition of GLN3 transcription in good nitrogen source; has glutathione peroxidase activity and can mutate to acquire GST activity; altered form creates [URE3] prion	16.8%	-2.6	0.0005	8	0	3 0	0
YGL107C	RMD9	Mitochondrial protein required for respiratory growth; mutant phenotype and genetic interactions suggest a role in delivering mt mRNAs to ribosomes; located on matrix face of the inner membrane and loosely associated with mitoribosomes	16.8%	-2.6	3E-05	0	0	0	0
YBR203 W	COS111	Protein required for resistance to the antifungal drug ciclopirox olamine; not related to the subtelomerically-encoded COS family; the authentic, non-tagged protein is detected in highly purified mitochondria in high-throughput studies	16.8%	-2.6	9E-06	0	0	0	0
YGL174W	BUD13	Subunit of the RES complex, which is required for nuclear pre-mRNA retention and splicing; involved in bud-site selection; diploid mutants display a unipolar budding pattern instead of the wild-type bipolar pattern	16.8%	-2.6	3E-05	0	0	0	0
YDR296 W	MHR1	Protein involved in homologous recombination in mitochondria and in transcription regulation in nucleus; binds to activation domains of acidic activators; required for recombination-dependent mtDNA partitioning	16.8%	-2.6	1E-05	0	0	0	0
YDR137 W	RGP1	Subunit of a Golgi membrane exchange factor (Ric1p-Rgp1p) that catalyzes nucleotide exchange on Ypt6p	16.8%	-2.6	1E-05	5	0	0	0
YML011C	RAD33	Protein involved in nucleotide excision repair; green fluorescent protein (GFP)-fusion protein localizes to the nucleus	16.8%	-2.6	6E-05	0	0	3 0	1 1
YDR512C	EMI1	Non-essential protein of unknown function required for transcriptional induction of the early meiotic-specific transcription factor IME1, also required for sporulation	16.9%	-2.6	0.0006	5	0	0	9
YMR257C	PET111	Mitochondrial translational activator specific for the COX2 mRNA; located in the mitochondrial inner membrane	17.0%	-2.6	1E-04	4	0	0	0
YBL093C	ROX3	Subunit of the RNA polymerase II mediator complex; associates with core polymerase subunits to form the RNA polymerase II holoenzyme	17.0%	-2.6	3E-05	1 9	0	2 1	0
YBL022C	PIM1	ATP-dependent Lon protease, involved in degradation of misfolded proteins in mitochondria; required for biogenesis and maintenance of mitochondria	17.0%	-2.6	6E-05	0	0	1 6	0
YMR098C	ATP25	Mitochondrial protein required for the stability of Oli1p (Atp9p) mRNA and for the Oli1p ring formation; YMR098C is not an essential gene	17.1%	-2.6	0.0003	0	0	0	0

Appendix A

ORF	Gene	Description	PRG	LF C	p-val	M M S	T B P	4 N Q O	U V
YCL058C	FYV5	Protein of unknown function, required for survival upon exposure to K1 killer toxin; involved in ion homeostasis	17.1%	-2.5	3E-05	0	0	6	0
YNL238W	KEX2	Subtilisin-like protease (proprotein convertase), a calcium-dependent serine protease involved in the activation of proproteins of the secretory pathway	17.3%	-2.5	2E-06	4	6	2 6	0
YDL045W -A	MRP10	Mitochondrial ribosomal protein of the small subunit	17.4%	-2.5	0.0005	0	0	0	4
YNL315C	ATP11	Molecular chaperone, required for the assembly of alpha and beta subunits into the F1 sector of mitochondrial F1F0 ATP synthase	17.4%	-2.5	0.0001	1 7	0	1 3	0
YER074 W	RPS24A	Protein component of the small (40S) ribosomal subunit; identical to Rps24Bp and has similarity to rat S24 ribosomal protein	17.6%	-2.5	5E-05	0	0	0	0
YAL024C	LTE1	Putative GDP/GTP exchange factor required for mitotic exit at low temperatures; acts as a guanine nucleotide exchange factor (GEF) for Tem1p, which is a key regulator of mitotic exit; physically associates with Ras2p-GTP	17.6%	-2.5	0.0002	1 2	0	1 8	0
YDR354 W	TRP4	Anthranilate phosphoribosyl transferase of the tryptophan biosynthetic pathway, catalyzes the phosphoribosylation of anthranilate, subject to the general control system of amino acid biosynthesis	17.7%	-2.5	0.0002	0	0	0	0
YMR219 W	ESC1	Protein localized to the nuclear periphery, involved in telomeric silencing; interacts with PAD4-domain of Sir4p	17.8%	-2.5	3E-05	0	0	0	0
YMR230 W	RPS10B	Protein component of the small (40S) ribosomal subunit; nearly identical to Rps10Ap and has similarity to rat ribosomal protein S10	17.9%	-2.5	0.0002	0	0	4	0
YER155C	BEM2	Rho GTPase activating protein (RhoGAP) involved in the control of cytoskeleton organization and cellular morphogenesis; required for bud emergence	18.0%	-2.5	8E-05	8	0	0	0
YML103C	NUP188	Subunit of the nuclear pore complex (NPC), involved in the structural organization of the complex and of the nuclear envelope, also involved in nuclear envelope permeability, interacts with Pom152p and Nic96p	18.0%	-2.5	1E-06	5	0	2 2	0
YOR039 W	CKB2	Beta' regulatory subunit of casein kinase 2, a Ser/Thr protein kinase with roles in cell growth and proliferation; the holoenzyme also contains CKA1, CKA2 and CKB1, the many substrates include transcription factors and all RNA polymerases	18.0%	-2.5	0.0012	1 5	0	1 2	5
YML062C	MFT1	Subunit of the THO complex, which is a nuclear complex comprised of Hpr1p, Mft1p, Rlr1p, and Thp2p, that is involved in transcription elongation and mitotic recombination; involved in telomere maintenance	18.1%	-2.5	1E-05	0	0	1 1	0
YLL014W	EMC6	Member of a transmembrane complex required for efficient folding of proteins in the ER; null mutant displays induction of the unfolded protein response	18.2%	-2.5	0.0003	0	0	0	0

Appendix A

ORF	Gene	Description	PRG	LF C	p-val	M M S	T B P	4 N Q O	U V
YOR275C	RIM20	Protein involved in proteolytic activation of Rim101p in response to alkaline pH; PalA/AIP1/Alix family member; interaction with the ESCRT-III subunit Snf7p suggests a relationship between pH response and multivesicular body formation	18.2%	-2.5	6E-06	1 5	2	0	0
YNL288W	CAF40	Evolutionarily conserved subunit of the CCR4-NOT complex involved in controlling mRNA initiation, elongation and degradation; binds Cdc39p	18.3%	-2.5	2E-05	7	2	0	0
YDR323C	PEP7	Multivalent adaptor protein that facilitates vesicle-mediated vacuolar protein sorting by ensuring high-fidelity vesicle docking and fusion, which are essential for targeting of vesicles to the endosome; required for vacuole inheritance	18.3%	-2.5	0.0006	1 0	2	2 6	4
YPL059W	GRX5	Hydroperoxide and superoxide-radical responsive glutathione-dependent oxidoreductase; mitochondrial matrix protein involved in the synthesis/assembly of iron-sulfur centers; monothiol glutaredoxin subfamily member along with Grx3p and Grx4p	18.4%	-2.4	0.004	5	7	0	0
YMR216C	SKY1	SR protein kinase (SRPK) involved in regulating proteins involved in mRNA metabolism and cation homeostasis; similar to human SRPK1	18.4%	-2.4	7E-05	7	0	2 3	0
YBR224W	N/A	Dubious open reading frame unlikely to encode a protein, based on available experimental and comparative sequence data; partially overlaps the verified gene TDP1	18.5%	-2.4	2E-05	0	0	0	0
YPL090C	RPS6A	Protein component of the small (40S) ribosomal subunit; identical to Rps6Bp and has similarity to rat S6 ribosomal protein	18.5%	-2.4	7E-06	0	0	2	0
YDL057W	N/A	Putative protein of unknown function; YDL057W is not an essential gene	18.6%	-2.4	0.0001	0	0	0	0
YLR403W	SFP1	Transcription factor that controls expression of ribosome biogenesis genes in response to nutrients and stress, regulates G2/M transitions during mitotic cell cycle and DNA-damage response, modulates cell size; regulated by TORC1 and Mrs6p	18.6%	-2.4	0.0001	1 5	0	0	1 3
YBR106W	PHO88	Probable membrane protein, involved in phosphate transport; pho88 pho86 double null mutant exhibits enhanced synthesis of repressible acid phosphatase at high inorganic phosphate concentrations	18.7%	-2.4	0.0004	0	0	0	0
YDR127W	ARO1	Pentafunctional arom protein, catalyzes steps 2 through 6 in the biosynthesis of chorismate, which is a precursor to aromatic amino acids	18.8%	-2.4	0.0004	0	0	0	0
YGL025C	PGD1	Subunit of the RNA polymerase II mediator complex; associates with core polymerase subunits to form the RNA polymerase II holoenzyme; essential for basal and activated transcription; direct target of Cyc8p-Tup1p transcriptional corepressor	18.8%	-2.4	0.0001	0	2	3 0	0

Appendix A

ORF	Gene	Description	PRG	LF C	p-val	M M S	T B P	4 N Q O	U V
YHR067 W	HTD2	Mitochondrial 3-hydroxyacyl-thioester dehydratase involved in fatty acid biosynthesis, required for respiratory growth and for normal mitochondrial morphology	18.9%	-2.4	0.0002	4	0	0	1 1
YLR218C	N/A	Putative protein of unknown function; green fluorescent protein (GFP)-fusion protein localizes to the cytoplasm; YLR218C is not essential; mutants exhibit glycogen storage defects and growth defects on a non-fermentable carbon source	18.9%	-2.4	1E-07	2	0	0	0
YGL253W	HXK2	Hexokinase isoenzyme 2 that catalyzes phosphorylation of glucose in the cytosol; predominant hexokinase during growth on glucose; functions in the nucleus to repress expression of HXK1 and GLK1 and to induce expression of its own gene	18.9%	-2.4	8E-05	0	0	7	0
YDR069C	DOA4	Ubiquitin isopeptidase, required for recycling ubiquitin from proteasome-bound ubiquitinated intermediates, acts at the late endosome/prevacuolar compartment to recover ubiquitin from ubiquitinated membrane proteins en route to the vacuole	18.9%	-2.4	1E-06	1 3	0	0	0
YDL069C	CBS1	Mitochondrial translational activator of the COB mRNA; membrane protein that interacts with translating ribosomes, acts on the COB mRNA 5'-untranslated leader	19.0%	-2.4	6E-05	0	0	0	0
YIL119C	RPI1	Putative transcriptional regulator; overexpression suppresses the heat shock sensitivity of wild-type RAS2 overexpression and also suppresses the cell lysis defect of an mpk1 mutation	19.0%	-2.4	2E-06	0	0	0	0
YHL027W	RIM101	Transcriptional repressor involved in response to pH and in cell wall construction; required for alkaline pH-stimulated haploid invasive growth and sporulation; activated by proteolytic processing; similar to <i>A. nidulans</i> PacC	19.1%	-2.4	1E-06	1 1	3	0	7
YDR418 W	RPL12B	Protein component of the large (60S) ribosomal subunit, nearly identical to Rpl12Ap; rpl12a rpl12b double mutant exhibits slow growth and slow translation; has similarity to <i>E. coli</i> L11 and rat L12 ribosomal proteins	19.2%	-2.4	4E-06	5	2	0	4
YML129C	COX14	Mitochondrial membrane protein, involved in translational regulation of Cox1p and assembly of cytochrome c oxidase (complex IV); associates with complex IV assembly intermediates and complex III/complex IV supercomplexes	19.2%	-2.4	4E-05	0	0	0	0
YPL165C	SET6	SET domain protein of unknown function; deletion heterozygote is sensitive to compounds that target ergosterol biosynthesis, may be involved in compound availability	19.3%	-2.4	1E-05	7	0	0	0
YPL179W	PPQ1	Putative protein serine/threonine phosphatase; null mutation enhances efficiency of translational suppressors	19.3%	-2.4	4E-05	0	0	0	0

Appendix A

ORF	Gene	Description	PRG	LF C	p-val	M M S	T B P	4 N Q O	U V
YOL068C	HST1	NAD(+)-dependent histone deacetylase; essential subunit of the Sum1p/Rfm1p/Hst1p complex required for ORC-dependent silencing and mitotic repression; non-essential subunit of the Set3C deacetylase complex; involved in telomere maintenance	19.3%	-2.4	4E-05	7	0	0	0
YNL302C	RPS19B	Protein component of the small (40S) ribosomal subunit, required for assembly and maturation of pre-40 S particles; mutations in human RPS19 are associated with Diamond Blackfan anemia; nearly identical to Rps19Ap	19.4%	-2.4	0.0003	0	0	7	0
YGR105 W	VMA21	Integral membrane protein that is required for vacuolar H ⁺ -ATPase (V-ATPase) function, although not an actual component of the V-ATPase complex; functions in the assembly of the V-ATPase; localized to the yeast endoplasmic reticulum (ER)	19.4%	-2.4	8E-06	1 1	0	2 2	2 2
YGR219 W	N/A	Dubious open reading frame unlikely to encode a protein, based on available experimental and comparative sequence data; partially overlaps the verified ORF MRPL9/YGR220C	19.5%	-2.4	4E-05	0	0	0	0
YJL164C	TPK1	cAMP-dependent protein kinase catalytic subunit; promotes vegetative growth in response to nutrients via the Ras-cAMP signaling pathway; inhibited by regulatory subunit Bcy1p in the absence of cAMP; partially redundant with Tpk2p and Tpk3p	19.5%	-2.4	0.0013	0	0	0	0
YDR405 W	MRP20	Mitochondrial ribosomal protein of the large subunit	19.5%	-2.4	0.0006	1 4	0	0	8
YLL044W	N/A	Dubious open reading frame unlikely to encode a protein, based on available experimental and comparative sequence data; transcription of both YLL044W and the overlapping gene RPL8B is reduced in the gcr1 null mutant	19.5%	-2.4	7E-05	0	0	0	0
YLL027W	ISA1	Mitochondrial matrix protein involved in biogenesis of the iron-sulfur (Fe/S) cluster of Fe/S proteins, isa1 deletion causes loss of mitochondrial DNA and respiratory deficiency; depletion reduces growth on nonfermentable carbon sources	19.5%	-2.4	0.0001	0	0	0	0
YML014 W	TRM9	tRNA methyltransferase, catalyzes esterification of modified uridine nucleotides in tRNA(Arg3) and tRNA(Glu), likely as part of a complex with Trm112p; deletion confers resistance to zymocin	19.6%	-2.3	7E-06	1 1	0	0	0
YMR008C	PLB1	Phospholipase B (lysophospholipase) involved in lipid metabolism, required for deacylation of phosphatidylcholine and phosphatidylethanolamine but not phosphatidylinositol	19.7%	-2.3	0.0004	0	0	4	0
YDR110 W	FOB1	Nucleolar protein that binds the rDNA replication fork barrier (RFB) site; required for replication fork blocking, recombinational hotspot activity, condensin recruitment to RFB and rDNA repeat segregation; related to retroviral integrases	19.7%	-2.3	3E-07	0	0	0	0

Appendix A

ORF	Gene	Description	PRG	LF C	p-val	M M S	T B P	4 N Q O	U V
YDR122 W	KIN1	Serine/threonine protein kinase involved in regulation of exocytosis; localizes to the cytoplasmic face of the plasma membrane; closely related to Kin2p	19.9%	-2.3	1E-05	0	0	0	0
YDL167C	NRP1	Putative RNA binding protein of unknown function; localizes to stress granules induced by glucose deprivation; predicted to be involved in ribosome biogenesis	19.9%	-2.3	4E-06	0	0	1 2	3
YDL115C	IWR1	Protein of unknown function, deletion causes hypersensitivity to the K1 killer toxin	19.9%	-2.3	0.0004	1 5	0	0	9
YMR193C -A	N/A	Dubious open reading frame unlikely to encode a functional protein, based on available experimental and comparative sequence data	19.9%	-2.3	6E-05	0	2	1 2	0
YPR191 W	QCR2	Subunit 2 of the ubiquinol cytochrome-c reductase complex, which is a component of the mitochondrial inner membrane electron transport chain; phosphorylated; transcription is regulated by Hap1p, Hap2p/Hap3p, and heme	20.0%	-2.3	6E-06	0	0	0	0
YFR040W	SAP155	Protein that forms a complex with the Sit4p protein phosphatase and is required for its function; member of a family of similar proteins including Sap4p, Sap185p, and Sap190p	20.0%	-2.3	7E-06	0	0	1 0	0
YLR111W	N/A	Dubious open reading frame unlikely to encode a protein, based on available experimental and comparative sequence data	20.1%	-2.3	0.0003	0	0	0	0
YPR101 W	SNT309	Component of NineTeen complex (NTC) containing Prp19p involved in mRNA splicing, interacts physically and genetically with Prp19p	20.2%	-2.3	0.0001	2	0	0	4
YGL127C	SOH1	Subunit of the RNA polymerase II mediator complex; associates with core polymerase subunits to form the RNA polymerase II holoenzyme; involved in telomere maintenance; conserved with other metazoan MED31 subunits	20.4%	-2.3	4E-05	7	0	7	0
YKL194C	MST1	Mitochondrial threonyl-tRNA synthetase	20.5%	-2.3	8E-05	0	0	1 6	0
YJR077C	MIR1	Mitochondrial phosphate carrier, imports inorganic phosphate into mitochondria; functionally redundant with Pic2p but more abundant than Pic2p under normal conditions; phosphorylated	20.6%	-2.3	3E-05	0	0	0	9
YLR366W	N/A	Dubious open reading frame unlikely to encode a protein, based on available experimental and comparative sequence data; partially overlaps the dubious ORF YLR364C-A	20.8%	-2.3	0.0003	0	0	0	0
YBL079W	NUP170	Abundant subunit of the nuclear pore complex (NPC), required for proper localization of specific nucleoporins within the NPC, involved in nuclear envelope permeability and in chromosome segregation, has similarity to Nup157p	20.9%	-2.3	2E-05	0	0	0	0

Appendix A

ORF	Gene	Description	PRG	LF C	p-val	M M S	T B P	4 N Q O	U V
YGL066W	SGF73	Subunit of SAGA histone acetyltransferase complex; involved in formation of the preinitiation complex assembly at promoters; null mutant displays defects in premeiotic DNA synthesis	21.0%	-2.3	0.0001	5	0	1 3	0
YCL038C	ATG22	Vacuolar integral membrane protein required for efflux of amino acids during autophagic body breakdown in the vacuole; null mutation causes a gradual loss of viability during starvation	21.0%	-2.3	9E-06	0	0	0	0
YLR065C	N/A	Putative protein of unknown function; YLR065C is not an essential gene	21.1%	-2.2	3E-06	0	0	0	0
YLR402W	N/A	Dubious open reading frame unlikely to encode a protein, based on available experimental and comparative sequence data	21.1%	-2.2	3E-05	1 2	0	0	0
YOR001 W	RRP6	Nuclear exosome exonuclease component; has 3'-5' exonuclease activity; involved in RNA processing, maturation, surveillance, degradation, tethering, and export; has similarity to E. coli RNase D and to human PM-Sc1 100 (EXOSC10)	21.1%	-2.2	5E-05	7	0	0	1 3
YDR144C	MKC7	GPI-anchored aspartyl protease (yapsin) involved in protein processing; shares functions with Yap3p and Kex2p	21.3%	-2.2	0.0002	1 0	0	0	0
YMR064 W	AEP1	Protein required for expression of the mitochondrial OLI1 gene encoding subunit 9 of F1-F0 ATP synthase	21.4%	-2.2	7E-05	0	0	0	0
YOR083 W	WHI5	Repressor of G1 transcription that binds to SCB binding factor (SBF) at SCB target promoters in early G1; phosphorylation of Whi5p by the CDK, Cln3p/Cdc28p relieves repression and promoter binding by Whi5; periodically expressed in G1	21.5%	-2.2	0.0003	8	0	0	7
YPL172C	COX10	Heme A:farnesyltransferase, catalyzes the first step in the conversion of protoheme to the heme A prosthetic group required for cytochrome c oxidase activity; human ortholog is associated with mitochondrial disorders	21.6%	-2.2	0.0001	4	0	0	8
YOL081W	IRA2	GTPase-activating protein that negatively regulates RAS by converting it from the GTP- to the GDP-bound inactive form, required for reducing cAMP levels under nutrient limiting conditions, has similarity to Ira1p and human neurofibromin	21.6%	-2.2	0.0002	1 5	5	2 2	0
YOL055C	THI20	Multifunctional protein with both hydroxymethylpyrimidine kinase and thiaminase activities; involved in thiamine biosynthesis and also in thiamine degradation; member of a gene family with THI21 and THI22; functionally redundant with Thi21p	21.7%	-2.2	7E-05	4	0	0	0
YLR052W	IES3	Subunit of the INO80 chromatin remodeling complex	21.7%	-2.2	0.0002	0	0	9	0
YEL036C	ANP1	Subunit of the alpha-1,6 mannosyltransferase complex; type II membrane protein; has a role in retention of glycosyltransferases in the Golgi; involved in osmotic sensitivity and resistance to aminonitrophenyl propanediol	21.7%	-2.2	0.0003	0	0	0	0

Appendix A

ORF	Gene	Description	PRG	LF C	p-val	M M S	T B P	4 N Q O	U V
YNR045 W	PET494	Mitochondrial translational activator specific for the COX3 mRNA, acts together with Pet54p and Pet122p; located in the mitochondrial inner membrane	21.7%	-2.2	1E-04	0	0	0	0
YPL206C	PGC1	Phosphatidyl Glycerol phospholipase C; regulates the phosphatidylglycerol (PG) content via a phospholipase C-type degradation mechanism; contains glycerophosphodiester phosphodiesterase motifs	21.8%	-2.2	9E-05	5	0	0	0
YBR189 W	RPS9B	Protein component of the small (40S) ribosomal subunit; nearly identical to Rps9Ap and has similarity to E. coli S4 and rat S9 ribosomal proteins	21.8%	-2.2	9E-06	0	0	0	0
YOR349 W	CIN1	Tubulin folding factor D involved in beta-tubulin (Tub2p) folding; isolated as mutant with increased chromosome loss and sensitivity to benomyl	21.9%	-2.2	0.0033	0	0	4	0
YER141 W	COX15	Protein required for the hydroxylation of heme O to form heme A, which is an essential prosthetic group for cytochrome c oxidase	22.0%	-2.2	2E-05	0	0	0	0
YDR450 W	RPS18A	Protein component of the small (40S) ribosomal subunit; nearly identical to Rps18Bp and has similarity to E. coli S13 and rat S18 ribosomal proteins	22.0%	-2.2	1E-05	0	0	0	0
YLR326W	N/A	Putative protein of unknown function, predicted to be palmitoylated	22.1%	-2.2	0.001	0	0	0	0
YER027C	GAL83	One of three possible beta-subunits of the Snf1 kinase complex, allows nuclear localization of the Snf1 kinase complex in the presence of a nonfermentable carbon source; contains glycogen-binding domain	22.1%	-2.2	0.0002	0	0	0	0
YLR068W	FYV7	Essential protein required for maturation of 18S rRNA; required for survival upon exposure to K1 killer toxin	22.1%	-2.2	0.0006	0	0	0	0
YCR081 W	SRB8	Subunit of the RNA polymerase II mediator complex; associates with core polymerase subunits to form the RNA polymerase II holoenzyme; essential for transcriptional regulation; involved in glucose repression	22.3%	-2.2	7E-05	0	0	3 0	0
YPL119C	DBP1	Putative ATP-dependent RNA helicase of the DEAD-box protein family; mutants show reduced stability of the 40S ribosomal subunit scanning through 5' untranslated regions of mRNAs	22.4%	-2.2	2E-05	0	0	0	0
YNL198C	N/A	Dubious open reading frame unlikely to encode a protein, based on available experimental and comparative sequence data	22.4%	-2.2	9E-05	4	0	2 2	0
YER050C	RSM18	Mitochondrial ribosomal protein of the small subunit, has similarity to E. coli S18 ribosomal protein	22.4%	-2.2	8E-07	0	0	0	0
YGR244C	LSC2	Beta subunit of succinyl-CoA ligase, which is a mitochondrial enzyme of the TCA cycle that catalyzes the nucleotide-dependent conversion of succinyl-CoA to succinate	22.5%	-2.2	0.0001	0	0	0	0

Appendix A

ORF	Gene	Description	PRG	LF C	p-val	M M S	T B P	4 N Q O	U V
YJL129C	TRK1	Component of the Trk1p-Trk2p potassium transport system; 180 kDa high affinity potassium transporter; phosphorylated in vivo and interacts physically with the phosphatase Ppz1p, suggesting Trk1p activity is regulated by phosphorylation	22.5%	-2.2	6E-05	0	0	0	0
YIL008W	URM1	Ubiquitin-like protein with weak sequence similarity to ubiquitin; depends on the E1-like activating enzyme Uba4p; molecular function of the Urm1p pathway is unknown, but it is required for normal growth, particularly at high temperature	22.6%	-2.1	5E-06	0	0	0	0
YML048 W	GSF2	ER localized integral membrane protein that may promote secretion of certain hexose transporters, including Gal2p; involved in glucose-dependent repression	22.7%	-2.1	0.0005	0	0	0	0
YER070 W	RNR1	One of two large regulatory subunits of ribonucleotide-diphosphate reductase; the RNR complex catalyzes rate-limiting step in dNTP synthesis, regulated by DNA replication and DNA damage checkpoint pathways via localization of small subunits	22.8%	-2.1	0.0039	5	0	0	5
YML008C	ERG6	Delta(24)-sterol C-methyltransferase, converts zymosterol to fecosterol in the ergosterol biosynthetic pathway by methylating position C-24; localized to both lipid particles and mitochondrial outer membrane	22.9%	-2.1	0.0016	9	3	2 3	4
YOL014W	N/A	Putative protein of unknown function	23.0%	-2.1	0.0004	0	0	0	0
YLR322W	VPS65	Dubious open reading frame, unlikely to encode a protein; not conserved in closely related Saccharomyces species; 75% of ORF overlaps the verified gene SFH1; deletion causes a vacuolar protein sorting defect and blocks anaerobic growth	23.1%	-2.1	7E-05	1 8	0	3 0	1 7
YPL155C	KIP2	Kinesin-related motor protein involved in mitotic spindle positioning, stabilizes microtubules by targeting Bik1p to the plus end; Kip2p levels are controlled during the cell cycle	23.1%	-2.1	0.0015	0	0	0	0
YBR111C	YSA1	Nudix hydrolase family member with ADP-ribose pyrophosphatase activity; shown to metabolize O-acetyl-ADP-ribose to AMP and acetylated ribose 5'-phosphate	23.2%	-2.1	0.0002	5	0	9	1 4
YNL225C	CNM67	Component of the spindle pole body outer plaque; required for spindle orientation and mitotic nuclear migration	23.2%	-2.1	0.0003	0	0	0	0
YOR351C	MEK1	Meiosis-specific serine/threonine protein kinase, functions in meiotic checkpoint, promotes recombination between homologous chromosomes by suppressing double strand break repair between sister chromatids	23.2%	-2.1	0.0051	0	0	0	0
YCR063 W	BUD31	Component of the SF3b subcomplex of the U2 snRNP; diploid mutants display a random budding pattern instead of the wild-type bipolar pattern	23.2%	-2.1	2E-05	0	0	0	0

Appendix A

ORF	Gene	Description	PRG	LF C	p-val	M M S	T B P	4 N Q O	U V
YGL129C	RSM23	Mitochondrial ribosomal protein of the small subunit, has similarity to mammalian apoptosis mediator proteins; null mutation prevents induction of apoptosis by overproduction of metacaspase Mca1p	23.3%	-2.1	0.0001	0	0	0	0
YNL055C	POR1	Mitochondrial porin (voltage-dependent anion channel), outer membrane protein required for the maintenance of mitochondrial osmotic stability and mitochondrial membrane permeability; phosphorylated	23.3%	-2.1	4E-05	1 0	0	3	4
YDR076 W	RAD55	Protein that stimulates strand exchange by stabilizing the binding of Rad51p to single-stranded DNA; involved in the recombinational repair of double-strand breaks in DNA during vegetative growth and meiosis; forms heterodimer with Rad57p	23.3%	-2.1	7E-06	3 0	0	2 1	0
YOR085 W	OST3	Gamma subunit of the oligosaccharyltransferase complex of the ER lumen, which catalyzes asparagine-linked glycosylation of newly synthesized proteins; Ost3p is important for N-glycosylation of a subset of proteins	23.3%	-2.1	0.0039	0	0	0	0
YER095 W	RAD51	Strand exchange protein, forms a helical filament with DNA that searches for homology; involved in the recombinational repair of double-strand breaks in DNA during vegetative growth and meiosis; homolog of Dmc1p and bacterial RecA protein	23.4%	-2.1	4E-06	3 0	0	3 0	0
YKR020 W	VPS51	Component of the GARP (Golgi-associated retrograde protein) complex, Vps51p-Vps52p-Vps53p-Vps54p, which is required for the recycling of proteins from endosomes to the late Golgi; links the (VFT/GARP) complex to the SNARE Tlg1p	23.4%	-2.1	0.0001	6	0	1 6	0
YLR265C	NEJ1	Protein involved in regulation of nonhomologous end joining; interacts with DNA ligase IV components Dnl4p and Lif1p; repressed by MAT heterozygosity; regulates cellular distribution of Lif1p	23.4%	-2.1	0.0007	0	0	0	0
YJL204C	RCY1	F-box protein involved in recycling plasma membrane proteins internalized by endocytosis; localized to sites of polarized growth	23.5%	-2.1	0.0142	1 5	0	1 8	0
YMR143 W	RPS16A	Protein component of the small (40S) ribosomal subunit; identical to Rps16Bp and has similarity to E. coli S9 and rat S16 ribosomal proteins	23.5%	-2.1	1E-05	0	0	0	0
YJL133W	MRS3	Iron transporter that mediates Fe ²⁺ transport across the inner mitochondrial membrane; mitochondrial carrier family member, similar to and functionally redundant with Mrs4p; active under low-iron conditions; may transport other cations	23.6%	-2.1	0.0001	0	0	0	0

Appendix A

ORF	Gene	Description	PRG	LF C	p-val	M M S	T B P	4 N Q O	U V
YPL138C	SPP1	Subunit of COMPASS (Set1C), a complex which methylates histone H3 on lysine 4 and is required in telomeric transcriptional silencing; interacts with Orc2p; PHD finger domain protein similar to human CGBP, an unmethylated CpG binding protein	23.7%	-2.1	0.0035	7	0	0	0
YLR018C	POM34	Integral membrane protein of the nuclear pore; has an important role in maintaining the architecture of the pore complex	23.7%	-2.1	4E-05	0	0	0	0
YDR348C	N/A	Protein of unknown function; green fluorescent protein (GFP)-fusion protein localizes to the cell periphery and bud neck; potential Cdc28p substrate	23.8%	-2.1	1E-05	9	2	0	7
YNL294C	RIM21	Component of the RIM101 pathway, has a role in cell wall construction and alkaline pH response; has similarity to <i>A. nidulans</i> PalH	24.0%	-2.1	0.0009	1 1	3	0	0
YBR214 W	SDS24	One of two <i>S. cerevisiae</i> homologs (Sds23p and Sds24p) of the <i>S. pombe</i> Sds23 protein, which is implicated in APC/cyclosome regulation; involved in cell separation during budding; may play an indirect role in fluid-phase endocytosis	24.0%	-2.1	2E-05	0	0	0	0
YKR085C	MRPL20	Mitochondrial ribosomal protein of the large subunit	24.1%	-2.1	0.0006	0	0	0	0
YMR123 W	PKR1	V-ATPase assembly factor, functions with other V-ATPase assembly factors in the ER to efficiently assemble the V-ATPase membrane sector (V0)	24.1%	-2.1	6E-06	0	0	3 0	0
YDL083C	RPS16B	Protein component of the small (40S) ribosomal subunit; identical to Rps16Ap and has similarity to <i>E. coli</i> S9 and rat S16 ribosomal proteins	24.2%	-2.0	5E-05	0	0	0	0
YJR004C	SAG1	Alpha-agglutinin of alpha-cells, binds to Aga1p during agglutination, N-terminal half is homologous to the immunoglobulin superfamily and contains binding site for alpha-agglutinin, C-terminal half is highly glycosylated and contains GPI anchor	24.2%	-2.0	0.0001	0	0	0	0
YOL003C	PFA4	Palmitoyltransferase with autoacylation activity, required for palmitoylation of amino acid permeases containing a C-terminal Phe-Trp-Cys site; required for modification of Chs3p; member of the DHHC family of putative palmitoyltransferases	24.3%	-2.0	0.0002	0	0	0	0
YMR214 W	SCJ1	One of several homologs of bacterial chaperone DnaJ, located in the ER lumen where it cooperates with Kar2p to mediate maturation of proteins	24.3%	-2.0	9E-06	0	3	0	0
YGL072C	N/A	Dubious open reading frame unlikely to encode a protein; partially overlaps the verified gene HSF1; null mutant displays increased resistance to antifungal agents gliotoxin, cycloheximide and H2O2	24.4%	-2.0	0.0003	0	0	1 5	0
YPR159 W	KRE6	Protein required for beta-1,6 glucan biosynthesis; putative beta-glucan synthase; appears functionally redundant with Skn1p	24.4%	-2.0	7E-05	4	0	5	0

Appendix A

ORF	Gene	Description	PRG	LF C	p-val	M M S	T B P	4 N Q O	U V
YDL061C	RPS29B	Protein component of the small (40S) ribosomal subunit; nearly identical to Rps29Ap and has similarity to rat S29 and E. coli S14 ribosomal proteins	24.4%	-2.0	2E-05	0	0	6	0
YKL009W	MRT4	Protein involved in mRNA turnover and ribosome assembly, localizes to the nucleolus	24.7%	-2.0	0.0002	0	2	9	4
YOR187 W	TUF1	Mitochondrial translation elongation factor Tu; comprises both GTPase and guanine nucleotide exchange factor activities, while these activities are found in separate proteins in S. pombe and humans	24.7%	-2.0	2E-05	0	0	0	0
YDR078C	SHU2	Protein involved in a Rad51p-, Rad54p-dependent pathway for homologous recombination repair, important for error-free repair of spontaneous and induced DNA lesions to protect the genome from mutation; associates with Shu1p, Psy3p, and Csm2p	24.7%	-2.0	4E-06	1 8	0	0	0
YGL080W	FMP37	Putative protein of unknown function; highly conserved across species and orthologous to human gene BRP44L; the authentic, non-tagged protein is detected in highly purified mitochondria in high-throughput studies	24.8%	-2.0	7E-05	0	0	0	0
YAL016W	TPD3	Regulatory subunit A of the heterotrimeric protein phosphatase 2A, which also contains regulatory subunit Cdc55p and either catalytic subunit Pph21p or Pph22p; required for cell morphogenesis and for transcription by RNA polymerase III	24.8%	-2.0	0.0006	1 0	0	2 4	6
YPL154C	PEP4	Vacuolar aspartyl protease (proteinase A), required for the posttranslational precursor maturation of vacuolar proteinases; important for protein turnover after oxidative damage; synthesized as a zymogen, self-activates	24.9%	-2.0	0.0013	4	0	0	0
YMR312 W	ELP6	Subunit of Elongator complex, which is required for modification of wobble nucleosides in tRNA; required for Elongator structural integrity	24.9%	-2.0	0.0001	2	2	0	0
YOR354C	MSC6	Protein of unknown function; mutant is defective in directing meiotic recombination events to homologous chromatids; the authentic, non-tagged protein is detected in highly purified mitochondria in high-throughput studies	25.0%	-2.0	0.0001	0	0	0	0
YML086C	ALO1	D-Arabinono-1,4-lactone oxidase, catalyzes the final step in biosynthesis of dehydro-D-arabinono-1,4-lactone, which is protective against oxidative stress	25.2%	-2.0	0.0001	0	0	0	0
YAL058C- A	0	Dubious open reading frame unlikely to encode a protein, based on available experimental and comparative sequence data	25.2%	-2.0	7E-05	4	2	0	0
YOL012C	HTZ1	Histone variant H2AZ, exchanged for histone H2A in nucleosomes by the SWR1 complex; involved in transcriptional regulation through prevention of the spread of silent heterochromatin	25.3%	-2.0	0.0031	1 9	0	1 3	0
YOL083W	N/A	Putative protein of unknown function	25.3%	-2.0	0.0021	4	0	0	0

Appendix A

ORF	Gene	Description	PRG	LF C	p-val	M M S	T B P	4 N Q O	U V
YBR181C	RPS6B	Protein component of the small (40S) ribosomal subunit; identical to Rps6Ap and has similarity to rat S6 ribosomal protein	25.5%	-2.0	6E-05	0	0	0	0
YEL059W	N/A	Dubious open reading frame unlikely to encode a functional protein	25.6%	-2.0	4E-06	2 2	0	1 2	0
YIL029C	N/A	Putative protein of unknown function; deletion confers sensitivity to 4-(N-(S-gluthionylacetyl)amino) phenylarsenoxide (GSAO)	25.6%	-2.0	0.0001	6	2	0	0
YOR142 W	LSC1	Alpha subunit of succinyl-CoA ligase, which is a mitochondrial enzyme of the TCA cycle that catalyzes the nucleotide-dependent conversion of succinyl-CoA to succinate; phosphorylated	25.7%	-2.0	0.0002	0	0	0	0
YKR027 W	BCH2	Member of the ChAPs family of proteins (Chs5p-Arf1p-binding proteins: Bch1p, Bch2p, Bud7p, Chs6p), that forms the exomer complex with Chs5p to mediate export of specific cargo proteins, including Chs3p, from the Golgi to the plasma membrane	25.8%	-2.0	8E-05	0	7	1 9	0
YML081C -A	ATP18	Subunit of the mitochondrial F1F0 ATP synthase, which is a large enzyme complex required for ATP synthesis; termed subunit I or subunit j; does not correspond to known ATP synthase subunits in other organisms	25.9%	-2.0	7E-05	2	0	0	1 0
YOL063C	CRT10	Protein involved in transcriptional regulation of RNR2 and RNR3; expression of the gene is induced by DNA damage and null mutations confer increased resistance to hydroxyurea; N-terminal region has a leucine repeat and a WD40 repeat	25.9%	-1.9	0.0007	4	0	0	0
YER111C	SWI4	DNA binding component of the SBF complex (Swi4p-Swi6p), a transcriptional activator that in concert with MBF (Mbp1-Swi6p) regulates late G1-specific transcription of targets including cyclins and genes required for DNA synthesis and repair	26.2%	-1.9	0.004	5	0	9	0
YBR218C	PYC2	Pyruvate carboxylase isoform, cytoplasmic enzyme that converts pyruvate to oxaloacetate; highly similar to isoform Pyc1p but differentially regulated; mutations in the human homolog are associated with lactic acidosis	26.2%	-1.9	0.0004	0	0	0	0
YOR330C	MIP1	Catalytic subunit of the mitochondrial DNA polymerase; conserved C-terminal segment is required for the maintenance of mitochondrial genome.	26.2%	-1.9	0.0092	0	0	0	7
YBR263 W	SHM1	Mitochondrial serine hydroxymethyltransferase, converts serine to glycine plus 5,10 methylenetetrahydrofolate; involved in generating precursors for purine, pyrimidine, amino acid, and lipid biosynthesis; reverse reaction generates serine	26.3%	-1.9	0.0002	0	0	0	0

Appendix A

ORF	Gene	Description	PRG	LF C	p-val	M M S	T B P	4 N Q O	U V
YDR101C	ARX1	Shuttling pre-60S factor; involved in the biogenesis of ribosomal large subunit biogenesis; interacts directly with Alb1; responsible for Tif6 recycling defects in absence of Rei1; associated with the ribosomal export complex	26.4%	-1.9	5E-06	0	2	0	0
YBR048 W	RPS11B	Protein component of the small (40S) ribosomal subunit; identical to Rps11Ap and has similarity to E. coli S17 and rat S11 ribosomal proteins	26.4%	-1.9	1E-05	0	0	0	0
YPR043 W	RPL43A	Protein component of the large (60S) ribosomal subunit, identical to Rpl43Bp and has similarity to rat L37a ribosomal protein; null mutation confers a dominant lethal phenotype	26.5%	-1.9	4E-05	0	2	0	0
YOL052C	SPE2	S-adenosylmethionine decarboxylase, required for the biosynthesis of spermidine and spermine; cells lacking Spe2p require spermine or spermidine for growth in the presence of oxygen but not when grown anaerobically	26.5%	-1.9	0.0007	5	0	0	0
YOR368 W	RAD17	Checkpoint protein, involved in the activation of the DNA damage and meiotic pachytene checkpoints; with Mec3p and Ddc1p, forms a clamp that is loaded onto partial duplex DNA; homolog of human and S. pombe Rad1 and U. maydis Rec1 proteins	26.5%	-1.9	0.0022	2 2	0	2 9	1 8
YBR183 W	YPC1	Alkaline ceramidase that also has reverse (CoA-independent) ceramide synthase activity, catalyzes both breakdown and synthesis of phytoceramide; overexpression confers fumonisin B1 resistance	26.6%	-1.9	0.0032	0	0	0	0
YDR148C	KGD2	Dihydrolipoyl transsuccinylase, component of the mitochondrial alpha-ketoglutarate dehydrogenase complex, which catalyzes the oxidative decarboxylation of alpha-ketoglutarate to succinyl-CoA in the TCA cycle; phosphorylated	26.6%	-1.9	0.0007	0	0	0	0
YPL270W	MDL2	Mitochondrial inner membrane half-type ATP-binding cassette (ABC) transporter	26.6%	-1.9	0.0017	4	0	0	0
YJL023C	PET130	Protein required for respiratory growth; the authentic, non-tagged protein is detected in highly purified mitochondria in high-throughput studies	26.7%	-1.9	0.0003	0	0	0	0
YML017 W	PSP2	Asn rich cytoplasmic protein that contains RGG motifs; high-copy suppressor of group II intron-splicing defects of a mutation in MRS2 and of a conditional mutation in POL1 (DNA polymerase alpha); possible role in mitochondrial mRNA splicing	26.9%	-1.9	5E-06	0	0	0	0
YLR349W	N/A	Dubious open reading frame unlikely to encode a protein, based on available experimental and comparative sequence data; overlaps the verified ORF DIC1/YLR348C	27.3%	-1.9	0.0133	0	0	0	0

Appendix A

ORF	Gene	Description	PRG	LF C	p-val	M M S	T B P	4 N Q O	U V
YBR082C	UBC4	Ubiquitin-conjugating enzyme (E2), mediates degradation of short-lived and abnormal proteins; interacts with E3-CaM in ubiquitinating calmodulin; interacts with many SCF ubiquitin protein ligases; component of the cellular stress response	27.4%	-1.9	0.0015	0	0	9	0
YGL013C	PDR1	Zinc cluster protein that is a master regulator involved in recruiting other zinc cluster proteins to pleiotropic drug response elements (PDREs) to fine tune the regulation of multidrug resistance genes	27.5%	-1.9	0.0038	0	0	9	0
YER123 W	YCK3	Palmitoylated, vacuolar membrane-localized casein kinase I isoform; negatively regulates vacuole fusion during hypertonic stress via phosphorylation of Vps41p; shares essential functions with Hrr25p; regulates vesicle fusion in AP-3 pathway	27.6%	-1.9	2E-05	0	0	0	0
YLR085C	ARP6	Actin-related protein that binds nucleosomes; a component of the SWR1 complex, which exchanges histone variant H2AZ (Htz1p) for chromatin-bound histone H2A	27.6%	-1.9	0.0007	1 5	0	0	0
YPL182C	N/A	Dubious open reading frame unlikely to encode a protein, based on available experimental and comparative sequence data; partially overlaps the verified gene CTI6/YPL181W	27.7%	-1.9	0.0004	1 0	2	0	0
YCL008C	STP22	Component of the ESCRT-I complex, which is involved in ubiquitin-dependent sorting of proteins into the endosome; homologous to the mouse and human Tsg101 tumor susceptibility gene; mutants exhibit a Class E Vps phenotype	27.7%	-1.9	4E-06	2 2	7	0	0
YER055C	HIS1	ATP phosphoribosyltransferase, a hexameric enzyme, catalyzes the first step in histidine biosynthesis; mutations cause histidine auxotrophy and sensitivity to Cu, Co, and Ni salts; transcription is regulated by general amino acid control	27.8%	-1.8	7E-07	0	2	0	0
YNR020C	ATP23	Putative metalloprotease of the mitochondrial inner membrane, required for processing of Atp6p; has an additional role in assembly of the F0 sector of the F1F0 ATP synthase complex	27.8%	-1.8	0.0008	6	0	0	1 4
YGR229C	SMI1	Protein involved in the regulation of cell wall synthesis; proposed to be involved in coordinating cell cycle progression with cell wall integrity	27.8%	-1.8	4E-05	8	0	1 9	0
YKL006W	RPL14A	N-terminally acetylated protein component of the large (60S) ribosomal subunit, nearly identical to Rpl14Bp and has similarity to rat L14 ribosomal protein; rpl14a csh5 double null mutant exhibits synthetic slow growth	27.9%	-1.8	1E-05	4	0	2 2	0
YPR160 W	GPH1	Non-essential glycogen phosphorylase required for the mobilization of glycogen, activity is regulated by cyclic AMP-mediated phosphorylation, expression is regulated by stress-response elements and by the HOG MAP kinase pathway	27.9%	-1.8	3E-05	2 3	0	0	0

Appendix A

ORF	Gene	Description	PRG	LF C	p-val	M M S	T B P	4 N Q O	U V
YDR083 W	RRP8	Nucleolar protein involved in rRNA processing, pre-rRNA cleavage at site A2; also involved in telomere maintenance; mutation is synthetically lethal with a gar1 mutation	27.9%	-1.8	2E-05	0	0	0	0
YOL001W	PHO80	Cyclin, negatively regulates phosphate metabolism; Pho80p-Pho85p (cyclin-CDK complex) phosphorylates Pho4p and Swi5p; deletion of PHO80 leads to aminoglycoside supersensitivity; truncated form of PHO80 affects vacuole inheritance	28.0%	-1.8	9E-05	1 8	3	2 3	0
YNL133C	FYV6	Protein of unknown function, required for survival upon exposure to K1 killer toxin; proposed to regulate double-strand break repair via non-homologous end-joining	28.1%	-1.8	3E-06	3	0	1 0	0
YMR055C	BUB2	Mitotic exit network regulator, forms GTPase-activating Bfa1p-Bub2p complex that binds Tem1p and spindle pole bodies, blocks cell cycle progression before anaphase in response to spindle and kinetochore damage	28.1%	-1.8	1E-05	6	0	8	0
YGL231C	EMC4	Member of a transmembrane complex required for efficient folding of proteins in the ER; null mutant displays induction of the unfolded protein response; human ortholog TMEM85 may function in apoptosis	28.3%	-1.8	0.0014	0	0	1 2	0
YBR240C	THI2	Zinc finger protein of the Zn(II)2Cys6 type, probable transcriptional activator of thiamine biosynthetic genes	28.3%	-1.8	0.0002	5	0	0	0
YER151C	UBP3	Ubiquitin-specific protease that interacts with Bre5p to co-regulate anterograde and retrograde transport between endoplasmic reticulum and Golgi compartments; inhibitor of gene silencing; cleaves ubiquitin fusions but not polyubiquitin	28.4%	-1.8	1E-05	0	0	0	0
YLR110C	CCW12	Cell wall mannoprotein, mutants are defective in mating and agglutination, expression is downregulated by alpha-factor	28.5%	-1.8	4E-05	0	0	2	0
YML001 W	YPT7	GTPase; GTP-binding protein of the rab family; required for homotypic fusion event in vacuole inheritance, for endosome-endosome fusion, similar to mammalian Rab7	28.7%	-1.8	0.0002	4	3	0	0
YHR028C	DAP2	Dipeptidyl aminopeptidase, synthesized as a glycosylated precursor; localizes to the vacuolar membrane; similar to Ste13p	28.7%	-1.8	7E-05	0	0	0	0
YDR200C	VPS64	Cytoplasmic protein required for cytoplasm to vacuole targeting of proteins; forms a complex with Far3p, Far7p, Far10p, and Far11p that is involved in pheromone-induced cell cycle arrest; also localized to the endoplasmic reticulum membrane	28.8%	-1.8	0.006	0	0	7	0
YPR170C	N/A	Dubious open reading frame unlikely to encode a protein, based on available experimental and comparative sequence data; partially overlaps the dubious ORFs YPR169W-A and YPR170W-B	28.9%	-1.8	0.0003	0	0	0	0

Appendix A

ORF	Gene	Description	PRG	LF C	p-val	M M S	T B P	4 N Q O	U V
YPL203W	TPK2	cAMP-dependent protein kinase catalytic subunit; promotes vegetative growth in response to nutrients via the Ras-cAMP signaling pathway; inhibited by regulatory subunit Bcy1p in the absence of cAMP; partially redundant with Tpk1p and Tpk3p	28.9%	-1.8	0.0003	4	2	0	0
YML081W	N/A	Putative protein of unknown function; green fluorescent protein (GFP)-fusion protein localizes to the nucleus; YML081w is not an essential gene	29.0%	-1.8	0.0008	0	0	0	3
YPL188W	POS5	Mitochondrial NADH kinase, phosphorylates NADH; also phosphorylates NAD(+) with lower specificity; required for the response to oxidative stress	29.0%	-1.8	0.0003	1 5	7	5	6
YBR221C	PDB1	E1 beta subunit of the pyruvate dehydrogenase (PDH) complex, which is an evolutionarily-conserved multi-protein complex found in mitochondria	29.0%	-1.8	0.0068	8	0	0	0
YHR051W	COX6	Subunit VI of cytochrome c oxidase, which is the terminal member of the mitochondrial inner membrane electron transport chain; expression is regulated by oxygen levels	29.1%	-1.8	2E-06	1 2	0	0	5
YML112W	CTK3	Gamma subunit of C-terminal domain kinase I (CTDK-I), which phosphorylates both RNA pol II subunit Rpo21p to affect transcription and pre-mRNA 3' end processing, and ribosomal protein Rps2p to increase translational fidelity	29.1%	-1.8	8E-06	1 6	0	0	3
YDL136W	RPL35B	Protein component of the large (60S) ribosomal subunit, identical to Rpl35Ap and has similarity to rat L35 ribosomal protein	29.2%	-1.8	0.0003	0	0	3	4
YNL246W	VPS75	NAP family histone chaperone; binds to histones and Rtt109p, stimulating histone acetyltransferase activity; possesses nucleosome assembly activity in vitro; proposed role in vacuolar protein sorting and in double-strand break repair	29.2%	-1.8	0.0006	1 2	0	0	9
YOR069W	VPS5	Nexin-1 homolog required for localizing membrane proteins from a prevacuolar/late endosomal compartment back to the late Golgi apparatus; structural component of the retromer membrane coat complex; forms a retromer subcomplex with Vps17p	29.2%	-1.8	6E-05	4	0	4	0
YER139C	RTR1	Protein with a role in transcription; interacts with Rpo21p; has a cysteine-rich motif required for function and conserved in eukaryotes; shuttles between the nucleus and cytoplasm; RTR1 shows genetic interactions with RPB4, 5, 7, and 9	29.3%	-1.8	0.0001	1 1	0	7	0
YOR315W	SFG1	Nuclear protein, putative transcription factor required for growth of superficial pseudohyphae (which do not invade the agar substrate) but not for invasive pseudohyphal growth; may act together with Phd1p; potential Cdc28p substrate	29.4%	-1.8	0.0085	0	0	0	0

Appendix A

ORF	Gene	Description	PRG	LF C	p-val	M M S	T B P	4 N Q O	U V
YAR014C	BUD14	Protein involved in bud-site selection, Bud14p-Glc7p complex is a cortical regulator of dynein; inhibitor of the actin assembly factor Bnr1p (formin); diploid mutants display a random budding pattern instead of the wild-type bipolar pattern	29.4%	-1.8	3E-05	0	0	6	0
YPL185W	N/A	Dubious open reading frame unlikely to encode a protein, based on available experimental and comparative sequence data; partially overlaps the verified gene UIP4/YPL186C	29.4%	-1.8	0.0001	0	0	0	0
YMR154C	RIM13	Calpain-like cysteine protease involved in proteolytic activation of Rim101p in response to alkaline pH; has similarity to <i>A. nidulans</i> paIB	29.4%	-1.8	0.0023	2 0	5	0	0
YJL052W	TDH1	Glyceraldehyde-3-phosphate dehydrogenase, isozyme 1, involved in glycolysis and gluconeogenesis; tetramer that catalyzes the reaction of glyceraldehyde-3-phosphate to 1,3 bis-phosphoglycerate; detected in the cytoplasm and cell-wall	29.5%	-1.8	0.0008	4	0	0	0
YKL213C	DOA1	WD repeat protein required for ubiquitin-mediated protein degradation, forms complex with Cdc48p, plays a role in controlling cellular ubiquitin concentration; also promotes efficient NHEJ in postdiauxic/stationary phase	29.6%	-1.8	0.0003	3 0	0	7	0
YPL197C	N/A	Dubious open reading frame unlikely to encode a protein, based on experimental and comparative sequence data; partially overlaps the ribosomal gene RPB7B	29.9%	-1.7	2E-05	4	0	0	0
YPL156C	PRM4	Pheromone-regulated protein, predicted to have 1 transmembrane segment; transcriptionally regulated by Ste12p during mating and by Cat8p during the diauxic shift	29.9%	-1.7	0.0031	0	0	0	0
YPL193W	RSA1	Protein involved in the assembly of 60S ribosomal subunits; functionally interacts with Dbp6p; functions in a late nucleoplasmic step of the assembly	29.9%	-1.7	0.0002	0	5	1 2	2
YOR211C	MGM1	Mitochondrial GTPase related to dynamin, present in a complex containing Ugo1p and Fzo1p; required for normal morphology of cristae and for stability of Tim11p; homolog of human OPA1 involved in autosomal dominant optic atrophy	29.9%	-1.7	0.0008	3	0	0	1 2
YOL057W	N/A	Putative member of the dipeptidyl-peptidase III group of enzymes that cleave dipeptides from the amino terminus of target proteins; mammalian ortholog may be a biomarker for some cancers	29.9%	-1.7	0.0067	4	0	0	0
YPL107W	N/A	Putative protein of unknown function; green fluorescent protein (GFP)-fusion protein localizes to mitochondria; YPL107W is not an essential gene	30.0%	-1.7	0.0008	0	0	0	0
YPL174C	NIP100	Large subunit of the dynactin complex, which is involved in partitioning the mitotic spindle between mother and daughter cells; putative ortholog of mammalian p150(glued)	30.0%	-1.7	0.0004	7	0	0	0
YDR109C	N/A	Putative kinase	30.0%	-1.7	8E-05	4	0	0	0

Appendix A

ORF	Gene	Description	PRG	LF C	p-val	M M S	T B P	4 N Q O	U V
YNL199C	GCR2	Transcriptional activator of genes involved in glycolysis; interacts and functions with the DNA-binding protein Gcr1p	30.0%	-1.7	2E-05	5	0	2 6	0
YHL013C	OTU2	Protein of unknown function that may interact with ribosomes, based on co-purification experiments; member of the ovarian tumor-like (OTU) superfamily of predicted cysteine proteases; shows cytoplasmic localization	30.1%	-1.7	8E-05	0	4	0	0
YFL007W	BLM10	Proteasome activator subunit; found in association with core particles, with and without the 19S regulatory particle; required for resistance to bleomycin, may be involved in protecting against oxidative damage; similar to mammalian PA200	30.1%	-1.7	9E-06	0	0	0	0
YMR194 W	RPL36A	N-terminally acetylated protein component of the large (60S) ribosomal subunit, nearly identical to Rpl36Bp and has similarity to rat L36 ribosomal protein; binds to 5.8 S rRNA	30.3%	-1.7	0.0008	0	2	0	0
YCL007C	N/A	Dubious ORF unlikely to encode a protein; overlaps verified ORF YCL005W-A; mutations in YCL007C were thought to confer sensitivity to calcofluor white, but this phenotype was later shown to be due to the defect in YCL005W-A	30.3%	-1.7	0.0013	4	1 2	2 2	2
YDL117W	CYK3	SH3-domain protein located in the mother-bud neck and the cytokinetic actin ring; mutant phenotype and genetic interactions suggest a role in cytokinesis	30.3%	-1.7	0.0003	0	0	0	0
YMR293C	HER2	Mitochondrial protein required for remodeling of ER caused by Hmg2p overexpression; null has decreased mitochondrial genome loss and decreased cardiolipin and phosphatidylethanolamine levels; like bacterial glutamyl-tRNA amidotransferases	30.4%	-1.7	0.0003	7	0	0	0
YFL013C	IES1	Subunit of the INO80 chromatin remodeling complex	30.4%	-1.7	3E-05	0	0	1 5	0
YCL037C	SRO9	Cytoplasmic RNA-binding protein that associates with translating ribosomes; involved in heme regulation of Hap1p as a component of the HMC complex, also involved in the organization of actin filaments; contains a La motif	30.4%	-1.7	0.0001	0	0	0	0
YLR271W	N/A	Putative protein of unknown function; green fluorescent protein (GFP)-fusion protein localizes to the cytoplasm and the nucleus and is induced in response to the DNA-damaging agent MMS	30.4%	-1.7	0.007	0	0	0	0
YLR062C	BUD28	Dubious open reading frame, unlikely to encode a protein; not conserved in closely related Saccharomyces species; 98% of ORF overlaps the verified gene RPL22A; diploid mutant displays a weak budding pattern phenotype in a systematic assay	30.5%	-1.7	3E-05	0	7	0	0
YLR039C	RIC1	Protein involved in retrograde transport to the cis-Golgi network; forms heterodimer with Rgp1p that acts as a GTP exchange factor for Ypt6p; involved in transcription of rRNA and ribosomal protein genes	30.5%	-1.7	9E-05	4	3	7	4

Appendix A

ORF	Gene	Description	PRG	LF C	p-val	M M S	T B P	4 N Q O	U V
YLR080W	EMP46	Integral membrane component of endoplasmic reticulum-derived COPII-coated vesicles, which function in ER to Golgi transport	30.6%	-1.7	1E-05	0	0	0	0
YMR056C	AAC1	Mitochondrial inner membrane ADP/ATP translocator, exchanges cytosolic ADP for mitochondrially synthesized ATP; phosphorylated; Aac1p is a minor isoform while Pet9p is the major ADP/ATP translocator	30.7%	-1.7	0.0002	0	0	0	0
YBR220C	N/A	Putative protein of unknown function; YBR220C is not an essential gene	30.8%	-1.7	0.0073	0	0	0	0
YJL175W	N/A	Dubious open reading frame unlikely to encode a functional protein; deletion confers resistance to cisplatin, hypersensitivity to 5-fluorouracil, and growth defect at high pH with high calcium; overlaps gene for SWI3 transcription factor	30.9%	-1.7	0.0003	0	5	1 0	0
YGR222 W	PET54	Mitochondrial inner membrane protein that binds to the 5' UTR of the COX3 mRNA to activate its translation together with Pet122p and Pet494p; also binds to the COX1 Group I intron AI5 beta to facilitate exon ligation during splicing	31.0%	-1.7	0.0002	0	0	0	0
YOL071W	EMI5	Non-essential protein of unknown function required for transcriptional induction of the early meiotic-specific transcription factor IME1, also required for sporulation; null mutant excretes excess acetic acid	31.1%	-1.7	0.0039	0	0	0	0
YML013C -A	0	Dubious open reading frame unlikely to encode a protein, based on available experimental and comparative sequence data; partially overlaps the verified gene SEL1	31.1%	-1.7	0.0012	4	2	0	0
YOR293 W	RPS10A	Protein component of the small (40S) ribosomal subunit; nearly identical to Rps10Bp and has similarity to rat ribosomal protein S10	31.1%	-1.7	0.001	0	0	2	0
YGL084C	GUP1	Plasma membrane protein involved in remodeling GPI anchors; member of the MBOAT family of putative membrane-bound O-acyltransferases; proposed to be involved in glycerol transport	31.1%	-1.7	0.0009	4	0	1 6	0
YBR230C	OM14	Integral mitochondrial outer membrane protein; abundance is decreased in cells grown in glucose relative to other carbon sources; appears to contain 3 alpha-helical transmembrane segments; ORF encodes a 97-basepair intron	31.2%	-1.7	0.0009	0	0	0	0
YER129 W	SAK1	Upstream serine/threonine kinase for the SNF1 complex; partially redundant with Elm1p and Tos3p; members of this family have functional orthology with LKB1, a mammalian kinase associated with Peutz-Jeghers cancer-susceptibility syndrome	31.2%	-1.7	0.0002	0	0	0	0
YDR521 W	N/A	Dubious ORF that overlaps YDR520C; mutant increases expression of PIS1 and RPL3 in glycerol	31.3%	-1.7	4E-05	0	0	0	0

Appendix A

ORF	Gene	Description	PRG	LF C	p-val	M M S	T B P	4 N Q O	U V
YGR214 W	RPS0A	Protein component of the small (40S) ribosomal subunit, nearly identical to Rps0Bp; required for maturation of 18S rRNA along with Rps0Bp; deletion of either RPS0 gene reduces growth rate, deletion of both genes is lethal	31.3%	-1.7	0.0006	0	0	0	3
YGR160 W	N/A	Dubious open reading frame unlikely to encode a functional protein, based on available experimental and comparative sequence data	31.4%	-1.7	3E-05	0	0	4	0
YDR500C	RPL37B	Protein component of the large (60S) ribosomal subunit, has similarity to Rpl37Ap and to rat L37 ribosomal protein	31.5%	-1.7	7E-05	0	0	1 4	0
YOL065C	INP54	Phosphatidylinositol 4,5-bisphosphate 5-phosphatase with a role in secretion, localizes to the endoplasmic reticulum via the C-terminal tail; lacks the Sac1 domain and proline-rich region found in the other 3 INP proteins	31.5%	-1.7	0.004	0	0	0	0
YIR004W	DJP1	Cytosolic J-domain-containing protein, required for peroxisomal protein import and involved in peroxisome assembly, homologous to E. coli DnaJ	31.6%	-1.7	1E-05	0	0	0	0
YGR292 W	MAL12	Maltase (alpha-D-glucosidase), inducible protein involved in maltose catabolism; encoded in the MAL1 complex locus	31.7%	-1.7	1E-06	0	0	0	0
YDR080 W	VPS41	Vacuolar membrane protein that is a subunit of the homotypic vacuole fusion and vacuole protein sorting (HOPS) complex; essential for membrane docking and fusion at the Golgi-to-endosome and endosome-to-vacuole stages of protein transport	31.9%	-1.6	9E-06	7	0	0	0
YNL235C	N/A	Dubious open reading frame unlikely to encode a protein, based on available experimental and comparative sequence data; partially overlaps the verified ORF SIN4/YNL236W, a subunit of the mediator complex	32.0%	-1.6	0.0005	0	0	1 2	0
YPL222W	FMP40	Putative protein of unknown function; proposed to be involved in responding to environmental stresses; the authentic, non-tagged protein is detected in highly purified mitochondria in high-throughput studies	32.2%	-1.6	4E-05	0	0	0	0
YJR034W	PET191	Protein required for assembly of cytochrome c oxidase; exists as an oligomer that is integral to the mitochondrial inner membrane and faces the intermembrane space; contains a twin Cx9C motif	32.3%	-1.6	2E-07	0	0	0	0
YPL191C	N/A	Putative protein of unknown function; diploid deletion strain exhibits high budding index; green fluorescent protein (GFP)-fusion protein localizes to the cytoplasm	32.3%	-1.6	0.0006	5	0	0	0
YOL053W	AIM39	Putative protein of unknown function; null mutant displays elevated frequency of mitochondrial genome loss	32.4%	-1.6	0.0004	4	0	0	0
YPL170W	DAP1	Heme-binding protein involved in regulation of cytochrome P450 protein Erg11p; damage response protein, related to mammalian membrane progesterone receptors; mutations lead to defects in telomeres, mitochondria, and sterol synthesis	32.4%	-1.6	0.0005	2 2	2	0	0

Appendix A

ORF	Gene	Description	PRG	LF C	p-val	M M S	T B P	4 N Q O	U V
YDR135C	YCF1	Vacuolar glutathione S-conjugate transporter of the ATP-binding cassette family, has a role in detoxifying metals such as cadmium, mercury, and arsenite; also transports unconjugated bilirubin; similar to human cystic fibrosis protein CFTR	32.4%	-1.6	0.0002	0	0	0	0
YDR174 W	HMO1	Chromatin associated high mobility group (HMG) family member involved in genome maintenance; rDNA-binding component of the Pol I transcription system; associates with a 5'-3' DNA helicase and Fpr1p, a prolyl isomerase	32.4%	-1.6	0.0004	0	0	0	0
YMR002 W	MIC17	Mitochondrial intermembrane space cysteine motif protein; MIC17 is not an essential gene	32.5%	-1.6	1E-05	0	2	0	0
YPR047 W	MSF1	Mitochondrial phenylalanyl-tRNA synthetase, active as a monomer, unlike the cytoplasmic subunit which is active as a dimer complexed to a beta subunit dimer; similar to the alpha subunit of E. coli phenylalanyl-tRNA synthetase	32.5%	-1.6	0.0004	0	0	0	0
YIL065C	FIS1	Protein involved in mitochondrial membrane fission and peroxisome abundance; required for localization of Dnm1p and Mdv1p during mitochondrial division; mediates ethanol-induced apoptosis and ethanol-induced mitochondrial fragmentation	32.6%	-1.6	2E-05	9	2	0	0
YOR334 W	MRS2	Mitochondrial inner membrane Mg(2+) channel, required for maintenance of intramitochondrial Mg(2+) concentrations at the correct level to support splicing of group II introns	32.7%	-1.6	0.0067	0	0	0	0
YGL076C	RPL7A	Protein component of the large (60S) ribosomal subunit, nearly identical to Rpl7Bp and has similarity to E. coli L30 and rat L7 ribosomal proteins; contains a conserved C-terminal Nucleic acid Binding Domain (NDB2)	32.7%	-1.6	6E-05	0	0	0	7
YNR042 W	N/A	Dubious open reading frame unlikely to encode a protein, based on available experimental and comparative sequence data; completely overlaps verified gene COQ2	32.7%	-1.6	0.001	4	0	0	0
YML036 W	CGI121	Protein involved in telomere uncapping and elongation as component of the KEOPS protein complex with Bud32p, Kae1p, Pcc1p, and Gon7p; also shown to be a component of the EKC protein complex; homolog of human CGI-121	32.9%	-1.6	0.0003	0	0	0	0
YDR345C	HXT3	Low affinity glucose transporter of the major facilitator superfamily, expression is induced in low or high glucose conditions	33.0%	-1.6	0.0002	0	0	0	0
YDR028C	REG1	Regulatory subunit of type 1 protein phosphatase Glc7p, involved in negative regulation of glucose-repressible genes	33.0%	-1.6	4E-05	5	5	2 1	0
YOR358 W	HAP5	Subunit of the heme-activated, glucose-repressed Hap2/3/4/5 CCAAT-binding complex, a transcriptional activator and global regulator of respiratory gene expression; required for assembly and DNA binding activity of the complex	33.1%	-1.6	0.0024	0	0	0	0
YNL319W	N/A	Dubious open reading frame unlikely to encode a protein; partially overlaps the verified gene HXT14	33.2%	-1.6	2E-05	7	0	0	0

Appendix A

ORF	Gene	Description	PRG	LF C	p-val	M M S	T B P	4 N Q O	U V
YKL211C	TRP3	Bifunctional enzyme exhibiting both indole-3-glycerol-phosphate synthase and anthranilate synthase activities, forms multifunctional hetero-oligomeric anthranilate synthase:indole-3-glycerol phosphate synthase enzyme complex with Trp2p	33.2%	-1.6	3E-05	2	0	0	0
YPL088W	N/A	Putative aryl alcohol dehydrogenase; transcription is activated by paralogous transcription factors Yrm1p and Yrr1p along with genes involved in multidrug resistance	33.3%	-1.6	0.0019	0	0	0	0
YJR063W	RPA12	RNA polymerase I subunit A12.2; contains two zinc binding domains, and the N terminal domain is responsible for anchoring to the RNA pol I complex	33.3%	-1.6	0.0001	0	0	0	0
YLR255C	N/A	Dubious ORF unlikely to encode a functional protein, based on available experimental and comparative sequence data	33.3%	-1.6	0.0019	0	0	0	0
YOR291 W	YPK9	Vacuolar protein with a possible role in sequestering heavy metals; has similarity to the type V P-type ATPase Spf1p; homolog of human ATP13A2 (PARK9), mutations in which are associated with Parkinson disease and Kufo?Rakeb syndrome	33.3%	-1.6	0.0151	0	0	0	0
YDR493 W	AIM8	Protein of unknown function; overexpression causes a cell cycle delay or arrest; null mutant displays severe respiratory growth defect and elevated frequency of mitochondrial genome loss; detected in mitochondria in high-throughput studies	33.3%	-1.6	5E-05	0	0	0	0
YMR221C	N/A	Putative protein of unknown function; the authentic, non-tagged protein is detected in highly purified mitochondria in high-throughput studies; physical interaction with Atg27p suggests a possible role in autophagy	33.3%	-1.6	0.0003	0	0	0	0
YJR105W	ADO1	Adenosine kinase, required for the utilization of S-adenosylmethionine (AdoMet); may be involved in recycling adenosine produced through the methyl cycle	33.3%	-1.6	0.002	2	0	2 3	0
YPL087W	YDC1	Alkaline dihydroceramidase, involved in sphingolipid metabolism; preferentially hydrolyzes dihydroceramide to a free fatty acid and dihydrosphingosine; has a minor reverse activity	33.4%	-1.6	4E-05	0	0	0	0
YHR034C	PIH1	Protein of unresolved function; may function in protein folding and/or rRNA processing, interacts with a chaperone (Hsp82p), two chromatin remodeling factors (Rvb1p, Rvb2p) and two rRNA processing factors (Rrp43p, Nop58p)	33.4%	-1.6	0.0001	0	0	0	0
YDR123C	INO2	Component of the heteromeric Ino2p/Ino4p basic helix-loop-helix transcription activator that binds inositol/choline-responsive elements (ICREs), required for derepression of phospholipid biosynthetic genes in response to inositol depletion	33.4%	-1.6	4E-05	0	0	0	0

Appendix A

ORF	Gene	Description	PRG	LF C	p-val	M M S	T B P	4 N Q O	U V
YDR369C	XRS2	Protein required for DNA repair; component of the Mre11 complex, which is involved in double strand breaks, meiotic recombination, telomere maintenance, and checkpoint signaling	33.6%	-1.6	0.0002	2 7	0	3 0	0
YKL139W	CTK1	Catalytic (alpha) subunit of C-terminal domain kinase I (CTDK-I), which phosphorylates both RNA pol II subunit Rpo21p to affect transcription and pre-mRNA 3' end processing, and ribosomal protein Rps2p to increase translational fidelity	33.7%	-1.6	0.0005	1 8	0	7 4	1 4
YMR066 W	SOV1	Mitochondrial protein of unknown function	33.7%	-1.6	1E-05	0	0	0	0
YIL028W	N/A	Dubious open reading frame unlikely to encode a protein, based on available experimental and comparative sequence data	33.9%	-1.6	2E-05	6	4	0	0
YGL203C	KEX1	Protease involved in the processing of killer toxin and alpha factor precursor; cleaves Lys and Arg residues from the C-terminus of peptides and proteins	34.0%	-1.6	8E-05	0	0	0	0
YLR017W	MEU1	Methylthioadenosine phosphorylase (MTAP), catalyzes the initial step in the methionine salvage pathway; affects polyamine biosynthesis through regulation of ornithine decarboxylase (Spe1p) activity; regulates ADH2 gene expression	34.2%	-1.5	0.0002	0	0	0	0
YIL085C	KTR7	Putative mannosyltransferase involved in protein glycosylation; member of the KRE2/MNT1 mannosyltransferase family	34.2%	-1.5	0.0001	0	0	0	0
YOR323C	PRO2	Gamma-glutamyl phosphate reductase, catalyzes the second step in proline biosynthesis	34.2%	-1.5	0.0216	4	0	0	0
YFL001W	DEG1	Non-essential tRNA:pseudouridine synthase, introduces pseudouridines at position 38 or 39 in tRNA, important for maintenance of translation efficiency and normal cell growth, localizes to both the nucleus and cytoplasm	34.3%	-1.5	2E-06	1 2	0	1 3	0
YPL192C	PRM3	Pheromone-regulated protein required for nuclear envelope fusion during karyogamy; localizes to the outer face of the nuclear membrane; interacts with Kar5p at the spindle pole body	34.4%	-1.5	0.0019	0	0	0	0
YOR313C	SPS4	Protein whose expression is induced during sporulation; not required for sporulation; heterologous expression in E. coli induces the SOS response that senses DNA damage	34.5%	-1.5	0.0195	4	0	0	0
YIL158W	AIM20	Putative protein of unknown function; overexpression causes a cell cycle delay or arrest; green fluorescent protein (GFP)-fusion protein localizes to the vacuole; null mutant displays elevated frequency of mitochondrial genome loss	34.5%	-1.5	4E-05	0	0	0	0
YKL053W	N/A	Dubious open reading frame unlikely to encode a protein, based on available experimental and comparative sequence data; partially overlaps verified ORF ASK1	34.6%	-1.5	3E-05	0	0	4	0

Appendix A

ORF	Gene	Description	PRG	LF C	p-val	M M S	T B P	4 N Q O	U V
YLR396C	VPS33	ATP-binding protein that is a subunit of the HOPS complex and the CORVET tethering complex; essential for membrane docking and fusion at both the Golgi-to-endosome and endosome-to-vacuole stages of protein transport	34.6%	-1.5	0.0002	7	1 9	1 9	0
YNL285W	N/A	Dubious open reading frame unlikely to encode a functional protein, based on available experimental and comparative sequence data	34.6%	-1.5	0.0002	0	0	0	0
YJL180C	ATP12	Conserved protein required for assembly of alpha and beta subunits into the F1 sector of mitochondrial F1F0 ATP synthase; mutation of human ATP12 reduces active ATP synthase levels and is associated with the disorder ATPAF2 deficiency	34.7%	-1.5	0.0031	2 3	0	1 8	1 5
YLR119W	SRN2	Component of the ESCRT-I complex, which is involved in ubiquitin-dependent sorting of proteins into the endosome; suppressor of rna1-1 mutation; may be involved in RNA export from nucleus	34.7%	-1.5	0.0002	6	2	0	0
YBR250W	SPO23	Protein of unknown function; associates with meiosis-specific protein Spo1p	34.7%	-1.5	0.0015	5	0	0	0
YDR495C	VPS3	Component of CORVET tethering complex; cytoplasmic protein required for the sorting and processing of soluble vacuolar proteins, acidification of the vacuolar lumen, and assembly of the vacuolar H ⁺ -ATPase	34.8%	-1.5	2E-05	1 0	7	1 7	0
YHR100C	GEP4	Protein of unknown function required for respiratory growth; detected in highly purified mitochondria in high-throughput studies; null mutation confers sensitivity to tunicamycin and DTT and decreased levels of phosphatidylethanol	34.8%	-1.5	4E-05	3 0	0	0	1 7
YJR033C	RAV1	Subunit of the RAVE complex (Rav1p, Rav2p, Skp1p), which promotes assembly of the V-ATPase holoenzyme; required for transport between the early and late endosome/PVC and for localization of TGN membrane proteins; potential Cdc28p substrate	34.9%	-1.5	0.0002	0	0	6	0
YIL005W	EPS1	ER protein with chaperone and co-chaperone activity, involved in retention of resident ER proteins; has a role in recognizing proteins targeted for ER-associated degradation (ERAD), member of the protein disulfide isomerase family	34.9%	-1.5	0.0002	2	2	0	0
YER044C	ERG28	Endoplasmic reticulum membrane protein, may facilitate protein-protein interactions between the Erg26p dehydrogenase and the Erg27p 3-ketoreductase and/or tether these enzymes to the ER, also interacts with Erg6p	35.0%	-1.5	0.0001	3 0	1 6	2 6	9
YOR026W	BUB3	Kinetochore checkpoint WD40 repeat protein that localizes to kinetochores during prophase and metaphase, delays anaphase in the presence of unattached kinetochores; forms complexes with Mad1p-Bub1p and with Cdc20p, binds Mad2p and Mad3p	35.0%	-1.5	0.0001	7	0	1 2	6

Appendix A

ORF	Gene	Description	PRG	LF C	p-val	M M S	T B P	4 N Q O	U V
YLR092W	SUL2	High affinity sulfate permease; sulfate uptake is mediated by specific sulfate transporters Sul1p and Sul2p, which control the concentration of endogenous activated sulfate intermediates	35.1%	-1.5	0.0002	0	0	0	0
YDR344C	N/A	Dubious open reading frame unlikely to encode a functional protein, based on available experimental and comparative sequence data	35.1%	-1.5	0.0001	0	0	0	0
YOR053W	N/A	Dubious open reading frame unlikely to encode a protein, based on available experimental and comparative sequence data; partially overlaps the verified gene VHS3/YOR054C	35.2%	-1.5	0.0003	0	0	0	0
YPL118W	MRP51	Mitochondrial ribosomal protein of the small subunit; MRP51 exhibits genetic interactions with mutations in the COX2 and COX3 mRNA 5'-untranslated leader sequences	35.3%	-1.5	0.0073	0	0	4	0
YNL162W	RPL42A	Protein component of the large (60S) ribosomal subunit, identical to Rpl42Bp and has similarity to rat L44 ribosomal protein	35.4%	-1.5	1E-06	0	0	0	0
YAL013W	DEP1	Transcriptional modulator involved in regulation of structural phospholipid biosynthesis genes and metabolically unrelated genes, as well as maintenance of telomeres, mating efficiency, and sporulation	35.4%	-1.5	0.0001	0	0	1 5	0
YOR344C	TYE7	Serine-rich protein that contains a basic-helix-loop-helix (bHLH) DNA binding motif; binds E-boxes of glycolytic genes and contributes to their activation; may function as a transcriptional activator in Ty1-mediated gene expression	35.4%	-1.5	0.0126	0	0	0	0
YLR414C	N/A	Putative protein of unknown function; localizes to bud and cytoplasm; co-localizes with Sur7p in punctate patches in the plasma membrane; null mutant displays decreased thermotolerance; transcription induced on cell wall damage	35.4%	-1.5	0.0016	7	5	9	0
YGL007W	BRP1	Dubious ORF located in the upstream region of PMA1, deletion leads to polyamine resistance due to downregulation of PMA1	35.5%	-1.5	0.0001	0	0	2 6	2 3
YLR273C	PIG1	Putative targeting subunit for the type-1 protein phosphatase Glc7p that tethers it to the Gsy2p glycogen synthase	35.5%	-1.5	0.0165	0	0	0	0
YDR360W	OPI7	Dubious open reading frame unlikely to encode a protein, based on available experimental and comparative sequence data; partially overlaps verified gene VID21/YDR359C.	35.5%	-1.5	2E-05	0	0	9	0
YER028C	MIG3	Probable transcriptional repressor involved in response to toxic agents such as hydroxyurea that inhibit ribonucleotide reductase; phosphorylation by Snf1p or the Mec1p pathway inactivates Mig3p, allowing induction of damage response genes	35.6%	-1.5	3E-06	0	2	0	0
YGL045W	RIM8	Protein of unknown function, involved in the proteolytic activation of Rim101p in response to alkaline pH; has similarity to A. nidulans PalF; essential for anaerobic growth	35.7%	-1.5	2E-05	1 4	2	0	0

Appendix A

ORF	Gene	Description	PRG	LF C	p-val	M M S	T B P	4 N Q O	U V
YJL157C	FAR1	Cyclin-dependent kinase inhibitor that mediates cell cycle arrest in response to pheromone; also forms a complex with Cdc24p, Ste4p, and Ste18p that may specify the direction of polarized growth during mating; potential Cdc28p substrate	35.7%	-1.5	0.0059	0	0	0	0
YLR441C	RPS1A	Ribosomal protein 10 (rp10) of the small (40S) subunit; nearly identical to Rps1Bp and has similarity to rat S3a ribosomal protein	35.9%	-1.5	1E-05	0	0	0	0
YML024 W	RPS17A	Ribosomal protein 51 (rp51) of the small (40s) subunit; nearly identical to Rps17Bp and has similarity to rat S17 ribosomal protein	35.9%	-1.5	0.0012	0	0	0	0
YER068 W	MOT2	Subunit of the CCR4-NOT complex, which has roles in transcription regulation, mRNA degradation, and post-transcriptional modifications; with Ubc4p, ubiquitinates nascent polypeptide-associated complex subunits and histone demethylase Jhd2p	35.9%	-1.5	0.0001	1 9	0	6	2 1
YBR233 W	PBP2	RNA binding protein with similarity to mammalian heterogeneous nuclear RNP K protein, involved in the regulation of telomere position effect and telomere length	36.0%	-1.5	0.0074	0	0	0	0
YIL131C	FKH1	Forkhead family transcription factor with a minor role in the expression of G2/M phase genes; negatively regulates transcriptional elongation; positive role in chromatin silencing at HML and HMR; regulates donor preference during switching	36.0%	-1.5	0.0002	0	0	0	0
YDR326C	YSP2	Protein involved in programmed cell death; mutant shows resistance to cell death induced by amiodarone or intracellular acidification	36.2%	-1.5	1E-05	9	0	0	0
YPL273W	SAM4	S-adenosylmethionine-homocysteine methyltransferase, functions along with Mht1p in the conversion of S-adenosylmethionine (AdoMet) to methionine to control the methionine/AdoMet ratio	36.2%	-1.5	0.0093	0	0	0	0
YIL038C	NOT3	Subunit of the CCR4-NOT complex, which is a global transcriptional regulator with roles in transcription initiation and elongation and in mRNA degradation	36.2%	-1.5	0.0007	4	0	0	0
YDR502C	SAM2	S-adenosylmethionine synthetase, catalyzes transfer of the adenosyl group of ATP to the sulfur atom of methionine; one of two differentially regulated isozymes (Sam1p and Sam2p)	36.3%	-1.5	0.0004	0	0	0	0
YKL148C	SDH1	Flavoprotein subunit of succinate dehydrogenase (Sdh1p, Sdh2p, Sdh3p, Sdh4p), which couples the oxidation of succinate to the transfer of electrons to ubiquinone	36.4%	-1.5	0.0001	0	0	0	0
YBR231C	SWC5	Protein of unknown function, component of the SWR1 complex, which exchanges histone variant H2AZ (Htz1p) for chromatin-bound histone H2A	36.4%	-1.5	0.0354	2 9	0	1 7	4
YDL206W	N/A	Putative protein of unknown function; YDL206W is not an essential protein	36.5%	-1.5	0.0004	0	0	0	0

Appendix A

ORF	Gene	Description	PRG	LF C	p-val	M M S	T B P	4 N Q O	U V
YMR144 W	N/A	Putative protein of unknown function; localized to the nucleus; YMR144W is not an essential gene	36.6%	-1.5	8E-05	0	0	0	0
YDR483 W	KRE2	Alpha1,2-mannosyltransferase of the Golgi involved in protein mannosylation	36.6%	-1.5	4E-05	0	0	0	0
YJL117W	PHO86	Endoplasmic reticulum (ER) resident protein required for ER exit of the high-affinity phosphate transporter Pho84p, specifically required for packaging of Pho84p into COPII vesicles	36.6%	-1.4	0.0007	7	5	8	0
YOL048C	RRT8	Putative protein of unknown function; identified in a screen for mutants with increased levels of rDNA transcription; green fluorescent protein (GFP)-fusion protein localizes to lipid particles	36.7%	-1.4	0.0002	4	0	0	0
YDR448 W	ADA2	Transcription coactivator, component of the ADA and SAGA transcriptional adaptor/HAT (histone acetyltransferase) complexes	36.7%	-1.4	2E-05	4	0	0	6
YPR173C	VPS4	AAA-ATPase involved in multivesicular body (MVB) protein sorting, ATP-bound Vps4p localizes to endosomes and catalyzes ESCRT-III disassembly and membrane release; ATPase activity is activated by Vta1p; regulates cellular sterol metabolism	36.8%	-1.4	4E-05	4	0	0	0
YGR289C	MAL11	Inducible high-affinity maltose transporter (alpha-glucoside transporter); encoded in the MAL1 complex locus; member of the 12 transmembrane domain superfamily of sugar transporters; broad substrate specificity that includes maltotriose	36.8%	-1.4	8E-05	0	0	0	0
YPL171C	OYE3	Conserved NADPH oxidoreductase containing flavin mononucleotide (FMN), homologous to Oye2p with slight differences in ligand binding and catalytic properties; expression induced in cells treated with the mycotoxin patulin	36.9%	-1.4	0.0147	4	5	0	0
YGL218W	N/A	Dubious open reading frame, unlikely to encode a protein; not conserved in closely related Saccharomyces species; 93% of ORF overlaps the verified gene MDM34; deletion in <i>cyr1</i> mutant results in loss of stress resistance	37.0%	-1.4	0.0004	5	0	0	4
YHR194 W	MDM31	Mitochondrial inner membrane protein with similarity to Mdm32p, required for normal mitochondrial morphology and inheritance; interacts genetically with MMM1, MDM10, MDM12, and MDM34	37.1%	-1.4	0.0043	1 8	0	0	0
YMR032 W	HOF1	Bud neck-localized, SH3 domain-containing protein required for cytokinesis; regulates actomyosin ring dynamics and septin localization; interacts with the formins, Bni1p and Bnr1p, and with Cyk3p, Vrp1p, and Bni5p	37.1%	-1.4	0.0025	7	0	1 3	0
YPL163C	SVS1	Cell wall and vacuolar protein, required for wild-type resistance to vanadate	37.1%	-1.4	0.0039	7	2	0	0

Appendix A

ORF	Gene	Description	PRG	LF C	p-val	M M S	T B P	4 N Q O	U V
YIL094C	LYS12	Homo-isocitrate dehydrogenase, an NAD-linked mitochondrial enzyme required for the fourth step in the biosynthesis of lysine, in which homo-isocitrate is oxidatively decarboxylated to alpha-ketoadipate	37.1%	-1.4	6E-05	0	0	0	0
YMR326C	N/A	Dubious open reading frame unlikely to encode a protein, based on available experimental and comparative sequence data; overlaps the telomere on the right arm of chromosome 13	37.2%	-1.4	3E-05	0	2	0	1 0
YIL042C	PKP1	Mitochondrial protein kinase involved in negative regulation of pyruvate dehydrogenase complex activity by phosphorylating the ser-133 residue of the Pda1p subunit; acts in concert with kinase Pkp2p and phosphatases Ptc5p and Ptc6p	37.2%	-1.4	5E-05	4	2	0	0
YDL198C	GGC1	Mitochondrial GTP/GDP transporter, essential for mitochondrial genome maintenance; has a role in mitochondrial iron transport; member of the mitochondrial carrier family	37.2%	-1.4	0.0135	2	0	0	0
YLR435W	TSR2	Protein with a potential role in pre-rRNA processing	37.3%	-1.4	0.001	0	0	7	0
YJL191W	RPS14B	Ribosomal protein 59 of the small subunit, required for ribosome assembly and 20S pre-rRNA processing; mutations confer cryptopleurine resistance; nearly identical to Rps14Ap and similar to E. coli S11 and rat S14 ribosomal proteins	37.3%	-1.4	0.0002	0	0	0	0
YIL056W	VHR1	Transcriptional activator, required for the vitamin H-responsive element (VHRE) mediated induction of VHT1 (Vitamin H transporter) and BIO5 (biotin biosynthesis intermediate transporter) in response to low biotin concentrations	37.3%	-1.4	3E-05	0	0	0	0
YOR364 W	N/A	Dubious open reading frame unlikely to encode a protein, based on available experimental and comparative sequence data; partially overlaps the uncharacterized ORF YOR365C	37.4%	-1.4	0.0004	4	0	0	0
YBR084C -A	RPL19A	Protein component of the large (60S) ribosomal subunit, nearly identical to Rpl19Bp and has similarity to rat L19 ribosomal protein; rpl19a and rpl19b single null mutations result in slow growth, while the double null mutation is lethal	37.4%	-1.4	0.0004	0	0	0	0
YOR068C	VAM10	Protein involved in vacuole morphogenesis; acts at an early step of homotypic vacuole fusion that is required for vacuole tethering	37.5%	-1.4	9E-05	0	0	0	0
YBR163 W	DEM1	Mitochondrial protein of unknown function; null mutant has defects in cell morphology and in response to air drying; may be regulated by the transcription factor Ace2	37.5%	-1.4	6E-05	0	0	0	0
YNL148C	ALF1	Alpha-tubulin folding protein, similar to mammalian cofactor B; Alf1p-GFP localizes to cytoplasmic microtubules; required for the folding of alpha-tubulin and may play an additional role in microtubule maintenance	37.5%	-1.4	0.0005	1 0	0	7	0

Appendix A

ORF	Gene	Description	PRG	LF C	p-val	M M S	T B P	4 N Q O	U V
YBR205 W	KTR3	Putative alpha-1,2-mannosyltransferase involved in O- and N-linked protein glycosylation; member of the KRE2/MNT1 mannosyltransferase family	37.6%	-1.4	0.0027	0	0	0	0
YEL046C	GLY1	Threonine aldolase, catalyzes the cleavage of L-allo-threonine and L-threonine to glycine; involved in glycine biosynthesis	37.6%	-1.4	0.0003	0	6	0	0
YER180C	ISC10	Protein required for sporulation, transcript is induced 7.5 hours after induction of meiosis, expected to play significant role in the formation of reproductive cells	37.6%	-1.4	0.0005	0	0	0	0
YER181C	N/A	Dubious open reading frame unlikely to encode a protein, based on available experimental and comparative data; extensively overlaps a Ty1 LTR; protein product is detected in highly purified mitochondria in high-throughput studies	37.7%	-1.4	7E-05	0	0	0	0
YPL149W	ATG5	Conserved protein involved in autophagy and the Cvt pathway; undergoes conjugation with Atg12p to form a complex involved in Atg8p lipidation; conjugated Atg12p also forms a complex with Atg16p that is essential for autophagosome formation	37.7%	-1.4	2E-05	4	0	0	0
YJL062W	LAS21	Integral plasma membrane protein involved in the synthesis of the glycosylphosphatidylinositol (GPI) core structure; mutations affect cell wall integrity	37.8%	-1.4	5E-05	0	2	0	0
YJR018W	N/A	Dubious open reading frame unlikely to encode a functional protein, based on available experimental and comparative sequence data	37.8%	-1.4	0.0009	1 8	0	3 0	0
YOL025W	LAG2	Protein involved in determination of longevity; LAG2 gene is preferentially expressed in young cells; overexpression extends the mean and maximum life span of cells	37.9%	-1.4	0.0045	0	0	0	0
YGR012 W	N/A	Putative cysteine synthase, localized to the mitochondrial outer membrane	37.9%	-1.4	0.0002	0	0	0	0
YGR233C	PHO81	Cyclin-dependent kinase (CDK) inhibitor, regulates Pho80p-Pho85p and Pcl7p-Pho85p cyclin-CDK complexes in response to phosphate levels; inhibitory activity for Pho80p-Pho85p requires myo-D-inositol heptakisphosphate (IP7) generated by Vip1p	37.9%	-1.4	0.0006	0	0	0	0
YKL204W	EAP1	eIF4E-associated protein, binds eIF4E and inhibits cap-dependent translation, also functions independently of eIF4E to maintain genetic stability; plays a role in cell growth, implicated in the TOR signaling cascade	37.9%	-1.4	0.0003	1 8	0	2 2	0
YGR188C	BUB1	Protein kinase that forms a complex with Mad1p and Bub3p that is crucial in the checkpoint mechanism required to prevent cell cycle progression into anaphase in the presence of spindle damage, associates with centromere DNA via Skp1p	38.0%	-1.4	0.0002	1 5	0	2 9	8
YBR021 W	FUR4	Uracil permease, localized to the plasma membrane; expression is tightly regulated by uracil levels and environmental cues	38.0%	-1.4	1E-06	0	0	0	0

Appendix A

ORF	Gene	Description	PRG	LF C	p-val	M M S	T B P	4 N Q O	U V
YBR207 W	FTH1	Putative high affinity iron transporter involved in transport of intravacuolar stores of iron; forms complex with Fet5p; expression is regulated by iron; proposed to play indirect role in endocytosis	38.0%	-1.4	0.0013	4	0	0	0
YBR026C	ETR1	2-enoyl thioester reductase, member of the medium chain dehydrogenase/reductase family; localized to in mitochondria, where it has a probable role in fatty acid synthesis	38.1%	-1.4	3E-05	9	0	0	0
YIL111W	COX5B	Subunit Vb of cytochrome c oxidase, which is the terminal member of the mitochondrial inner membrane electron transport chain; predominantly expressed during anaerobic growth while its isoform Va (Cox5Ap) is expressed during aerobic growth	38.1%	-1.4	0.0002	0	2	0	0
YER182 W	FMP10	Putative protein of unknown function; the authentic, non-tagged protein is detected in highly purified mitochondria in high-throughput studies	38.1%	-1.4	9E-05	0	0	0	0
YPR124 W	CTR1	High-affinity copper transporter of the plasma membrane, mediates nearly all copper uptake under low copper conditions; transcriptionally induced at low copper levels and degraded at high copper levels	38.3%	-1.4	1E-05	8	0	1 0	4
YGR220C	MRPL9	Mitochondrial ribosomal protein of the large subunit	38.3%	-1.4	0.0003	0	0	0	0
YMR058 W	FET3	Ferro-O ₂ -oxidoreductase required for high-affinity iron uptake and involved in mediating resistance to copper ion toxicity, belongs to class of integral membrane multicopper oxidases	38.3%	-1.4	6E-05	0	0	0	0
YDR074 W	TPS2	Phosphatase subunit of the trehalose-6-phosphate synthase/phosphatase complex, which synthesizes the storage carbohydrate trehalose; expression is induced by stress conditions and repressed by the Ras-cAMP pathway	38.4%	-1.4	0.0018	4	2	0	0
YHR033 W	N/A	Putative protein of unknown function; epitope-tagged protein localizes to the cytoplasm	38.5%	-1.4	7E-05	0	0	0	0
YIL006W	YIA6	Mitochondrial NAD ⁺ transporter, involved in the transport of NAD ⁺ into the mitochondria (see also YEA6); member of the mitochondrial carrier subfamily; disputed role as a pyruvate transporter; has putative mouse and human orthologs	38.5%	-1.4	0.0001	9	2	0	0
YBR194 W	AIM4	Protein proposed to be associated with the nuclear pore complex; null mutant is viable, displays elevated frequency of mitochondrial genome loss and is sensitive to freeze-thaw stress	38.6%	-1.4	0.0008	8	3	1 6	4
YDL190C	UFD2	Ubiquitin chain assembly factor (E4) that cooperates with a ubiquitin-activating enzyme (E1), a ubiquitin-conjugating enzyme (E2), and a ubiquitin protein ligase (E3) to conjugate ubiquitin to substrates; also functions as an E3	38.6%	-1.4	3E-06	0	0	0	0
YPL263C	KEL3	Cytoplasmic protein of unknown function	38.6%	-1.4	0.0035	0	0	0	0

Appendix A

ORF	Gene	Description	PRG	LF C	p-val	M M S	T B P	4 N Q O	U V
YOR241 W	MET7	Folypolyglutamate synthetase, catalyzes extension of the glutamate chains of the folate coenzymes, required for methionine synthesis and for maintenance of mitochondrial DNA	38.7%	-1.4	0.0021	2	0	0	9
YIL007C	NAS2	Protein with similarity to the p27 subunit of mammalian proteasome modulator; not essential; interacts with Rpn4p	38.8%	-1.4	0.0005	6	2	0	0
YLR081W	GAL2	Galactose permease, required for utilization of galactose; also able to transport glucose	38.8%	-1.4	2E-06	0	0	0	0
YGR050C	N/A	Dubious open reading frame unlikely to encode a protein, based on available experimental and comparative sequence data	38.8%	-1.4	5E-05	4	0	0	0
YOL033W	MSE1	Mitochondrial glutamyl-tRNA synthetase, predicted to be palmitoylated	39.0%	-1.4	1E-04	0	0	0	2
YDR358 W	GGA1	Golgi-localized protein with homology to gamma-adaptin, interacts with and regulates Arf1p and Arf2p in a GTP-dependent manner in order to facilitate traffic through the late Golgi	39.1%	-1.4	3E-05	5	0	0	0
YBR289 W	SNF5	Subunit of the SWI/SNF chromatin remodeling complex involved in transcriptional regulation; functions interdependently in transcriptional activation with Snf2p and Snf6p	39.1%	-1.4	2E-05	7	3	2	0
YMR294 W	JNM1	Component of the yeast dynactin complex, consisting of Nip100p, Jnm1p, and Arp1p; required for proper nuclear migration and spindle partitioning during mitotic anaphase B	39.1%	-1.4	0.0015	7	0	0	0
YGR112 W	SHY1	Mitochondrial inner membrane protein required for assembly of cytochrome c oxidase (complex IV); associates with complex IV assembly intermediates and complex III/complex IV supercomplexes; similar to human SURF1 involved in Leigh Syndrome	39.1%	-1.4	5E-05	0	0	0	0
YDR515 W	SLF1	RNA binding protein that associates with polysomes; proposed to be involved in regulating mRNA translation; involved in the copper-dependent mineralization of copper sulfide complexes on cell surface in cells cultured in copper salts	39.1%	-1.4	5E-05	0	0	7	0
YNL322C	KRE1	Cell wall glycoprotein involved in beta-glucan assembly; serves as a K1 killer toxin membrane receptor	39.1%	-1.4	0.0034	4	2	1	0
YCL046W	N/A	Dubious open reading frame unlikely to encode a protein, based on available experimental and comparative sequence data; partially overlaps the uncharacterized ORF YCL045C	39.2%	-1.4	0.0003	0	0	0	0
YPL180W	TCO89	Subunit of TORC1 (Tor1p or Tor2p-Kog1p-Lst8p-Tco89p), a complex that regulates growth in response to nutrient availability; cooperates with Ssd1p in the maintenance of cellular integrity; deletion strains are hypersensitive to rapamycin	39.2%	-1.4	0.0024	1 0	0	0	0

Appendix A

ORF	Gene	Description	PRG	LF C	p-val	M M S	T B P	4 N Q O	U V
YOL148C	SPT20	Subunit of the SAGA transcriptional regulatory complex, involved in maintaining the integrity of the complex	39.2%	-1.4	5E-05	7	4	0	0
YLR138W	NHA1	Na ⁺ /H ⁺ antiporter involved in sodium and potassium efflux through the plasma membrane; required for alkali cation tolerance at acidic pH	39.4%	-1.3	0.0006	0	0	0	0
YLR049C	N/A	Putative protein of unknown function	39.5%	-1.3	3E-06	0	0	0	0
YER120 W	SCS2	Integral ER membrane protein that regulates phospholipid metabolism via an interaction with the FFAT motif of Opi1p, also involved in telomeric silencing, disruption causes inositol auxotrophy above 34 degrees C, VAP homolog	39.6%	-1.3	0.0007	0	0	0	0
YPL201C	YIG1	Protein that interacts with glycerol 3-phosphatase and plays a role in anaerobic glycerol production; localizes to the nucleus and cytosol	39.6%	-1.3	0.0004	4	0	0	0
YML010C -B	0	Dubious open reading frame unlikely to encode a functional protein, based on available experimental and comparative sequence data	39.7%	-1.3	7E-06	7	0	0	0
YHL029C	OCA5	Cytoplasmic protein required for replication of Brome mosaic virus in <i>S. cerevisiae</i> , which is a model system for studying replication of positive-strand RNA viruses in their natural hosts	39.8%	-1.3	0.0001	0	0	0	0
YLL042C	ATG10	Conserved E2-like conjugating enzyme that mediates formation of the Atg12p-Atg5p conjugate, which is a critical step in autophagy	39.9%	-1.3	9E-05	0	0	0	0
YBR185C	MBA1	Protein involved in assembly of mitochondrial respiratory complexes; may act as a receptor for proteins destined for export from the mitochondrial matrix to the inner membrane	40.0%	-1.3	0.0003	0	0	0	0
YBR209 W	N/A	Dubious open reading frame unlikely to encode a protein, based on available experimental and comparative sequence data; YBR209W is not an essential gene	40.0%	-1.3	0.0142	0	0	0	0
YFL012W	N/A	Putative protein of unknown function; transcribed during sporulation; null mutant exhibits increased resistance to rapamycin	40.2%	-1.3	0.007	0	0	0	0
YDR461 W	MFA1	Mating pheromone a-factor, made by a cells; interacts with alpha cells to induce cell cycle arrest and other responses leading to mating; biogenesis involves C-terminal modification, N-terminal proteolysis, and export; also encoded by MFA2	40.3%	-1.3	2E-05	0	0	8	0
YMR063 W	RIM9	Protein of unknown function, involved in the proteolytic activation of Rim101p in response to alkaline pH; has similarity to <i>A. nidulans</i> Pall; putative membrane protein	40.3%	-1.3	0.0027	1 0	5	0	0
YGL088W	N/A	Dubious open reading frame unlikely to encode a protein, based on available experimental and comparative sequence data; partially overlaps snR10, a snoRNA required for preRNA processing	40.3%	-1.3	7E-05	0	0	4	0

Appendix A

ORF	Gene	Description	PRG	LF C	p-val	M M S	T B P	4 N Q O	U V
YCR004C	YCP4	Protein of unknown function, has sequence and structural similarity to flavodoxins; predicted to be palmitoylated; the authentic, non-tagged protein is detected in highly purified mitochondria in high-throughput studies	40.3%	-1.3	9E-05	0	0	0	0
YAL023C	PMT2	Protein O-mannosyltransferase, transfers mannose residues from dolichyl phosphate-D-mannose to protein serine/threonine residues; acts in a complex with Pmt1p, can instead interact with Pmt5p in some conditions; target for new antifungals	40.3%	-1.3	0.0008	0	0	0	0
YBR197C	N/A	Putative protein of unknown function; green fluorescent protein (GFP)-fusion protein localizes to the cytoplasm and nucleus; YBR197C is not an essential gene	40.3%	-1.3	0.0002	0	0	0	0
YJL206C	N/A	Putative protein of unknown function; similar to transcriptional regulators from the Zn[2]-Cys[6] binuclear cluster protein family; mRNA is weakly cell cycle regulated, peaking in S phase; induced rapidly upon MMS treatment	40.3%	-1.3	0.0002	0	0	0	0
YBR191 W	RPL21A	Protein component of the large (60S) ribosomal subunit, nearly identical to Rpl21Bp and has similarity to rat L21 ribosomal protein	40.4%	-1.3	5E-05	1 6	0	1 0	0
YDR444 W	N/A	Putative protein of unknown function	40.5%	-1.3	0.0002	0	2	0	0
YMR057C	N/A	Dubious open reading frame unlikely to encode a protein, based on available experimental and comparative sequence data; partially overlaps verified ORF AAC1	40.5%	-1.3	0.0001	0	0	0	0
YKR006C	MRPL13	Mitochondrial ribosomal protein of the large subunit, not essential for mitochondrial translation	40.6%	-1.3	0.0001	0	0	0	0
YDR414C	ERD1	Predicted membrane protein required for the retention of luminal endoplasmic reticulum proteins; mutants secrete the endogenous ER protein, BiP (Kar2p)	40.7%	-1.3	2E-05	9	0	0	0
YOR350C	MNE1	Mitochondrial protein similar to <i>Lucilia illustris</i> mitochondrial cytochrome oxidase	40.8%	-1.3	0.02	0	0	0	0
YIL053W	RHR2	Constitutively expressed isoform of DL-glycerol-3-phosphatase; involved in glycerol biosynthesis, induced in response to both anaerobic and, along with the Hor2p/Gpp2p isoform, osmotic stress	40.8%	-1.3	6E-05	4	2	0	0
YGL046W	RIM8	Protein of unknown function, involved in the proteolytic activation of Rim101p in response to alkaline pH; has similarity to <i>A. nidulans</i> PalF; essential for anaerobic growth	40.8%	-1.3	7E-05	1 4	2	1 4	0
YLL038C	ENT4	Protein of unknown function, contains an N-terminal epsin-like domain	40.9%	-1.3	0.0009	0	0	0	0
YKR094C	RPL40B	Fusion protein, identical to Rpl40Ap, that is cleaved to yield ubiquitin and a ribosomal protein of the large (60S) ribosomal subunit with similarity to rat L40; ubiquitin may facilitate assembly of the ribosomal protein into ribosomes	41.0%	-1.3	9E-05	0	0	0	0

Appendix A

ORF	Gene	Description	PRG	LF C	p-val	M M S	T B P	4 N Q O	U V
YOR298 W	MUM3	Protein of unknown function involved in the organization of the outer spore wall layers; has similarity to the tafazzins superfamily of acyltransferases	41.0%	-1.3	0.0123	0	0	0	0
YER093C -A	N/A	Putative protein of unknown function; YER093C-A contains an intron; YER093C-A is not an essential gene	41.1%	-1.3	0.0007	9	0	0	0
YKL081W	TEF4	Translation elongation factor EF-1 gamma	41.1%	-1.3	1E-05	0	0	2 2	0
YPL234C	TFP3	Vacuolar ATPase V0 domain subunit c', involved in proton transport activity; hydrophobic integral membrane protein (proteolipid) containing four transmembrane segments; N and C termini are in the vacuolar lumen	41.2%	-1.3	0.0005	0	0	0	0
YFR012W	N/A	Putative protein of unknown function	41.2%	-1.3	0.0001	3 0	0	1 8	0
YDR363 W	ESC2	Protein involved in silencing; may recruit or stabilize Sir proteins; role in Rad51-dependent homologous recombination repair and intra S-phase DNA damage checkpoint; member of the RENi (Rad60-Esc2-Nip45) family of SUMO-like domain proteins	41.2%	-1.3	0.0014	1 9	0	1 5	0
YGR062C	COX18	Mitochondrial integral inner membrane protein required for membrane insertion of C-terminus of Cox2p; interacts genetically and physically with Mss2p and Pnt1p; similar to <i>S. cerevisiae</i> Oxa1, <i>N. crassa</i> Oxa2p, and <i>E. coli</i> YidC	41.4%	-1.3	6E-05	0	0	0	5
YER019 W	ISC1	Mitochondrial membrane localized inositol phosphosphingolipid phospholipase C, hydrolyzes complex sphingolipids to produce ceramide; activated by phosphatidylserine, cardiolipin, and phosphatidylglycerol; mediates Na ⁺ and Li ⁺ halotolerance	41.4%	-1.3	5E-06	0	2	1 0	0
YGR243 W	FMP43	Putative protein of unknown function; expression regulated by osmotic and alkaline stresses; the authentic, non-tagged protein is detected in highly purified mitochondria in high-throughput studies	41.4%	-1.3	1E-05	0	0	0	0
YER185 W	PUG1	Plasma membrane protein with roles in the uptake of protoporphyrin IX and the efflux of heme; expression is induced under both low-heme and low-oxygen conditions	41.4%	-1.3	7E-06	0	0	0	0
YPL145C	KES1	Member of the oxysterol binding protein family, which includes seven yeast homologs; involved in negative regulation of Sec14p-dependent Golgi complex secretory functions, peripheral membrane protein that localizes to the Golgi complex	41.7%	-1.3	0.0005	0	5	0	0
YMR190C	SGS1	Nucleolar DNA helicase of the RecQ family involved in genome integrity maintenance; regulates chromosome synapsis and meiotic joint molecule/crossover formation; similar to human BLM and WRN proteins implicated in Bloom and Werner syndromes	41.7%	-1.3	0.0002	2 5	0	2 7	3
YIR005W	IST3	Component of the U2 snRNP, required for the first catalytic step of splicing and for spliceosomal assembly; interacts with Rds3p and is required for Mer1p-activated splicing	41.8%	-1.3	4E-05	0	0	0	0

Appendix A

ORF	Gene	Description	PRG	LF C	p-val	M M S	T B P	4 N Q O	U V
YDR471 W	RPL27B	Protein component of the large (60S) ribosomal subunit, nearly identical to Rpl27Ap and has similarity to rat L27 ribosomal protein	41.8%	-1.3	9E-06	0	0	0	0
YAR018C	KIN3	Nonessential protein kinase with unknown cellular role	41.8%	-1.3	0.0003	0	0	1 0	0
YOR051C	N/A	Nuclear protein that inhibits replication of Brome mosaic virus in <i>S. cerevisiae</i> , which is a model system for studying replication of positive-strand RNA viruses in their natural hosts	41.9%	-1.3	0.0007	7	0	0	0
YOL115W	PAP2	Catalytic subunit of TRAMP, a nuclear poly (A) polymerase complex involved in RNA quality control; catalyzes polyadenylation of unmodified tRNAs, and snoRNA and rRNA precursors; has 5'-dRP lyase activity; disputed role as a DNA polymerase	41.9%	-1.3	6E-05	4	0	0	0
YMR175 W	SIP18	Protein of unknown function whose expression is induced by osmotic stress	41.9%	-1.3	0.0002	0	0	0	0
YGR122C -A	N/A	Dubious open reading frame unlikely to encode a functional protein, similar to YLR334C and YOL106W	42.0%	-1.3	2E-05	0	0	1 0	0
YGL261C	N/A	Putative protein of unknown function; mRNA expression appears to be regulated by SUT1 and UPC2; YGL261C is not an essential gene	42.0%	-1.3	0.0018	0	0	0	0
YLR118C	N/A	Acyl-protein thioesterase responsible for depalmitoylation of Gpa1p; green fluorescent protein (GFP)-fusion protein localizes to both the cytoplasm and nucleus and is induced in response to the DNA-damaging agent MMS	42.1%	-1.2	0.0003	4	0	0	0
YHL033C	RPL8A	Ribosomal protein L4 of the large (60S) ribosomal subunit, nearly identical to Rpl8Bp and has similarity to rat L7a ribosomal protein; mutation results in decreased amounts of free 60S subunits	42.1%	-1.2	0.0014	0	0	0	0
YNL086W	N/A	Putative protein of unknown function; green fluorescent protein (GFP)-fusion protein localizes to endosomes	42.1%	-1.2	0.0016	0	0	0	0
YMR054 W	STV1	Subunit a of the vacuolar-ATPase V0 domain, one of two isoforms (Stv1p and Vph1p); Stv1p is located in V-ATPase complexes of the Golgi and endosomes while Vph1p is located in V-ATPase complexes of the vacuole	42.2%	-1.2	0.0015	0	0	0	0
YDR506C	N/A	Possible membrane-localized protein	42.2%	-1.2	0.0002	0	0	4	0
YLR131C	ACE2	Transcription factor that activates expression of early G1-specific genes, localizes to daughter cell nuclei after cytokinesis and delays G1 progression in daughters, localization is regulated by phosphorylation; potential Cdc28p substrate	42.2%	-1.2	2E-05	0	0	0	0
YGL202W	ARO8	Aromatic aminotransferase I, expression is regulated by general control of amino acid biosynthesis	42.3%	-1.2	0.0002	0	0	0	0
YBR259 W	N/A	Putative protein of unknown function; YBR259W is not an essential gene	42.3%	-1.2	0.0038	0	0	0	0

Appendix A

ORF	Gene	Description	PRG	LF C	p-val	M M S	T B P	4 N Q O	U V
YGR100W	MDR1	Cytoplasmic GTPase-activating protein for Ypt/Rab transport GTPases Ypt6p, Ypt31p and Sec4p; involved in recycling of internalized proteins and regulation of Golgi secretory function	42.3%	-1.2	0.0003	0	0	1 2	0
YDL182W	LYS20	Homocitrate synthase isozyme, catalyzes the condensation of acetyl-CoA and alpha-ketoglutarate to form homocitrate, which is the first step in the lysine biosynthesis pathway; highly similar to the other isozyme, Lys21p	42.4%	-1.2	5E-05	0	0	0	0
YGR018C	N/A	Dubious open reading frame unlikely to encode a protein, based on available experimental and comparative sequence data; partially overlaps the uncharacterized ORF YGR017W	42.4%	-1.2	6E-05	0	0	1 2	0
YIL073C	SPO22	Meiosis-specific protein essential for chromosome synapsis, involved in completion of nuclear divisions during meiosis; induced early in meiosis	42.4%	-1.2	0.0001	2	0	0	0
YGR122W	N/A	Probable ortholog of <i>A. nidulans</i> PalC, which is involved in pH regulation and binds to the ESCRT-III complex; null mutant does not properly process Rim101p and has decreased resistance to rapamycin; GFP-fusion protein is cytoplasmic	42.5%	-1.2	0.0003	1 9	0	0	0
YOR014W	RTS1	B-type regulatory subunit of protein phosphatase 2A (PP2A); homolog of the mammalian B' subunit of PP2A	42.6%	-1.2	0.0006	4	0	0	0
YLR413W	N/A	Putative protein of unknown function; YLR413W is not an essential gene	42.6%	-1.2	0.0001	0	0	0	0
YJR094W-A	RPL43B	Protein component of the large (60S) ribosomal subunit, identical to Rpl43Ap and has similarity to rat L37a ribosomal protein	42.7%	-1.2	0.0001	0	0	0	0
YIL069C	RPS24B	Protein component of the small (40S) ribosomal subunit; identical to Rps24Ap and has similarity to rat S24 ribosomal protein	42.7%	-1.2	0.0001	2	0	9	0
YJR102C	VPS25	Component of the ESCRT-II complex, which is involved in ubiquitin-dependent sorting of proteins into the endosome	42.7%	-1.2	0.003	1 4	5	0	0
YLR391W	CCW14	Covalently linked cell wall glycoprotein, present in the inner layer of the cell wall	42.7%	-1.2	0.0011	0	0	0	0
YNL082W	PMS1	ATP-binding protein required for mismatch repair in mitosis and meiosis; functions as a heterodimer with Mlh1p, binds double- and single-stranded DNA via its N-terminal domain, similar to <i>E. coli</i> MutL	42.8%	-1.2	0.0014	8	0	0	0
YGR197C	SNG1	Protein involved in nitrosoguanidine (MNNG) resistance; expression is regulated by transcription factors involved in multidrug resistance	42.9%	-1.2	4E-05	2	0	0	0
YDL047W	SIT4	Type 2A-related serine-threonine phosphatase that functions in the G1/S transition of the mitotic cycle; cytoplasmic and nuclear protein that modulates functions mediated by Pkc1p including cell wall and actin cytoskeleton organization	43.0%	-1.2	0.0065	0	4	1 3	6

Appendix A

ORF	Gene	Description	PRG	LF C	p-val	M M S	T B P	4 N Q O	U V
YCL006C	0	Dubious ORF unlikely to encode a protein; overlaps verified ORF YCL005W-A; mutations in YCL007C were thought to confer sensitivity to calcofluor white, but this phenotype was later shown to be due to the defect in YCL005W-A	43.0%	-1.2	0.0002	0	0	0	0
YDR133C	N/A	Dubious open reading frame unlikely to encode a protein, based on available experimental and comparative sequence data; partially overlaps YDR134C	43.0%	-1.2	0.0001	0	0	0	0
YDL082W	RPL13A	Protein component of the large (60S) ribosomal subunit, nearly identical to Rpl13Bp; not essential for viability; has similarity to rat L13 ribosomal protein	43.0%	-1.2	0.0003	0	2	0	0
YMR019 W	STB4	Protein that binds Sin3p in a two-hybrid assay; contains a Zn(II)2Cys6 zinc finger domain characteristic of DNA-binding proteins; computational analysis suggests a role in regulation of expression of genes encoding transporters	43.0%	-1.2	6E-05	0	3	0	0
YDR105C	TMS1	Vacuolar membrane protein of unknown function that is conserved in mammals; predicted to contain eleven transmembrane helices; interacts with Pdr5p, a protein involved in multidrug resistance	43.1%	-1.2	6E-05	0	0	0	0
YIL136W	OM45	Protein of unknown function, major constituent of the mitochondrial outer membrane; located on the outer (cytosolic) face of the outer membrane	43.1%	-1.2	8E-05	0	0	0	0
YHR021C	RPS27B	Protein component of the small (40S) ribosomal subunit; nearly identical to Rps27Ap and has similarity to rat S27 ribosomal protein	43.2%	-1.2	0.0002	0	0	1 8	0
YIL092W	N/A	Putative protein of unknown function; green fluorescent protein (GFP)-fusion protein localizes to the cytoplasm and to the nucleus	43.3%	-1.2	0.0002	0	4	0	0
YDR096 W	GIS1	JmjC domain-containing histone demethylase; transcription factor involved in the expression of genes during nutrient limitation; also involved in the negative regulation of DPP1 and PHR1	43.3%	-1.2	2E-05	0	0	0	0
YJL057C	IKS1	Putative serine/threonine kinase; expression is induced during mild heat stress; deletion mutants are hypersensitive to copper sulphate and resistant to sorbate; interacts with an N-terminal fragment of Sst2p	43.3%	-1.2	0.0002	4	0	0	0
YFL010W -A	AUA1	Protein required for the negative regulation by ammonia of Gap1p, which is a general amino acid permease	43.4%	-1.2	0.0002	0	0	0	0
YOR385 W	N/A	Putative protein of unknown function; green fluorescent protein (GFP)-fusion protein localizes to the cytoplasm; YOR385W is not an essential gene	43.4%	-1.2	0.0114	4	0	0	0
YPR045C	N/A	Protein of unknown function; involvement in splicing based on pre-mRNA accumulation defect for many intron-containing genes; contains a SAC3 domain; physically interacts with Csn12p; YRP045C is not an essential gene	43.4%	-1.2	4E-05	1 8	0	0	0

Appendix A

ORF	Gene	Description	PRG	LF C	p-val	M M S	T B P	4 N Q O	U V
YJR127C	RSF2	Zinc-finger protein involved in transcriptional control of both nuclear and mitochondrial genes, many of which specify products required for glycerol-based growth, respiration, and other functions	43.4%	-1.2	0.0434	2	2	0	0
YER179 W	DMC1	Meiosis-specific protein required for repair of double-strand breaks and pairing between homologous chromosomes; homolog of Rad51p and the bacterial RecA protein	43.5%	-1.2	4E-05	0	0	0	0
YPL037C	EGD1	Subunit beta1 of the nascent polypeptide-associated complex (NAC) involved in protein targeting, associated with cytoplasmic ribosomes; enhances DNA binding of the Gal4p activator; homolog of human BTF3b	43.5%	-1.2	0.0007	0	2	0	0
YPL078C	ATP4	Subunit b of the stator stalk of mitochondrial F1F0 ATP synthase, which is a large, evolutionarily conserved enzyme complex required for ATP synthesis; phosphorylated	43.5%	-1.2	0.0002	0	0	0	0
YMR228 W	MTF1	Mitochondrial RNA polymerase specificity factor with structural similarity to S-adenosylmethionine-dependent methyltransferases and functional similarity to bacterial sigma-factors, interacts with mitochondrial core polymerase Rpo41p	43.5%	-1.2	0.0001	0	0	0	0
YDR338C	N/A	Putative protein of unknown function	43.6%	-1.2	0.0001	4	0	0	0
YER183C	FAU1	5,10-methenyltetrahydrofolate synthetase, involved in folic acid biosynthesis	43.6%	-1.2	6E-06	0	0	0	0
YIL122W	POG1	Putative transcriptional activator that promotes recovery from pheromone induced arrest; inhibits both alpha-factor induced G1 arrest and repression of CLN1 and CLN2 via SCB/MCB promoter elements; potential Cdc28p substrate; SBF regulated	43.7%	-1.2	0.0004	0	0	0	0
YMR077C	VPS20	Myristoylated subunit of ESCRTIII, the endosomal sorting complex required for transport of transmembrane proteins into the multivesicular body pathway to the lysosomal/vacuolar lumen; cytoplasmic protein recruited to endosomal membranes	43.7%	-1.2	0.0001	3 0	5	0	0
YFL004W	VTC2	Vacuolar membrane protein involved in vacuolar polyphosphate accumulation; functions as a regulator of vacuolar H ⁺ -ATPase activity and vacuolar transporter chaperones; involved in protein localization and non-autophagic vacuolar fusion	43.7%	-1.2	5E-05	0	0	7	0
YDR245 W	MNN10	Subunit of a Golgi mannosyltransferase complex also containing Anp1p, Mnn9p, Mnn11p, and Hoc1p that mediates elongation of the polysaccharide mannan backbone; membrane protein of the mannosyltransferase family	43.7%	-1.2	0.0023	0	0	0	0

Appendix A

ORF	Gene	Description	PRG	LF C	p-val	M M S	T B P	4 N Q O	U V
YKL143W	LTV1	Component of the GSE complex, which is required for proper sorting of amino acid permease Gap1p; required for ribosomal small subunit export from nucleus; required for growth at low temperature	43.9%	-1.2	0.0029	0	0	1 2	0
YMR179 W	SPT21	Protein required for normal transcription at several loci including HTA2-HTB2 and HHF2-HHT2, but not required at the other histone loci; functionally related to Spt10p; involved in telomere maintenance	43.9%	-1.2	0.0013	9	0	1 9	6
YKL170W	MRPL38	Mitochondrial ribosomal protein of the large subunit; appears as two protein spots (YmL34 and YmL38) on two-dimensional SDS gels	44.0%	-1.2	5E-06	0	0	0	0
YIL017C	VID28	Protein involved in proteasome-dependent catabolite degradation of fructose-1,6-bisphosphatase (FBPase); localized to the nucleus and the cytoplasm	44.0%	-1.2	0.0001	6	2	0	0
YNL228W	N/A	Dubious open reading frame unlikely to encode a functional protein, based on available experimental and comparative sequence data; almost completely overlaps ORF YNL227C/JJJ1	44.1%	-1.2	3E-05	0	0	0	0
YPL186C	UIP4	Protein that interacts with Ulp1p, a Ubl (ubiquitin-like protein)-specific protease for Smt3p protein conjugates; detected in a phosphorylated state in the mitochondrial outer membrane; also detected in ER and nuclear envelope	44.2%	-1.2	0.0111	0	0	0	0
YPL167C	REV3	Catalytic subunit of DNA polymerase zeta, which is involved in DNA repair and translesion synthesis; required for mutagenesis induced by DNA damage	44.2%	-1.2	0.0018	1 8	0	1 9	0
YDR382 W	RPP2B	Ribosomal protein P2 beta, a component of the ribosomal stalk, which is involved in the interaction between translational elongation factors and the ribosome; regulates the accumulation of P1 (Rpp1Ap and Rpp1Bp) in the cytoplasm	44.3%	-1.2	0.0037	0	0	0	0
YPR141C	KAR3	Minus-end-directed microtubule motor that functions in mitosis and meiosis, localizes to the spindle pole body and localization is dependent on functional Cik1p, required for nuclear fusion during mating; potential Cdc28p substrate	44.3%	-1.2	0.0007	1 8	0	3 0	7
YOR030 W	DFG16	Probable multiple transmembrane protein, involved in diploid invasive and pseudohyphal growth upon nitrogen starvation; required for accumulation of processed Rim101p	44.4%	-1.2	0.0509	1 4	2	0	5
YCL045C	EMC1	Member of a transmembrane complex required for efficient folding of proteins in the ER; null mutant displays induction of the unfolded protein response; interacts with Gal80p	44.4%	-1.2	0.0001	0	0	0	0
YLR063W	N/A	Putative S-adenosylmethionine-dependent methyltransferase; green fluorescent protein (GFP)-fusion protein localizes to the cytoplasm; YLR063W is not an essential gene	44.4%	-1.2	0.0006	0	2	0	0

Appendix A

ORF	Gene	Description	PRG	LF C	p-val	M M S	T B P	4 N Q O	U V
YOR384 W	FRE5	Putative ferric reductase with similarity to Fre2p; expression induced by low iron levels; the authentic, non-tagged protein is detected in highly purified mitochondria in high-throughput studies	44.4%	-1.2	0.049	0	0	0	0
YMR089C	YTA12	Component, with Afg3p, of the mitochondrial inner membrane m-AAA protease that mediates degradation of misfolded or unassembled proteins and is also required for correct assembly of mitochondrial enzyme complexes	44.5%	-1.2	0.0002	0	0	0	0
YML080 W	DUS1	Dihydrouridine synthase, member of a widespread family of conserved proteins including Smm1p, Dus3p, and Dus4p; modifies pre-tRNA(Phe) at U17	44.5%	-1.2	0.0002	6	0	0	0
YLR019W	PSR2	Functionally redundant Psr1p homolog, a plasma membrane phosphatase involved in the general stress response; required with Psr1p and Whi2p for full activation of STRE-mediated gene expression, possibly through dephosphorylation of Msn2p	44.5%	-1.2	2E-05	0	2	0	0
YPL005W	AEP3	Peripheral mitochondrial inner membrane protein, located on the matrix face of the membrane; stabilizes the bicistronic AAP1-ATP6 mRNA encoding subunits 6 and 8 of the ATP synthase complex	44.6%	-1.2	0.0004	0	0	0	0
YOR378 W	N/A	Putative protein of unknown function; belongs to the DHA2 family of drug:H ⁺ antiporters; YOR378W is not an essential gene	44.6%	-1.2	0.0008	0	0	0	0
YKL055C	OAR1	Mitochondrial 3-oxoacyl-[acyl-carrier-protein] reductase, may comprise a type II mitochondrial fatty acid synthase along with Mct1p	44.6%	-1.2	0.0001	4	0	0	0
YLR057W	N/A	Putative protein of unknown function; YLR050C is not an essential gene	44.6%	-1.2	2E-06	4	0	0	0
YDR340 W	N/A	Putative protein of unknown function	44.6%	-1.2	3E-05	0	0	9	0
YMR167 W	MLH1	Protein required for mismatch repair in mitosis and meiosis as well as crossing over during meiosis; forms a complex with Pms1p and Msh2p-Msh3p during mismatch repair; human homolog is associated with hereditary non-polyposis colon cancer	44.6%	-1.2	4E-05	7	0	0	0
YGR254 W	ENO1	Enolase I, a phosphopyruvate hydratase that catalyzes the conversion of 2-phosphoglycerate to phosphoenolpyruvate during glycolysis and the reverse reaction during gluconeogenesis; expression is repressed in response to glucose	44.6%	-1.2	0.0007	0	0	0	0
YAL047C	SPC72	Component of the cytoplasmic Tub4p (gamma-tubulin) complex, binds spindle pole bodies and links them to microtubules; has roles in astral microtubule formation and stabilization	44.7%	-1.2	0.0003	7	0	2 2	0

Appendix A

ORF	Gene	Description	PRG	LF C	p-val	M M S	T B P	4 N Q O	U V
YJR087W	N/A	Dubious open reading frame, unlikely to encode a protein; not conserved in closely related <i>Saccharomyces</i> species; partially overlaps the verified gene STE18 and uncharacterized ORF YJR088C	44.7%	-1.2	4E-06	0	0	0	0
YHR191C	CTF8	Subunit of a complex with Ctf18p that shares some subunits with Replication Factor C and is required for sister chromatid cohesion	44.8%	-1.2	0.0003	1 8	0	1 8	0
YML050 W	AIM32	Putative protein of unknown function; null mutant is viable and displays elevated frequency of mitochondrial genome loss	44.9%	-1.2	0.0006	0	0	0	0
YGL115W	SNF4	Activating gamma subunit of the AMP-activated Snf1p kinase complex (contains Snf1p and a Sip1p/Sip2p/Gal83p family member); activates glucose-repressed genes, represses glucose-induced genes; role in sporulation, and peroxisome biogenesis	44.9%	-1.2	0.0008	0	0	0	0
YLR083C	EMP70	Protein with a role in cellular adhesion and filamentous growth; similar to Tmn2p and Tmn3p; member of Transmembrane Nine family of proteins with 9 transmembrane segments; 24kDa cleavage product found in endosome-enriched membrane fractions	44.9%	-1.2	6E-05	0	0	0	0
YOL017W	ESC8	Protein involved in telomeric and mating-type locus silencing, interacts with Sir2p and also interacts with the Gal11p, which is a component of the RNA pol II mediator complex	44.9%	-1.2	0.018	0	0	0	0
YOL013C	HRD1	Ubiquitin-protein ligase required for endoplasmic reticulum-associated degradation (ERAD) of misfolded proteins; genetically linked to the unfolded protein response (UPR); regulated through association with Hrd3p; contains an H2 ring finger	44.9%	-1.2	0.0448	0	0	0	0
YDR007 W	TRP1	Phosphoribosylanthranilate isomerase that catalyzes the third step in tryptophan biosynthesis; in 2004, the sequence of TRP1 from strain S228C was updated by changing the previously annotated internal STOP (TAA) to serine (TCA)	44.9%	-1.2	0.0014	0	0	0	0
YDR525 W	API2	Dubious open reading frame, unlikely to encode a protein; not conserved in closely related <i>Saccharomyces</i> species; 26% of ORF overlaps the dubious ORF YDR524C-A; insertion mutation in a <i>cdc34-2</i> mutant background causes altered bud morphology	44.9%	-1.2	0.0002	0	0	0	0
YLR053C	N/A	Putative protein of unknown function	45.0%	-1.2	4E-05	0	0	0	0
YER086 W	ILV1	Threonine deaminase, catalyzes the first step in isoleucine biosynthesis; expression is under general amino acid control; ILV1 locus exhibits highly positioned nucleosomes whose organization is independent of known ILV1 regulation	45.0%	-1.2	0.0002	7	0	1 2	0

Appendix A

ORF	Gene	Description	PRG	LF C	p-val	M M S	T B P	4 N Q O	U V
YOL027C	MDM38	Mitochondrial inner membrane protein, involved in membrane integration of a subset of mitochondrial proteins; required for K ⁺ /H ⁺ exchange; associates with mitochondrial ribosomes; human ortholog Letm1 implicated in Wolf-Hirschhorn syndrome	45.0%	-1.2	0.0014	0	0	0	0
YML051 W	GAL80	Transcriptional regulator involved in the repression of GAL genes in the absence of galactose; inhibits transcriptional activation by Gal4p; inhibition relieved by Gal3p or Gal1p binding	45.2%	-1.1	0.0002	0	0	0	0
YML021C	UNG1	Uracil-DNA glycosylase, required for repair of uracil in DNA formed by spontaneous cytosine deamination, not required for strand-specific mismatch repair, cell-cycle regulated, expressed in late G1, localizes to mitochondria and nucleus	45.2%	-1.1	0.0004	0	0	0	0
YMR285C	NGL2	Protein involved in 5.8S rRNA processing; Ccr4p-like RNase required for correct 3'-end formation of 5.8S rRNA at site E; similar to Ngl1p and Ngl3p	45.2%	-1.1	0.0009	2	0	0	0
YIL041W	GVP36	BAR domain-containing protein that localizes to both early and late Golgi vesicles; required for adaptation to varying nutrient concentrations, fluid-phase endocytosis, polarization of the actin cytoskeleton, and vacuole biogenesis	45.3%	-1.1	0.0001	9	2	0	0
YGL260W	N/A	Putative protein of unknown function; transcription is significantly increased in a NAP1 deletion background; deletion mutant has increased accumulation of nickel and selenium	45.3%	-1.1	0.008	0	0	0	0
YGR054 W	N/A	Eukaryotic initiation factor (eIF) 2A; associates specifically with both 40S subunits and 80 S ribosomes, and interacts genetically with both eIF5b and eIF4E; homologous to mammalian eIF2A	45.3%	-1.1	8E-06	0	0	0	0
YDR133C	N/A	Dubious open reading frame unlikely to encode a protein, based on available experimental and comparative sequence data; partially overlaps YDR134C	45.3%	-1.1	0.0001	0	0	0	0
YOL110W	SHR5	Subunit of a palmitoyltransferase, composed of Shr5p and Erf2p, that adds a palmitoyl lipid moiety to heterolipidated substrates such as Ras1p and Ras2p through a thioester linkage; palmitoylation is required for Ras2p membrane localization	45.4%	-1.1	2E-05	4	0	0	0
YLR047C	FRE8	Protein with sequence similarity to iron/copper reductases, involved in iron homeostasis; deletion mutant has iron deficiency/accumulation growth defects; expression increased in the absence of copper-responsive transcription factor Mac1p	45.4%	-1.1	0.0004	0	0	0	0
YER184C	N/A	Putative zinc cluster protein; deletion confers sensitivity to Calcufluor white, and prevents growth on glycerol or lactate as sole carbon source	45.5%	-1.1	1E-04	0	0	0	0

Appendix A

ORF	Gene	Description	PRG	LF C	p-val	M M S	T B P	4 N Q O	U V
YKL205W	LOS1	Nuclear pore protein involved in nuclear export of pre-tRNA	45.5%	-1.1	0.0019	0	0	0	0
YGR014 W	MSB2	Mucin family member involved in the Cdc42p- and MAP kinase-dependent filamentous growth signaling pathway; also functions as an osmosensor in parallel to the Sho1p-mediated pathway; potential Cdc28p substrate	45.6%	-1.1	0.0003	0	0	0	0
YLR073C	N/A	Protein of unknown function; green fluorescent protein (GFP)-fusion protein localizes to endosomes; YLR073C is not an essential gene	45.6%	-1.1	3E-06	0	0	0	0
YLR020C	YEH2	Steryl ester hydrolase, catalyzes steryl ester hydrolysis at the plasma membrane; involved in sterol metabolism	45.6%	-1.1	0.0002	0	0	0	0
YEL051W	VMA8	Subunit D of the eight-subunit V1 peripheral membrane domain of the vacuolar H ⁺ -ATPase (V-ATPase), an electrogenic proton pump found throughout the endomembrane system; plays a role in the coupling of proton transport and ATP hydrolysis	45.7%	-1.1	0.0018	1 8	9	3 0	0
YGR276C	RNH70	3'-5' exoribonuclease; required for maturation of 3' ends of 5S rRNA and tRNA-Arg3 from dicistronic transcripts	45.8%	-1.1	0.0004	0	0	0	0
YBR222C	PCS60	Peroxisomal AMP-binding protein, localizes to both the peroxisomal peripheral membrane and matrix, expression is highly inducible by oleic acid, similar to E. coli long chain acyl-CoA synthetase	45.8%	-1.1	0.0138	0	0	0	0
YPL077C	N/A	Putative protein of unknown function; regulates PIS1 expression; mutant displays spore wall assembly defect in ether sensitivity screen; YPL077C is not an essential gene	45.8%	-1.1	0.0028	0	0	0	0
YER089C	PTC2	Type 2C protein phosphatase; dephosphorylates Hog1p to limit maximal osmostress induced kinase activity; dephosphorylates Ire1p to downregulate the unfolded protein response; dephosphorylates Cdc28p; role in DNA checkpoint inactivation	45.8%	-1.1	0.0003	0	0	0	0
YDR124 W	N/A	Putative protein of unknown function; non-essential gene; expression is strongly induced by alpha factor	45.9%	-1.1	0.0001	0	0	0	0
YDR349C	YPS7	Putative GPI-anchored aspartic protease, located in the cytoplasm and endoplasmic reticulum	45.9%	-1.1	2E-05	0	0	0	0
YDR242 W	AMD2	Putative amidase	46.0%	-1.1	0.0006	4	0	3	0
YBR290 W	BSD2	Heavy metal ion homeostasis protein, facilitates trafficking of Smf1p and Smf2p metal transporters to the vacuole where they are degraded, controls metal ion transport, prevents metal hyperaccumulation, functions in copper detoxification	46.0%	-1.1	0.0006	0	3	0	0
YML102C -A	N/A	Dubious open reading frame unlikely to encode a functional protein, based on available experimental and comparative sequence data	46.1%	-1.1	5E-05	1 5	0	1 2	0

Appendix A

ORF	Gene	Description	PRG	LF C	p-val	M M S	T B P	4 N Q O	U V
YPL244C	HUT1	Protein with a role in UDP-galactose transport to the Golgi lumen, has similarity to human UDP-galactose transporter UGTrel1, exhibits a genetic interaction with <i>S. cerevisiae</i> ERO1	46.3%	-1.1	0.0046	0	0	0	0
YPL066W	N/A	Putative protein of unknown function; green fluorescent protein (GFP)-fusion protein localizes to the bud neck and cytoplasm; null mutant is viable and exhibits growth defect on a non-fermentable (respiratory) carbon source	46.3%	-1.1	2E-05	0	0	0	0
YDR146C	SWI5	Transcription factor that activates transcription of genes expressed at the M/G1 phase boundary and in G1 phase; localization to the nucleus occurs during G1 and appears to be regulated by phosphorylation by Cdc28p kinase	46.3%	-1.1	0.0001	7	0	0	0
YGL027C	CWH41	Processing alpha glucosidase I, ER type II integral membrane N-glycoprotein involved in assembly of cell wall beta 1,6 glucan and asparagine-linked protein glycosylation; also involved in ER protein quality control and sensing of ER stress	46.4%	-1.1	0.0273	0	0	0	0
YOR301 W	RAX1	Protein involved in bud site selection during bipolar budding; localization requires Rax2p; has similarity to members of the insulin-related peptide superfamily	46.4%	-1.1	0.0359	0	0	0	0
YDR120C	TRM1	tRNA methyltransferase, localizes to both the nucleus and mitochondrion to produce the modified base N2,N2-dimethylguanosine in tRNAs in both compartments	46.5%	-1.1	0.0001	0	0	4	0
YLR452C	SST2	GTPase-activating protein for Gpa1p, regulates desensitization to alpha factor pheromone; also required to prevent receptor-independent signaling of the mating pathway; member of the RGS (regulator of G-protein signaling) family	46.6%	-1.1	0.0002	0	0	0	0
YJL121C	RPE1	D-ribose-5-phosphate 3-epimerase, catalyzes a reaction in the non-oxidative part of the pentose-phosphate pathway; mutants are sensitive to oxidative stress	46.6%	-1.1	0.0003	0	0	0	0
YGL110C	CUE3	Protein of unknown function; has a CUE domain that binds ubiquitin, which may facilitate intramolecular monoubiquitination	46.6%	-1.1	3E-05	0	0	1 2	1 0
YPR074C	TKL1	Transketolase, similar to Tkl2p; catalyzes conversion of xylulose-5-phosphate and ribose-5-phosphate to sedoheptulose-7-phosphate and glyceraldehyde-3-phosphate in the pentose phosphate pathway; needed for synthesis of aromatic amino acids	46.8%	-1.1	0.0017	7	0	0	0
YER116C	SLX8	Subunit of the Six5-Six8 SUMO-targeted ubiquitin ligase (STUbL) complex; stimulated by prior attachment of SUMO to the substrate; contains a C-terminal RING domain	46.8%	-1.1	6E-05	1 1	0	7	6
YKR030 W	GMH1	Golgi membrane protein of unknown function, interacts with Gea1p and Gea2p; required for localization of Gea2p; computational analysis suggests a possible role in either cell wall synthesis or protein-vacuolar targeting	46.8%	-1.1	0.0001	2	0	0	0

Appendix A

ORF	Gene	Description	PRG	LF C	p-val	M M S	T B P	4 N Q O	U V
YDR377 W	ATP17	Subunit f of the F0 sector of mitochondrial F1F0 ATP synthase, which is a large, evolutionarily conserved enzyme complex required for ATP synthesis	46.9%	-1.1	0.0004	0	0	0	4
YMR307 W	GAS1	Beta-1,3-glucanosyltransferase, required for cell wall assembly; localizes to the cell surface via a glycosylphosphatidylinositol (GPI) anchor	46.9%	-1.1	0.0006	4	5	9	0
YOR054C	VHS3	Functionally redundant (see also SIS2) inhibitory subunit of Ppz1p, a PP1c-related ser/thr protein phosphatase Z isoform; synthetically lethal with sis2; putative phosphopantothencycysteine decarboxylase involved in coenzyme A biosynthesis	47.1%	-1.1	0.0009	4	0	9	7
YMR006C	PLB2	Phospholipase B (lysophospholipase) involved in phospholipid metabolism; displays transacylase activity in vitro; overproduction confers resistance to lysophosphatidylcholine	47.1%	-1.1	0.0081	0	3	0	0
YDR111C	ALT2	Putative alanine transaminase (glutamic pyruvic transaminase)	47.1%	-1.1	0.0001	0	0	0	0
YAL054C	ACS1	Acetyl-coA synthetase isoform which, along with Acs2p, is the nuclear source of acetyl-coA for histone acetylation; expressed during growth on nonfermentable carbon sources and under aerobic conditions	47.2%	-1.1	0.0005	4	0	0	0
YIL077C	N/A	Putative protein of unknown function; the authentic, non-tagged protein is detected in highly purified mitochondria in high-throughput studies; deletion confers sensitivity to 4-(N-(S-glutathionylacetyl)amino) phenylarsenoxide (GSAO)	47.3%	-1.1	0.0008	2	2	0	0
YNL068C	FKH2	Forkhead family transcription factor with a major role in the expression of G2/M phase genes; positively regulates transcriptional elongation; negative role in chromatin silencing at HML and HMR; substrate of the Cdc28p/Cib5p kinase	47.3%	-1.1	7E-05	8	0	0	0
YPL071C	N/A	Putative protein of unknown function; green fluorescent protein (GFP)-fusion protein localizes to both the cytoplasm and the nucleus	47.4%	-1.1	0.0005	0	0	0	0
YLR003C	CMS1	Subunit of U3-containing 90S preribosome processome complex involved in production of 18S rRNA and assembly of small ribosomal subunit; overexpression rescues suppressor mutant of mcm10; null mutant is viable	47.4%	-1.1	2E-05	0	0	0	0
YLR352W	N/A	Putative protein of unknown function with similarity to F-box proteins; interacts with Skp1p and Cdc53p; YLR352W is not an essential gene	47.4%	-1.1	0.0012	0	0	0	0
YNL064C	YDJ1	Protein chaperone involved in regulation of the HSP90 and HSP70 functions; involved in protein translocation across membranes; member of the DnaJ family	47.4%	-1.1	0.0002	1 5	0	2 6	1 5

Appendix A

ORF	Gene	Description	PRG	LF C	p-val	M M S	T B P	4 N Q O	U V
YLR123C	N/A	Dubious open reading frame unlikely to encode a protein, based on available experimental and comparative sequence data; partially overlaps the dubious ORF YLR122C; contains characteristic aminoacyl-tRNA motif	47.5%	-1.1	0.0009	0	0	0	0
YOL105C	WSC3	Partially redundant sensor-transducer of the stress-activated PKC1-MPK1 signaling pathway involved in maintenance of cell wall integrity; involved in the response to heat shock and other stressors; regulates 1,3-beta-glucan synthesis	47.5%	-1.1	2E-05	4	0	0	0
YGR165 W	MRPS3 5	Mitochondrial ribosomal protein of the small subunit	47.5%	-1.1	5E-05	0	0	0	0
YDR121 W	DPB4	Shared subunit of DNA polymerase (II) epsilon and of ISW2/yCHRAC chromatin accessibility complex; involved in both chromosomal DNA replication and in inheritance of telomeric silencing	47.5%	-1.1	0.0005	0	0	0	0
YMR202 W	ERG2	C-8 sterol isomerase, catalyzes the isomerization of the delta-8 double bond to the delta-7 position at an intermediate step in ergosterol biosynthesis	47.5%	-1.1	0.0008	1 2	0	2 9	0
YBR077C	SLM4	Component of the EGO complex, which is involved in the regulation of microautophagy, and of the GSE complex, which is required for proper sorting of amino acid permease Gap1p; gene exhibits synthetic genetic interaction with MSS4	47.5%	-1.1	5E-05	2	0	0	0
YBR031 W	RPL4A	N-terminally acetylated protein component of the large (60S) ribosomal subunit, nearly identical to Rpl4Bp and has similarity to E. coli L4 and rat L4 ribosomal proteins	47.6%	-1.1	2E-07	0	0	0	0
YML078 W	CPR3	Mitochondrial peptidyl-prolyl cis-trans isomerase (cyclophilin), catalyzes the cis-trans isomerization of peptide bonds N-terminal to proline residues; involved in protein refolding after import into mitochondria	47.7%	-1.1	0.0002	0	0	0	0
YLR067C	PET309	Specific translational activator for the COX1 mRNA, also influences stability of intron-containing COX1 primary transcripts; localizes to the mitochondrial inner membrane; contains seven pentatricopeptide repeats (PPRs)	47.8%	-1.1	2E-05	0	0	0	0
YER054C	GIP2	Putative regulatory subunit of the protein phosphatase Glc7p, involved in glycogen metabolism; contains a conserved motif (GVNK motif) that is also found in Gac1p, Pig1p, and Pig2p	47.8%	-1.1	2E-05	0	0	0	0
YBR081C	SPT7	Subunit of the SAGA transcriptional regulatory complex, involved in proper assembly of the complex; also present as a C-terminally truncated form in the SLIK/SALSA transcriptional regulatory complex	47.9%	-1.1	2E-05	1 0	1 1	2 2	0
YML100 W	TSL1	Large subunit of trehalose 6-phosphate synthase (Tps1p)/phosphatase (Tps2p) complex, which converts uridine-5'-diphosphoglucose and glucose 6-phosphate to trehalose, homologous to Tps3p and may share function	47.9%	-1.1	9E-05	0	2	0	0

Appendix A

ORF	Gene	Description	PRG	LF C	p-val	M M S	T B P	4 N Q O	U V
YOR092 W	ECM3	Non-essential protein of unknown function; involved in signal transduction and the genotoxic response; induced rapidly in response to treatment with 8-methoxypsoralen and UVA irradiation	47.9%	-1.1	0.0061	0	0	0	0
YLR077W	FMP25	Putative protein of unknown function; the authentic, non-tagged protein is detected in highly purified mitochondria in high-throughput studies	48.0%	-1.1	0.0002	0	0	0	0
YDR456 W	NHX1	Endosomal Na ⁺ /H ⁺ exchanger, required for intracellular sequestration of Na ⁺ ; required for osmotolerance to acute hypertonic shock	48.0%	-1.1	7E-05	7	0	2 1	0
YDR073 W	SNF11	Subunit of the SWI/SNF chromatin remodeling complex involved in transcriptional regulation; interacts with a highly conserved 40-residue sequence of Snf2p	48.0%	-1.1	6E-05	0	0	0	0
YDR455C	N/A	Dubious open reading frame unlikely to encode a protein, based on available experimental and comparative sequence data; partially overlaps the verified gene YDR456W	48.1%	-1.1	0.0024	1 0	0	2 1	0
YCL044C	MGR1	Subunit of the mitochondrial (mt) i-AAA protease supercomplex, which degrades misfolded mitochondrial proteins; forms a subcomplex with Mgr3p that binds to substrates to facilitate proteolysis; required for growth of cells lacking mtDNA	48.2%	-1.1	0.0002	0	0	7	0
YLL040C	VPS13	Protein of unknown function; heterooligomeric or homooligomeric complex; peripherally associated with membranes; homologous to human COH1; involved in sporulation, vacuolar protein sorting and protein-Golgi retention	48.2%	-1.1	9E-05	4	0	0	0
YDR108 W	GSG1	Subunit of TRAPP (transport protein particle), a multi-subunit complex involved in targeting and/or fusion of ER-to-Golgi transport vesicles with their acceptor compartment; protein has late meiotic role, following DNA replication	48.3%	-1.1	0.0002	0	0	0	0
YOL059W	GPD2	NAD-dependent glycerol 3-phosphate dehydrogenase, homolog of Gpd1p, expression is controlled by an oxygen-independent signaling pathway required to regulate metabolism under anoxic conditions; located in cytosol and mitochondria	48.3%	-1.1	0.0006	0	0	0	0
YIL064W	SEE1	Protein with a role in intracellular transport; has sequence similarity to S-adenosylmethionine-dependent methyltransferases of the seven beta-strand family	48.3%	-1.0	7E-05	4	2	0	0
YNL099C	OCA1	Putative protein tyrosine phosphatase, required for cell cycle arrest in response to oxidative damage of DNA	48.3%	-1.0	0.0003	0	0	0	0
YDR257C	RKM4	Ribosomal lysine methyltransferase specific for monomethylation of Rpl42ap and Rpl42bp (lysine 55); nuclear SET-domain containing protein	48.4%	-1.0	0.0008	2	2	0	0

Appendix A

ORF	Gene	Description	PRG	LF C	p-val	M M S	T B P	4 N Q O	U V
YMR313C	TGL3	Triacylglycerol lipase of the lipid particle, responsible for all the TAG lipase activity of the lipid particle; contains the consensus sequence motif GXSXG, which is found in lipolytic enzymes; required with Tgl4p for timely bud formation	48.4%	-1.0	0.0004	2	0	0	0
YCR034 W	FEN1	Fatty acid elongase, involved in sphingolipid biosynthesis; acts on fatty acids of up to 24 carbons in length; mutations have regulatory effects on 1,3-beta-glucan synthase, vacuolar ATPase, and the secretory pathway	48.4%	-1.0	0.01	0	0	0	0
YCR031C	RPS14A	Ribosomal protein 59 of the small subunit, required for ribosome assembly and 20S pre-rRNA processing; mutations confer cryptopleurine resistance; nearly identical to Rps14Bp and similar to E. coli S11 and rat S14 ribosomal proteins	48.5%	-1.0	0.001	0	0	0	0
YDR474C	JIP4	Protein of unknown function; previously annotated as two separate ORFs, YDR474C and YDR475C, which were merged as a result of corrections to the systematic reference sequence	48.6%	-1.0	0.0003	0	0	0	0
YHR203C	RPS4B	Protein component of the small (40S) ribosomal subunit; identical to Rps4Ap and has similarity to rat S4 ribosomal protein	48.6%	-1.0	0.0004	0	0	3	0
YGR228 W	N/A	Dubious open reading frame unlikely to encode a protein, based on available experimental and comparative sequence data; partially overlaps the verified ORF SMI1/YGR229C	48.7%	-1.0	0.0003	0	0	9	0
YMR053C	STB2	Protein that interacts with Sin3p in a two-hybrid assay and is part of a large protein complex with Sin3p and Stb1p	48.7%	-1.0	7E-05	0	0	0	0
YDR485C	VPS72	Htz1p-binding component of the SWR1 complex, which exchanges histone variant H2AZ (Htz1p) for chromatin-bound histone H2A; required for vacuolar protein sorting	48.7%	-1.0	0.0001	1 3	0	0	0
YLR320W	MMS22	Protein that acts with Mms1p in a repair pathway that may be involved in resolving replication intermediates or preventing the damage caused by blocked replication forks; required for accurate meiotic chromosome segregation	48.7%	-1.0	0.0008	2 9	0	3 0	0
YGL230C	N/A	Putative protein of unknown function; non-essential gene	48.8%	-1.0	0.0097	0	0	0	0
YPL072W	UBP16	Deubiquitinating enzyme anchored to the outer mitochondrial membrane, probably not important for general mitochondrial functioning, but may perform a more specialized function at mitochondria	48.8%	-1.0	7E-05	0	0	0	0
YHR041C	SRB2	Subunit of the RNA polymerase II mediator complex; associates with core polymerase subunits to form the RNA polymerase II holoenzyme; general transcription factor involved in telomere maintenance	48.8%	-1.0	0.0043	1 3	0	2 1	7

Appendix A

ORF	Gene	Description	PRG	LF C	p-val	M M S	T B P	4 N Q O	U V
YLL028W	TPO1	Polyamine transporter that recognizes spermine, putrescine, and spermidine; catalyzes uptake of polyamines at alkaline pH and excretion at acidic pH; phosphorylation enhances activity and sorting to the plasma membrane	48.8%	-1.0	0.0015	0	0	0	0
YGL147C	RPL9A	Protein component of the large (60S) ribosomal subunit, nearly identical to Rpl9Bp and has similarity to E. coli L6 and rat L9 ribosomal proteins	48.9%	-1.0	0.0006	0	0	0	0
YAL011W	SWC3	Protein of unknown function, component of the SWR1 complex, which exchanges histone variant H2AZ (Htz1p) for chromatin-bound histone H2A; required for formation of nuclear-associated array of smooth endoplasmic reticulum known as karmellae	49.0%	-1.0	0.0001	2 3	0	0	0
YIL027C	KRE27	Member of a transmembrane complex required for efficient folding of proteins in the ER; null mutant displays induction of the unfolded protein response, and also shows K1 killer toxin resistance	49.1%	-1.0	8E-05	5	0	0	0
YDR496C	PUF6	Pumilio-homology domain protein that binds ASH1 mRNA at PUF consensus sequences in the 3' UTR and represses its translation, resulting in proper asymmetric localization of ASH1 mRNA	49.1%	-1.0	7E-05	0	2	1 8	4
YNL291C	MID1	N-glycosylated integral membrane protein of the ER membrane and plasma membrane, functions as a stretch-activated Ca ²⁺ -permeable cation channel required for Ca ²⁺ influx stimulated by pheromone; interacts with Cch1p; forms an oligomer	49.1%	-1.0	0.0004	7	0	0	0
YIR023W	DAL81	Positive regulator of genes in multiple nitrogen degradation pathways; contains DNA binding domain but does not appear to bind the dodecanucleotide sequence present in the promoter region of many genes involved in allantoin catabolism	49.2%	-1.0	0.0009	9	0	1 3	0
YNL073W	MSK1	Mitochondrial lysine-tRNA synthetase, required for import of both aminoacylated and deacylated forms of tRNA(Lys) into mitochondria and for aminoacylation of mitochondrially encoded tRNA(Lys)	49.3%	-1.0	0.0012	0	0	0	4
YER014C -A	BUD25	Protein involved in bud-site selection; diploid mutants display a random budding pattern instead of the wild-type bipolar pattern	49.3%	-1.0	0.0045	0	0	0	0
YDR138 W	HPR1	Subunit of THO/TREX complexes that couple transcription elongation with mitotic recombination and with mRNA metabolism and export, subunit of an RNA Pol II complex; regulates lifespan; involved in telomere maintenance; similar to Top1p	49.3%	-1.0	0.0001	1 6	0	2 0	1 8

Appendix A

ORF	Gene	Description	PRG	LF C	p-val	M M S	T B P	4 N Q O	U V
YMR238 W	DFG5	Putative mannosidase, essential glycosylphosphatidylinositol (GPI)-anchored membrane protein required for cell wall biogenesis in bud formation, involved in filamentous growth, homologous to Dcw1p	49.3%	-1.0	0.0002	0	0	0	0
YBR215 W	HPC2	Subunit of the HIR complex, a nucleosome assembly complex involved in regulation of histone gene transcription; mutants display synthetic defects with subunits of FACT, a complex that allows passage of RNA Pol II through nucleosomes	49.3%	-1.0	0.0421	6	0	0	0
YPR096C	N/A	Protein of unknown function that may interact with ribosomes, based on co-purification experiments	49.3%	-1.0	0.0002	4	2	7	5
YDR463 W	STP1	Transcription factor, undergoes proteolytic processing by SPS (Ssy1p-Ptr3p-Ssy5p)-sensor component Ssy5p in response to extracellular amino acids; activates transcription of amino acid permease genes and may have a role in tRNA processing	49.3%	-1.0	0.0003	4	0	0	0
YML028 W	TSA1	Thioredoxin peroxidase, acts as both a ribosome-associated and free cytoplasmic antioxidant; self-associates to form a high-molecular weight chaperone complex under oxidative stress; deletion results in mutator phenotype	49.4%	-1.0	0.0005	0	0	1 0	0
YGR001C	N/A	Putative protein of unknown function with similarity to methyltransferase family members; green fluorescent protein (GFP)-fusion protein localizes to the cytoplasm; required for replication of Brome mosaic virus in <i>S. cerevisiae</i>	49.4%	-1.0	0.0002	0	0	0	2
YNL295W	N/A	Putative protein of unknown function	49.4%	-1.0	0.0002	0	0	0	0
YLR447C	VMA6	Subunit d of the five-subunit V0 integral membrane domain of vacuolar H ⁺ -ATPase (V-ATPase), an electrogenic proton pump found in the endomembrane system; stabilizes V0 subunits; required for V1 domain assembly on the vacuolar membrane	49.4%	-1.0	0.0002	7	0	7	0
YJL096W	MRPL49	Mitochondrial ribosomal protein of the large subunit	49.5%	-1.0	7E-06	0	0	0	0
YER048C	CAJ1	Nuclear type II J heat shock protein of the <i>E. coli</i> dnaJ family, contains a leucine zipper-like motif, binds to non-native substrates for presentation to Ssa3p, may function during protein translocation, assembly and disassembly	49.5%	-1.0	3E-05	0	0	0	0
YMR166C	N/A	Predicted transporter of the mitochondrial inner membrane; has similarity to human mitochondrial ATP-Mg/Pi carriers; YMR166C is not an essential gene	49.6%	-1.0	0.0049	7	0	0	0
YHL006C	SHU1	Protein involved in a Rad51p-, Rad54p-dependent pathway for homologous recombination repair, important for error-free repair of spontaneous and induced DNA lesions to protect the genome from mutation; associates with Shu2p, Psy3p, and Csm2p	49.6%	-1.0	2E-05	2 2	0	9	0

Appendix A

ORF	Gene	Description	PRG	LF C	p-val	M M S	T B P	4 N Q O	U V
YOR309C	N/A	Dubious open reading frame unlikely to encode a protein, based on available experimental and comparative sequence data; partially overlaps the verified gene NOP58	49.6%	-1.0	0.0006	0	0	6	0
YJR129C	N/A	Putative protein of unknown function; predicted S-adenosylmethionine-dependent methyltransferase of the seven beta-strand family; green fluorescent protein (GFP)-fusion protein localizes to the cytoplasm	49.7%	-1.0	0.0047	0	0	0	0
YHR200 W	RPN10	Non-ATPase base subunit of the 19S regulatory particle (RP) of the 26S proteasome; N-terminus plays a role in maintaining the structural integrity of the RP; binds selectively to polyubiquitin chains; homolog of the mammalian S5a protein	49.7%	-1.0	8E-05	0	0	0	0
YML009C	MRPL39	Mitochondrial ribosomal protein of the large subunit	49.7%	-1.0	0.0028	8	0	0	0
YHR013C	ARD1	Subunit of N-terminal acetyltransferase NatA (Nat1p, Ard1p, Nat5p); acetylates many proteins and thus affects telomeric silencing, cell cycle, heat-shock resistance, mating, and sporulation; human Ard1p levels are elevated in cancer cells	49.7%	-1.0	0.0006	2 2	0	2	6
YKL207W	AIM27	Member of a transmembrane complex required for efficient folding of proteins in the ER; required for respiratory growth; null mutant displays induction of the unfolded protein response	49.8%	-1.0	0.0008	6	0	0	0
YKR016 W	AIM28	Mitochondrial protein of unknown function; null mutant displays a slow growth defect in combination with a null mutation in the mitochondrial GTPase GEM1; null mutant displays reduced frequency of mitochondrial genome loss	49.8%	-1.0	0.0038	0	0	0	0
YNL278W	CAF120	Part of the evolutionarily-conserved CCR4-NOT transcriptional regulatory complex involved in controlling mRNA initiation, elongation, and degradation	49.8%	-1.0	0.0006	0	0	0	0
YDR469 W	SDC1	Subunit of the COMPASS (Set1C) complex, which methylates histone H3 on lysine 4 and is required in transcriptional silencing near telomeres; has similarity to <i>C. elegans</i> Dpy-30	49.8%	-1.0	6E-05	8	0	0	0
YLR235C	N/A	Dubious open reading frame unlikely to encode a protein, based on available experimental and comparative sequence data; partially overlaps the verified gene TOP3	49.8%	-1.0	0.0044	3 0	0	3 0	8
YHR183 W	GND1	6-phosphogluconate dehydrogenase (decarboxylating), catalyzes an NADPH regenerating reaction in the pentose phosphate pathway; required for growth on D-glucono-delta-lactone and adaptation to oxidative stress	49.9%	-1.0	0.0027	0	0	7	0
YPL184C	MRN1	RNA-binding protein proposed to be involved in translational regulation; binds specific categories of mRNAs, including those that contain upstream open reading frames (uORFs) and internal ribosome entry sites (IRES)	49.9%	-1.0	0.0075	0	0	0	0

Appendix A

ORF	Gene	Description	PRG	LF C	p-val	M M S	T B P	4 N Q O	U V
YKL109W	HAP4	Subunit of the heme-activated, glucose-repressed Hap2p/3p/4p/5p CCAAT-binding complex, a transcriptional activator and global regulator of respiratory gene expression; provides the principal activation function of the complex	50.0%	-1.0	1E-05	0	0	0	0

Appendix B

**Effects of the Medium Components on 11 β -Dichloro
Toxicity in *Saccharomyces cerevisiae***

B.1 Introduction

This appendix highlights some interesting results yielded by an investigation of the effects of various medium components on the sensitivity of several *S. cerevisiae* strains to 11 β -dichloro exposure. This work was started following the observation that yeast cells are not sensitive to 11 β -dichloro when treated in rich medium (YPD), yet many strains are sensitive when exposed to 11 β -dichloro in phosphate buffered saline (PBS). We discovered that 11 β -dichloro toxicity is dramatically increased in conditions of low ionic strength. Surprisingly, the toxicity is alleviated by the presence of glucose or calcium in the PBS buffer during treatment.

B.2 Materials & Methods

The compounds 11 β -dichloro and 11 β -dimethoxy were synthesized using previously reported schemes (Marquis et al., 2005). Mechlorethamine (HN2) and chlorambucil were purchased from Sigma-Aldrich (St. Louis, MO, USA). Stock solutions (100 mM for chlorambucil, 10 mM for all other compounds) were prepared in anhydrous DMSO (Sigma). All other inorganic salts and reagents were from Sigma-Aldrich. All media components (yeast extract, peptone, glucose) were from BD Biosciences.

All experiments included here are relative growth assays performed as described in Chapter 2 Materials and Methods. Whenever indicated, the PBS vehicle has been supplemented with various chemical components at the concentration indicated. Another buffering system, TBS, (Tris buffered saline, pH = 7.4) has been utilized instead of PBS for some of the experiments involving calcium, to circumvent the formation of an insoluble calcium phosphate precipitate.

B.3 Results and Discussion

B.3.1 The phenotypes of the control strains

We investigated the effect of different treatment conditions on the sensitivity to 11 β -dichloro (Figure B.1 A) of the four control strains utilized in the complete library screen. Figure B.1 highlights the phenotypic properties of these strains. Both Δ COX9 and Δ ERG6 mutants are very sensitive to 20 μ M 11 β -dichloro and somewhat sensitive to 40 μ M 11 β -dimethoxy (Figure B.1 B). This sensitivity was the basis for selecting them as positive controls for the library screen. WT and Δ REV1 strains show similar phenotypes when treated with the 11 β compounds. Although unaffected by 11 β -dichloro, the Δ REV1 mutant is very sensitive to the crosslinking agent mechlorethamine (HN2) at 10 μ M and somewhat sensitive to a high dose (400 μ M) of chlorambucil. The patterns of sensitivity of Δ REV1 are in agreement with overall screening results, which indicated that an important number of mutants lacking proteins involved in DNA repair and therefore highly sensitive to DNA damaging agents, are not very sensitive to 11 β -dichloro. The ability of 11 β -dimethoxy to elicit a similar pattern of toxicity with 11 β -dichloro, albeit of smaller magnitude, constitutes further evidence that there is a component of the mechanism of toxicity of 11 β -dichloro in yeast that is DNA-damage independent.

B.3.2 The influence of the low ionic strength of the buffer

We investigated whether the ionic strength of the PBS solution in which we treat the yeast cells can influence their sensitivity to 11 β -dichloro. We employed dilutions of the PBS stock in doubly-distilled water (ddH₂O) to achieve lower ionic strengths of the buffer. Undiluted PBS contains ~150 mM of monocations (sodium and potassium). At a lower concentration of monocations (120 mM corresponding to a 0.8 X dilution), corresponding to a lower ionic strength solution, the viability of the untreated yeast does not change (data not shown). However, in a 0.8X PBS buffer, the sensitivity to 11 β -dichloro increases dramatically in all the strains, especially in the WT and Δ REV1, strains that are not sensitive to 11 β -dichloro in a 1.0X PBS buffer. This experimental observation may underline the importance of transport

of 11 β -dichloro across the yeast cell wall and plasma membrane. In lower ionic strength solutions, the cells swell up and become more permeable to biomolecules, including 11 β -dichloro. The higher toxicity is then achieved by the increased amounts of compound entering the cell. Alternatively, one of the putative mechanisms of 11 β -dichloro may involve perturbations of the cell membrane and ion homeostasis. The low ionic strength buffer may already perturb the cell membrane on its own; in that case, the 11 β -dichloro exposure is just the last drop that pushes the cell over the edge.

B.3.3 The influence of glucose

A careful analysis was done on discreet elements of the YPD media, to identify those elements that might confer the yeast cells resistance to 11 β -dichloro. One such element was found to be glucose (Figure B.3). When the PBS solution is supplemented with glucose at 0.025% or higher, the Δ COX9 mutant, highly sensitive to 11 β -dichloro, becomes unaffected. The presence of glucose also abolishes the small sensitivity of the WT and Δ REV1 strains. Curiously, the presence of glucose does not affect the sensitivity of the Δ ERG6 strain, which remains just as sensitive as it were in PBS without glucose. The unaffected sensitivity of Δ ERG6 discards the simple explanation that the observed results are due to glucose interfering with 11 β -dichloro solubility or bioavailability, suggesting that a more complicated mechanism might be involved. One possibility is of active efflux; the glucose is used by the cells to produce ATP, which can then be used to power various drug-efflux pumps. The activity of such transporter proteins may potentially lower significantly the intracellular concentration of 11 β -dichloro, and thus, avert its toxicity. One problem with this hypothesis may be the low level of glucose necessary to achieve the striking rescue effect on the Δ COX9 mutant; the 0.025% concentration is 20 to 50 times lower than the usual glucose concentrations present in the rich medium YPD. Additionally, this hypothesis cannot explain the fact that other compounds that can be used to generate energy in the cell, such as glutamate, methylpyruvate and galactose, do not elicit the same phenotype. Even when the PBS buffer is supplemented with high levels of glutamate, methylpyruvate or galactose, the Δ COX9 mutant remains highly sensitive to 11 β -dichloro (data not shown). Furthermore, the “glucose effect” is not limited to Δ COX9. A large number of mutants sensitive to 11 β -

dichloro are rescued by addition of small amounts of glucose. Nevertheless, Δ ERG6 is not the singular example of a mutant that cannot be rescued by glucose. Although very few, we identified several others. Curiously, most of the mutants that are rescued by glucose have defects in mitochondrial function (similar to Δ COX9), whereas the mutants that do not respond to glucose, tend to have defects in membrane properties (similar to Δ ERG6). All these observations suggest that the “glucose effect” is related to the mechanism of toxicity of the compound in yeast cells. Unfortunately, the exact details of the mechanism are still a mystery.

B.3.4 The influence of divalent cations

A study done on mutants from the ERG6 pathway indicated that the presence of calcium can alleviate their growth defects and even render them more resistant to antifungal compounds (Crowley et al., 1998). Therefore, we investigated whether addition of millimolar levels of calcium in the PBS buffer, during treatment might alleviate the toxicity of 11 β -dichloro to Δ ERG6. Surprisingly, the results indicated that the presence of calcium during exposure of the yeast cells to our compound had significant consequences (Figure B.5). A 10 mM concentration of calcium was sufficient to significantly rescue the phenotype of Δ ERG6. The presence of calcium had also notable effects on all the strains, including Δ COX9, which was however rescued to a lesser extent. We also discovered that magnesium, another biologically relevant divalent cation elicits a similar response. Additionally, we investigated whether the addition of a calcium or magnesium chelator such as EDTA or EGTA would have the opposite effect, increasing sensitivity of the strains to 11 β -dichloro. The experimental results confirm our supposition (Figure B.5). Taken together, all these results suggest that one aspect of the mechanism of toxicity of 11 β -dichloro may be related to membrane damage. The mutants in the ergosterol pathway such as Δ ERG6 have impaired membrane function and consequently have difficulty in maintaining the homeostasis of various ions and small molecules (Gaber et al., 1989). Therefore, the mutants in the ERG pathway would be expected to be very sensitive to a compound that exacerbates the membrane impairment.

B.4 Figures

<i>Figure B.1 The molecular structures of 11β-dichloro and 11β-dimethoxy.....</i>	<i>275</i>
<i>Figure B.2 The phenotypes of the control strains exposed to 11β-dichloro and nitrogen mustards.....</i>	<i>276</i>
<i>Figure B.3 The effect of ionic strength of the PBS buffer on the sensitivity of the control strains to 11β-dichloro.....</i>	<i>277</i>
<i>Figure B.4 The effect of glucose on the sensitivity of the control strains to 11β-dichloro .</i>	<i>278</i>
<i>Figure B.5 The effect of calcium and magnesium on sensitivity of the control strains to 11β- dichloro.....</i>	<i>279</i>

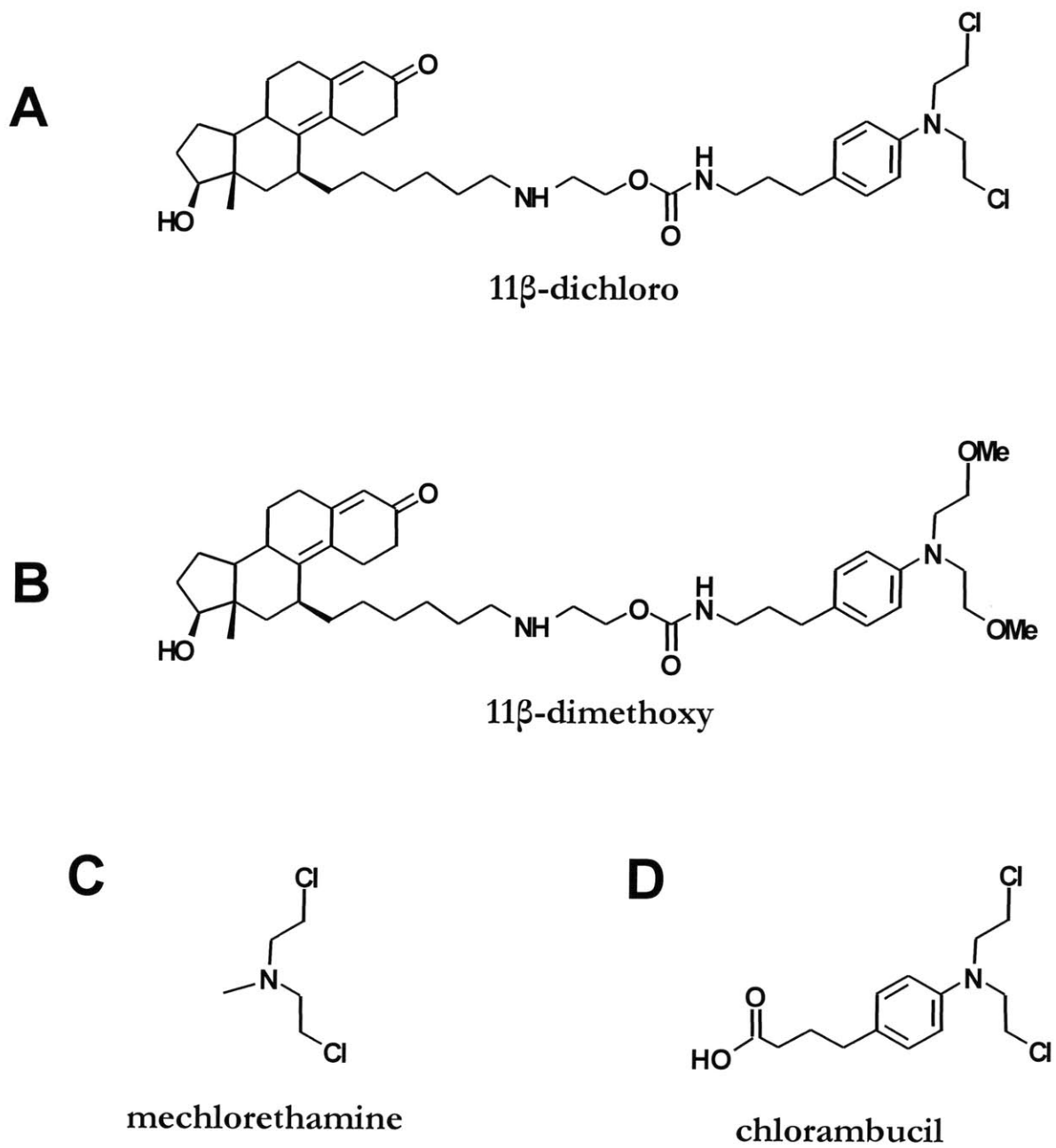


Figure B.1 The molecular structures of 11 β -dichloro, 11 β -dimethoxy, HN2 and chlorambucil

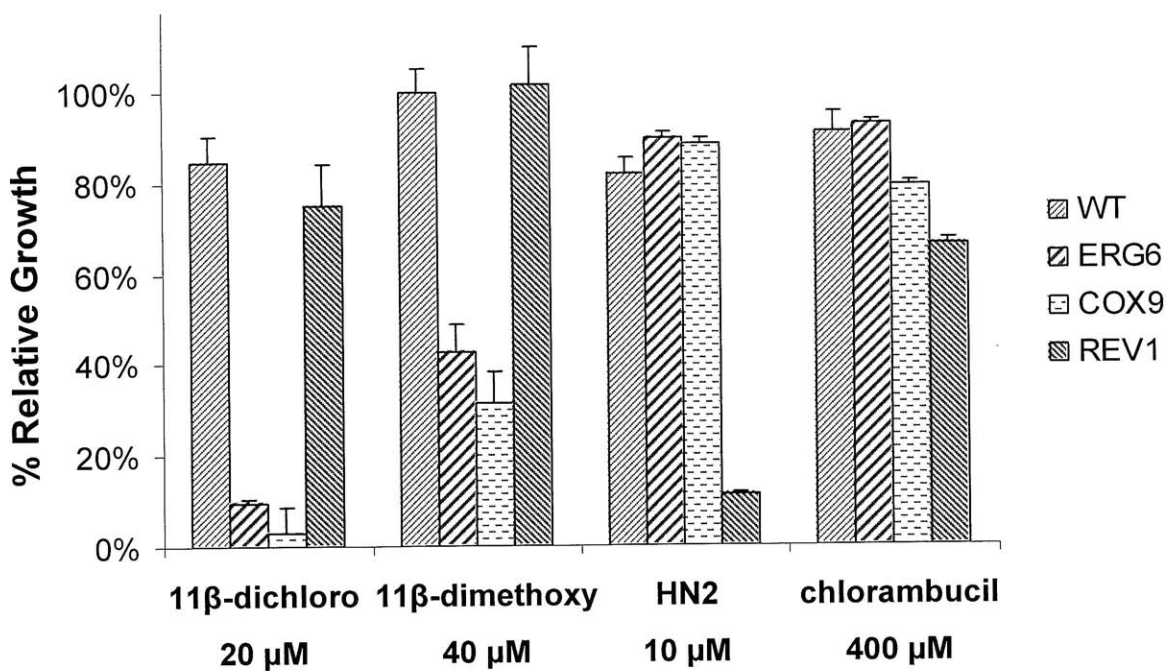


Figure B.2 The phenotypes of the control strains exposed to 11β-dichloro, 11β-dimethoxy and the nitrogen mustards HN2 and chlorambucil

Mutants such as Δ ERG6 and Δ COX9 are very sensitive to 11β-dichloro and somewhat sensitive to 11β-dimethoxy, yet they are quite resistant to HN2 or chlorambucil. The mutant Δ REV1 is not sensitive to 11β compounds, but very sensitive to DNA crosslinking agent HN2. Chlorambucil is not very toxic for yeast cells; however, the most sensitive mutants to chlorambucil in our group is Δ REV1.

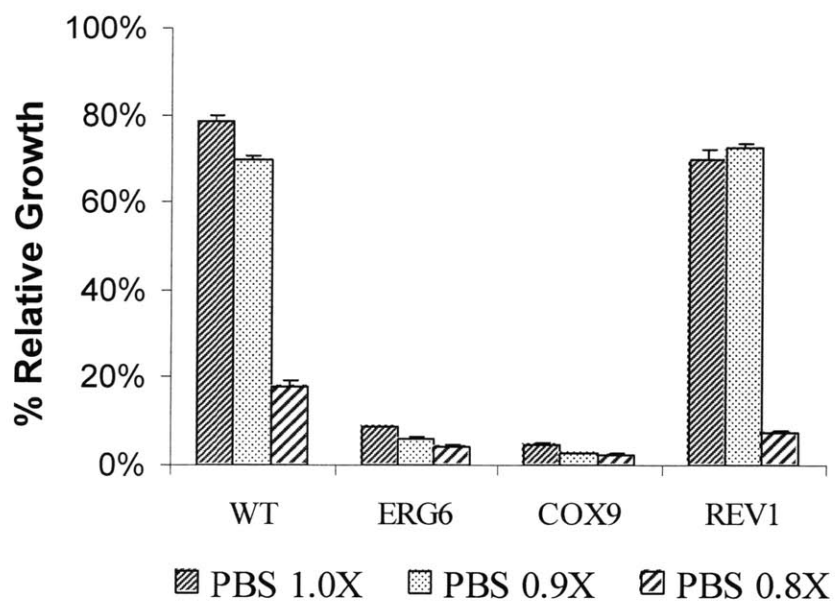


Figure B.3 The effect of ionic strength of the PBS buffer on the sensitivity of the control strains to 11 β -dichloro

Cells were treated with 20 μ M 11 β -dichloro for 4 hours. The cells were then washed and incubated in rich medium for 12 hours. The extent of growth was determined spectrophotometrically. These data show that the ionic strength of the buffer in which the drug is dissolved is important in modulating 11 β -dichloro toxicity.

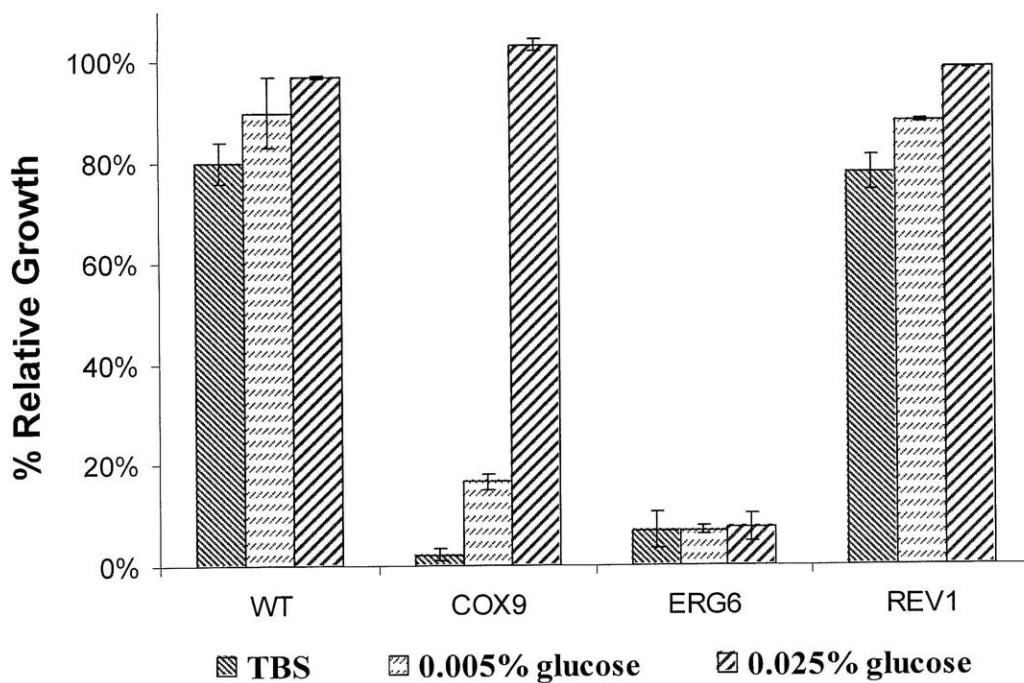


Figure B.4 The effect of glucose on the sensitivity of the control strains to 11 β -dichloro

The yeast strains were treated with 20 μ M 11 β -dichloro for 4 hours. The solution of 11 β -dichloro was made in TBS or in TBS supplemented with glucose at the concentration indicated. The results highlight the surprising recovery of Δ COX9 mutant when at least 0.025% glucose is present during treatment. The other sensitive mutant, Δ ERG6, is not rescued by glucose.

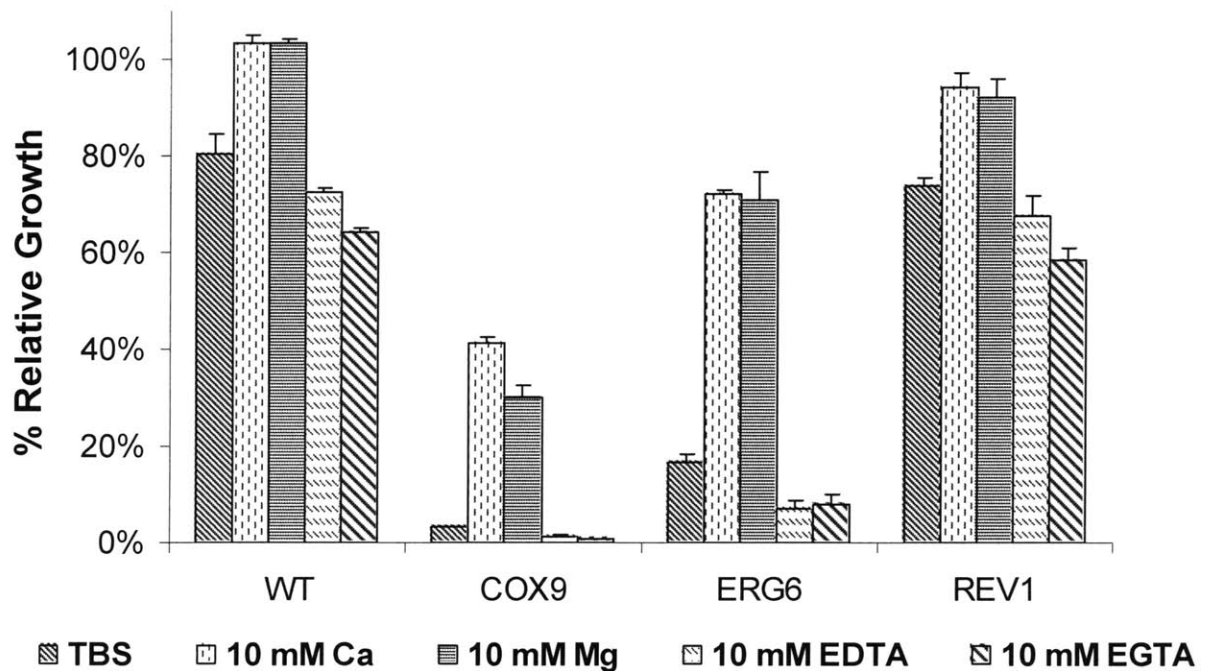


Figure B.5 The effect of calcium and magnesium on sensitivity of the control strains to 11 β -dichloro

The yeast strains were incubated with 20 μ M 11 β -dichloro for 4 hours. The solution of 11 β -dichloro was prepared in TBS, or TBS supplemented with 10 mM CaCl₂ or 10 mM MgCl₂. In a parallel experiment, 10 mM EDTA or 10 mM EGTA were added to the TBS buffer. The results highlight the ability of divalent cations to diminish the sensitivity of Δ ERG6 mutant to 11 β -dichloro. The addition of the calcium and magnesium chelating agents EDTA and EGTA increases toxicity in all strains.

B.5 References

- Crowley, J. H., Tove, S., and Parks, L. W. (1998). A calcium-dependent ergosterol mutant of *Saccharomyces cerevisiae*. *Curr. Genet* 34, 93-99.
- Gaber, R. F., Copple, D. M., Kennedy, B. K., Vidal, M., and Bard, M. (1989). The yeast gene *ERG6* is required for normal membrane function but is not essential for biosynthesis of the cell-cycle-sparking sterol. *Mol. Cell. Biol* 9, 3447-3456.

Curriculum Vitae
BOGDAN I. FEDELEȘ

Massachusetts Institute of Technology 32 Vassar Street, 56-670 Cambridge, MA 02139 857-928-0072 bogdan@mit.edu		268 Harvard Street, Apt #6 Cambridge MA, 02139
--	--	---

Education **Massachusetts Institute of Technology** Cambridge, MA
 Ph.D. in Biological Engineering, June 2009
 Thesis topic: The Androgen Receptor Independent Mechanism of Toxicity of a Novel Aniline Mustard-Estradienone Anti-tumor Agent

Massachusetts Institute of Technology Cambridge, MA
 Bachelor of Science in Chemistry,
 Bachelor of Science in Biology,
 Minor in Music, June 2002. GPA 4.8/5.0

“B.P.Hasdeu” High School Buzau, Romania
 Valedictorian, first in a 450 class. June 1998. GPA 9.92/10.00

Awards Ragnar& Margaret Naess Award (2008)
 1st Prize and Intempco Best Design Award for MIT 6.270 Autonomous Robot Design Competition (2006)
 Biogen Idec Fellowship (2004-2005)
 Ashdown Award for Community Service, (2003)
 Frederick D. Greene Teaching Award (MIT Chemistry Department, 2002)
 National Collegiate Natural Science Award (2001)
 International Chemistry Olympiad medalist, (silver - Melbourne 1998, bronze - Montreal 1997, gold - Yakutsk 1996)

Research experience **Massachusetts Institute of Technology** Cambridge, MA
 Advisor: John Essigmann
 Characterized novel, synthetic chemotherapeutic agents.
 Investigated the effect of different linkers between the mustard and steroid moieties using gel shift assays.
 Investigated the mechanism of toxicity by phenotypic screening of a yeast mutant library and GO terms mapping.
 Developed high-throughput protocol for yeast phenotypic screening.
 Used yeast data to identify pathways involved in the mechanism of toxicity in human cell lines.
 Investigated the link between mitochondrial function and drug toxicity using cell viability assays, mitochondrial probes and rt-PCR techniques.
 Investigated the nature and role of reactive oxygen species (ROS) in the drug toxicity using spectrophotometry and flow cytometry techniques.
 (July 2002-at present)

Curriculum Vitae

Massachusetts Institute of Technology

Cambridge, MA

Advisor: Matthew Wilson

Undergraduate research opportunity program.

Set-up electrophysiology experiments which included building custom drives & tetrodes, surgical implantation, and neuronal ensembles *in-vivo* recordings in mutant mice.

Run behavior experiments with mutant mice, including Morris watermaze, rotarod and fear conditioning tests.

Developed software for data analysis including statistical analysis, database manipulations, image processing and GUI design. (Feb 1999-May 2002)

Teaching experience

MIT, Department of Biological Engineering

Cambridge, MA

Teaching assistant for 20.440 - *Analysis of biological networks*.

Assisted students in understanding the course material at office hours and in writing the final project. Assisted with critical reading and grading of final projects (Feb-May 2004)

Mentor for 20.UR – *Undergraduate Research Opportunity Program*

Taught undergraduate students various relevant lab techniques. Formulated and assigned small projects. Supervised and assisted with experimental work. (2005-at present)

MIT, Department of Chemistry

Cambridge, MA

Teaching assistant for 5.12 & 5.13 - *Organic Chemistry I & II*

Held recitation sections where class material was reviewed and practice problems were presented; held office hours, graded problem sets, proctored and graded exams (Sep2000-May 2002).

Lab teaching assistant for 5.301 - *Intro to Experimental Chemistry*

Setup experimental materials and optimized conditions for basic chemistry experiments; supervised and assisted students during lab work; graded results and assignments (Jan 2002).

Presentations & posters

Fedeles B, Zhu AY, Young KS, Essigmann JM, Croy RG (2008) Investigating the cellular responses to a novel bifunctional genotoxicant. DNA Repair and Mutagenesis Group, Cambridge, MA.

Fedeles B, Zhu AY, Young KS, Essigmann JM, Croy RG (2008) Investigating the toxicity mechanism of a nitrogen mustard in *S. cerevisiae* and HeLa cells. MIT Center for Environmental Health Sciences, Cambridge, MA

Sun LD, **Fedeles B**, Yu H, Shen J, Wilson MA (2001) Behavioral Analysis of *Presenilin-1* Conditional Knockout: Spatial Memory Impairment and Beyond. Society for Neuroscience National Conference, San Diego, CA

Curriculum Vitae

Publications Sharma U, Marquis JC, Dinaut AN, Hillier S, **Fedeles B**, Rye PT, Essigmann JM, Croy RG (2004) Synthesis and Evaluation of Estradiol-linked genotoxins. Bio-organic & Medicinal Chemistry Letters 14: 3829-3833.

Marquis JC, Sharma U, Dinaut N, Hillier S, **Fedeles B**, Rye PT, Essigmann JM, Croy RG (2003) Molecular variations in the linker determine biological activities of estradiol-bis-(2-chloroethyl)aniline conjugates. Clinical Cancer Research 9 (16): 6075S-6075S.

Yu H, Saura CA, Choi S, Sun LD, Yang X, Handler M, Kawarabayashi T, Younkin L, **Fedeles B**, Wilson MA, Younkin S, Kandel ER, Kirkwood A and Shen J (2001) APP Processing and Synaptic Plasticity in *Presenilin-1* Conditional Knockout Mice. Neuron 31: 713-726.

Languages: Native Romanian, fluent in English and French, basic German, basic Chinese

Computer Skills: Programming: C/C++, Java, MATLAB, Perl/Python, HTML, Visual Basic

Activities : Arts writer for the MIT newspaper "The Tech" (2000-at present)
Member of the MIT Chamber Music Society (2000-at present)
AHEC Operations Officer (2004-2005)
Interests include: piano performance, music writing, skiing, ping-pong, tennis, soccer, strategy games.

References: Professor John M. Essigmann
Department of Biological Engineering & Department of Chemistry
Massachusetts Institute of Technology
56-669
Cambridge, MA 02139
617-253-6227
jessig@mit.edu

Professor Forest M. White
Department of Biological Engineering
Massachusetts Institute of Technology
56-787A
Cambridge, MA 02139
617-258-8949
fwhite@mit.edu

Professor Leona D. Samson
Center for Environmental Health Sciences
Massachusetts Institute of Technology
56-235
Cambridge, MA 02139
617-258-7813
lsamson@mit.edu

Curriculum Vitae